

GEOSPATIAL MODELLING OF RANGELANDS PRODUCTIVITY IN WATER-LIMITED ENVIRONMENTS OF SOUTH AFRICA

Report to the
WATER RESEARCH COMMISSION

by

**O MUTANGA¹, T MABHAUDHI¹, T DUBE², M SIBANDA², T BANGIRA¹ &
R LOTTERING¹**

¹ School of Agricultural, Earth and Environmental Sciences
Centre for Transformative Agricultural and Food Systems
University of KwaZulu-Natal, Pietermaritzburg, South Africa

² Faculty of Science and Faculty of Arts
University of the Western Cape, Cape Town, South Africa

WRC Report No. 3126/1/24
ISBN 978-0-6392-0601-1

April 2024



Obtainable from

Water Research Commission
Bloukrans Building, Lynnwood Bridge Office Park
4 Daventry Street
Lynnwood Manor
PRETORIA

orders@wrc.org.za or download from www.wrc.org.za

This is the final report for WRC project no. C2020/2021-00490.

DISCLAIMER

This report has been reviewed by the Water Research Commission (WRC) and approved for publication. Approval does not signify that the contents necessarily reflect the views and policies of the WRC, nor does mention of trade names or commercial products constitute endorsement or recommendation for use.

EXECUTIVE SUMMARY

Grasslands are renowned for their socioeconomic, ecological and environmental functions, yet they remain the most contested biome that is also extensively impacted by climate change. Specifically, grasslands provide several ecosystem services, which include providing fodder for livestock while regulating elements of the hydrological cycle at various scales. In South Africa, grasslands are the third largest biomes incurring extensive spatiotemporal transformations. Their spatiotemporal dynamics are predominantly a result of anthropogenic activities and climate change. Climate change is associated with temperature and precipitation variations that in turn regulates grassland productivity. Meanwhile, competitive anthropogenic activities which include crop farming, development, overgrazing, and mining activities continue to transform grasslands.

Optimal management of grassland resources requires spatially explicit information on their dynamics as well as an understanding of the drivers of that change. However, there is paucity of spatial information on the changes in grassland productivity. Past research efforts were mostly directed to specific and strategic localities, with limited spatial extents due to the tedious fieldwork and processing tools. Subsequently, accurate, perpetual, and constant monitoring of grasslands as well as the associated decisions made were somewhat compromised as they lacked spatial explicitness. Remote sensing technologies have emerged as the most convenient, accurate, time- and cost-effective approach in mapping and monitoring the dynamics of various grassland attributes at various spatiotemporal scales. The application of remote sensing technologies and data for monitoring grasslands has substantially progressed. The recent advances in satellite data provision as well as the introduction of big data cloud computing and storage facilities have availed opportunities to conduct research on grasslands at various spatial scales. In this regard, this project sought to map and monitor grassland ecosystem attributes using geospatial technologies. The application of wall-to-wall geospatial applications for monitoring grasslands in South Africa could contribute towards achieving and addressing Sustainable Development Goals on poverty and hunger alleviation, provision of clean water, contribute to climate action and life on land (biodiversity) by 2030, SDGs 1, 2, 13 and 15, respectively. The focus of this project was on assessing the utility of geospatial data and techniques in providing spatially explicit information on grassland productivity suitable for reinforcing the decision-making process for sustainable utilisation of grasslands. In the long run, this could assist farmers in planning activities such as grazing rotation, fodder management, thereby sustainably utilising this natural capital resource with preparedness in the light of climate change. Specifically, the project contractual aims were:

- (i) to conduct a comprehensive and state of the art literature review on the potential use of remote sensing-based models for grassland productivity monitoring in the light of climate change,
- (ii) to review the importance of grasslands as an ecosystem service, particularly the contribution of leaf area index (LAI), canopy storage capacity and biomass in water management,
- (iii) to characterise and model communal grassland productivity status in a changing climate at three sites within the uMgungundlovu District Municipality, and
- (iv) to assess intra- and interannual changes in grassland productivity and proportionate land use change within the catchment and explain the changes thereof.

To address the contractual objectives, the project was sub-structured into four work packages. The first work package addressed objectives No 1 and 2 presented as two systematic literature reviews. Work package 2 addressed objective No 3 and 4 by first assessing the changes in the areal extent of grasslands between 2010 and 2020 using geospatial data acquired from free and readily available satellite-based archival sources. This was followed by mapping and modelling the intra- and interannual grassland productivity attributes (i.e. LAI, biomass, canopy storage capacity). Work package 3 partially addressed objectives No 3 and 4 by incorporating environmental factors in assessing the water-related ecosystem services. Work package 4 focussed on research dissemination to ensure that the research output informed practice, thereby maximising the benefit to key stakeholders. It provided a report on capacity development. The following specific objectives were drawn to address the outlined work packages and the contractual aims and objectives,

- (i) To review scientific peer-reviewed articles comprehensively and systematically on using remotely sensed data within the explicit theme of estimating grass productivity (GP) proxies, such as above ground biomass (AGB), leaf area index (LAI), canopy storage capacity (CSC).
- (ii) To systematically review the progress, emerging gaps, and opportunities on the application of remote sensing technologies in quantifying grasslands ecosystem services.
- (iii) To assess the spatiotemporal variability of rangelands within a typical southern African communal area from the year 2000 to 2020 using multi-temporal Landsat datasets in conjunction with the random forest.
- (iv) To predict the future spatial distribution of grasslands in communal rangelands using the CA-Markov model between the year 2020 and 2040. The project also compared

the magnitude of grass fragmentation in the forthcoming 20 years since the same year intervals were considered in generating input maps for modelling.

- (v) To compare the predictive performance of shallow artificial neural networks (ANNs) and deep convolutional neural networks (CNNs) in estimating aboveground grass biomass using Sentinel 2 MSI during the dry season.
- (vi) To predict inter-seasonal variations of grass biomass in using Sentinel 2 MSI remotely sensed data in conjunction with convolutional neural networks (CNNs).
- (vii) To test the utility of multi-source data in estimating LAI, CSC, CWC, and EWT within communal grasslands across wet and dry seasons.

The study was supposed to focus on three areas in KwaZulu-Natal, namely, Swayimane (uMshwathi Municipality), Vulindlela (Msunduzi Municipality) and Nhlazuka (Richmond Municipality). Upon realising that in Swayimane, the dominant agricultural activity was crop farming with limited and fragmented rangelands, this study site was left out. All sites are within the uMgungundlovu District Municipality and the Greater Umgeni Catchment. A District model approach implemented by government was adopted in conducting this project. The project sought to build on action research approaches to ensure community participation and beneficiation in the target locations. Already, the UKZN team had been working within the target sites since 2012 and has built significant social capital within the communities. Thus, the project leveraged on such social capital. Specifically, the UKZN Project Facilitators and Community Mobilisation Officers who were already working within these communities supporting action learning were integrated into the project.

GIS shapefiles of administrative boundaries (i.e. Provinces, Districts and Wards), were downloaded from the Department of Forestry Fisheries and the Environment websites. The districts and selected wards were utilised to generate random sampling points in ArcGIS 10.8. The generated points were then used as general guide for the sampling procedure for different research inquiries addressing the contractual objectives. Specifically, data from the Landsat, Sentinel and Shuttle Radar Topographic Missions was accessed and utilised using the readily accessible big data cloud computing Google Earth Engine in conjunction with various machine learning algorithms. In terms of the systematic literature reviews, the Preferred Reporting Items for Systematic Reviews and Meta-Analyses (PRISMA) approach and checklist were utilised to generate the key search words, for retrieving literature from databases such as Web of Science, Scopus, and Science Direct.

In conducting a comprehensive and state of the art literature review on the potential use of remote sensing-based models for grassland productivity (GP) monitoring in the light of climate change, results of the systematic literature review showed that the most used proxies of GP in ecological studies are aboveground biomass (AGB), leaf area index (LAI), canopy storage capacity (CSC), and chlorophyll and nitrogen content. The systematic review of research published between 1970 and October 2021 (n= 203) peer reviewed articles indicated the growing demand for high resolution hyperspectral sensors and computationally efficient image-processing techniques for the accurate and time-efficient prediction of GP at various scales of application. Further research is required to attract the synthesis of optical and radar data, multi-sensor data, and the selection of appropriate techniques for GP prediction at different scales. Results implied that there is a need to understand the major uncertainties associated with various algorithms employed for predicting GP and striving to reduce these errors.

In reviewing the importance of grasslands as an ecosystem service, particularly the contribution of leaf area index (LAI), canopy storage capacity and biomass in water management, a systematic review of 178 peer-reviewed articles from Web of Science, Scopus and Institute of Electrical and Electronics Engineers were analysed. The findings showed that most of the studies were conducted in Asia with a particular focus on biomass and primary production being the major researched ecosystem services. Results demonstrated that biomass, CSC and LAI are prominent attributes in deriving insights on evapotranspiration, infiltration, run-off, soil water availability, groundwater restoration and surface water balance. Hence an understanding of such hydrological processes is critical for understanding water redistribution and balance within grassland ecosystems which is important for water management.

To assess the proportionate land use change within the catchment and explaining the changes thereof, two specific objectives were drawn. The first assessed the land cover (LU/LC) changes and the spatial variation of communal rangelands (between the years 2000, 2010 and 2020). The second specific objective predicted the future changes (2020 to 2040) in the spatial distribution of rangelands in communal areas using the CA-Markov model.

Results showed that the rangelands decreased at a rate of 37.52 hectares per year from 2000 to 2010 and at 76.46 hectares per year from 2010 to 2020 in Vulindlela. Meanwhile, in Inhlazuka they decreased at 40 hectares per year between the years 2000 and 2010 then increased at a rate of 45.28 hectares per year between 2010 and 2020 due to a decline in the forest class. These changes were detected at overall accuracies of 75%, 79% and 83% for

Inhlazuka and overall accuracies of 89%, 85%, and 89% for Vulindlela during the years 2000, 2010 and 2020, respectively. In terms of fragmentation analysis, results showed that the rangeland mean patch sizes in Vulindlela decreased from 32 ha to 22 ha and then to 9 ha between 2000, 2010 and 2020, respectively, because of the increase in built-up areas. On the other hand, in Inhlazuka, the grasslands mean patch area decreased from 2 ha to a hectare between 2000 and 2010 and then it increased by 1 hectare between 2010 and 2020.

In predicting the future changes (2020 to 2040) in the spatial distribution of rangelands in communal areas using the CA-Markov model, results showed that the spatial extent of grasslands in Vulindlela will continue to decline from 6660.04 ha in 2020 to 5740.30 ha by 2040, whereas in Inhlazuka, the grasslands are expected to increase from 2567.55 ha in 2020 to 2987.03 ha by 2040. Results also showed that the patch area is anticipated to increase from 8.5 ha in 2020 to 55.94 ha by 2040 in Vulindlela and increase in Inhlazuka from 1.7 ha in 2020 to 7.20 ha by 2040. Meanwhile, patch isolation (Euclidean Nearest Neighbor Distance) is predicted to increase from 73.0 ha in 2020 to 172.20 ha by 2040 in Vulindlela and increase from 75.0 ha to 120.60 ha in Inhlazuka within the same period. These findings highlight the urgent need for the development of robust spatially explicit rangeland monitoring mechanisms for implementing sound conservation strategies.

The final contractual objectives (iii) to characterise and model communal grassland productivity status in a changing climate at three sites within the uMgungundlovu District Municipality and (iv) to assess intra- and interannual changes in grassland productivity and proportionate land use change within the catchment and explain the changes thereof, were addressed in three specific objectives. The project compared the predictive performance of shallow artificial neural network (ANNs) and deep convolutional neural network (CNN) in estimating aboveground grass biomass using Sentinel 2 MSI. The second specific objective predicted inter-seasonal (dry season and wet season) fodder quantity in selected wards of Umgeni catchment area using high resolution satellite imagery. Finally, the project tested the utility of multi-source data in estimating leaf area index (LAI), canopy storage capacity (CSC), canopy water content (CWC), and equivalent water thickness (EWT) within communal grasslands across wet and dry seasons. It was hypothesized that integrating multi-source data with a robust machine learning algorithm would improve the prediction accuracies of GWC indicators as a step towards building spatially explicit communal rangeland monitoring frameworks.

In comparing the predictive performance of shallow artificial neural network (ANNs) and deep convolutional neural network (CNN) in estimating aboveground grass biomass using Sentinel

2 MSI, results showed that deep CNN outperforms the ANN in estimating aboveground biomass with a best R^2 of 0,83, RMSE of 3,36 g/m^2 and RMSE% of 6,09. In comparison, the ANN produced a best R^2 of 0,75, RMSE of 5,78 g/m^2 and RMSE% of 8,90. The sensitivity analysis suggests that the blue band, Green Chlorophyll index (GCI) and Green normalised difference vegetation index (GBNDVI) were the most significant indices for model development by both neural network architectures. Subsequently, the CNN ensemble was adopted in predicting inter-seasonal (dry season and wet season) fodder quantity in selected wards of Umgeni catchment area using high resolution satellite imagery.

Results showed that seasonal grass productivity trends could be predicted to a R^2 of 0,83, RMSE of 3,36 g/m^2 and a RMSE% of 6,09 in the dry season and a R^2 of 0,85, RMSE of 2,41 g/m^2 and a RMSE% of 3,71 in the wet season, respectively using optimal spectral variables which included Band 2 (blue), Green Chlorophyll index (GCI) and Green normalised difference vegetation index (GNDVI). These findings suggested that grass biomass was substantially influenced by changes in rainfall and temperature as noted in other grassland studies abroad.

In testing the utility of multi-source data in estimating LAI, CSC, CWC, and EWT within communal grasslands across wet and dry seasons based on the random forest regression ensemble in GEE results showed that LAI was optimally estimated in the wet season with an RMSE of 0.03 m^{-2} and R^2 of 0.83, comparable to the dry season results which exhibited an RMSE of 0.04 m^{-2} and R^2 of 0.90. Meanwhile, CSC was estimated with high accuracy in the wet season (RMSE = 0.01 mm and R^2 = 0.86) when compared to an RMSE of 0.03 mm and R^2 of 0.93 obtained in the dry season. r CWC, the wet season results yielded RMSE of 19.42 g/m^2 and R^2 of 0.76 which was lower than an accuracy of RMSE = 1.35 g/m^2 and R^2 = 0.87 obtained in the dry season. Finally, EWT was best estimated in the dry season yielding a model accuracy of RMSE = 2.01 g/m^2 and R^2 = 0.91 as compared to the wet season (RMSE = 10.75 g/m^2 and R^2 = 0.65). CSC was most optimally predicted amongst all grass water content (GWC) variable in both seasons. The most optimal prediction variables for estimating these GWC variables included the red-edge, near-infrared region (NIR), short-wave infrared region (SWIR) bands, their derivatives, and environmental variables such as rainfall and temperature across both seasons. The use of multi-source data significantly improved the prediction accuracies on GWC indicators across both seasons.

New knowledge and innovation

Despite the impeccable progress on the application of advanced geospatial techniques and data in mapping and monitoring grassland productivity in general, there is paucity of such research efforts in developing countries such as South Africa. In this regard, the project sought to generate knowledge on the optimal remote sensing data and methods that can map the extent and spatial-temporal distribution of rangeland productivity in the communal grazing lands of Umgeni catchments. Specifically, new knowledge on the utility of Geospatial techniques in modelling the spatial distribution of biomass, leaf area index (LAI), equivalent moisture thickness (EWT), canopy storage capacity (CSC), foliar moisture content (FMC), and canopy water content (CWC) was generated through this project. The project quantitatively generated spatially explicit maps on various grassland productivity elements in communal rangeland areas. The project also demonstrated that there is promise in interpreting and simplifying the attained spatially explicit information on grassland productivity. Furthermore, the project notes that if this information is converted, simplified, and well interpreted, it is suitable for reinforcing the decision-making process for sustainable utilisation of the grasslands. In the long run, this could assist farmers in planning activities such as grazing rotation, fodder management, thereby sustainably utilising this natural capital resource with preparedness in the light of climate change. Meanwhile, this could also assist the policy makers in drawing informed decision on how to reduce the magnitude of rangeland degradation.

Capacity Building

The project comprehensively addressed its capacity building mandate by recruiting and mentoring three master's students, a postdoctoral fellow, and three early career and emerging researchers, enhancing both the institutional and individual capabilities. Of these three master's students, two completed Cum Laude. The project is still going to recruit one more master student by leveraging on other funding streams to address any other issues lurking in the objectives. In this project, the postdoctoral fellows played an active role in student supervision along with the early career researchers. This cohort of researchers benefited from the active mentorship by the mid-career and seasoned researchers in the project, specifically in terms of conceptualization and project management skills.

Conclusion

The project's findings underscore the importance of geospatial technologies and data in spatially quantifying changes in grassland productivity elements in the context of climate change and anthropogenic activities. Specifically, grassland productivity elements which include biomass, leaf area index, equivalent moisture thickness, canopy storage capacity, foliar moisture content, and canopy water content were all optimally estimated using the readily accessible Landsat and Sentinel 2 MSI data and robust machine learning techniques. This project is a pathway towards the development of an automated and real time geospatial model for Monitoring grassland ecosystems. This will provide actionable information services to grassland assessment and monitoring across different key land management areas. Specifically, the assessment and monitoring service will deliver satellite-based Earth observation spatiotemporal models that will assist users in their operational grassland management as well as policy and decision making in the target areas.

Recommendations

Several research gaps remain regarding the utility of geospatial technologies and data in mapping and monitoring the spatiotemporal dynamics of grassland productivity, especially in communal rangelands.

- There is still a need to assess the utility of integrating deep Machine learning geospatial technologies and multi-source data in mapping and monitoring grass ecophysiological attributes such as the canopy chlorophyll content and crops' structural attributes.
- The varying pixel size and radiometric resolutions of different earth observation sensors utilised in this project could have an impact on the accuracy estimates obtained in modelling grass productivity and water-related ecosystem services elements. In this regard, future research still needs to test and compare the utility of various sensors including the newly launched Landsat-9 OLI-2 and, EnMAP.
- Research efforts should also be exerted towards understanding the general distribution, productivity, water-related ecosystem services and forage quality attributes of specifically the sourveld and sweetveld grasses in uMngeni catchment to improve and inform the sustainable utilisation of communal grasslands.
- There is a need for advancing the theoretical and practical knowledge of machine learning techniques in assisting decision-making in both small-scale and large-scale grassland ecosystems.

- There is still an urgent need to increase research efforts on rangeland management strategies that can be implemented in the communal areas to create awareness on the vital importance of protecting these ecosystems. Future studies could also assess the impact of activities such as livestock production and grazing intensity/patterns as well as fire administration in the communal areas as individual agents impacting on the quality and quantity rangelands.

ACKNOWLEDGMENTS

The research presented here was a component of an unsolicited project initiated, funded, and overseen by the Water Research Commission (WRC) in the Key Strategic of Water Utilisation in Agriculture. The project team expresses their sincere gratitude to the WRC for their funding and project management. The project team also wishes to sincerely thank the following members of the Reference Group for their valuable contributions and guidance:

Prof. S Mpandeli	:	Water Research Commission (Chairman)
Dr L Nhamo	:	Water Research Commission
Dr S Hlophe-Ginindza	:	Water Research Commission
Prof. A Ramoelo	:	University of Pretoria
Dr E Mashimbye	:	Stellenbosch University
Dr O Gwate	:	University of Free State
Mr T Mudau	:	Agricultural Research Council
Ms A Mshengu	:	(Committee Secretary)

We would also like to thank the following individuals:

- South African Research Chair (SARChI) in Landuse management in the School of Agricultural, Earth & Environmental Science, Discipline of Geography, University of KwaZulu-Natal, for logistical support and leverage funding.
- The uMgeni Resilience Project, funded by the Adaptation Fund, for supporting part of the fieldwork as part of building the resilience of smallholder farmers to climate change.
- The postgraduate students who participated in the project: A Masenyama, X Zuma, and M Vawda.
- The administrative staff from the Centre for Transformative Agricultural and Food Systems (CTAFS) and the Centre for Water Resources Research for supporting the project.
- The community members from Swayimane for allowing the field trials to be conducted on their land.
- The many stakeholders whose contributions laid the groundwork for the data used in the report.

Table of Contents

EXECUTIVE SUMMARY	iii
ACKNOWLEDGMENTS.....	xii
Table of Contents.....	xiii
List of Figures	xx
List of Tables	xxiv
LIST OF ACRONYMS AND ABBREVIATIONS	xxvi
REPOSITORY OF DATA.....	xxvii
1. Introduction and Project Overview	1
1.1. Background and Rationale.....	1
1.2. Project aims and objectives.	3
1.2.1. Specific objectives	3
1.3. Scope and the Overview of the Report.....	4
2. Remote Sensing Grassland Productivity Attributes: A Systematic Review	7
2.1. Introduction	7
2.2. Materials and Methods.....	8
2.3. Results.....	12
2.3.1. Searched Literature Traits: Published Trends	12
2.3.2. Keyword Analysis	13
2.3.3. Geographic Patterns	14
2.3.4. Remote-Sensing Sensor Technologies in Mapping Grassland Productivity (Paying Particular Attention to Prediction Accuracies).....	16
2.3.5. Utility of Vegetation Indices as Proxy for Estimating Grassland Productivity ..	21

2.3.6.	Algorithms Used for Grassland Productivity Using Remote Sensing	24
2.4.	Discussion	26
2.4.1.	Algorithms Used for Grassland Productivity Using Remote Sensing	26
2.4.2.	State-of-the-Art Approaches for Improving GP Monitoring Using Remote-Sensing Techniques	28
2.4.3.	Limitations and Future Expectations on Applications and Sensors.....	29
2.5.	Conclusions	31
3.	A systematic review on the application of remote sensing technologies in grasslands ecosystem services.....	32
3.1.	Introduction.....	32
3.2.	Materials and Methods.....	34
3.2.1.	Literature search, inclusion, and exclusion strategy	34
3.2.2.	Data Extraction	36
3.2.3.	Data analysis	36
3.3.	Results.....	38
3.3.1.	Literature search characteristics	38
3.3.2.	Progress in the use of remote sensing technologies to monitor grasslands ecosystem services.....	40
3.3.2.1.	Grassland ecosystem services identified in literature.....	40
3.3.2.2.	Geographic distribution and publication trends.....	41
3.3.2.3.	Sensor technologies, spectral settings, and derived vegetation indices	43
3.3.2.4.	The role of remote sensing prediction and modelling algorithms in grassland ecosystem services.....	47
3.4.	Discussion	50

3.4.1.	Progress in remote sensing of grassland ecosystem services	50
3.4.1.1.	Geographic distribution and publication trends.....	50
3.4.1.2.	Earth observation sensors	50
3.4.1.3.	Spectral features (wavebands and vegetation indices)	51
3.4.1.4.	Prediction, modelling and classification algorithms.....	52
3.4.2.	Remote sensing of biomass, LAI, and CSC to characterize water-related grassland ecosystem services	53
3.4.3.	Limitation of the study	55
3.4.4.	Research gaps and opportunities.....	55
3.5.	Conclusion	57
	Chapter 3 Appendix.....	58
4.	Land use land cover changes in a typical communal area in Southern Africa	61
4.1.	Introduction	61
4.2.	Methods and Materials.....	63
4.2.1.	Study Site	63
4.2.2.	Satellite Data	65
4.2.3.	Classification and Change Detection	65
4.2.4.	Rate of Change.....	67
4.3.	Results.....	69
4.3.1.	Classifications.....	69
4.3.2.	Changes in the Spatial Extent of Rangelands	73
4.3.3.	Patch Analysis at Class Level Metric	75
4.4.	Discussion	76

4.5.	Conclusion.....	79
5.	Assessing current and future dynamics of landcover using the CA-Markov model in typical communal rangelands Southern Africa	80
5.1.	Introduction.....	80
5.2.	Methods and Materials.....	82
5.2.1.	Study Site	82
5.2.2.	Satellite Data	82
5.2.3.	Projections.....	84
5.2.4.	CA-Markov.....	86
5.2.5.	Accuracy assessment.....	86
5.2.6.	Rangeland Patch Analysis for the projected year 2040	87
5.3.	Results.....	88
5.3.1.	Image Classifications	88
5.3.2.	Validation Results	89
5.3.3.	Projections.....	90
5.3.4.	Rangeland Patch Analysis 2020 and 2040 comparison	96
5.4.	Discussion	97
5.5.	Conclusion.....	100
6.	Comparing the utility of Artificial Neural Networks (ANN) and Convolutional Neural Networks (CNN) in tandem with Sentinel-2 MSI in estimating dry season aboveground grass biomass.....	101
6.1.	Introduction.....	101
6.2.	Methods.....	103

6.2.1.	Study Area.....	103
6.2.2.	Sentinel 2 MSI satellite imagery.....	105
6.2.3.	Field data collection and measurements.....	105
6.2.4.	Sentinel 2 spectral bands and variables.....	106
6.2.5.	Statistical analysis and machine learning.....	109
6.3.	Results.....	112
6.3.1.	Descriptive Statistics.....	112
6.3.2.	Comparison of the performance of ANN and CNN.....	112
6.4.	Discussion.....	115
6.5.	Conclusion.....	121
7.	Predicting inter-seasonal grass biomass utilising satellite remote sensing in the Vulindlela area of the Umgeni catchment, KwaZulu-Natal.....	122
7.1.	Introduction.....	122
7.2.	Methods.....	125
7.2.1.	Study Area.....	125
7.2.2.	Sentinel 2 MSI satellite imagery.....	126
7.2.3.	Field data collection and measurements.....	126
7.2.4.	Sentinel 2 spectral bands and variables.....	127
7.2.5.	Statistical analysis and machine learning.....	130
7.2.6.	Accuracy Assessment.....	132
7.3.	Results.....	133
7.3.1.	Descriptive Statistics.....	133
7.3.2.	CNN Training History.....	134

7.3.3.	Dry season vs Wet season	135
7.3.4.	Sensitivity Analysis	136
7.4.	Discussion	137
7.5.	Conclusion	143
8.	Inter-seasonal estimation of grass water content indicators using multisource remotely sensed data metrics and cloud-computing Google Earth Engine platform.....	145
8.1.	Introduction	145
8.2.	Materials and methods.....	148
8.2.1.	Spatial analyses.....	155
8.2.2.	Accuracy assessment	156
8.3.	Results.....	156
8.3.1.	Estimating grass water content variables using spectral and topo-climatic variables	156
8.3.2.	Comparing the optimal seasonal models of grass water content elements between the dry and the wet seasons.	159
8.3.3.	Spatial distribution of modelled grass water content variables	164
8.4.	Discussion	166
8.4.1.	Predictive performance of spectral and environmental variables in determining grass water content indicators	166
8.4.2.	Comparing predictor variables for estimating grass water content indicators	167
8.4.3.	Relevance of the study	169
8.5.	Conclusion	169
9.	General discussion, conclusions and recommendations	171
9.1.	General Discussion.....	171

9.2. Limitations of The Study.....	174
9.3. Conclusion.....	175
9.4. Recommendations.....	176
REFERENCES	178
APPENDICES.....	218
Appendix A: List of Publications.....	218
Appendix B: List of Conferences Presentations	219
Appendix C: Keynote Addresses	219
Appendix D: Policy Briefs & Reports.....	219
Appendix E: Policy Briefs & Reports.....	219
Appendix F: Workshops	220
Appendix G: List of Post Doctoral Fellows and Graduated Students.....	220

List of Figures

Figure 2.1: Steps followed for the articles considered in this review.	11
Figure 2.2: Evolution in the time of the published articles that used remotely sensed data for GP monitoring.	12
Figure 2.3: Evolution of key terms in estimating grassland productivity using remote sensing, based on the data derived from the abstracts and titles of the selected literature.	14
Figure 2.4: Global distribution of studies (from 1975 to 2021) that used remote sensing data to estimate grassland productivity.	15
Figure 2.5: Frequency of studies conducted at different spatial scales (i.e. the extent of the study areas).	15
Figure 2.6: Popularly used remote-sensing sensors used in GP monitoring. WV = WorldView, S-1 = Sentinel-1, S-2 = Sentinel-2, OLI = Operational Land Imager, ETM = Enhanced Thematic Mapper, and MSS = Multi-Spectral Scanner.	16
Figure 2.7: Temporal development of the remote-sensing systems used to analyze GP for the period between 1986 and the end of 2021.	17
Figure 2.8: Overall accuracies of the various sensors used in monitoring grassland vegetation attributes.	18
Figure 3.1: PRISMA flow diagram for selection of studies considered in the review.	35
Figure 3.2: Topical concepts in grasslands ecosystem services studies derived using data from titles, abstract and keywords.	39
Figure 3.3: The number of studies that utilized remote sensing to assess grasslands ecosystem services. Studies with multi-ecosystem services were counted several times. ..	41
Figure 3.4: Spatial distribution of remote sensing studies in the context of grassland ecosystem services. Studies conducted at regional and global scales are not shown.	42
Figure 3.5: Frequency of studies published on remote sensing applications in grassland ecosystem services.	43

Figure 3.6: Frequency of studies that utilized a specific sensor system within reviewed studies. Studies with multi-sensors were counted several times.	44
Figure 3.7: Progression of Earth observation sensors used within the reviewed studies between December 1983 and September 2021.	45
Figure 3.8: Box plots showing average correlation coefficients values for Earth observation sensors used in the ecosystem services studies. Sensors utilized in less than three studies are excluded.	45
Figure 3.9: Box plots showing average coefficient of determination (R^2) values produced by remote sensing algorithms applied in the studies. Numbers in italics represent the number of times an algorithm was utilized. (a) CASA= Carnegie-Ames-Stanford Approach; LUE= light use efficiency; PROSAIL= prospect + sail, (b) ANN= artificial neural networks; RF= random forest; SVM= support vector machines, (c) DA= discriminant analysis; ER= exponential regression; LR= linear regression; MLR= multiple linear regression; OLSR= ordinary least square regression; PLSR= partial least square regression; PR= power regression; SPLSR= sparse partial least square regression.....	49
Figure 4.1: Inhlazuka and Vulindlela communal areas In Pietermaritzburg, KwaZulu-Natal South Africa.	64
Figure 4.2: Typical communal rangeland areas in a) Vulindlela and b) Inhlazuka.....	65
Figure 4.3: Classification overall accuracies and kappa scores in the areas of a) Vulindlela and b) Inhlazuka	69
Figure 4.4: Variable importance scores from the image classifications in Vulindlela for the year a) 2000, b) 2010, and c) 2020 as well as Nhlazuka for the year d) 2000, e) 2010, and f) 2020. (NDWI = normalised difference water index, EVI = enhanced vegetation index, GNDVI = green normalised vegetation index, SAVI = soil adjusted vegetation index, RVI = ratio vegetation index, NDVI = normalised vegetation index, DVI = difference vegetation index, IPVI = Integrated Polarization Vegetation Index, and VARI = Visible Atmospherically Resistant Index)	71
Figure 4.5: Changes in the mapped land cover types in a) Vulindlela and b) Inhlazuka	72
Figure 4.6: Spatial distribution of grasslands in a) Vulindlela and b) Inhlazuka from 2000 to 2020.....	74

Figure 4.7: Changes in the rangeland spatial extent from 2000 to 2020 in Vulindlela and Inhlazuka.	75
Figure 5.1: The already classified images of land use land cover changes in a) Vulindlela and b) Inhlazuka during the years 2010 and 2022.....	85
Figure 5.2: A flow chart of the simulation process.	87
Figure 5.3: Classification overall accuracies and kappa scores in the areas of a) Vulindlela and b) Nhlazuka.....	89
Figure 5.4: Prediction images of 2020 for a) Inhlazuka and b) Vulindlela	90
Figure 5.5: The projected changes in a) Vulindlela and b) Inhlazuka for the year 2040.....	92
Figure 5.6: A comparison in the rangeland distribution between 2020 and 2040 in (a) Vulindlela and (b) iNhlazuka.....	93
Figure 5.7: The changes in the distribution of rangelands between 2020 and 2040 in (a) Vulindlela and (b) iNhlazuka.....	94
Figure 5.8: (a, b and c) is presenting the gains and losses of each feature class and the Net changes in grasslands in Vulindlela between the years 2010 and 2010 and (d, e and f,) presenting the grassland changes in Inhlazuka, respectively.	95
Figure 5.9: The areal difference in the land cover types between 2020 and 2040 in the areas of a) Vulindlela and b) Nhlazuka	96
Figure 6.1: Location of Vulindlela area relative to South Africa and KZN.....	104
Figure 6.2: (a) <i>Aristida junciformis</i> dominated grassland and (b) typical grassland within the study area during the dry season.	106
Figure 6.3: The general architecture of an ANN	109
Figure 6.4: The general architecture of a CNN	110
Figure 6.5: Number of epochs for each model. The arrows indicate that for the CNN and ANN models the number of epochs that gave the lowest error was 30 and 50, respectively.	112

Figure 6.6: Scatterplots showing biomass over the dry season for a. ANN and b. CNN. ...	113
Figure 6.7: Biomass (g/m^2) over the dry season for (a). ANN and (b). CNN	114
Figure 6.8: Ranking the importance of variables for developing the a. ANN and b. CNN models for biomass detection.....	115
Figure 7.1: Images of the study area (a) during the wet season (b) in the context of grazing, (c and d). during the dry season (March 2022).....	127
Figure 7.2: A general structure of a CNN.	131
Figure 7.3: Number of epochs for each model. The arrows indicate that for the CNN-Dry and CNN-Wet models the number of epochs that gave the lowest error was both 30.	134
Figure 7.4: Scatterplots showing observed and predicted biomass over the a. dry season and b. wet season using CNN.	135
Figure 7.5: Predicted biomass (g/m^2) over the a. dry and b. wet season using CNN.	136
Figure 7.6: Ranking the importance of variables for developing the CNN model for biomass detection in the (a) dry season and (b) wet season.	137
Figure 7.7: Total monthly rainfall in Vulindlela during the (a) dry season and (b) wet season (Data provided by South African Weather Services).....	138
Figure 7.8: Average maximum daily temperature in Vulindlela over the a. dry season and b. wet season (Data provided by South African Weather Services).....	139
Figure 8.1: Location of the study area	149
Figure 8.2: Relationship between observed and predicted grass LAI (a and b), CSC (c and d), CWC (e and f) and EWT (g and h) derived using optimally selected predictor variables for the wet and dry seasons respectively.....	161
Figure 8.3: Variable importance scores of selected variables in estimating (a and b) LAI, (c and d) CSC, (e and f) CWC and (g and h) EWT for the wet season and dry seasons respectively	163
Figure 8.4: Spatial distribution of modelled LAI (<i>a and b</i>), CSC (<i>c and d</i>), CWC (<i>e and f</i>) and EWT (<i>g and h</i>) for the wet and dry seasons respectively.....	165

List of Tables

Table 2.1: Key terms utilized in the literature search.	10
Table 2.2: Characteristics of the most frequently used sensors.....	19
Table 2.3: Available algorithms for grass productivity prediction using remotely sensed data.	25
Table 3.1: Non-exhaustive grassland-related ecosystem services classification based on Millennium Ecosystem Assessment as explained in Leemans and De Groot (2003).	37
Table 3.2: Summary of the commonly used vegetation indices in grassland ecosystem services studies.	47
Table 3.3: Additional remote sensing algorithms applied in the studies.	58
Table 4.1: Class level Fragmentation Metrics and their descriptions	67
Table 4.2: Vulindlela and Inhlazuka grassland patch metrics variations between 2000 and 2020.....	76
Table 5.1: Image collections used in the study.....	83
Table 5.2: The kappa coefficient scores for quantity and location for the year 2020 prediction.	89
Table 5.3: The kappa coefficient scores for quantity and location for the 2040 prediction. ..	91
Table 5.4: Rangeland Patch Analysis of the year 2020 and 2040	97
Table 6.1: Sentinel 2B spectral bands (https://eos.com/find-satellite/sentinel-2/).....	107
Table 6.2: Various vegetation indices (VIs) used in this study.....	107
Table 6.3: Hyper-parameters used to train the ANN and CNN models.....	110
Table 6.4: Descriptive statistics of the observed biomass (g/m ²) over the dry season	112
Table 7.1: Vegetation indices used in this study derived from Sentinel 2 spectral data.	128
Table 7.2: Hyper-parameters used to train the CNN model.....	132

Table 7.3: Descriptive statistics of the observed biomass (g/m ²) over the wet and dry season	134
Table 8.1: Spectral vegetation indices used in this study.	153
Table 8.2: Topographic variables used in this study as explained in Odebiri, Mutanga et al. (2020).	154
Table 8.3: Estimation accuracies of LAI, CSC, CWC, and EWT derived using spectral data and topo-climatic variables.....	158

LIST OF ACRONYMS AND ABBREVIATIONS

AGB	Above-Ground Biomass
ANN	Artificial Neural Networks
CSC	Canopy Storage Capacity
ETM+	Thematic Mapper Plus
GDP	Gross Domestic Products
GIS	Geographic information systems
LAI	leaf area index
MSI	Multispectral instrument
NIR	Near Infrared
OLI	Operational Land Imager
RF	Random forest
SVM	Support Vector Machines
SWIR	Shortwave Infrared
TIRS	Thermal Infrared Sensor
TM	Thematic Mapper
VI(s)	Vegetation Index (Indices)
WRC	Water Research Commission

REPOSITORY OF DATA

For details related to the project's data, please contact:

South African Research Chair (SARChI) in Landuse management
Discipline of Geography and Environmental Science
School of Agricultural, Earth and Environmental Sciences
University of KwaZulu-Natal
P Bag X0,1 Scottsville 3209
Pietermaritzburg, South Africa
Email: Mutangao@ukzn.ac.za

This page was intentionally left blank

1. Introduction and Project Overview

M Sibanda, O Mutanga, T Bangira, T Mabhaudhi, T Dube, and R Lottering

1.1. Background and Rationale

Grasslands provide various forms of ecosystem services at local, regional, and global scales. Other than offering agricultural services (i.e. fodder to livestock, and food), grasslands have a critical water regulatory role in the hydrological cycle by regulating interception, percolation and stream flows (Bengtsson, Bullock et al. 2019). Grasslands also play a significant role in soil erosion control, carbon sequestration and anthropogenic regulatory activities, including biological control.

Meanwhile, grasslands support economic activities, such as smallholder and commercial livestock production systems and tourism activities. In southern Africa, these grassland services have been reported to be significant in raising the income per capita of rural communities. In South Africa, grasslands had a total economic value of R9.7 billion in 2006, which includes a consumptive value of R1.59 million as well as an indirect value of about R8 million (De Witt and Blignaut 2006). Despite the ecological and socio-economic importance of grasslands, they are characterized by perpetual conflicts between conservation endeavours and anthropogenic activities such as agriculture (Franke, Keuck et al. 2012).

However, much of the grasslands are showing signs of degradation and more recently, the ecosystem has declined significantly in size (FAO 2010). In South Africa, the grasslands are among the most threatened biomes yet they are the third-largest biome covering about 336,544 km² (de Wit, Blignaut et al. 2006, Egoh, Reyers et al. 2011). Specifically, 35% of the change in size of grasslands has been mainly due to competition from other land uses such as crop production and human settlements. Degradation has been linked mostly to agriculture, overgrazing, invasive alien plants, droughts and climatic change (Egoh, Reyers et al. 2011). Even though climate change is associated with uncertainties with regard to the extent and magnitude of changes in conditions that could occur, literature predicts that grasslands and livestock farming will be adversely affected (Rust and Rust 2013). An understanding of changes in the productivity of grassland ecosystems will provide insights into how the hydrological system is altered through variations of available biomass across space and time. This will in turn assist water resource managers and communities to prioritise hot spot areas for intervention and restoration. This will also improve the management of grazing resources

pertinent to the livelihoods of the disadvantaged communal smallholder farmers rearing livestock for subsistence purposes. Productivity here refers to the amount (biomass/Leaf Area Index) and areal extent of grassland ecosystems.

From a livestock production perspective, modelling of grassland productivity provides communities and extension officers with relevant information on the amount of forage contained by the respective rangelands. This information is required in determining the optimum number of livestock to be kept on the veld without degradation. With robust predictive information on future climate variabilities and drought risk occurrences, farmers can take early decisions to reduce the population of their livestock in a systematic manner to reduce the overuse of grazing lands. The fodder bank of grass that is available during the dry season is the key determinant of the survival of livestock through the dry season.

Meanwhile, characterising the variability of biomass, leaf area index, foliar water content as well as canopy storage capacity of grass could offer an effective method of assessing grassland health. This is because, biomass, leaf area index, foliar water content and canopy storage capacity are associated with plant physiological processes like stomatal conductance, transpiration, and photosynthesis. Also, these have a significant influence on the nutrient (e.g. nitrogen) concentrations, distribution, and palatability of grasses. For example, understanding grass Canopy Storage Capacity (CSC) is critical in deriving insights into soil water reserves, particularly in grassland areas. Wietzke and Zimmermann (2014) defined CSC as the amount of water retained in the canopy, which is an important parameter in modelling interception. Various studies have illustrated that CSC plays a critical role in wall-to-wall hydrological models (Keim et al. 2006; Wietzke and Zimmermann 2014). CSC alters infiltration, spatial distribution, and timing of rainwater input to the surface. This in turn has overarching implications on surface runoff and soil water availability, as well as the general water balance within the catchment over a long period. There is therefore a need to implement spatially explicit and time-efficient methods to understand the variations in grassland resource quantity if ecosystem services are to be maintained and livelihoods sustained.

There is a paucity of spatial information on changes in the productivity of the grassland ecosystem in both space and time. Past research concentrated on specific and strategic localities, with limited spatial extents due to tedious fieldwork and lack of large spatial data and processing tools. This affected monitoring and decisions at a planetary scale.

Until recently, lack of field data, satellite data and computing technology implied that spatial data would be refreshed after a few years and hardly done in developing countries where data

availability remains a challenge. With the recent advancement in satellite data provision, as well as Big data cloud computing and storage capabilities, there is a possibility to conduct planetary-scale analysis and consistently monitor the productivity of grasslands over time.

We, therefore, propose the development of a geospatial Framework for Monitoring grassland ecosystems. For the first time, the study will monitor grasslands over broad spatial scales as well as at intra- and interannual temporal scales, informed by an understanding of the temporal relationships among measurements. The framework will provide actionable information services for grassland assessment and monitoring across different key land management areas. Specifically, the assessment and monitoring service will deliver satellite-based Earth observation spatio-temporal models that will assist users in their operational grassland management as well as policy and decision-making in the target areas.

1.2. Project aims and objectives.

1. To conduct a comprehensive and state-of-the-art literature review and potential use of remote sensing-based models for grassland productivity monitoring in the light of climate change
2. To review the importance of grasslands as an ecosystem service, particularly the contribution of leaf area index (LAI), Canopy storage capacity and Biomass in water management
3. To characterise and model communal grassland productivity status in a changing climate at sites within the uMgungundlovu District Municipality
4. To assess intra- and interannual temporal changes in grassland productivity and proportionate land use change within the catchment and explain the changes thereof.

1.2.1. Specific objectives

The above stated contractual objectives on the project were addressed by drawing the following specific objectives.

1. To review scientific peer-reviewed articles comprehensively and systematically on using remotely sensed data within the explicit theme of estimating grass productivity (GP) proxies, such as above ground biomass (AGB), leaf area index (LAI), canopy storage capacity (CSC).

2. To systematically review the progress, emerging gaps, and opportunities on the application of remote sensing technologies in quantifying grasslands ecosystem services.
3. To assess the spatiotemporal variability of rangelands within a typical southern African communal area from the year 2000 to 2020 using multi-temporal Landsat datasets in conjunction with the random forest.
4. To predict the future spatial distribution of grasslands in communal rangelands using the CA-Markov model between the year 2020 and 2040. The project also compared the magnitude of grass fragmentation in the forthcoming 20 years since the same year intervals were considered in generating input maps for modelling.
5. To compare the predictive performance of shallow artificial neural networks (ANNs) and deep convolutional neural networks (CNNs) in estimating aboveground grass biomass using Sentinel 2 MSI during the dry season.
6. To predict inter-seasonal variations of grass biomass in using Sentinel 2 MSI remotely sensed data in conjunction with convolutional neural networks (CNNs).
7. To test the utility of multi-source data in estimating LAI, CSC, CWC, and EWT within communal grasslands across wet and dry seasons.

1.3. Scope and the Overview of the Report

This report is presented as stand-alone chapters written by different authors. Each of these chapters fully or partially addresses at least one of the project's contractual objectives based on the guidance of the WRC project managers, the technical reference group members, and the critical international peer reviewed system for some of the chapters published in peer-reviewed journals. In this regard, the general methodology chapter is not included since the report is presented in a paper format. Considering that each of the objectives or stand-alone chapters are addressing the same overarching aim, and the paper approach adopted in presenting this report, there are inevitable overlaps or repetitions, especially in the methods and materials sections within the scope of this project report. This was deemed insignificant, since all these chapters present a seamless flow of methods and principles that underpin the current scientific setting to address the same overarching aim. Furthermore, some of the chapters were adapted from articles already published in internationally peer reviewed journals. The report is structured to address all the project's contractual objectives in a logical framework.

Specifically, the chapters in this report are as follows;

Chapter 1: offers a comprehensive introduction, background, and conceptualization of the entire study. It provides rationale for the overarching study outlined in the terms of reference, outlining the project's goals and specific objectives as stipulated in the contract.

Chapter 2: is a comprehensive and state-of-the-art systematic review of the literature on the potential use of remote sensing-based models for grassland productivity monitoring in the light of climate change. This chapter directly addresses contractual objective number 1.

Chapter 3: provides a systematic review of the literature on the utility of remote sensing, with a special focus on the importance of grasslands as an ecosystem service. It delves into specific contributions of leaf area index (LAI), Canopy storage capacity, equivalent Water thickness (EWT), canopy water content (CWC) and biomass in water management. The conclusions derived from these literature reviews informed the methodology followed by the application chapters (4 to 8). The chapter addressed contractual objective number 2.

Chapters 4 to 8 addressed contractual objectives number 3 & 4.

Chapter 4: assessed the spatiotemporal variability of rangelands within a typical southern African communal area from the year 2000 to 2020 using multi-temporal Landsat datasets in conjunction with random forest. This section of the project assessed the magnitude and extent of grassland fragmentation in these communal rangelands using fragmentation statistics. This chapter partially addresses contractual objectives number 4, wherein the proportionate land use change within the catchment and the changes thereof are assessed and explained.

Chapter 5: assessed the current and future dynamics of the extent, spatial distribution and magnitude of grassland fragmentation using the CA-Markov model in conjunction with the random forest regression ensemble. This chapter also partially addresses contractual objectives number 4.

Chapter 6: presents a comparative assessment of the performance of artificial neural networks (ANN) and convolutional neural networks (CNN) in estimating dry season aboveground grass biomass using Sentinel-2 MSI remotely sensed data. The findings in this chapter suggested that CNN could optimally estimate dry season aboveground grass biomass. Subsequently, the proceeding chapter adopted deep CNN in estimating grass biomass. This chapter partially addresses contractual objectives number 3 & 4 which was to characterise AND assess intra seasonal changes in grassland productivity.

Chapter 7: predicts the inter-seasonal grass biomass using deep CNN and Sentinel-2 MSI remote data in selected wards of the uMngeni catchment in KwaZulu-Natal. Also, this chapter

partially addresses contractual objectives number 3 &4 which was to characterise AND assess interannual changes in grassland productivity. The findings of this chapter highlight the significance of precipitation and temperature as key drivers regulating changes in grassland productivity.

Chapter 8: involves the inter-seasonal estimation of grass water content indicators using multisource remotely sensed data metrics and cloud-computing google earth engine (GEE) platform. It focuses on estimating LAI, CSC, CWC, and EWT of communal grasslands using GEE random forest across wet and dry seasons, using Sentinel-2 MSI and topo-climatic variables. Additionally, this chapter partially addresses contractual objectives 3 & 4 by assessing seasonal changes in grassland productivity which in turn regulates seasonal spatial variations of the grass water-related ecosystem services.

Chapter 9: presents a comprehensive discussion of the entire project, connecting all individual studies to fulfil the project objectives. The chapter also delivers conclusions and suggestions for future research.

2. Remote Sensing Grassland Productivity Attributes: A Systematic Review

T Bangira, O Mutanga, M Sibanda, T Dube and T Mabhaudhi.

2.1. Introduction

Grasslands, covering at least one-third of the Earth's land surface, provide different ecosystem services, including carbon sequestration, biodiversity conservation, forage, and opportunities for tourism and recreation (Franke, Keuck et al. 2012, Xu and Guo 2015, Ali, Cawkwell et al. 2016, Bengtsson, Bullock et al. 2019). From a climate change perspective, grasslands, both in tropical and temperate regions, play a significant function in maintaining the carbon (C) cycle and balancing greenhouse gases (GHGs) (Jones and Donnelly 2004, Ali, Cawkwell et al. 2016). These ecosystems contribute roughly 12% of the total terrestrial carbon stocks, and any changes in their quality and quantity can potentially change their role in the C cycle (Smith, Powsoln et al. 1997, Jones and Donnelly 2004).

Over 20% of the world's grasslands appear to be threatened, and more than 7.5% of them appear to be disturbed (Yang, Hao et al. 2019). Over the past ten years, grassland degradation has been estimated to have cost the global livestock industry more than USD 7 billion. The impact on socioeconomic life is particularly alarming in underdeveloped areas, where most communities depend on grasslands for feeding livestock (Bardgett, Bullock et al. 2021). As a result, grassland degradation portrays a critical problem that has to be addressed to maximize their potential to provide ecosystem services in the future.

To accurately assess grassland ecological status, certain traits and indicators need to be investigated (Théau, Lauzier-Hudon et al. 2021). Indicators are measurable parameters that can be used to assess the current state of key ecological attributes and provide warnings about potential threats to the ecosystem (Soubry, Doan et al. 2021). Grass quantity and quality are indicators of grassland productivity (GP), management practices, and the ecological processes that affect them. The quantitative and qualitative traits of GP monitoring include aboveground biomass (AGB), yield, leaf area index (LAI), canopy storage capacity (CSC), and photosynthetic activity. Recently, RS has been widely used to acquire information on the quality and quantity of grasslands over large areas and is relatively cheaper than conventional field surveys (Mutanga, Skidmore et al. 2005, Chen, Guerschman et al. 2021). These quantitative and qualitative proxies are frequently used, equally, for GP monitoring in RS studies. As a result, these grassland output monitoring attributes and indicators are also evaluated in this context. There have been several successful studies on the prospective and capability of RS systems for GP monitoring (Reichstein, Ciais et al. 2007, Kong, Yu et al. 2019,

Guerini Filho, Kuplich et al. 2020). For example, Naidoo, van Deventer et al. (2019) utilized random forest regression models, derived from WorldView space-borne sensors (WV3), to yield the highest AGB prediction accuracies (RMSE = 169.28 g/m²). Similarly, Guerini Filho, Kuplich et al. (2020) made use of Sentinel-2 data to predict biomass in the Brazilian Pampa using a multiple linear regression analyses approach and produced high modelling accuracies ($R^2 > 0.8$). In another study, Quan, He et al. (2017) compared radiative transfer model (RTM) AGB estimation to those obtained using an exponential regression, a partial least square regression (PLSR), and artificial neural networks (ANNs). The RTM-based method (RMSE = 41.65 gm⁻²) performed better than the exponential regression (RMSE = 42.67 gm⁻²) and the ANN (RMSE = 46.26 gm⁻²). However, to date, RS-based approaches for predicting proxies for GP are still in their infancy, not used extensively, and frequently implemented with undetermined accuracy (Ramoelo, Cho et al. 2015, Palmer, Samuels et al. 2016, Liu, Atzberger et al. 2020). There is a dearth of consistent approaches, particularly for grassland ecosystems (Yu, Wu et al. 2021). Robust and transferable techniques to estimate proxies for GP are still needed. Furthermore, the introduction of new and more sophisticated sensors demonstrates that RS data will continue to contribute significantly to studies on GP estimation (Dube, Shoko et al. 2021, Yu, Yao et al. 2021, Zumo, Hashim et al. 2021).

This study presents a comprehensive systematic review of the scientific peer-reviewed articles on using remotely sensed data within the explicit theme of estimating GP proxies, such as AGB, LAI, CSC, yield, and chlorophyll content. The study presents examples from the literature that summarize the remote sensing of the GP landscape, chronicling the evolution of sensors and associated methodologies, and analysing the geographic distribution of studies at various spatial scales. In this instance, specific search terms were used to locate information on the RS platform used, the characteristics of the sensor used, the extent of the study, and the prediction accuracy of the algorithms used.

2.2. Materials and Methods

The phrases and definitions of grasslands differ from study to study, according to its scope and objectives. The tag, grasslands, is used to symbolize unidentified graminoids (Dixon, Faber-Langendoen et al. 2014) or as a broad term for different kinds of grasses (e.g. pasture lands) (Conant, Cerri et al. 2017, Wigley-Coetsee and Staver 2020). Terms such as rangelands, pasturelands, or savanna can be found in the pertinent literature (Bengtsson, Bullock et al. 2019) to represent the land use activities of grasslands, whether natural or man-made. This study assessed natural grasslands that provide regulatory and provisioning ecosystem services.

This review used a systematic approach (Gough, Oliver et al. 2017) to identify peer-reviewed articles that published original research on estimating GP proxies using RS. This review is divided into two sections to accomplish its research objectives. The initial section focuses on the growth achieved, to date, in estimating and monitoring GP using remotely sensed data. The biophysical variable parameters, sensor characteristics, sensor platforms, approaches, and suitable spectral characteristics that have been utilized to date are reported in this section. The last section highlights the recommendations and the way forward for future studies focusing on GP. The detailed literature search and analysis were conducted in four stages:

1. Stage 1: Literature search

The preliminary stage of the relevant articles search was to compile a list of all key texts, words, phrases, and terms found in search strings. These terms must appear in the article title and keywords of the abstract. The preliminary literature was searched in Google Scholar, and the few top articles were downloaded and analysed for keywords. The following texts and their alternatives were used: “grassland productivity”, “remote sensing”, “GIS”, “grassland productivity monitoring”, “above ground biomass”, “leaf area index”, “yield”, “grassland nutrients AND Remote Sensing & GIS”, “grassland productivity AND remote sensing”, “grassland productivity monitoring”, “grassland above ground biomass AND Remote sensing & GIS”, “grassland LAI and Remote sensing & GIS”, “grassland canopy storage capacity and remote sensing”, and “grassland productivity AND yield AND remote sensing & GIS.” In some searches, the word grassland was replaced with any of the following terms: prairie*, meadow*, pasture*, savanna*, veld*, steppe*, ‘old field’*, and shrub*. The inclusion/exclusion criteria were restricted to title, abstract, and keywords. Table 2.1 shows the query strings used across the databases.

The identified keywords were pasted in the SCOPUS, ScienceDirect, and the Web of Science databases to build the relevant literature database. The missing papers from Web of Science, Scopus, and ScienceDirect were located using Google Scholar. Pertinent articles were also found in the list of references of the relevant studies through a reverse reference list inspection (Gough, Oliver et al. 2017). The literature was further screened and filtered to ensure that the primary focus of the review was the RS of grassland productivity. Peer-reviewed articles published between 1975 and the end of November 2021 were considered.

2. Stage 2: Screening

Preliminary literature searches in SCOPUS, ScienceDirect, Web of Science, and Google Scholar yielded 1403, 2348, 869, and 135 studies, respectively (Figure 2.1 and Table 2.1). In preparation for screening, the abstracts and keywords from the retrieved papers were

exported to Endnote. The initial screening procedure included the removal of duplicate articles as well as those written in languages other than English. The next step involved a comprehensive examination of the articles based on the use of RS to estimate AGB, LAI, and grass nutrient and chlorophyll content as proxies of GP. Only full-length articles of the chosen abstracts were included for detailed analysis. The detailed information for each article was then captured in a spreadsheet. Two hundred and three articles were considered for the quantitative and qualitative analysis of this review.

3. Stage 3: Data retrieval

All articles retained from the preceding stage were used to comprehensively indicate the current development, gaps, problems, and strengths in using RS techniques to estimate GP. To answer the research questions of this study, the third stage extracted data from the identified articles. The data recorded included details on the year the research was conducted, the spatial extent of the study site, the sensor attributes (such as spatial, temporal, radiometric, and spectral resolution), the proxy used to estimate GP, vegetation indices used, prediction accuracies, and the algorithms used. The explicit attributes were then changed to measurable variables, in preparation for the data analysis phase. Concurrently, key bibliometric data, including author names, country, publication year, article title, and abstract, were also gathered during this stage. Missing studies not identified in previous stages were captured during this stage. Accordingly, the stage evaluated the systematic review's applicability and quality assessment stage.

Table 2.1: Key terms utilized in the literature search.

Database	Search Strings	Studies Reserved
SCOPUS	TITLE-ABS-KEY (("grassland") AND ("remote sensing") AND ("aboveground biomass")) OR ("leaf area index") OR (("grass chlorophyll content ") AND ("remote sensing")) OR (("grassland yield") AND ("remote sensing") & AND GIS)) OR (("grassland quality") AND ("remote sensing" & GIS)) OR ((grassland nitrogen) ("remote sensing" & AND GIS)) OR (("grassland canopy storage capacity") OR ("remote sensing")) OR (("grassland productivity") AND ("remote sensing" & GIS)) AND (LIMIT-TO (LANGUAGE, "English"))	1403
ScienceDirect	"grassland" OR "remote sensing" AND "grassland chlorophyll content" AND "grassland canopy water storage" OR "grassland aboveground biomass" OR "yield" OR "grassland quality" AND "Remote sensing & GIS" OR "leaf area index"	869
Web of Science	TS = (("grassland") AND ("remote sensing" OR "GIS") OR (grassland "leaf area index") OR ("canopy storage capacity") OR (grassland "aboveground biomass") OR ("grassland quality"))	2348
Google Scholar	No key terms were used. Articles from the reference list.	135
	Full-text articles assessed for eligibility	1289
	Articles	203

4. Stage 4: Data analysis

The literature that was gathered and extracted was analysed both qualitatively and quantitatively. Regarding the quantitative analysis of studies focusing on the quantification of proxies of GP, a principal statistical analysis, such as trends, progress, and future projections, was conducted. A bibliometric survey was also performed to disclose the trends of principal words and phrases in monitoring GP. In addition, this aided in identifying research hotspots, development trends, the most cited authors, most relevant publications, and most frequently utilized keywords within a research area (Pritchard 1969, Zhang, Huang et al. 2017).

VOSviewer software developed by van Eck and Waltman (2010) was used for text mining and presenting bibliometric maps of key terms used to estimate and monitor GP. The titles, keywords, and abstracts of the studies in the resultant database (203 articles) were entered into VOSviewer to investigate GP. Literature analyses can be biased but considering that only the existence and co-existence of important texts and frequency distributions were evaluated, a bias evaluation was not prepared. To avoid biased reporting, the PRISMA (<http://www.prisma-statement.org/>, accessed on Day Month Year) statement was used as a guide (Moher, Liberati et al. 2009).

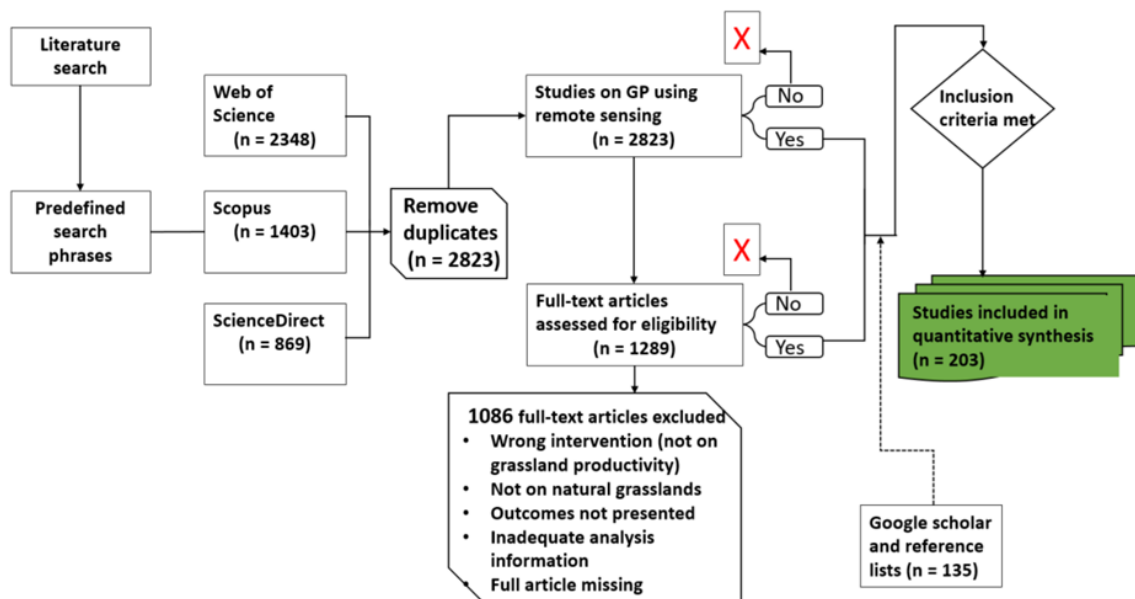


Figure 2.1: Steps followed for the articles considered in this review.

The study area of each article was evaluated in terms of country and continent. The spatial scale of the analysis was also considered. The scale of the studies was grouped into five categories, namely, local (<1000 km²), landscape (≥1000 km²), national (entire country),

regional (multiple countries), and global. If the study included multiple countries, all the countries were listed.

The detailed analysis of data usage included an extensive assessment of the different RS systems used in GP monitoring. Both microwave and optical sensors were considered in this review. These sensors can be on board either satellite, ground, or airborne platforms. The category of reference data used for the accuracy assessments was also identified.

2.3. Results

2.3.1. Searched Literature Traits: Published Trends

The first publications for GP monitoring using remote sensing were made in 1976 (Pearson, Tucker et al. 1976, Tucker, Miller et al. 1976), considering that the first Earth-observing satellite launched to monitor and study terrestrial ecosystems became functional in 1972. Since then, the number of studies has increased steadily, with a significant number of articles published by the end of 2021 (Figure 2.2). The first steady increase in publication activity occurred in the early 2000s. Between 2010 and 2018, a span of eight years, the annual publication rate increased to at least one article per month on average. The period of 2018-2020 is clearly noticeable since the publication amounts nearly doubled this period in contrast to the previous era.

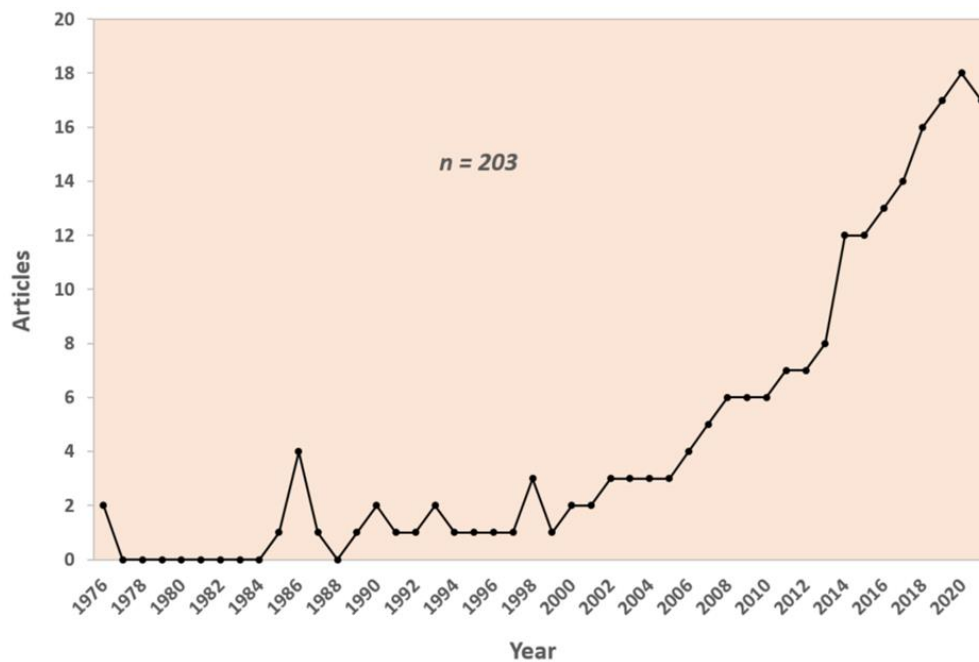


Figure 2.2: Evolution in the time of the published articles that used remotely sensed data for GP monitoring.

2.3.2. Keyword Analysis

Figure 2.3 depicts the development and direction of research based on key terms taken from the published paper titles, abstracts, and keywords used in this study. Text mining makes it possible to discover the development of the occurrence of research phrases in the analysis period. Three clusters in purple, green, and yellow across the past four decades are visible. The purple cluster has the most centralized, historical terms and is characterized by words such as “avhrr”, “ndvi”, “savi”, “wavelength”, “biophysical parameter”, “nitrogen”, and “phytomass”. The co-occurrence of the coarse resolution AVHRR sensor and regional study sites, such as China and the Tibetan Plateau, implies the preference for a coarse resolution sensor when the study area is large.

The green cluster, which covers the years from 1995 to 2005, has the terms “vegetation index”, “leaf area index (lai)”, “canopy chlorophyll content (ccc)”, “radiative transfer model (rtm)”, “MODIS”, “artificial neural network (ann)”, “vegetation index”, “landsat”, “red-edge”, “quality”, and “quantity”. The studies conducted during this period were more based on the indicators of forage quantity (e.g. AGB and LAI) (Friedl, Michaelsen et al. 1994, Lamb, Steyn-Ross et al. 2002, Samimi and Kraus 2004) rather than quality (canopy chlorophyll content and nutrients) parameters.

The yellow cluster showed “sentinel”, “operational land imager (oli)”, “machine learning regression (mlr)”, “random forest regression (rfr)”, “worldview”, “unmanned aerial vehicle (uav)”, and “PLSR”. This indicates a noticeable shift from conventional classification techniques to more robust MLAs, such as the partial least squares regression (PLSR) and random forest (RF) ensembles, in predicting proxies of GP. The trend in the sensors illustrates the peak in the utilization of AVHRR and MODIS in the historical studies published before 2015. This trend shifted towards the recently launched Landsat-8 OLI (launched February 2013) and Sentinel-2 (S-2) MSI (launched June 2015) instruments associated with improvements in estimation algorithms.

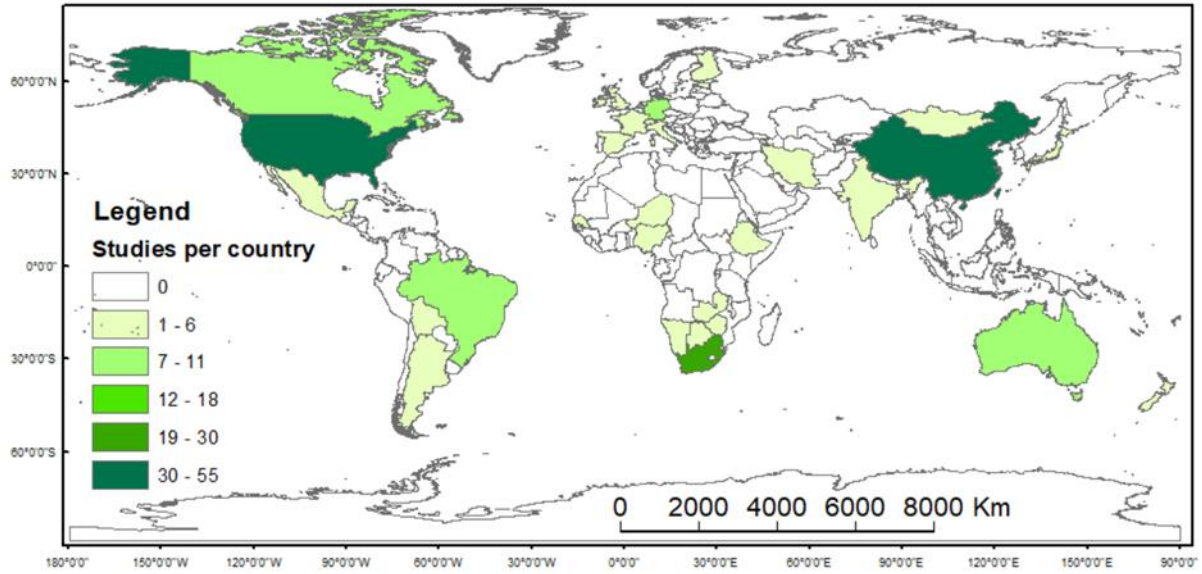


Figure 2.4: Global distribution of studies (from 1975 to 2021) that used remote sensing data to estimate grassland productivity.

Based on the articles considered in this study, it was observed that most research using RS techniques in GP was mostly conducted at the local scale (Figure 2.5). The least number of articles were those conducting analyses at the regional and landscape scales. While studies at the global and national scales do not demonstrate a trend, the overall number of landscape- and regional-scale articles has gradually increased over the temporal window examined in this research.

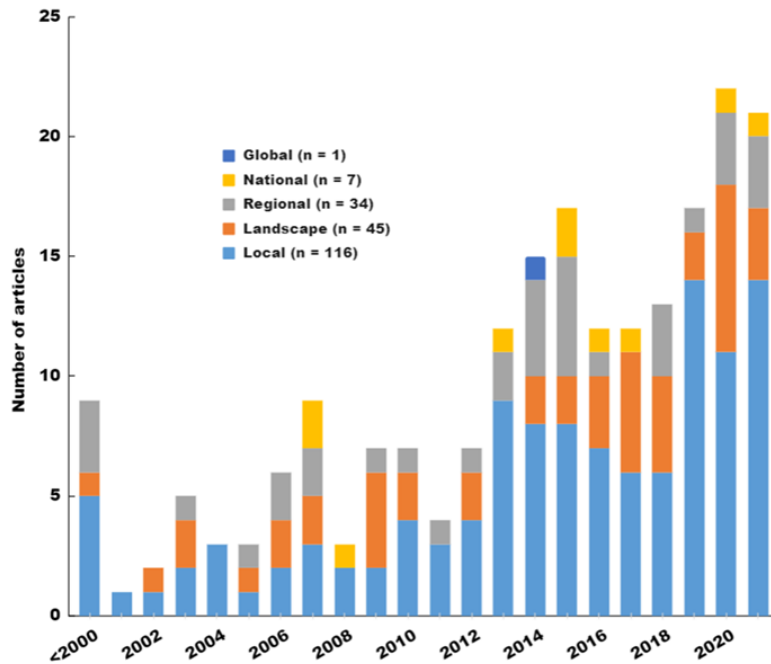


Figure 2.5: Frequency of studies conducted at different spatial scales (i.e. the extent of the study areas).

2.3.4. Remote-Sensing Sensor Technologies in Mapping Grassland Productivity (Paying Particular Attention to Prediction Accuracies)

Currently, various RS platforms with various image acquisition features are used for short-term and long-term GP monitoring. Although some studies used ground-based readings (such as the LI-COR LAI-2000 Plant Canopy Analyzer and MSR5 field-portable radiometer) and airborne sensors (such as the ASPIS sensor and HyMap hyperspectral), satellite-borne sensors account for the majority of the RS data used (Figure 2.6). The most widely used sensors are Landsat-8 (OLI), AVHRR, MODIS, SPOT, and the S-2.

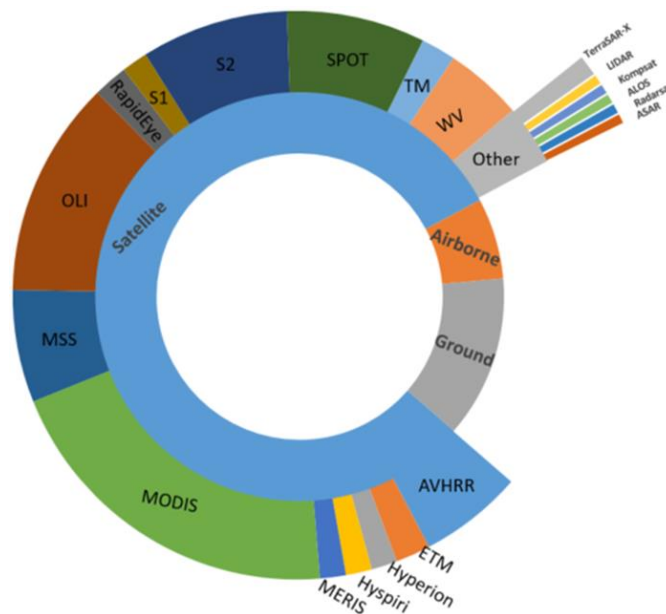


Figure 2.6: Popularly used remote-sensing sensors used in GP monitoring. WV = WorldView, S-1 = Sentinel-1, S-2 = Sentinel-2, OLI = Operational Land Imager, ETM = Enhanced Thematic Mapper, and MSS = Multi-Spectral Scanner.

The characteristics of the most frequently used satellite sensors are shown in Table 2.2. There is a sharp increase in the number of studies estimating GP using satellite-borne remotely sensed data. This is supported by the recent launch of new multispectral satellite sensors, such as the S-2 and Landsat-8, which can systematically acquire imagery at a high spatial resolution at no cost. However, few studies have used airborne data for estimating grassland productivity. As revealed in the literature analysis, Figure 2.7 shows that the few studies using radar data for grassland productivity monitoring only picked up in 2019 after the launch of S-1.

The MODIS sensor was the most frequently used sensor, accounting for nearly 30% of all the studies, followed by Landsat 1-8 series data (23%) (Figures 2.6 and 2.7). The increasing availability of low-cost and free satellite data with moderate-coarse (100-1000 m) and

moderate (10-100 m) spatial resolutions means that these are the most frequently exploited data sources for GP algorithms in the 21st century. The dominant image spatial resolutions in GP algorithms are 10 m, 30 m, and 250 m, which correlate to the S-2, Landsat series, and MODIS data. The superiority of MODIS data is explained by its frequent revisit time and large pixel size, which is computationally inexpensive for large-scale studies.

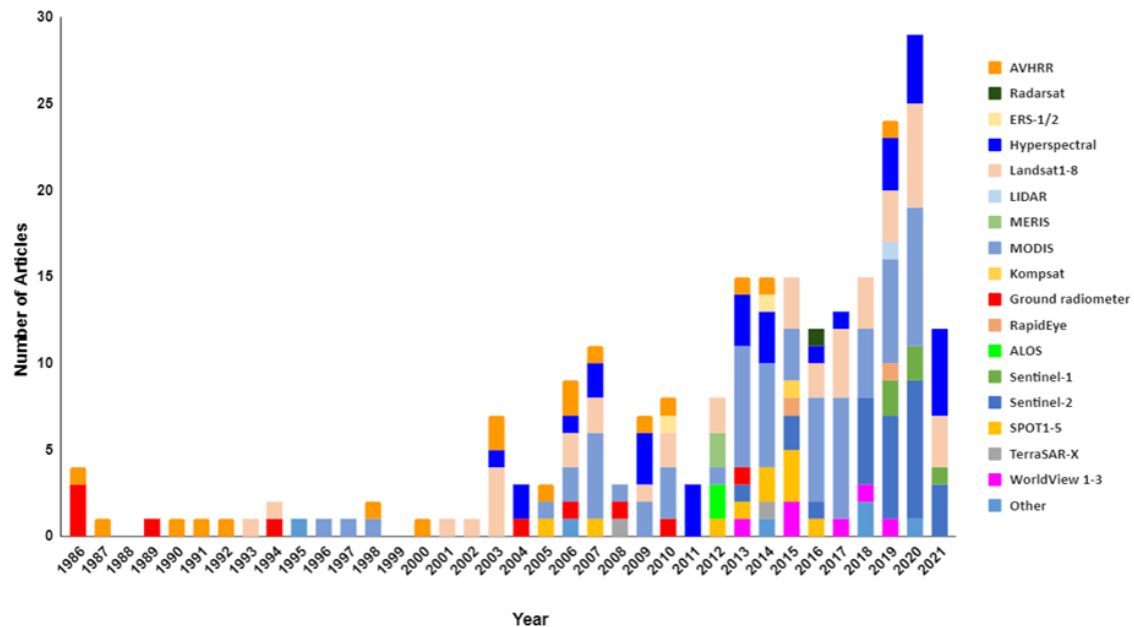


Figure 2.7: Temporal development of the remote-sensing systems used to analyse GP for the period between 1986 and the end of 2021.

Although RS provides a profitable instrument for GP, the sensor characteristics (i.e. spectral, spatial, and temporal resolution) influence the exact retrieval of spectral reflectance observations, playing an important role in GP monitoring (Gupta, Vijayan et al. 2003, Mutanga, Adam et al. 2012, Dube, Mutanga et al. 2016). For instance, Bédard, Crump et al. (2006) highlighted that different sensors exhibit unique characteristics over time and space, which affect the spectral reflectance observed by the sensor. The fine spectral resolution allows discrimination between grass and other land covers to estimate GP accurately. In addition, the phenology of the plants determines the temporal variability of their productivity (Shoko, Mutanga et al. 2016), which can be clearly mapped by sensors with a short revisit time. Matongera, Mutanga et al. (2021) stated that, at distinct phenological stages, grasses show variations in their productivity and water storage for the entire growing season, affecting the quantity and quality of biophysical proxies for evaluating and monitoring GP. Considering the sensor characteristics and phenology of grass species, this review found that most studies used coarse to medium spatial resolution data with high temporal resolutions. This is supported by the studies of Xu, Yang et al. (2008) and Zhang, Zhang et al. (2019), which

highlighted that significant changes in GP need frequent, repeated monitoring to be noticeable.

Figure 2.8 shows the overall accuracies of the sensors that appeared in five or more studies for estimating grassland vegetation attributes. In general, the sensors show a diverse range of median overall accuracies. Hyperspectral sensors, spectra radiometers, WorldView, and S-2, have the highest median overall accuracies. The sensors with the lowest median overall accuracies include MODIS and SPOT. MODIS, Hyperspectral, S-2, and AVHRR delivered the greatest range of results, while RapidEye and WorldView provided the smallest range.

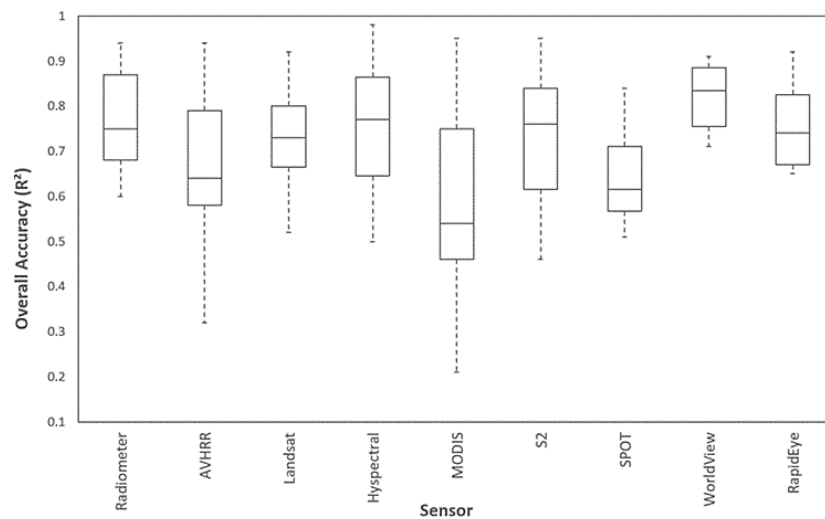


Figure 2.8: Overall accuracies of the various sensors used in monitoring grassland vegetation attributes.

The Landsat and MODIS satellites have imaged Earth’s terrestrial surfaces for over forty and twenty years, respectively. This explains the extensive number of studies utilizing these datasets in estimating the proxies of GP. Extended temporal monitoring also increases the efficacy of GP and the exploration of appropriate management practices, which increases productivity (Atzberger, Klisch et al. 2014). For instance, Wang, Gamon et al. (2020) used MODIS data to determine the annual grassland productivity of North American grassland in the period from 2000 to 2010, covering a decade, whereas Zhang, Lal et al. (2016) covered a period of five (2004-2008) years.

Although coarse spatial resolution sensors have a limitation of mixed pixels, this review has found that at least 90% of the studies used data with a low spatial resolution to estimate GP over regional or global scales. Higher-resolution hyperspectral sensors yield greater precision for estimating GP by producing finer details from every pixel generated in an image. The concurrent improvements in high-resolution remotely sensed data and computer hardware

and software have created an appropriate opportunity to effectively predict and map GP, regardless of the spatial and temporal extent. Thus recently, much attention has been paid to using high-resolution satellite sensors (e.g. RapidEye and WorldView-2). The study conducted by Naidoo, van Deventer et al. (2019) found that WorldView-3 produced the highest AGB estimation accuracies ($R^2 = 0.65$ and $RMSE = 170.28 \text{ g/m}^2$) when compared to S-1 ($R^2 = 0.56$ and $RMSE = 186.56$) and S-2 data ($R^2 = 0.60$ and 175.08 g/m^2) to estimate grassland AGB. On the other hand, Gao, Dong et al. (2020) found that utilising high-resolution multispectral and hyperspectral datasets has limitations mainly coupled with the saturation of the optical signal at a high biomass density, issues in pre-processing large datasets “big data”, and multi-regression and multi-collinearity problems. There are high computational costs incurred through the processing of large datasets.

Table 2.2: Characteristics of the most frequently used sensors.

Sensor	Bands	Spectral Range (nm)	Swath (km)	Pixel Size (m)	Temporal Resolution (Days)	Execution Scale
Hyperspectral *	>100	-	-	<1	User-defined	Farm
AVHRR	5	550-12,400	3000	1100	1	Regional-global
HyspIRI *	213	380-2500	600	60	19	Local-regional
	8	3000-12,000	150		5	
MERIS #	15	410-900	1150	300	3	Local to regional
Landsat TM	7	450-2350				Local to regional
ETM	8	450-2350	185	30	16	
OLI	11	430-12,510				
MODIS	36	620-14,385	2330	250, 500, 1000	1	Regional to global
RapidEye *	5	440-850	77	5	5.5	Local
Sentinel-2 MSI	13	492-1373	290	10, 20, 60	5, 10	Local to regional
SPOT	4	480-890	120	6,10, 20	26	Local to regional
SPOTVGT	1	437-1695	2200	1150	1	Regional to global
Worldview 2,3 *	8	400-2245	16.4	<1	1-1.37	Local
ALOS PALSAR *	VV, HH	L-band	70	10	14	Local
Sentinel-1	HV, VHHH, VH	C-band	250	5, 20	6, 12	Local to regional
COSMO-SkyMed *	HH	X-band	≥40	5	16	Local
TerraSAR-X *	VV, HH VH, HV	X-band	270	1	2.5	Local

Note: The sensors with * and # have expensive acquisition costs, and the mission has ended.

Although several researchers (Gao, Xu et al. 2013, Li, Huffman et al. 2013, Ardö, Tagesson et al. 2018) found strong biases caused by mixed pixels when using coarse resolution data for

the estimation of GP, this review found that a few studies (about 6%) have used hyperspectral sensors (Figure 2.6). This is mainly because such type of data is not freely available. Thus, GP techniques are focused mostly on moderate spatial resolution satellite data, such as Landsat, SPOT, and S-2. Using such sensors produced higher predictive accuracy (Figure 2.8) than MODIS and AVHRR, which have a low spatial resolution.

The deployment of SAR sensors presents a state-of-the-art opportunity for retrieving biophysical parameters regardless of the weather conditions and time of day, thus holding greater potential for GP monitoring. However, few studies (<5%) have used radar data acquired by SAR sensors for GP (Figure 2.6). The success of SAR-based GP algorithms is reliant on the sensor (e.g. microwave frequency, polarization, and incident angle) and environmental characteristics (canopy structure, topography, soil moisture, and depth) (El Hajj, Baghdadi et al. 2019).

A couple of SAR systems with different characteristics were placed in orbit during the 21st century, allowing radar RS' advancement on GP monitoring. Examples include X-band sensors, namely, TerraSAR-X with a very-small pixel size (up to 1 m) and COSMO-SkyMed, a constellation of four systems; Japanese ALOS and ALOS-2 L-band instruments; and C-band instruments on European Space Agency ASAR and S-1 sensors. Lately, systematically collected and freely available SAR datasets, such as that from the constellation of the S-1 system (Berger et al., 2012), have been unavailable. As explained in the above presentation of literature, the trends of studies based on SAR data picked up not long ago, after the launch of the S1 satellite that provides SAR data at no cost.

To date, the RS of GP using SAR data has focused on interpreting SAR backscattering observations and the polarimetric or interferometric attributes of individual or multiple scenes to estimate vegetation parameters using linear regression models (Svoray and Shoshany 2002, McNairn and Brisco 2004, Wang, Ge et al. 2013, Abdel-Hamid, Dubovyk et al. 2021). For example, Wang, Ge et al. (2013) analysed the GP with COSMO-SkyMed, ASAR, and ALOS PALSAR datasets through the linear relationship between the SAR backscattering coefficient. The analysis showed that the X-band of the COSMO-SkyMed has the highest correlation ($R^2 = 0.71$) for the spatial and seasonal vegetation biomass. In another study, Wang, Xiao et al. (2019) estimated the seasonal dynamics of LAI and AGB using S-1, OLI, and S2 data, individually and integrally. The results from that study indicated that S-1 data performed poorly ($R^2 = 0.44$) in recording the seasonal changes in biomass, but the accuracy improved when SAR data were integrated with optical data.

Regarding the seasonal GP using SAR data, Hajj, Baghdadi et al. (2014) observed a lower sensitivity at the X-band compared to the C-band between the microwave backscatter and the vegetation biophysical parameters with restricted possibilities of the X-band to predict GP. Inoue, Kurosu et al. (2002) and Gao, Niu et al. (2013) undertook studies to compare the sensitivity of individual portions of the electromagnetic spectrum to plant biomass, while Barrett, Nitze et al. (2014) demonstrated how the most accurate monitoring of grasslands could be attained with the integrated use of L- and C-bands time-series. In addition to using multiple wavelengths, different polarimetric acquisition capabilities can be exploited. For instance, Pairman, McNeill et al. (2008) utilized TerraSAR-X dual polarimetric SAR multi-images to estimate pasture biomass. In addition, using the multiple angles of Radarsat-2 quad-polarization, Buckley and Smith (2010) monitored GP for prairie grasslands. Their comparison with a single incidence angle showed better results for grassland classification.

While SAR data have many advantages, such as the ability to observe the ground even during cloudy conditions, there are also challenges related to SAR image analysis and its interpretation for estimating biophysical parameters for GP monitoring (Ali, Barrett et al. 2017). A further limitation associated with SAR imagery is the presence of speckles, which can affect observation accuracy and therefore cause a decrease in classification accuracy (Ali, Barrett et al. 2017). The backscatter signal from grasslands is governed by several variables, including the radar system, vegetation (i.e. stems and leaves), soil surface, and the biophysical parameters of the scatterers in the grass water content. Wang, Ge et al. (2013) concluded that the accuracy of SAR data in GP can be influenced by rain due to its sensitivity to water drops on leaves. To date, SAR data use in GP has remained rudimentary, except for a few studies (Chiarito, Cigna et al. 2021). Therefore, a few (<5%) studies have used these sensors. However, recently, Wang, Xiao et al. (2019) found the best performance from the integration of LS8, S1, and S2 ($R^2 = 0.76$) than the S-1 backscatter signals ($R^2 = 0.04-0.44$).

Recently, the performance of light detection and ranging (LiDAR) technique was reported in estimating grassland biophysical parameters using RS data (Jansen, Kolden et al. 2019, Zhang, Bao et al. 2021). Meanwhile, Zhang, Bao et al. (2021) found that the ground-measured biomass was correlated ($R^2 = 0.54$) with LiDAR estimates.

2.3.5. Utility of Vegetation Indices as Proxy for Estimating Grassland Productivity

An important and widely studied method of GP prediction is the use of RS-derived vegetation indices (VI) in conjunction with in-situ observations (Anderson, Hanson et al. 1993, Piao, Mohammad et al. 2006, Gu, Wylie et al. 2013). Most VIs uses the red, red-edge, and near-infrared wavelengths (Piao, Mohammad et al. 2006, Clevers and Gitelson 2013, Guerini Filho,

Kuplich et al. 2020). Over 80% of the studies tested the utility of NDVI in estimating grassland productivity. NDVI is influenced by the soil background signature and is associated with saturation problems at high LAI (Mutanga and Skidmore 2004, Liu, Huang et al. 2007, Nestola, Calfapietra et al. 2016). This has meant that more studies have incorporated the modified version of NDVI and other red-edge-based vegetation indices to address saturation issues (Mutanga and Skidmore 2004, Vescovo, Wohlfahrt et al. 2012, Wang, Liu et al. 2018). According to Mutanga and Skidmore (2004), the integration of narrow bands in the shorter wavelengths of the red edge (700-750 nm) and longer wavelengths of the red edge (750-780 nm) produce higher correlations (average $R^2 = 0.77$ for the top 20 NDVI values) with grass biomass than the standard NDVI alone.

The second most used VI for estimating grassland productivity is the enhanced vegetation index (EVI), which was formulated to improve biomass estimation in areas with elevated biomass by eliminating the canopy background signal and depletion in atmospheric influences (Yang, Fang et al. 2009, Meshesha, Ahmed et al. 2020, Villoslada Peciña, Bergamo et al. 2021). EVI uses the blue band, which is absent in most sensors. This drawback has resulted in the development of the two-band EVI_2 for sensors such as the AVHRR, which have a missing blue band (Jiang, Huete et al. 2007). The articles by Kim, Huete et al. (2010) and Jarchow, Didan et al. (2018) reported the similar performance of the EVI and EVI_2 bands when estimating grassland productivity at large scales. The earlier study's accuracy was very high for EVI ($R^2 = 0.97$) and EVI_2 ($R^2 = 0.98$). Therefore, EVI_2 can provide the continuity of the monitoring of grassland productivity across sensors with different spectral bands.

Transformed normalized difference vegetation index (TNDVI), perpendicular vegetation index (PVI), soil-adjusted vegetation index (SAVI), modified soil-adjusted vegetation index (MSAVI), transformed soil atmospherically resistant vegetation index (TSARVI), and transformed soil-adjusted vegetation index (TSAVI) is another group of modified VIs used in GP monitoring to minimize the effects of the soil on the vegetation spectral profile. The evidence from the literature has shown that the applications of this group of VIs in GP are primarily appropriate for regions with reduced grass cover, where the influence of soil brightness is high (Liu, Huang et al. 2007, Psomas, Kneubühler et al. 2011, Ullah, Si et al. 2012). For instance, Ullah, Si et al. (2012) examined natural GP in the northern Netherlands, characterized by short grass cover, and found that SAVI ($R^2 = 0.54$), TSAVI ($R^2 = 0.52$), and NDVI ($R^2 = 0.51$) have similar performances. In another interesting study conducted by Jin, Yang et al. (2014) over a large landscape (193,000 km²), the statistical analysis showed that the R^2 of NDVI, SAVI, and MSAVI were 0.686, 0.702, and 0.69, respectively.

The renormalized difference vegetation index (RDVI) is another VI widely used for GP (Liu, Huang et al. 2007, Ghorbani, Dadjou et al. 2020, Pang, Zhang et al. 2020). RDVI combines the advantages of difference vegetation index (DVI) and NDVI for low and high vegetation cover, respectively. The literature shows that RDVI is sensitive to LAI changes, making it suitable for productivity monitoring in grasslands with a high LAI (Vescovo, Wohlfahrt et al. 2012). For example, Tagesson, Ardö et al. (2017) found that RDVI ($R^2 = 0.90$) performed better than NDVI ($R^2 = 0.79$) in areas with a high LAI.

VIs based on the red edge (680-780 nm) have been proposed to minimize the impacts of the bidirectional reflectance distribution function and background noise, resulting in a better performance when estimating grassland productivity (Gupta, Vijayan et al. 2003, Sibanda, Mutanga et al. 2016, Lin, Li et al. 2019). For instance, Lin, Li et al. (2019) evaluated the efficacy of using VIs based on red-edge reflectance from S2 over a small local area to estimate grassland productivity. The results showed a high correlation ($R^2 = 0.77$). Recently, Imran, Gianelle et al. (2020) observed a strong correlation ($R^2 > 0.8$) between VIs based on the red edge and grassland LAI in a local grassland using S2 data. The major problem in using the VIs obtained from red bands is the small sensitivity to over-story vegetation conditions (Chen 1996).

Lately, advances in hyperspectral and commercial multispectral sensors have facilitated the evolution of narrowband greenness VIs, which have become the most suitable approach for assessing GP (Naidoo, van Deventer et al. 2019, Shoko, Mutanga et al. 2019). These narrowband indices can successfully discriminate discrete grass biochemical properties, such as chlorophyll.

Although VI remains the most used GP indicator, some vegetation biophysical parameters, such as LAI (Darvishzadeh, Skidmore et al. 2008, Kiala, Odindi et al. 2016, Wang, Xiao et al. 2019), the fraction of absorbed photosynthetically active radiation (FAPAR) (Lin, Li et al. 2019), canopy storage capacity (Xiong, Chen et al. 2021), canopy chlorophyll content (Darvishzadeh, Skidmore et al. 2008, Yin, He et al. 2016), and the greenness factor, have also been used to estimate productivity in grassland ecosystems. The evidence from the literature shows that these biophysical parameters provide detailed information about the grassland's physiological health, which is a very important indicator of photosynthetic potential (Darvishzadeh, Skidmore et al. 2008, Xiong, Chen et al. 2021).

Although VI regression models have been reported in the literature to have very-high accuracies in estimating biomass (Bella, Faivre et al. 2004, Xu, Yang et al. 2007), their major limitation is that these models are site-specific and cannot deal with highly non-linear and

complex patterns in the data. A major challenge in using VIs to assess GP is to minimize the influence of external factors and maximize the sensitivity of the relationship between VIs and biophysical parameters.

2.3.6. Algorithms Used for Grassland Productivity Using Remote Sensing

This study noted that the RS of GP can be performed using either physical-based (i.e. radiative transfer models (RTMs)) or empirical/statistical models (Table 2.3). Although 1-D and 3-D RTM inversion approaches have proven to be a promising way to retrieve the biophysical and biochemical variables of proxies of vegetation, such as the leaf area index (LAI), canopy water content, canopy or leaf chlorophyll content, and fuel moisture content (Darvishzadeh, Skidmore et al. 2008, Quan, He et al. 2017), this review found that only 6% of the studies used this technique for GP. RTM-based approaches have the benefit of reproducibility. These models are more general and are based on physical laws that establish explicit relationships between canopy properties and spectra. Outstanding results, with an R^2 greater than 0.7, were reported for using RTMs (Darvishzadeh, Skidmore et al. 2008, Vohland and Jarmer 2010). For example, Quan, He et al. (2017) used the PROSAILH (PROSPECT + SAILH) model and reflectance from OLI product to derive LAI and AGB in a grassland wetland. The RTM-based approach yielded a higher accuracy ($R^2 = 0.64$) than the exponential regression ($R^2 = 0.48$) and the ANN ($R^2 = 0.43$). Another example of a successful ($R^2 > 0.7$) RTM-based estimation of GP is the function of the crop growth model by Bella, Faivre et al. (2004) in France. RTM approaches, on the other hand, are computationally demanding, particularly when complex models are used. This makes retrieving biophysical variables over vast geographic areas impossible (Darvishzadeh, Skidmore et al. 2008, Darvishzadeh, Skidmore et al. 2008).

NDVI and in situ measurements of the empirical/statistical algorithms used to obtain a correlation between the spectral data or VIs with biomass are the widely used approaches in GP (Shoko, Mutanga et al. 2016, Sibanda, Mutanga et al. 2019). The empirical approach relates RS variables to in situ grass biomass via parametric or non-parametric regression models (Shoko, Mutanga et al. 2016). Linear regression, which has been used for decades, is the widely used algorithm for GP because of its simplicity and computational efficiency. However, the derived statistical relationships (R^2 ranging from 0.25 to 0.70) are considered sensor-specific, site- and sampling-conditions-dependent, and are anticipated to change in space and time (Shoko, Mutanga et al. 2016). Using MODIS-derived grass biomass, Xu, Yang et al. (2010) compared three different regression models, and the best correlation was shown by an exponential algorithm ($R^2 = 0.80$), followed by the PLSR ($R^2 = 0.79$) and linear ($R^2 = 0.67$).

Table 2.3: Available algorithms for grass productivity prediction using remotely sensed data.

Algorithm	Remote-Sensing Datasets	Performance	GP Parameter(s)	References
Linear regression	MODIS	R ² varied between 0.25 and 0.68.	AGB	(Grant, Johnson et al. 2014)
	AVHRR	R ² ranged from 0.39 to 0.47.	AGB	(Schino, Borfecchia et al. 2003)
	MERIS	R ² ranged from 0.51 to 0.72.	Nitrogen and AGB	(Ullah, Si et al. 2012)
Exponential regression PLSR PROSAILH	Landsat 8 OLI	The RTM-based algorithm yielded higher prediction values (R ² = 0.64) than the exponential regression (R ² = 0.48) and ANN (R ² = 0.43).	LAI, leaf chlorophyll content, leaf water content, and AGB	(Quan, He et al. 2017)
SML	Sentinel-2	The RMSE was 10.86 g/m ² , and the R ² accuracy was 82.84%.	AGB	(Pang, Zhang et al. 2020)
SPLSR	Sentinel-2 and HypsIRI	HypsIRI data showed higher AGB prediction accuracies (RMSE = 6.65 g/m ² , R ² = 0.69) than those from S-2 (RMSE = 6.79 g/m ² , R ² = 0.58).	AGB	(Sibanda, Mutanga et al. 2016)
PLSR	Hyperspectral	Results showed that PLSR models could retrieve LAI on hyperspectral images with accuracy values ranging from 0.81 to 0.93.	LAI	(Kiala, Odindi et al. 2017)
RF	WorldView-2	Results showed that random forest and vegetation indices achieved >89%.	Leaf nitrogen and AGB	(Ramoelo, Cho et al. 2015)
	S-2 and OLI	R ² ranges from 0.84 to 0.87.	LAI	(Li, Zhou et al. 2021)
SVM	Radarsat-2	The SVM yielded the best overall prediction (R ² = 0.98) for GP in central-north Brittany, France.	LAI	(Dusseux, Corpetti et al. 2014)
	MODIS	SVM (R ² = 0.58 and RMSE = 5.6 g/m ²).	AGB	(Zhou, Li et al. 2021)
	Hyperspectral	SVM models yielded higher accuracies (R ² = 0.90) than PLSR models (R ² = 0.87).	LAI	(Kiala, Odindi et al. 2016)
ANN	Landsat 7 ETM+	The study showed the AGB values modelled by ANN (R ² = 0.817) were not far from the observed values than MLR (R ² = 0.591).	AGB	(Xie, Sha et al. 2009)
DT	ENVISAT ASAR, ERS-2	Overall accuracies R ² ≥ 88.7% were achieved for most datasets.	AGB	(Barrett, Nitze et al. 2014)
PROSAIL	S-2	The R ² ranged from 0.22 to 0.76.	LAI, AGB, and leaf chlorophyll and water content	(Punalekar, Verhoef et al. 2018)

While parametric models can yield moderate estimates for GP, they are associated with several challenges. For instance, Verrelst, Camps-Valls et al. (2015) indicated that parametric algorithms lack proficiency in expressing the complex relationships between RS variables and grass aboveground biomass. Furthermore, researchers have noted that parametric methods

suffer from multi-collinearity, overfitting, and produce unstable predictions, when working with small sample sizes and missing values (Sibanda, Mutanga et al. 2016, Li, Xin et al. 2017).

Conversely, the new-fashioned and resilient non-parametric MLAs, including support vector machines (SVM), random forest (RF), partial least squares regression (PLSR), sparse PLSR (SPLSR), boosted regression trees (BRT), and artificial neural network (ANN), presents a robust tool for estimating GP. MLAs have been reported to be powerful, efficient, and less affected by the dimensionality of data than parametric algorithms (Ramoelo, Cho et al. 2015, Dube, Pandit et al. 2019). Furthermore, non-parametric algorithms overcome the challenges associated with using parametric algorithms, such as multi-collinearity, overfitting, handling small sample sizes, and missing values (Sibanda, Mutanga et al. 2015, Shoko, Mutanga et al. 2016). Though these algorithms are increasingly replacing parametric algorithms for GP, they are still considered rudimentary in the domain of GP (Kiala, Odindi et al. 2016, Zhang, Lal et al. 2016, Gao, Dong et al. 2020).

However, some inevitable limitations are associated with using MLAs for GP. The accuracy of the results is strongly determined by the quality of the training dataset. The existence of outliers and erroneous values in the training data may weaken the model performance (Shoko, Mutanga et al. 2016). Some MLAs, such as ANNs, are complex, computationally demanding, and require adjustments of several parametrizations, such as the kernel size (Ali, Greifeneder et al. 2015). In addition, some MLAs tend to be suitable for specific locations; hence, the models developed are not adapted to other environments, and in the case of RF, it has been documented that the algorithm tends to underestimate the high values and exaggerate the low values of AGB (Shoko, Mutanga et al. 2016). However, these issues are notable, and researchers try to minimize these limitations with precise strategies. For instance, the availability of vast datasets will aid remotely sensed data-driven models to achieve better generalization.

2.4. Discussion

2.4.1. Algorithms Used for Grassland Productivity Using Remote Sensing

As discussed in the previous sections, GP monitoring has been widely studied in the last five decades. However, many studies have been conducted in Asia, and few attempts have been made to estimate grassland AGB using RS in African and Australian grasslands, especially on indigenous grasses (Naidoo, van Deventer et al. 2019, Zhang, Chen et al. 2020). The limited number of studies in estimating grassland productivity using RS in some countries undermines the appreciation of grasslands in the carbon cycle.

Currently, there is a great demand for GP information at larger scales. Therefore, the future of regional studies for GP is invested in using RS datasets with applicable pixel sizes, spectral resolution, and repeat cycles in conjunction with algorithms, which can improve performance accuracy. The progress in satellite RS and using UAVs for collecting images at fine resolutions have revived GP monitoring (Villoslada Peciña, Bergamo et al. 2021). Grasslands play a significant role in carbon sequestration and support ecosystem services; therefore, the use of RS in GP monitoring will be uninterruptedly enhanced in the next decades as climate change mitigations increase.

Consequently, the availability of affordable and advanced sensors with a fine pixel size (e.g. RapidEye and WorldView 3), quick revisit time (e.g. Hyperspectral InfraRed Imager (HyspIRI) and the constellation of S-1A and 1B, S-2A and 2B, and S-3), fine spectral resolution (e.g. S-2 MSI), and radiometric resolution (e.g. Landsat 8 OLI) creates advanced opportunities for GP monitoring. We draw attention to the newly launched HyspIRI sensor, which has 213 spectral bands between 380 and 2500 nm, aiding the observation and characterization of exquisite contrast in grass species that are unnoticeable using broadband multispectral sensors (Shoko, Mutanga et al. 2016, Matongera, Mutanga et al. 2021). In addition, the OLI has finer spectral bands, sophisticated calibration and signal-to-noise characteristics, higher 12-bit radiometric resolution, and more advanced geometry compared to its predecessors (Roy, Kovalskyy et al. 2016). Therefore, these sensors provide greater possibilities for future studies in quantifying grassland quantity parameters (i.e. biomass, LAI, and CSC).

Studies that have used datasets acquired by new-generation sensors have shown that they have great potential to predict GP. For instance, Sibanda, Mutanga et al. (2017) and Naidoo, van Deventer et al. (2019) discovered that the WorldView-3 sensor has a special red-edge band, which has a high potential to estimate grassland productivity. In a related study, Sibanda, Mutanga et al. (2016) reported that the hyperspectral resolution of the HyspIRI imagery has a high potential to monitor grassland productivity, especially in heterogeneous environments. Given this, future research on the GP is enlightened. The advanced properties of new-generation datasets are more likely to offer an improved temporal characterization of grasslands to effectively manage grasslands and maintain ecosystem services.

Studies that have used SAR datasets have proved they have the potential for estimating proxies of GP, especially in areas where cloud cover is very high most of the time, which limits the use of optical satellite data (Dusseux, Corpetti et al. 2014, Abdel-Hamid, Dubovyk et al. 2021). Dusseux, Corpetti et al. (2014) found that the classification accuracy of SAR variables is significantly higher than those using optical data (0.98 compared to 0.81). The authors

highlighted that integrating optical and SAR remotely sensed data is of prime interest in distinguishing grass classes from other features.

The use of advanced MLAs in GP has also been successful when compared to conventional algorithms, even when using broadband multispectral sensors. Advanced MLAs improve the use of RS data to quantify GP (Li, Xin et al. 2017, Vundla, Mutanga et al. 2020). Generally, studies conducted in grassland ecosystems have reported the potential of MLAs in estimating GP (Mountrakis, Im et al. 2011, Ramoelo, Cho et al. 2015).

When satellite remotely sensed datasets are absent, it is also possible to collect remotely sensed data using UAVs to explore the potential of remotely sensed data in predicting GP (Villoslada Peciña, Bergamo et al. 2021). The resampling of hyperspectral images collected from UAVs is becoming a reliable alternative in testing the potential of available or upcoming sensors' spectral configurations, especially considering the limitations linked with hyperspectral datasets.

This study revealed that most research on estimating vegetation chlorophyll at the leaf and canopy scale has been for precision agriculture or forests, and few have been conducted for grassland ecosystems. There is a need to improve the generality and applicability of VIs for estimating GP at the leaf level. Studies at this scale can reveal key information applicable to ecosystem health, such as grass' physiological status, productivity, or phenology.

2.4.2. State-of-the-Art Approaches for Improving GP Monitoring Using Remote-Sensing Techniques

While great progress has been made in sensor development and GP monitoring approaches, several important issues for improving estimating GP – especially in complex environments (e.g. woody grasslands and grasslands with mixed grass species) such as in many places – need to be paid more attention to. Firstly, notwithstanding the extensive research on land use and land cover classification, few studies have focused on solving the issue of mixed pixels, which is relevant to the mapping of GP using coarse-spatial, high-temporal resolution imagery. There is a cut-off between studies on RS for GP in heterogeneous environments and the operationalization of remotely sensed data for grasslands application. A transformation from science-driven techniques to explicit, user-oriented approaches of RS is required for monitoring grasslands and the dynamics of grasses in heterogeneous environments.

More research is required to assess the prospects of the SAR and hyperspectral datasets, specifically those from S1 satellite and airborne (e.g. unmanned aerial vehicles (UAVs))

sensors. S-1 data sources hold much potential for GP as they are freely available, weather- and daylight-independent radar systems, have relatively high spatial resolutions and have short revisit periods. In addition, regarding the poor economic states of most countries, GP-monitoring techniques should be robust, cheap, and autonomous. When it comes to GP at the farm scale, the use of UAVs proved to be useful. Farmers can plan their pasture management methods and grazing capacity accordingly. This economically viable and easy technique will greatly improve the sustainable management of grasslands. Eventually, the compilation of robust and fruitful local-to-regional frameworks and policies to ease sustainable grassland management practices are more likely to be accomplished.

The emergence of remotely sensed datasets with a high temporal resolution has paved the way for near-real-time GP monitoring. Every day, a large number of space-borne and airborne sensors provide a considerable amount of remotely sensed data. These data are becoming an economic asset and a new important resource in estimating grassland productivity. There is, thus, a need to develop powerful data analysis techniques, such as MLAs, data fusion, multi-sensor approaches, and cloud-based storage and processing systems (e.g. Google Earth Engine) to handle large datasets.

RTM inversion algorithms have been demonstrated to be a promising way to retrieve proxies of GP. These models are more adaptable as they are based on physical laws that provide straightforward connections between canopy and LAI properties and spectra (Quan, He et al. 2017). Furthermore, these RTM-based approaches have the advantages of replicability and robustness at a large scale without the need to gather field samples. Consequently, there is a need to channel research towards using RTMs in estimating GP, especially in large areas. The recent study by Berger, Atzberger et al. (2018) proved that RTMs are computationally expensive and require high-end computers to perform quickly. This is no longer a drawback since computer technology is advancing rapidly, particularly with the advent of cloud computing platforms such as Google Earth Engine.

2.4.3. Limitations and Future Expectations on Applications and Sensors

Given the spatial and spectral variability of grass species, finding the correct dataset, with the optimal spectral and spatial resolution, remains a crucial drawback for estimating GP using RS data. Currently, GP estimates in light of climate change are required at the regional or national scale. These sensors must have the optimum spectral and spatial resolution sufficient to provide very-high spatial resolution data. However, the spatial resolution of current multispectral data products acquired in wide swaths have a low temporal resolution (10 days

at the equator with one satellite), negatively affecting the performance of techniques for explicitly estimating GP.

The available data on predicting GP over large areas have been derived using coarse spatial resolution datasets, such as MODIS (Figure 2.5). Despite having global coverage, a short revisit time, and being in operation for more than five decades, which are prerequisites for prolonged monitoring, MODIS data have a low prediction accuracy (see Figure 2.8 and Table 2.2), especially in heterogeneous grasslands. The limitations of the MODIS pixel size are inappropriate to adequately estimate GP in mixed grassland ecosystems (Jarchow, Didan et al. 2018). Although the coarse resolution sensors are associated with vast errors in the estimation of AGB, LAI, and CSC, they are still widely used for large-scale GP monitoring.

Fine spectral and spatial resolution input data are crucial for GP estimation approaches. To date, space-borne hyperspectral data have not been easily accessible, constraining studies to the local scale using UAV data. Studies using broadband multispectral data have produced low prediction accuracies in contrast with hyperspectral datasets, for example, the research conducted by Jarchow, Didan et al. (2018). In this regard, the trade-offs between pixel sizes, image acquisition costs, swath width, and spectral resolution were reported by many authors as a major drawback of RS for estimating GP and their function in the C cycle (Dube, Mutanga et al. 2016, Shoko, Mutanga et al. 2016, Tong and He 2017).

This review study showed several proposed RS techniques for GP monitoring. To date, there is not much information about which algorithm is superior in performance, because a limited number of the reported approaches have been validated for their accuracy. To date, few comparative studies have been undertaken. In addition, although Vis are successful in GP monitoring, it is not suitable in heterogeneous grasslands, particularly when scattered trees or shrubs are present. These indices are not robust and are site-specific. The conventional NDVI, developed from the red and NIR bands, have been reported to perform poorly in sparsely vegetated areas and associated with saturation challenges in thickly vegetated areas (Mutanga and Skidmore 2004, Pang, Zhang et al. 2020). This has led to the development of other indices with better accuracies than the NDVI, such as the red-edge NDVI (NDVI derived using red edge bands), EVI, SAVI, and MSAVI. Using the MODIS data, Zhou, Zhang et al. (2014) found that MSAVI, EVI, and SAVI indices outperformed the NDVI in quantifying the productivity of northern China grasslands.

There is a need to adopt novel methods to enhance the accuracy of estimating proxies of GP. Deep learning has been widely used in many areas of image processing due to its effective

performance in processing high-dimensional data and non-linear relationships. Estimating GP proxies using time series of hyperspectral imageries over large areas takes significant effort using machine-learning regression approaches. This means that deep learning is an outstanding alternative. Deep learning can also deal with multi-source inputs and learn weights to combine important information from them.

Despite the greater use of remotely sensed data in grassland monitoring, fewer studies have combined the several features of GP to develop an exhaustive, consistent biophysical monitoring system. In order to improve the eligibility and transferability of biophysical simulation models, it is also necessary to integrate multiple-source remote-sensing data.

2.5. Conclusions

The progress of RS systems and the introduction of new advanced classification algorithms have gained the attention of researchers to use these potential data and tools for GP monitoring. RS is fully used to obtain accurate information on GP proxies: AGB, LAI, CSC, and chlorophyll content. The present study analysed a substantial body of literature by gathering a comprehensive dataset (203 articles) for estimating grassland productivity using RS until the end of 2021.

The number of studies on estimating GP using remotely sensed data has risen significantly, but most strongly in the last two decades. The prevalence of research on GP is unequally distributed globally, as China has the highest number of studies, followed by the USA. Few studies have been conducted in Africa and Europe.

Multispectral satellite data was used in 88% of studies, especially in studies focusing on the retrieval of AGB. Few studies (10%) used microwave systems, and only 2% combined optical and radar data. Although hyperspectral data are associated with better accuracy than multispectral data, they have a small swath width, high acquisition costs, and high pre-processing. These challenges have limited their use, enabling researchers to focus more extensively on unrestrained broadband multispectral datasets.

The progress in techniques can further enhance the accuracy in estimating GP using the optimal RS datasets. The selection of the most appropriate image classification algorithm is one of the current topics of discussion in GP monitoring using RS data. Thus, there is a call for future research to test the applicability of broadband multispectral and hyperspectral sensors with state-of-the-art image acquisition traits, combined with powerful MLAs, such as DA, RF, PLSR, SVM, and ANN, for the well-informed management of grasslands.

3. A systematic review on the application of remote sensing technologies in grasslands ecosystem services

A Masenyama, O Mutanga, T Dube, T Bangira, M Sibanda, and T Mabhaudhi

3.1. Introduction

Grasslands represent the most extensive land cover on the earth's surface (Briske 2017). They are a mixture of grass, clover and other leguminous species, herbs and shrubs and are generally managed as natural ecosystems (Carlier, Rotar et al. 2009, Zerga 2015). Grasslands are particularly important because they occupy a large area of rangeland vegetation types, covering 31.5% of the global landmass and occurring naturally on all continents excluding Antarctica (Latham, Cumani et al. 2014). Globally, grasslands are recognized for their significant role in biodiversity conservation and the provision of a variety of ecosystem services (Habel, Dengler et al. 2013, Jin, Yang et al. 2014).

The last decade has seen rapid progress in ecosystem services-related (ES) research activities. While the past research mostly focused on forests and wetlands, grasslands were largely neglected, yet they also provide a variety of provisioning (forage production, genetic resources), supporting (nutrient cycling, primary production), cultural (recreation, educational), and regulating (water regulation, climate regulation) ecosystem services (Havstad, Peters et al. 2007, Zhao, Liu et al. 2020). Grassland ES refer to physical and non-physical resources provided by ecosystem structure and functioning of grasslands to meet human survival as well as biodiversity maintenance (Lemaire, Hodgson et al. 2011, Sala, Yahdjian et al. 2017). This implies that accurate and timely information about the geographic extent and health condition of grasslands is of crucial importance for the management of this natural capital.

One of the most valuable services provided by grasslands is that of water management. In terms of water flow regulation, grasslands mainly occur in the main catchment areas (Cadman, De Villiers et al. 2013). As such, they form an effective system for water capture by inducing high infiltration rates, reducing run-off and soil erosion while regulating stream flows (Egoh, Reyers et al. 2011, Cadman, De Villiers et al. 2013). However, grasslands are becoming more vulnerable to land-use changes (Alkemade, Reid et al. 2013), alien plant invasion (Seastedt and Pyšek 2011) and climate change (Bellocchi and Picon-Cochard 2021). Such threats compromise their ecosystem productivity resulting in the deterioration of the role of grassland biomes in water flow regulation.

Grass biophysical parameters such as biomass, leaf area index (LAI) and canopy storage capacity (CSC) are prominent attributes that could offer valuable information to understand

hydrological processes and water balance within grasslands (Xu, Gichuki et al. 2006, Bulcock and Jewitt 2010). Biomass refers to the mass of plant organic matter per unit area (Pang, Zhang et al. 2020). It is a critical component of global carbon cycling and it directly influences hydrological processes such as surface run-off and infiltration (Duley and Domingo 1949, Jin, Yang et al. 2014). LAI is the ratio of a leaf area per unit ground surface area (Zheng and Moskal 2009). It is a major control of vegetation productivity, biophysical feedback on atmospheric energy and water exchanges (Law, Cescatti et al. 2001). CSC is the amount of water retained in plant canopies that controls rainfall interception, evaporation from vegetation canopy, throughfall, interception, infiltration, and ground water restoration (Bulcock and Jewitt 2010, Zou, Caterina et al. 2015).

Remote sensing has become a cost-effective tool for regional and global mapping (Feng, Fu et al. 2010), modelling (Andrew, Wulder et al. 2014) and quantifying ecosystem properties (de Araujo Barbosa, Atkinson et al. 2015). Several studies (Ustin, Darling et al. 2004, Jiang, Qin et al. 2007, Muraoka and Koizumi 2009, Vargas, Willemen et al. 2019, del Río-Mena, Willemen et al. 2020, Niu, He et al. 2021, Wang, Chen et al. 2021) have demonstrated the capability of remote sensing technologies in quantifying ES. A notable advantage of Earth observation technologies is their capability to provide synoptic, unlimited, spatially explicit and frequent information at varying spatial and temporal resolutions (Xu, Yang et al. 2008, Wachendorf, Fricke et al. 2018). With recent advances in remote sensing technology, there is a possibility that Earth observation data could contribute extensively to research on grasslands ES (Soubry, Doan et al. 2021).

In terms of literature, grasslands ecosystem reviews have been carried out (Ceotto 2008, Prochnow, Heiermann et al. 2009, Prochnow, Heiermann et al. 2009, Modernel, Rossing et al. 2016, Zhao, Liu et al. 2020). However, most of the above-mentioned reviews did not focus on remote sensing applications in grassland ES. Within the remote sensing context, there are several reviews that look at the development and significant advances of remote sensing technologies within grassland studies (Ali, Cawkwell et al. 2016, Wachendorf, Fricke et al. 2018, Reinermann, Asam et al. 2020). To the best of our knowledge, the aforementioned studies did not conduct any bibliometric analysis of the studies that focus on remote sensing of ES provided by grasslands, with particular attention to their accuracies. Additionally, few studies have assessed literature on the utility of remote sensing on deriving grasslands biophysical parameters with a special interest in characterizing water-related grassland ES (Soubry, Doan et al. 2021). The recent systematic review by Soubry, Doan et al. (2021) specifically looked at application of geospatial techniques in characterizing ecosystem health attributes, indicators, and measures of forest and grassland. Nevertheless, the study focused on ecological indicators and attributes derived from GIS and remote sensing data in the

context of ecosystem health assessment, not the application of Earth observation data in characterizing ES provided by grassland ecosystems, with particular attention to model accuracies.

Therefore, the current study conducted a systematic literature review to understand the progress, emerging gaps and opportunities on the use of remote sensing technologies in quantifying grasslands ES including those that are related to water. The study seeks to further explore the contribution of variables such as biomass, LAI, and CSC in water management. An understanding of the contribution of such parameters will provide insights of their significant role in the hydrological cycle. This will, in turn, assist water resource managers to facilitate mapping hotspot areas for interventions within degraded grasslands.

3.2. Materials and Methods

3.2.1. Literature search, inclusion, and exclusion strategy

The studies included in this systematic literature review were retrieved through an extensive search for peer-reviewed journal articles published in Web of Science (WOS), Scopus and Institute of Electrical and Electronics Engineers (IEEE). The following search terms combination were used in all the three databases: “grassland productivity AND remote sensing OR GIS”, “grassland productivity monitoring”, “grassland ecosystems AND remote sensing OR GIS”, “grassland ecosystem services AND remote sensing OR GIS”, “grassland LAI AND remote sensing OR GIS”, “grassland canopy storage capacity AND remote sensing”, “grassland productivity AND water management AND remote sensing OR GIS”. The literature search was conducted without any restrictions on the year of publication.

A total of 784 references from WOS, 773 from Scopus and 89 references from IEEE were collected. Following the literature search, the retrieved references (n = 1646) were exported in Endnote for screening. The number of studies identified, included, or excluded were recorded following the Preferred Reporting Items for Systematic Reviews and Meta-analysis statement (Page, McKenzie et al. 2021) (Figure 3.1). The articles eligible for the meta-analysis had to meet the following criteria:

- (1) The study focuses on grasslands and no other vegetation types (e.g. forests, crops) are included since those will be denoting different ecosystems.
- (2) The study focuses on grasslands productivity concepts (biophysical and biochemical parameters of grasslands).
- (3) The study is based on GIS or remote sensing techniques in grassland productivity monitoring and management.

- (4) Results or prediction accuracies of remote sensing technology (sensors or algorithms or vegetation indices) used in the study are stated.
- (5) The article is published in an accredited journal.
- (6) The article is written in English.

From the retrieved literature searches, the study carried out the first exclusion process of removing all duplicates. In total, 641 records were excluded. Secondly, essential bibliography information (title and abstract) of the remaining articles (n = 1005) were examined to check whether the studies applied remote sensing to examine grasslands parameters. Upon title and abstract screening, irrelevant articles (n = 819) were excluded including studies that were not written in English. Of the 186 articles remaining, 45 of them were unavailable in portable document format (pdf), and inaccessible in full length. As a result, they were excluded. The remaining 141 articles were assessed for eligibility and additional articles (n = 81) were identified through the reference lists of the included articles using the backward reference searching (Horsley, Dingwall et al. 2011). These were retrieved using the Google scholar web search engine. In total, 222 articles met the selection criteria and were used for data extraction.

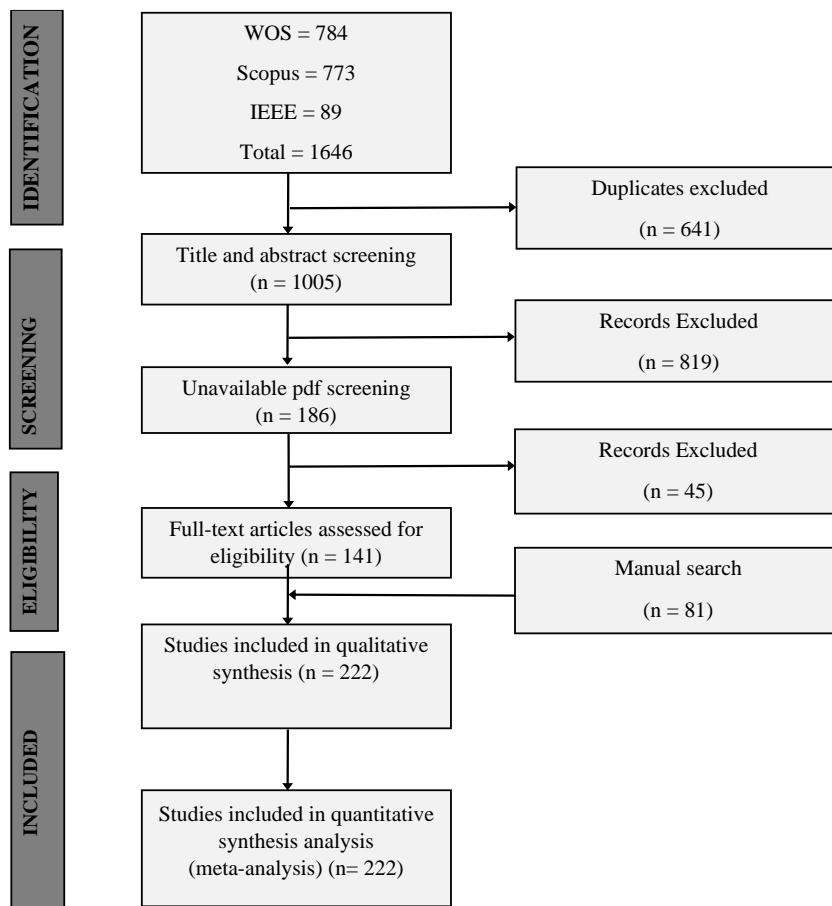


Figure 3.1: PRISMA flow diagram for selection of studies considered in the review.

3.2.2. Data Extraction

The data from Endnote was exported into an excel spreadsheet. Endnote was set to export key bibliographic information such as author name, publication year, article title, journal name, keywords, abstract digital object identifier (DOI), uniform resource locator (URL). In addition to this, information on study area location (country and continent), Earth observation sensor technology utilized, type of vegetation indices, remote sensing algorithms with special attention on derived accuracies and biophysical or biochemical parameter(s) being investigated were extracted after reading through each article. With regards to accuracies, the root mean square error values were not used in this study because ES variables are measured in different SI units. Consequently, the coefficient of determination (R^2) value was used in assessing the accuracies derived in estimating these grasslands ES. The R^2 value is a common accuracy estimation parameter used to explain the magnitude of variation between the predicted and measured samples of a specific grassland variable also known as the goodness of the model's fit (Cameron and Windmeijer 1997, Chicco, Warrens et al. 2021). The R^2 ranges from 0 to 1, with values closer to 1 indicating a great model fit or a more accurate model depending on what is predicted (Singh, Mutanga et al. 2017). The frequency of articles was used in this study for quantification purposes. Specifically, the measures used for the extracted data included counts and percentages while the R^2 s were extracted from respective manuscripts.

3.2.3. Data analysis

The retrieved articles and extracted data were subjected to quantitative and qualitative synthesis and analysis. Firstly, bibliometric analysis was performed to visualize occurrence and co-occurrence networks of key terms from the retrieved literature. Bibliometric analysis is a widely used meta-analytical tool that can identify interconnections of key terms related to a given topic or field from published papers (Han, Kang et al. 2020). This was carried out using VOSviewer software (van Eck and Waltman 2010). VOSviewer provides network visualization of key terms in the form of linked clusters. Creating a map in VOSviewer include four steps which are:

- (1) Selecting a counting method (binary counting or full counting).
- (2) Selecting minimum number of occurrences for a term (calculating similarity index).
- (3) Calculating relevance score for the co-occurrence terms and based on this score, display most relevant items.
- (4) Displaying a map based on the selected terms.

The functionality of VOSviewer for bibliometric mapping and analysis is detailed in van Eck and Waltman (2010). The titles, abstracts, and keywords of the final database were used as input text data in VOSviewer to provide graphical visualization based on occurrence and co-occurrence of key terms. To assess the progress of remote sensing technologies in grassland ES, basic statistical frequencies and trend analysis were conducted using Microsoft Excel (Carlberg 2014). ES provided by grasslands were categorized using the classification scheme proposed by the Millennium ecosystem assessment report (MA 2005) (Table 3.1). The Millennium Assessment (MA) classification scheme was chosen following its present wide recognition as a robust classification approach in distinguishing ecosystem functions into regulating, provisioning, supporting and cultural services.

Table 3.1: Non-exhaustive grassland-related ecosystem services classification based on Millennium Ecosystem Assessment as explained in Leemans and De Groot (2003).

Category	Ecosystem service	Explanation
Provisioning services	Food (fodder)	Range of food products derived from plants, animals, and microbes.
	Genetic resources	Genes and genetic information used for animal and plant breeding and biotechnology.
Regulating services	Fresh water	Water is obtained from different water ecosystems (dams, rivers, oceans).
	Climate regulation	Regulation processes related to the greenhouse effect, atmospheric chemical composition, ozone layer, and atmospheric weather conditions at both local and global scales. Regulation of both temperature and precipitation at a local scale. On a global scale, ecosystems play an important role in climate by Carbon sequestration storage.
	Water regulation	Regulation of hydrological flows, water storage and water retention (i.e. timing and magnitude of runoff, flooding, aquifer recharge and the system's water storage potential) are regulated by changes in land cover.
	Air quality regulation	Sequestration and storage of carbon as well as the release of oxygen, influence air quality.
Supporting services	Erosion regulation	Soil retention and regulation of soil erosion and landslides.
	Water purification and waste treatment	Purification of water through filtering out and decomposing organic wastes introduced into inland waters, coastal and marine ecosystems.
	Natural hazard regulation	Ecosystems can dramatically regulate the damage caused by landslides, wildfires, etc.
	Nutrient cycling	Nutrients such as nitrogen, and phosphorus cycle through ecosystems.
	Primary production or photosynthesis	Assimilation of energy and nutrients by biota. Production of energy required by most living organisms through photosynthesis.
Cultural services	Habitat	Providing living spaces for animals or plants while maintaining biodiversity.
	Soil formation	Soil formation and changes in soil formation which impact human well-being
	Recreation and ecotourism	Provision of recreational parks and touristic attractions.
	Educational values	Provide a basis for both formal and informal education in societies.
	Aesthetic values	Provide aesthetic value in the light of urban development.

Grassland biophysical and biochemical parameters are key indicators of ecosystem services (Lavorel, Grigulis et al. 2011). Given this context, biophysical and biochemical parameters were used to identify ES within the reviewed studies. Additionally, biochemical parameters relating to chemical components such as chlorophyll content and nitrogen concentration are an indirect measure of vegetation nutrient status which in turn relates to nutrient regulation services (Tong and He 2017, Wang, Deng et al. 2017). Therefore, studies relating to the proportion of nitrogen and chlorophyll concentration were classified under nutrient regulation service.

The review was then separated in two sections to address the research objectives. The first section explored the progress in remote sensing technologies applied in grassland ES. This section detailed the literature search characteristics, identified ecosystem services, trends in the distribution of studies and remote sensing technologies applied within grassland ES studies. The outcomes of the first phase were then used to articulate existing research gaps on the role of remote sensing in quantifying grassland water-related ES in the second phase.

3.3. Results

3.3.1. Literature search characteristics

In analysing literature characteristics of the retrieved studies, the network map in Figure 3.2 categorized the identified literature into four clusters of concepts. The green cluster had its key terms being “prediction accuracy”, “performance”, “ann”, “support vector machines”, “multiple linear regression”, “plsr”, “prospect”, “random forest” “biophysical parameters”. This cluster links accuracy assessment of algorithm performance with estimating biophysical parameters. The inclusion of terms such as “Landsat”, “hyperspectral data”, “spectroradiometer” in this cluster presents the linkage between satellite imagery, ground-level spectral reflectance, remote sensing modelling techniques and principal biophysical parameters which directly implies the utility of various remote sensing technologies in grasslands ecosystem services.

The second cluster (yellow) had its key terms as “band”, “spectral bands”, “sensor”, “red-edge”, “sentinel”, “worldview”. This relates to the influence of the spectral band settings (reflectance measured) on the sensor’s performance in estimating grass productivity (Wang, Xiao et al. 2019). The blue cluster had “synthetic aperture radar” and “soil moisture” as its key terms which directly implies the potential of synthetic aperture radar (SAR) sensors in estimating soil moisture content. Lastly, the red cluster connected terms such as “China”, “modis ndvi”, “carbon cycle”. This articulates the wide usage of MODIS derived NDVI as proxy for studying grasslands as major component of carbon cycling, with most studies carried out

in China (Fu, Tang et al. 2014, Liu, Cheng et al. 2017, Kong, Yu et al. 2019). The red cluster also categorized terms such as “climate change”, “net primary productivity”, “precipitation”, “temperature”. Precipitation and temperature are crucial variables in controlling net primary production which is a key measure of ecosystem functioning used in understanding global climate change (Jia, Xie et al. 2015).

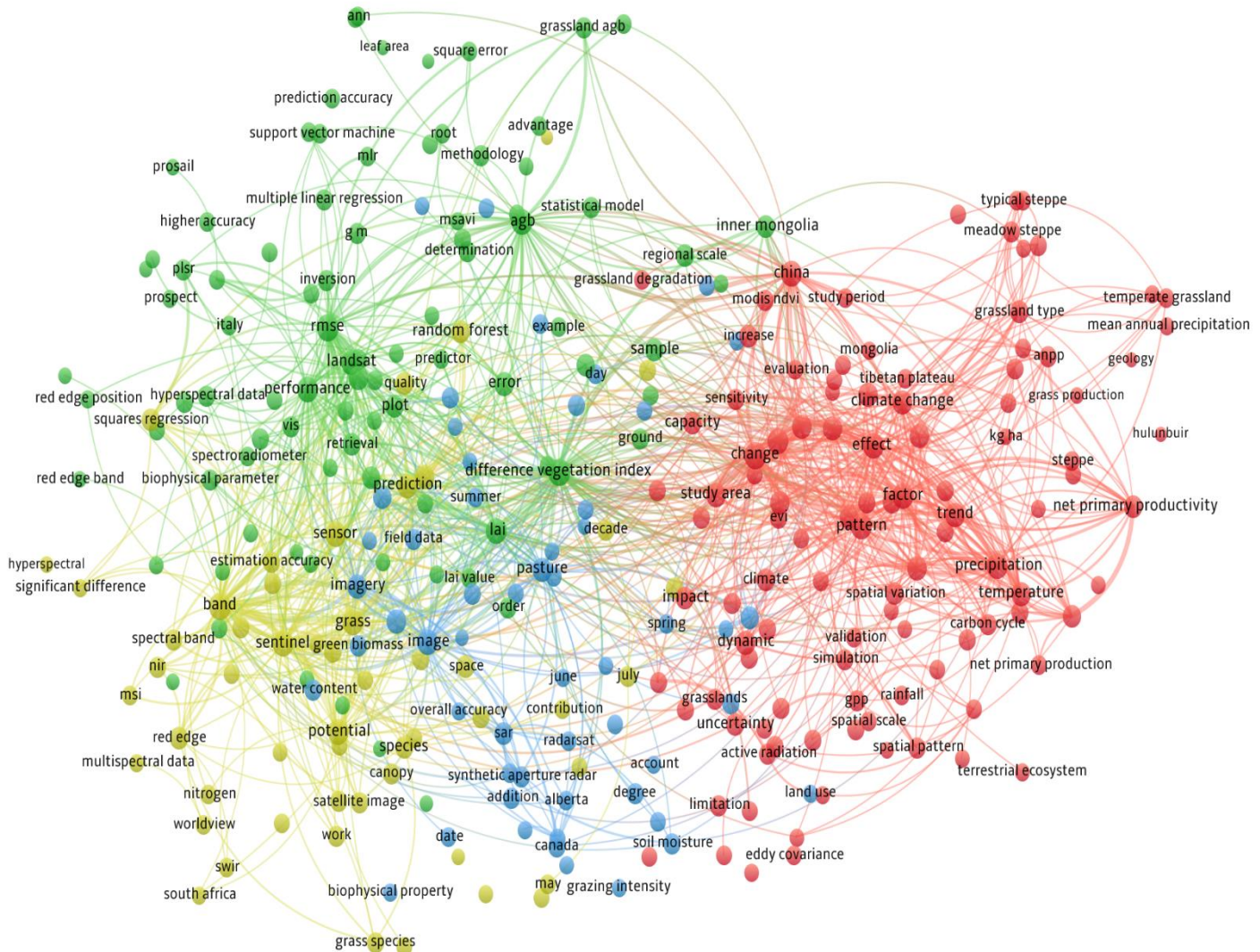


Figure 3.2: Topical concepts in grasslands ecosystem services studies derived using data from titles, abstract and keywords.

3.3.2. Progress in the use of remote sensing technologies to monitor grasslands ecosystem services.

3.3.2.1. Grassland ecosystem services identified in literature.

Results of this study illustrate that nine-grassland ES were mentioned in the retrieved articles (Figure 3.3). A total of 79 studies utilized remote sensing in studying grassland provisioning services of which forage provision had the highest frequency of studies (n =75). Forty-three studies investigated grassland supporting services relating to primary production, seventeen studies focused on nutrient cycling and thirteen studies were based on habitat for wildlife species. Seventy-five studies focused on grassland regulating services, of which 51 studies focused on climate regulation. The results show that only one study (Ge, Yang et al. 2014) utilized Earth observation data to monitor grasslands tourist seasons which relates to cultural ecosystem services.

For water regulation service, three studies (Davidson, Wang et al. 2006, Hajj, Baghdadi et al. 2014, Sibanda, Onisimo et al. 2021) evaluated the utility of remotely sensed data in mapping moisture content elements related to biomass. In addition, studies by Pan and Shangguan (2006) and Kautz, Collins et al. (2019) used the spatial extent of vegetation cover derived using remotely sensed data to estimate run-off while Xing, He et al. (2014) use it to estimate soil moisture within grasslands. Meanwhile, 5 studies (Shimoda and Oikawa 2008, Vetter, Schaffrath et al. 2012, Schaffrath and Bernhofer 2013, Zhu, Su et al. 2013, Castelli, Anderson et al. 2018) utilized remotely sensed data to characterize LAI in the context of hydrological models linked to evapotranspiration. Remotely-sensed LAI was also used as input data to understand hydrological processes relating to water balance (Nouvellon, Moran et al. 2001, Sridhar and Wedin 2009), ecological water requirement (Zhang, Yang et al. 2010) and precipitation use efficiency (Jia, Xie et al. 2015) within grasslands ecosystems. Qi, Murray et al. (2017) used process-based models which simulate LAI as a dynamic input in a grass growth model. The model was used to estimate evapotranspiration, drainage and water productivity within different grassland systems.

In terms of CSC, one study (Yu, Pypker et al. 2012) utilized water budget balance and artificial wetting methods to model canopy rainfall storage capacity in relation to grassland degradation and its impact on the hydrological cycle. Additionally, a study by Sibanda, Onisimo et al. (2021) utilized remote sensing methods to assess grassland CSC. Three studies (Bertoldi, Della Chiesa et al. 2014, Baghdadi, El Hajj et al. 2015, El Hajj, Baghdadi et al. 2015) were based on the use of remotely sensed data to estimate soil moisture content in grasslands which is a key parameter for many hydrological processes. Paruelo, Lauenroth et al. (1999) used remotely sensed aboveground net primary production data as an estimate of water availability

within grasslands. Saatchi, van Zyl et al. (1995) used synthetic aperture radar (SAR) data to estimate soil moisture and canopy water content of natural grasslands which is of fundamental importance to understanding eco-hydrological processes.

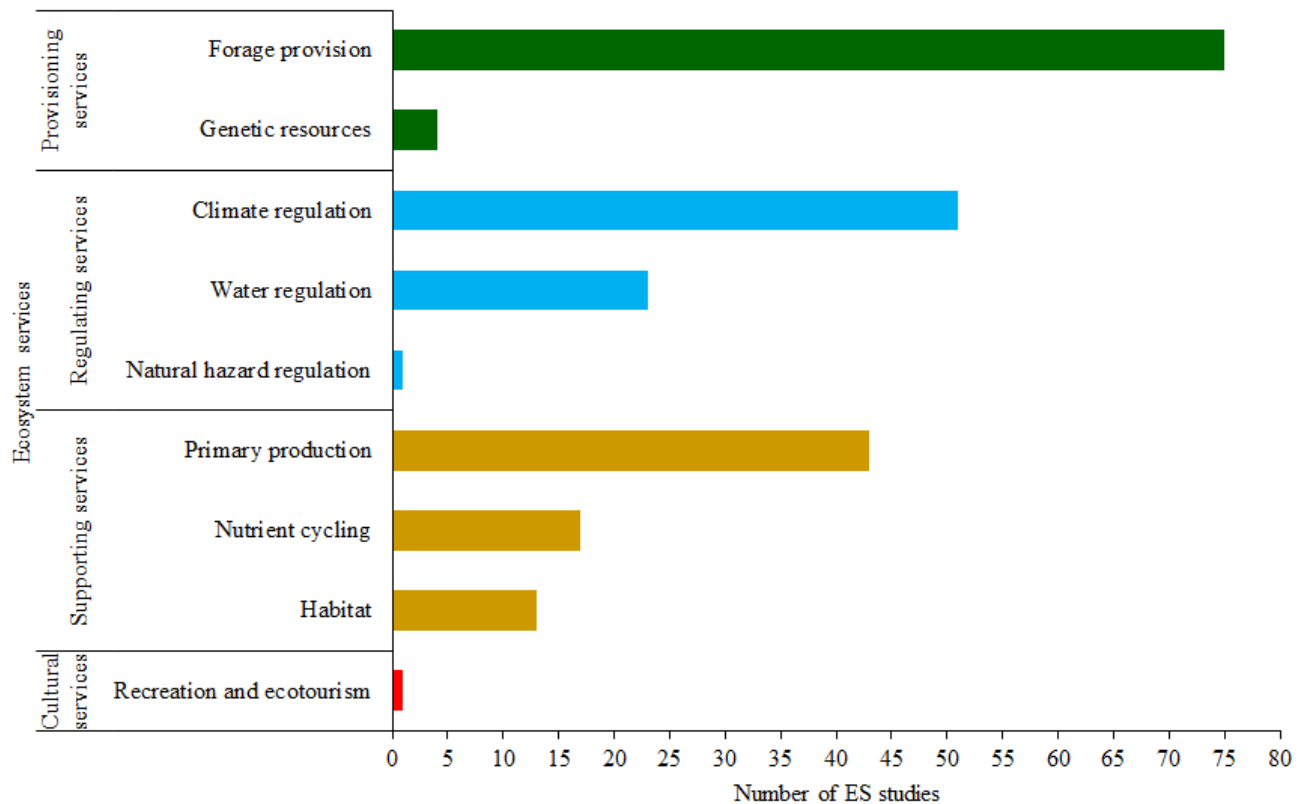


Figure 3.3: The number of studies that utilized remote sensing to assess grasslands ecosystem services. Studies with multi-ecosystem services were counted several times.

3.3.2.2. Geographic distribution and publication trends

In terms of spatial distribution, the studies included in the meta-analysis were conducted in thirty-one different countries (Figure 3.4). Ten articles were large-scale studies conducted at a regional scale and two studies (Xia, Liu et al. 2014, Yang, Wang et al. 2017) were conducted on a global scale. These studies were included in the meta-analysis but could not be classified under a certain country in Figure 3.4. In assessing the frequency of publications per nation, it was observed that studies on grasslands ES were conducted across all continents excluding Antarctica. Thirty-three per cent of these studies were conducted in Asia, with China having most studies.

Although 18% of the studies were conducted in Africa, (13%) were conducted in Southern Africa, mostly in South Africa. About 22% of the studies were conducted in Europe, 18% in North America, 5% in South America and 3% in Australia. 1% of the studies collected in this

study were conducted at a global-scale. From Figure 3.4, considerable gaps in the geographic distribution of published articles can be observed especially in South America, Australia and most parts of Africa. Interestingly, 11 out of 23 studies on water-related ecosystem services were conducted in the global south and 12 in the global north. More research efforts need to be exerted towards the utilization of remotely sensed data in assessing grassland water-related ES globally.

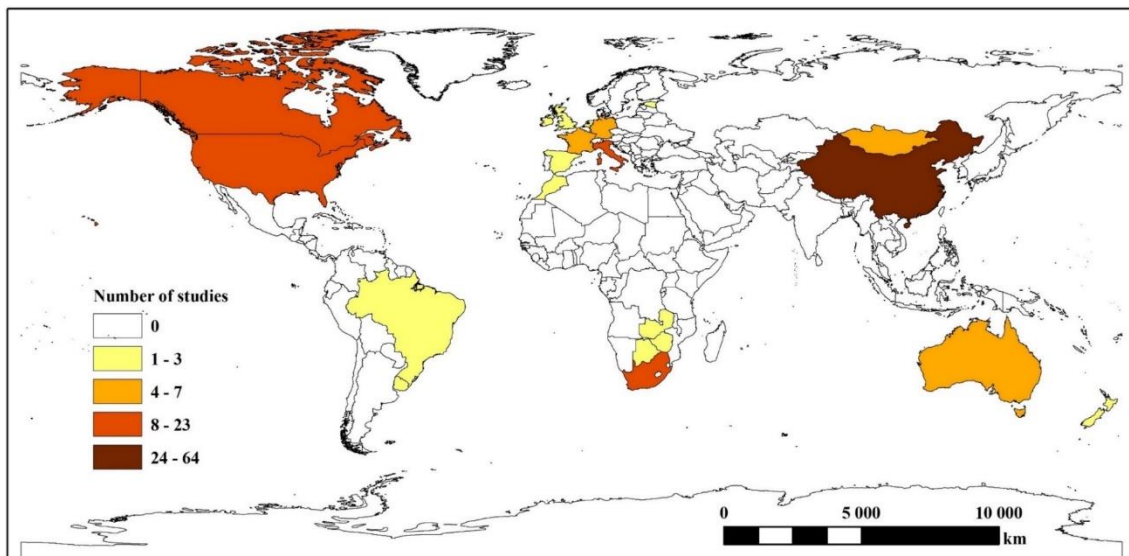


Figure 3.4: Spatial distribution of remote sensing studies in the context of grassland ecosystem services. Studies conducted at regional and global scales are not shown.

The earliest publication of grassland ES was in 1983 (Figure 3.5). Meanwhile, few articles ($n = 10$) were published between 1983 and 1996. A constant number of publications occurred between 1997 and 2001 after which a considerable fluctuation in publications was observed. Since then, the use of remote sensing in grassland ES studies has been increasing steadily reaching a total of 222 published articles in 2021 (Figure 3.5).

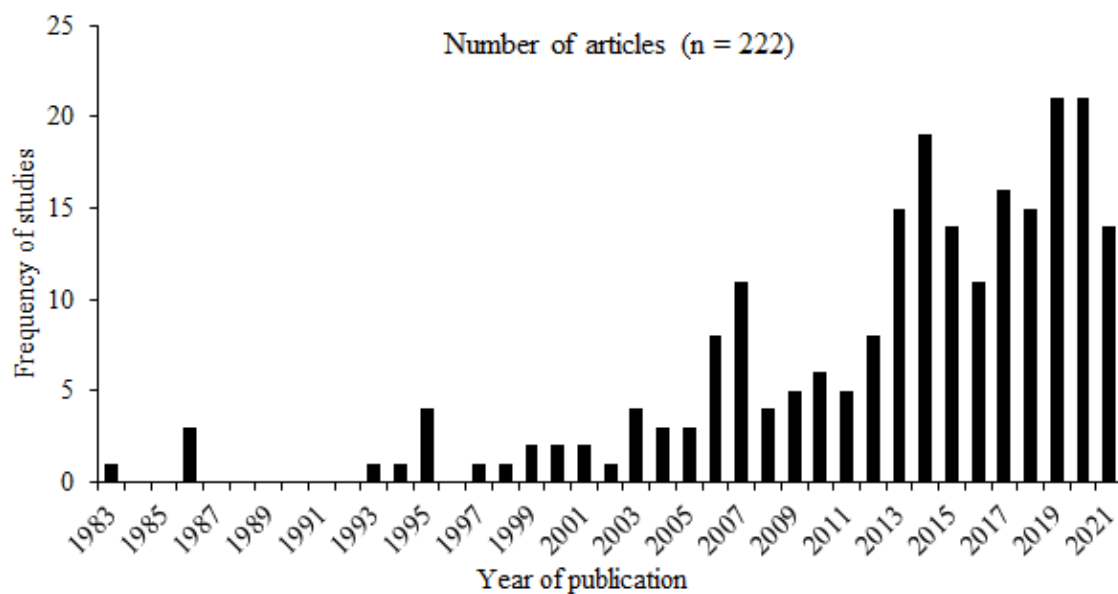


Figure 3.5: Frequency of studies published on remote sensing applications in grassland ecosystem services.

3.3.2.3. Sensor technologies, spectral settings, and derived vegetation indices

The use of Earth observation sensors used in remote sensing of grassland ES studies has considerably increased. Thirty-nine sensor types were noted in the literature reviewed (Figure 3.6). As illustrated in the characterization of literature in Figure 3.2 (red cluster), Moderate Resolution Imaging Spectroradiometer (MODIS) had the highest frequency of studies (34%), followed by the Landsat system (25% (TM = 11%, OLI = 8%, ETM+ = 6%)).

Meanwhile, a significant number of studies (18%) have used handheld hyperspectral devices for the in-situ acquisition of remotely sensed data for characterizing grass biophysical and biochemical parameters. The findings of this study also illustrate that 14% of the studies utilized digital elevation models (DEM) in estimating and mapping grassland ecosystem services. Of these studies, about 4% specifically used the Shuttle Radar Topography Mission (STRM) and 2% used the Advanced Spaceborne Thermal Emission and Reflection Radiometer (ASTER) derived digital elevation models.

The new generation of sensors such as Sentinel 2 multispectral instrument (MSI) has shown great potential in grassland ES studies (13%). High spatial resolution satellites such as Worldview-2 and Worldview-3 have also been utilized in 3% of the studies. Although applied in a few studies, results from the searched literature showed that recent technologies in remote sensing such the Unmanned Aerial Vehicle (UAV) based sensors have also been utilized in grasslands ES studies (3%) (Figure 3.6).

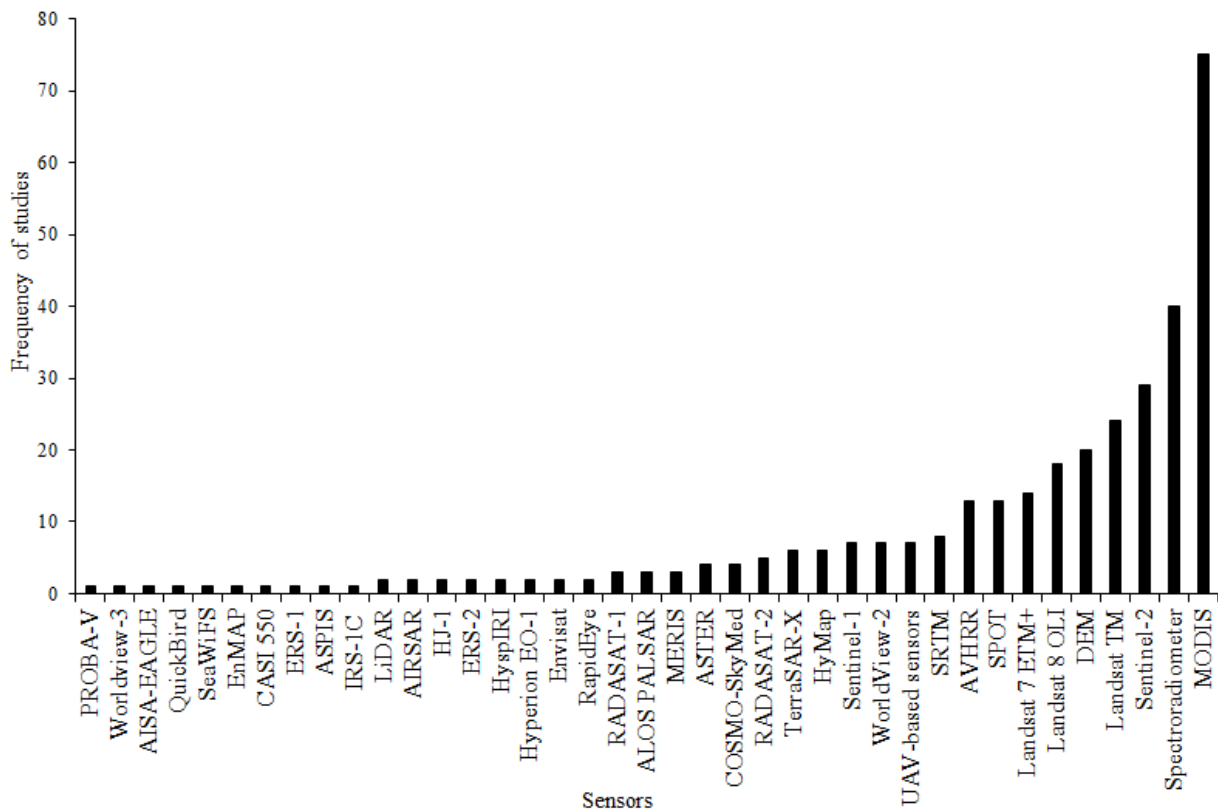


Figure 3.6: Frequency of studies that utilized a specific sensor system within reviewed studies. Studies with multi-sensors were counted several times.

Results show that the use of sensors such as Advanced Very High-Resolution Radiometer (AVHRR), spectroradiometer and platforms such as UAVs began to increase in the 1980's (Figure 3.7). The 1990's saw the introduction of sensors such as SPOT and Landsat TM sensor-system within the grassland ES research. The use of MODIS sensor can be observed from 2005 and it has been used almost in all years. Additionally, the use of Landsat ETM+ started trending in 2001 up until now. Although the results show that Worldview-2 had also been utilized in mapping grassland ES, it was observed to have been utilized for five years, from 2013 to 2018. The period from 2014 to 2021 witnessed a shift in the frequent use of Sentinel-2 and Landsat 8 OLI sensors.

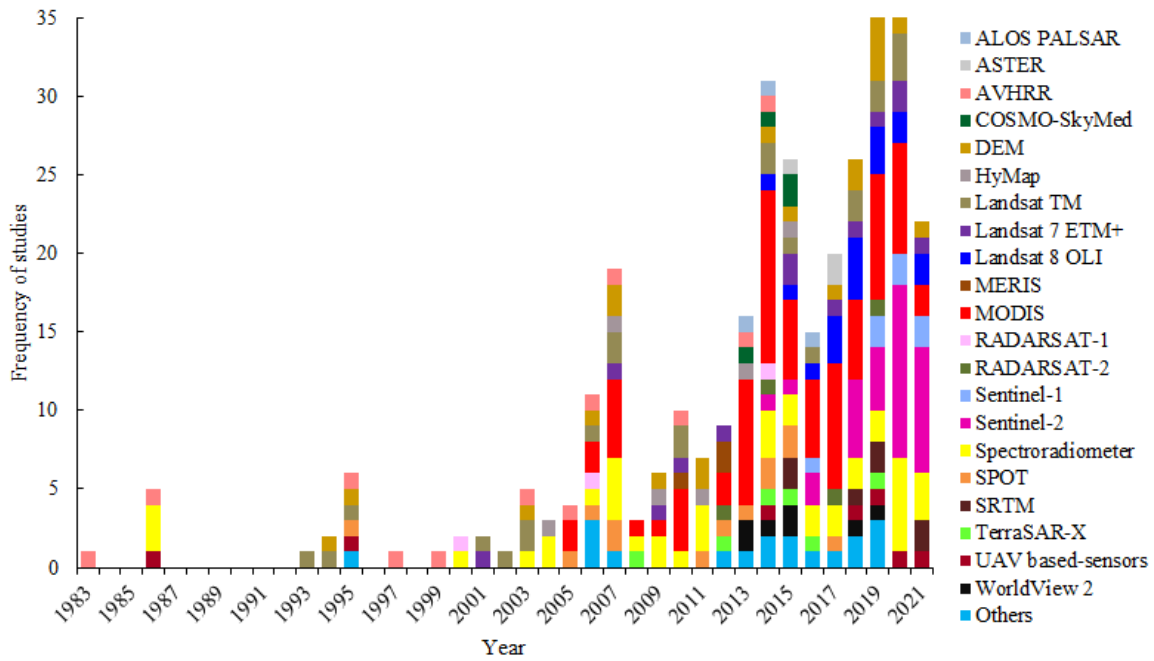


Figure 3.7: Progression of Earth observation sensors used within the reviewed studies between December 1983 and September 2021.

The sensors used in the grassland ES studies show a high range of average prediction accuracies with R^2 values of 55% to 90.5% (Figure 3.8). The highest average R^2 value (90.5%) was obtained from the utility of UAVs. Meanwhile, freely available moderate spatial resolution satellites such as Landsat TM, OLI and ETM+ had high mean prediction accuracies of 70, 76 and 83%, respectively. Additionally, the high spatial resolution Sentinel 2 satellite data yielded a high mean prediction accuracy of 77%. Interestingly, SAR systems yielded considerable average prediction accuracies ranging from 58%-73% (Figure 3.8).

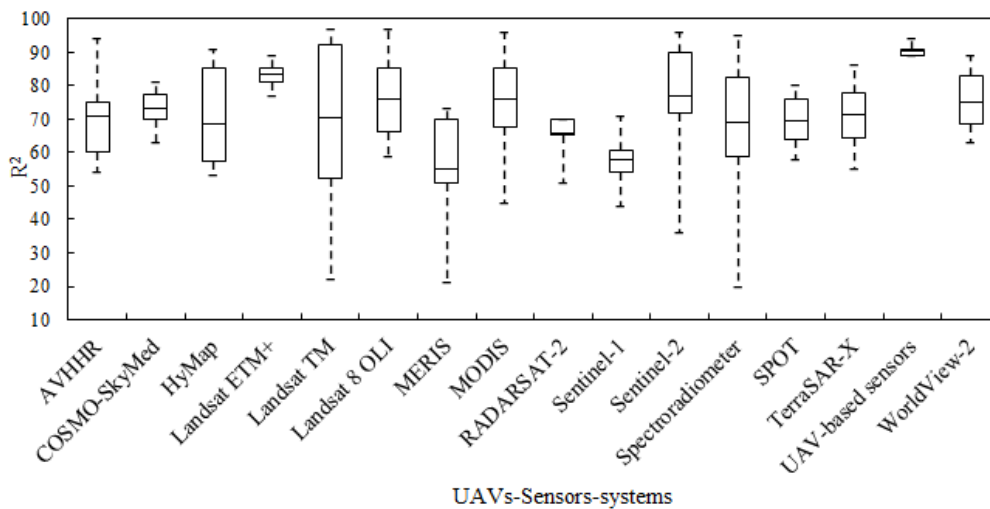


Figure 3.8: Box plots showing average correlation coefficients values for Earth observation sensors used in the ecosystem services studies. Sensors utilized in less than three studies are excluded.

Numerous vegetation indices have been derived from Earth observation sensors for mapping and monitoring grasslands ES. Although a plethora of vegetation indices were identified in the literature considered in this study, Table 3.2 only shows the vegetation indices applied in more than three studies. Most indices were not captured because they were used in less than three studies. Subsequently, the study reports on the sections of the electromagnetic spectrum that have been widely utilized to derive those vegetation indices as in Loris and Damiano (2006), Boschetti, Bocchi et al. (2007), Lu and He (2019), Wang, Liu et al. (2019) and Sibanda, Onisimo et al. (2021).

The widely used sections of the electromagnetic spectrum for the derived vegetation indices were the red and near-infrared regions (NIR). In this regard, the Normalized Difference Vegetation Index (NDVI) was utilized in 65% of the studies, the Enhanced vegetation index (EVI) in 13%, the Soil adjusted vegetation index (SAVI) in 10% and the Simple Ratio (SR) in 6% of the studies. A considerable number of studies (6%) used red-edge based vegetation indices which are calculated based on the red-edge region of the electromagnetic spectrum (Guerini Filho, Kuplich et al. 2020). Although most studies used vegetation indices, the results of this review showed that about 8% of the studies assessed the utility of topographic indices derived from DEM in predicting and estimating grassland ecosystem services.

In terms of water-related ES, the used sensors were COSMO-SkyMed, RADARSAT-2, MERIS, MODIS, Sentinel 2, SPOT, TerraSAR-X, Landsat fleet and hand-held spectral devices. Vegetation indices utilized in these studies were Soil Adjusted Total Vegetation Index (SATVI), NDVI and SR. Additionally, red-edge, NIR and short-wave infrared (SWIR) bands were reported to be critical in characterizing water-related ES. Moreover, only three studies (Saatchi, van Zyl et al. 1995, Bertoldi, Della Chiesa et al. 2014, Sibanda, Onisimo et al. 2021) used topographic indices in estimating water-related ES.

Table 3.2: Summary of the commonly used vegetation indices in grassland ecosystem services studies.

Index name	Abbreviation	Formula	R ² range	Reference
Enhanced Vegetation Index	EVI	$G \frac{NIR - RED}{NIR + C1 \times RED - C2 \times BLUE + L}$	0.44-0.95	(Liu and Huete 1995)
Normalized difference vegetation index	NDVI	$\frac{NIR - RED}{NIR + RED}$	0.22-0.95	(Rouse, Haas et al. 1974)
Sentinel 2 Normalized difference red edge index	NDRE	$\frac{NIR - RED\ EDGE}{NIR + RED\ EDGE}$	0.47-0.84	(Liu, Wang et al. 2018)
Soil adjusted vegetation index	SAVI	$(1 + L) \frac{NIR - RED}{NIR + RED + L}$	0.49-0.75	(Huete 1988)
Simple ratio	SR	$\frac{NIR}{RED}$	0.27-0.83	(Jordan 1969)

G = gain factor; C1, C2 = coefficients of the aerosol resistance term, which uses the blue band to correct for aerosol resistance term; L = soil brightness correction factor (Liu and Huete 1995).

3.3.2.4. The role of remote sensing prediction and modelling algorithms in grassland ecosystem services

Results of this review show that there are thirty-seven algorithms that have been utilized in studying grasslands ES. These thirty-seven algorithms fall into three categories that are as follows:

- (1) production efficiency models (n = 18)
- (2) machine learning algorithms (n = 10)
- (3) multivariate analysis techniques (n = 9)

Figure 3.9a shows the average coefficient of determination accuracies of production-efficiency models that were used in more than three studies. Fifteen of the eighteen production efficiency models were excluded from Figure 3.9a as they were used in less than three studies (Table 3.11: Appendix). The included models yielded high average R²s ranging from 60.6% to 72.8% (Figure 3.9a). Results of this study show that PROSAIL was the most widely used model among the production efficiency models. Results also show that light use efficiency (LUE) models are utilized in estimating ecosystem primary production services. For LUE and Carnegie-Ames-Stanford approach (CASA), it was observed that the major inputs for the

models were a fraction of Photosynthetic Active Radiation (fPAR) derived from remote sensing data and meteorological data.

Figure 3.9b shows the average coefficient of determination accuracies of three widely used machine-learning algorithms. Seven of the algorithms were excluded from Figure 3.9b because they were applied in less than three studies (Table 3A: Appendix). The average R^2 s of the algorithms ranged from 64.5% to 75%, showing considerable high prediction accuracies across all the algorithms used in estimating grassland ES. Random forest (RF) had the highest average prediction accuracy (75%) followed by artificial neural networks (ANN) and support vector machines (SVM) with average accuracies of 68% and 64.5%, respectively. These algorithms were detected using the network analysis in Figure 3.2 (green cluster) as topical elements of grassland ES mapping. Meanwhile, multivariate analysis techniques reported in most studies are illustrated in Figure 3.9c. The R^2 average accuracies ranged from 54% to 86.5%, indicating high model prediction accuracies (Richter, Hank et al. 2012). Discriminant analysis (DA) had the highest average prediction accuracy (86.5%) followed by sparse partial least square regression (SPLSR) and partial least square regression (PLSR) with average accuracies of 78% and 71% respectively. Exponential regression had the lowest average prediction accuracy of 54%.

Algorithms reported in studies that focused on water-related ES include hydrological models (Soil-vegetation-atmosphere transfer (SVAT), Water cloud, Process-based model, NOAH Land Surface Model (LSM), Rangeland Hydrology and Erosion Model (RHEM), Two Source Energy Balance Atmosphere Land Exchange Inverse (TSEB ALEXI), GEOTop and BROOK90 models), ordinary least square regression (OLSR), linear regression (LR), SPLSR and RF. However, most of these models are excluded from Figure 3.9 analysis because they were applied in less than three studies (Table 3.11: Appendix). Overall, it was observed that most multivariate techniques and machine learning algorithms (i.e. RF, SVM, ANN, PLSR, OLSR) performed well in literature considered in this study. Also, it was observed that they had a feature selection capability for identifying the most influential spectral features for estimating grass biophysical parameters.

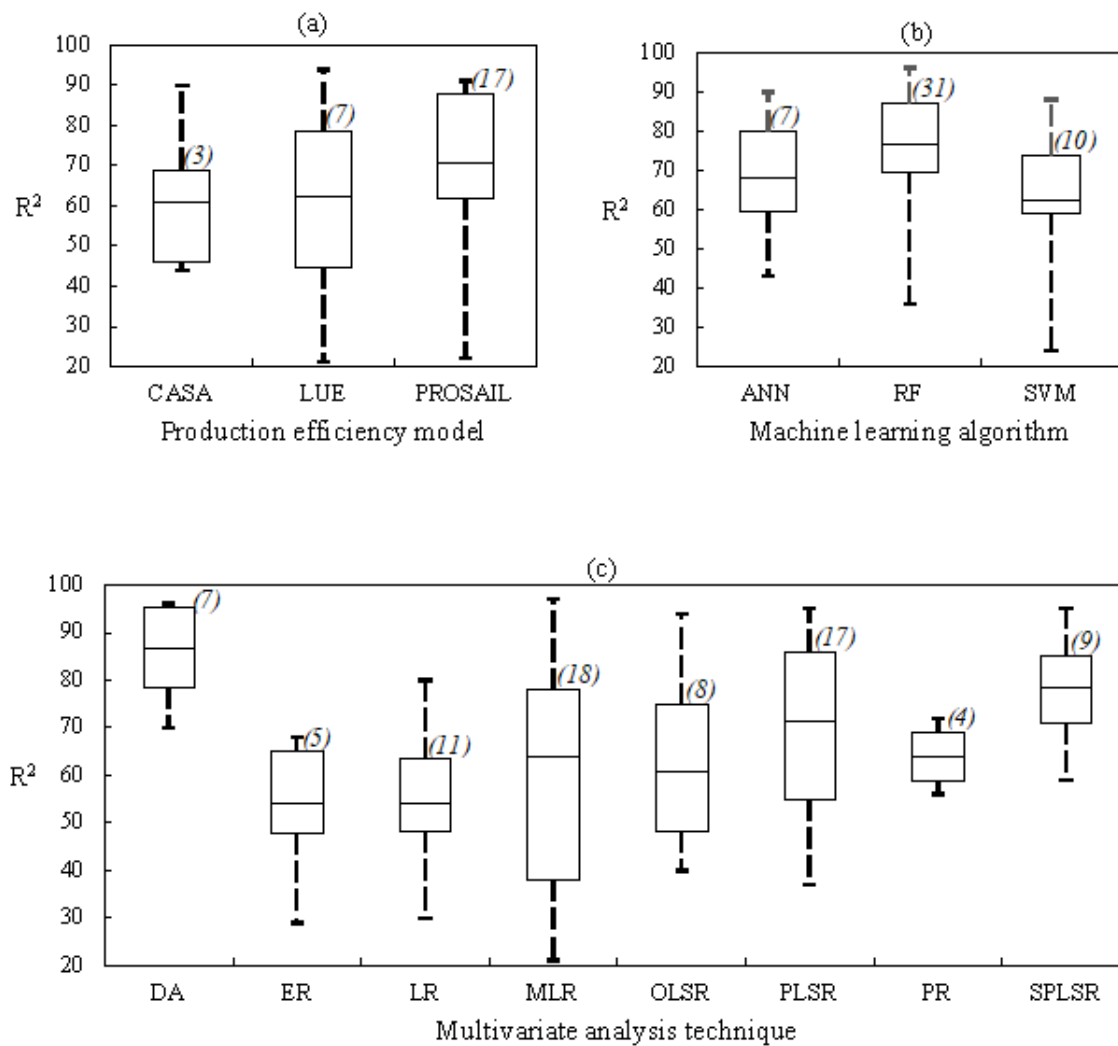


Figure 3.9: Box plots showing average coefficient of determination (R^2) values produced by remote sensing algorithms applied in the studies. Numbers in italics represent the number of times an algorithm was utilized. (a) CASA= Carnegie-Ames-Stanford Approach; LUE= light use efficiency; PROSAIL= prospect + sail, (b) ANN= artificial neural networks; RF= random forest; SVM= support vector machines, (c) DA= discriminant analysis; ER= exponential regression; LR= linear regression; MLR= multiple linear regression; OLSR= ordinary least square regression; PLSR= partial least square regression; PR= power regression; SPLSR= sparse partial least square regression.

3.4. Discussion

3.4.1. Progress in remote sensing of grassland ecosystem services

3.4.1.1. Geographic distribution and publication trends

Results in this study showed that most grassland ES were conducted in China. This could be explained by the fact that China possesses vast grassland ecosystems that include alpine steppe, meadow steppe, desert steppe, and typical steppe which accounts for 10% of the total grasslands area (Dai, Huang et al. 2016). Additionally, China has experienced relative scientific advancement of ecological science and technology (Li, Pei et al. 2020). As an example, China designed and launched environmental and disaster monitoring HJ-1 satellites. Such datasets have become operational in ecological monitoring, including grassland ecosystems (Xing, He et al. 2014, Meng, Ge et al. 2017).

On the other hand, results also showed considerable gaps in the spatial distribution of published articles in Africa, Australia and South America. This is an interesting finding contrary to the notion that large areas in these continents are covered with tropical grasslands (Lehmann, Archibald et al. 2011). Overall, it was observed that studies on remote sensing of grassland ES are significantly increasing (Figure 3.5). Remote sensing technologies have rapidly developed, providing grassland researchers with multi-source and multiplatform remotely sensed data (Li, Cui et al. 2021). Additionally, remote sensing provides the possibility of complimenting ground truth data through remote sensing inversion and data assimilation (Li, Cui et al. 2021). This could possibly explain the increase in grassland remote sensing ES research.

3.4.1.2. Earth observation sensors

Results in this study showed that MODIS and the Landsat fleet had the highest utilization frequency. Soubry, Doan et al. (2021) also noted an extensive utilization of data from the MODIS and Landsat sensors fleets in grassland remote sensing research. The high utilization frequency of such sensors could be attributed to the fact that until recently, Earth observation imagery has been dominated by traditional optical sensors such as MODIS and Landsat (Thenkabail, Smith et al. 2002). Such sensors have been in orbit for the longest time, and they have global coverage, consistently supplying researchers with freely available remotely sensed imagery suitable for retrieving grass biophysical parameters. Meanwhile, the results of this study also showed that a significant number of studies have explored the utilization of

handheld hyperspectral devices. These findings are similar to those of Soubry, Doan et al. (2021) who also noted a significant number of studies (16.5%) that were conducted based on hyperspectral sensors. Such sensors provide a wide range of sections of the electromagnetic spectrum in relation to other sensors (i.e. Landsat and MODIS), hence they provide higher, and optimal accuracies in estimating and mapping biophysical and optical properties of vegetation (Cerasoli, Campagnolo et al. 2018). In this regard, the use of in situ hyperspectral sensors has the potential of minimizing several errors since data is acquired proximal to the canopy when compared to satellite and airborne sensors (Agapiou, Hadjimitsis et al. 2012). Results showed that the application of remote sensing technologies in grassland ecosystems draws back to the 1980s. Initially, this era was associated with aerial photography (Dancy, Webster et al. 1986). The changes in remote sensing techniques from aerial images to satellite-borne sensors have achieved a significant advancement in the grassland ES research community. Specifically, the launch of MODIS in 2000 marked a shift within the remote sensing field which may probably explain the constant frequency in the publications on grassland ES occurring in the 2000s decade (Kawamura, Akiyama et al. 2005, Li, Wang et al. 2013, Yu, Wu et al. 2021). More so, recent advancements in Earth observation sensors include the launching of Sentinel 2 MSI and the Landsat 8 OLI, offering data on free access policy. With such advancements, the number of studies on mapping and monitoring grassland ES has increased along with the associated accuracies.

A considerable number of studies explored the possibility of using SAR sensors in estimating grassland ES; especially those related to water. SAR has several advantages which include an all-weather capability, independence from solar energy and the ability to select an appropriate wavelength for studying belowground properties and soil substrates (Holmes 1992). Furthermore, changes in vegetation and soil moisture contents contribute to the total backscattered radar signal which influences the absorption, transmission and reflection of microwave energy (Wang, Ge et al. 2013, He, Xing et al. 2014). Being active sensors, acquiring data in all weather conditions and being sensitive to vegetation and soil moisture content explains their prospective utility in assessing water-related ES.

3.4.1.3. Spectral features (wavebands and vegetation indices)

This review highlights that the widely used vegetation indices relied on near infrared and red bands with NDVI being the widely used index. NDVI is calculated through a normalization procedure using spectral reflectance from the red and the near-infrared bands which makes it simple to assess vegetation health and vigour (Xue and Su 2017). Despite the wide application of NDVI, it is sensitive to atmospheric effects, leaf canopy, soil brightness and cloud shadow

(Thenkabail, Smith et al. 2000, Xue and Su 2017). As a result, SR, EVI and SAVI have been proposed to reduce noise effects from non-vegetation matter (Zhengxing, Chuang et al. 2003, Xue and Su 2017). The application of such indices has greatly promoted the prediction of ES such as forage provision (Kawamura, Akiyama et al. 2005) and primary production (Zhou, Zhang et al. 2014).

Additionally, the advent of Sentinel 2 MSI offers fine spatial and robust spectral resolution covering the red-edge section of the electromagnetic spectrum. This section is very important for characterizing vegetation attributes (Boochs, Kupfer et al. 1990, Curran, Dungan et al. 1990, Pu, Gong et al. 2003, Mutanga and Skidmore 2007, Sibanda, Mutanga et al. 2019). In several studies (Ramoelo, Cho et al. 2015, Tong and He 2017, Munyati, Balzter et al. 2020), indices that utilized wavelengths from the red-edge region (i.e. NDRE) performed well in estimating grassland ES as compared to the normal broadband indices (i.e. NDVI), especially in relation to characterizing water-related ecosystems (Sibanda, Onesimo et al. 2021). The reflectance in the red-edge (680-780 nm) provides information on the rapid rise of vegetation reflectance at 680 nm with the highest absorption occurring at 780 nm which better estimates vegetation pigment, physical and chemical parameters (Gao, Wu et al. 2019). As such, red-edge based indices have been suggested to effectively correct variations caused by atmospheric influence, bidirectional reflectance distribution function and background noise (Tong and He 2017).

3.4.1.4. Prediction, modelling and classification algorithms.

In terms of remote sensing algorithms, the use of multivariate analysis techniques in grassland ES has been widely reported (Sakowska, Juszczak et al. 2016, Pang, Zhang et al. 2020). Multivariate analysis techniques were the most widely used algorithms probably because of their simplicity and ease of implementation. However, multivariate techniques are generally associated with data assumptions which are not always easy to attain based on ecological data (Finch 2005). For instance, to utilize multivariate techniques data must meet the assumptions of normality and homogeneous covariance matrices. Meanwhile, Arjasakusuma, Swahyu Kusuma et al. (2020) illustrated that multivariate techniques are susceptible to high data dimensionality and noted that they tend to overfit the models which reduce the model accuracies.

More research has also been conducted based on machine learning algorithms (Mutanga and Skidmore 2004, Lehnert, Meyer et al. 2015, Gao, Dong et al. 2020). The successful application of machine learning algorithms can be explained by the notion that they are non-parametric and therefore do not rely on any assumptions about data distribution (Barrett, Nitze et al.

2014). In this regard, they are insensitive to over-fitting and could be the best option for modelling grasslands biophysical parameters (Cawley and Talbot 2010). Overall, the majority of the multivariate and the machine learning algorithms showed optimal performance in estimating grassland ES mainly due to their feature selection capability. In this regard, the development of accurate remote sensing models for predicting grass biophysical parameters seems to largely depend on the algorithm used in selecting optimal spectral features from remotely sensed data as noted by Verrelst, Malenovský et al. (2019) and Richter, Hank et al. (2012).

Results of this study also showed that production efficiency models are prominent for monitoring ES such as primary production (Propastin, Kappas et al. 2012, Zhang, Lal et al. 2016). A review by Reinermann, Asam et al. (2020) also showed that most studies used CASA, LUE and PROSAIL modelling approaches in analysing grassland production traits and management. Most of the production efficiency models take into consideration the LUE theory which states that there is a constant relationship between photosynthetic carbon uptake and radiation interception at the plant canopy level (Monteith 1972, Anderson, Norman et al. 2000). Results also showed that the major input for these models is fraction of photosynthetically active radiation (fPAR). This can be explained by the notion that production efficiency models require inputs of meteorological data and satellite Earth observation derived fPAR in order to simulate the total primary production (McCallum, Wagner et al. 2009). The integration of remote sensing and production efficiency models represents an important approach for monitoring terrestrial carbon exchange across a wide range of spatial and temporal scales. The high average prediction accuracies obtained from these production efficiency models imply that they all exhibit robust techniques to evaluate remote sensing data that can effectively quantify and map grassland ES.

3.4.2. Remote sensing of biomass, LAI, and CSC to characterize water-related grassland ecosystem services

Results of this present study have shown that various remote sensing technologies have been widely applied in characterizing ES such as forage provision, genetic resource, climate regulation, natural hazard regulation, primary production, nutrient cycling and habitat support. However, very few studies were noted that sought to understand the role of remote sensing in characterizing biomass, LAI and CSC in relation to water-related ecosystems services management.

Results in this study showed that only three studies evaluated the utility of remotely sensed data in mapping the grass moisture content elements related to biomass. There is paucity of

literature that directly focus on the role of remote sensing in estimating grass biomass in relation to water resources even though grass prevalence has a considerable effect on some hydrological elements. For instance, dense biomass coverage has a direct impact on grass and soil water holding capacity through induced infiltration (Duley and Domingo 1949). This promotes soil water availability, groundwater restoration and surface water balance within grassland biomes.

Meanwhile, results showed that few studies have sought to utilize LAI in the context of estimating evapotranspiration. Remote sensing provides spatial and temporal estimations of LAI which can be coupled with meteorological variables in hydrological modelling mostly in evapotranspiration processes (Tesemma, Wei et al. 2015, Gan, Zhang et al. 2018). Evapotranspiration is the combination of two ecohydrological processes which are plant-mediated transpiration and evaporation (soil surface evaporation and evaporation of rainfall intercepted by plant canopies) (Smallman and Williams 2019). As such, it is a crucial terrestrial component of the hydrological cycle which impacts the magnitude of surface water and variability of catchment water yield and ultimately water balance (Zhang, Chiew et al. 2008). Although LAI is a critical variable in evapotranspiration, it should be noted that it is also an important structural parameter driving biophysical processes such as transpiration and precipitation interception which in turn influence hydrological processes such as the provision of water by stream flow, superficial runoff as well as the absolute water balance (Boussetta, Balsamo et al. 2013, Li, Wang et al. 2016).

Results showed that two studies (Yu, Pypker et al. 2012, Sibanda, Onisimo et al. 2021) utilized remote sensing methods to understand the impact of CSC on the hydrological cycle. CSC is an important attribute in controlling actual canopy interception which determines the amount of water reaching the ground (Ochoa-Sánchez, Crespo et al. 2018). It is an important component of the water balance influencing hydrological processes such as run-off, erosion, infiltration, and flood generation (Tsiko, Makurira et al. 2012). An understanding of such hydrological processes is crucial in understanding water redistribution within grassland ecosystems which is important for water management. Additionally, CSC is a prominent variable that depends on various canopy structural parameters including biomass and LAI (Xiong, Chen et al. 2021). The dense canopy coverage of grasslands biomass means high LAI which reduces surface run-off, thus leading to aquifer water recharge, water flow regulation and balance amongst other elements.

Results in this study show that there are very few studies that considered the utility of DEM derived topographic metrics in estimating water-related grassland ES. DEM provide ecohydrological information on the profile of the terrain regarding its direct impact on nutrient resources and moisture availability for plants, its impact on hydrological components such as

runoff percolation and how these variables interact with each other (Lukyanchuk, Kovalchuk et al. 2020). The work by Sibanda, Onisimo et al. (2021) concluded that topographic variables such as Topographic Wetness Index, maximum curvature and aspect were important in characterising eco-hydrological proxies such as LAI and CSC that are associated with hydrological ES. There is, therefore, a need for more research efforts to be exerted towards understanding the impact and contribution of topographic variables in mapping and monitoring water-related grassland ES using remotely sensed data.

3.4.3. Limitation of the study

In conducting the literature search, some studies were unavailable in full length, and others were not written in English. This may have a negative effect on quantifying all the studies which focus on grassland ES. More so, the exclusion of these studies has an impact on the spatial distribution of grassland ES studies.

The fundamental basis of utilising remote sensing technologies is based on their reliability to provide accurate spatially explicit information. This implies that accuracy assessment and validation of remotely sensed data is essential for decision making and sustainable ecosystem monitoring. However, in this study R^2 was used as the indicator of prediction accuracy since other accuracy assessment measures are based on different SI units of measurement. It is important to note that R^2 is one performance value amongst other parameters such as RMSE, relative root mean square error (RRMSE), standard error of prediction (SEP). It also must be outlined that R^2 assesses the goodness-of-model-fit. Furthermore, accuracy assessment parameters associated with remotely sensed data models, inclusive of R^2 , are impacted by many factors that include data sample size, sampling techniques, sensor type, vegetation indices or modelling approach being applied. That needs to be also considered in interpreting and contextualising the findings of this study.

Considering that we intended to explore whether there were generally significant differences in the accuracies derived using different sensors, algorithms, or vegetation indices, we assumed that the international peer review system followed by each of the journals considered in this study was sufficient and robust in evaluating the credibility and verification of the accuracies presented in each article.

3.4.4. Research gaps and opportunities

The following gaps and opportunities have been identified from the results of this study in the context of applications of remote sensing technologies in grassland ES studies:

- Considerable gaps still exist around the world and more specifically in the African continent on the integration of remote sensing into grassland ES.

- Grasslands provide more ES than the ones stated in this review. For instance, grasslands offer ES that are related to the hydrological cycle such as the canopy storage capacity, facilitation of infiltration and underground water storage refills. There is paucity of literature on the application of Earth observation data in quantifying the full range of such grassland ES. Meanwhile, some of these ES such as CSC that are related to LAI, can be characterized using remotely sensed data. LAI is arguably the most important vegetation structural parameter responsible for water and carbon exchange of vegetated land surfaces. Spatial distribution of LAI has an impact on the total water interception by plant canopy which directly influence plant CSC. Remotely sensed LAI and CSC data combined with remote sensing algorithms have a clear advantage of modelling ecohydrological processes (evapotranspiration, run-off, precipitation interception, surface water variability) which are crucial for understanding water balance within grasslands.
- The application of remote sensing technologies for estimating biomass in relation to water management has not attracted significant attention from the research community. Remote sensing-based modelling can be a useful tool for large scale prediction or estimation of surface water supply within grasslands. Remotely sensed biomass data can be used as an input in hydrological models. Such data can be simulated with run-off datasets to predict surface water supply.
- Erosion regulation can be estimated using remote sensing-based vegetation indices such as modified normalised vegetation index (mNDVI), normalized difference soil index (NDSI) and tasselled cap transformation (TCT) based vegetation indices. These indices are frequently used to investigate soil exposure, assess soil properties and estimate soil erosion processes (Xu, Hu et al. 2019).
- There is a paucity on studies that have sought to evaluate the influence of variations in topographic metrics on water-related grass ES. The integration of vegetation indices and topographic metrics may provide robust models capable of predicting water-related grasslands ES especially at local scales.
- Integration of remote sensing data and public participation geographic information systems (PPGIS) may be useful for quantitative evaluation of cultural services offered by grasslands. PPGIS pertains to the use of geographic information systems to produce local knowledge with the goal of including and empowering marginalized populations (Brown, Montag et al. 2012). Remote sensing of land use/land cover changes and local spatial knowledge may help in understanding how social and ecological systems are interacting over time. Also, PPGIS may help integrate people's cultural values to grasslands ecosystems. The capabilities of PPGIS have been

successfully implemented to assess ES provided by wetlands (Loc, Park et al. 2021) and protected forests (Peng, Liu et al. 2019).

- There is also need to consider the impact on newly launched sensors such as Landsat 9 OLI in characterizing water-related grasslands ES.

3.5. Conclusion

The objective of this study was to conduct a systematic review of literature, specifically assessing progress, identifying research gaps and opportunities on the application of remote sensing technologies in quantifying grassland ecosystem services, with particular attention to water-related services. Nine-grasslands ecosystem services were mentioned in the reviewed studies with forage provision, climate regulation and primary production having the highest frequencies. Over the past decade, grassland ES studies have experienced exponential growth, reaching a total of 222 published articles in September 2021. The results show that the integration of remote sensing technologies into grassland ES has been well incorporated. This is explained by the ability of Earth observation sensors-systems, vegetation indices and remote sensing algorithms to quantify and map several ES with considerable high prediction accuracies. Grass biophysical parameters such as biomass, LAI and CSC are prominent attributes for understanding hydrological processes and water balance within grasslands. The remote sensing-based estimation of such parameters in relation to water management is still in infancy. In this regard, there is room for more research efforts in understanding their effective contribution to the hydrological cycle which is important in water management.

Chapter 3 Appendix

Table 3.3: Additional remote sensing algorithms applied in the studies.

	Algorithm	Application	Results	Reference
Machine learning Algorithms	Adaptive neuro-fuzzy inference system (ANFIS)	Grassland yield estimation	$R^2 = 0.86$ & $RMSE = 11.07$ kgDM / ha	(Ali, Cawkwell et al. 2014)
	Extremely randomised trees (ETR)	Classifying grassland types	OA > 87.4% Kappa > 85%	(Barrett, Nitze et al. 2014)
	Classification and regression trees	Species distribution modelling	OA = 90.62% Kappa = 79.07%	(De Simone, Allegranza et al. 2021)
	Cubist regression trees	Canopy cover Aboveground biomass	$R^2 = 0.67$ & $RMSE = 14.4\%$ $R^2 = 0.68$ & $RMSE = 76.9$ g m ⁻²	(John, Chen et al. 2018)
	Stochastic gradient boosting	Grass nutrients	R^2 range of 0.65-0.72 RMSE range of 2.42 to 3.11% DM	(Singh, Mutanga et al. 2018)
	Decision trees	Pasture productivity	90.9% prediction accuracy	(Zhang, Valentine et al. 2006)
	High-Accuracy-Surface-modelling (HASM)	Aboveground biomass	$R^2 = 0.8459$ & $RMSE = 29$ g/m ²	(Zhou, Li et al. 2021)
Production Efficiency models	Alpine vegetation model (AVM)	GPP	$R^2 = 0.857$ & Conversion co-efficient 19.91 g C m ⁻²	(Li, Wang et al. 2013)
	Vegetation photosynthesis model (VPM)	GPP	GPP predicted relative error range 1.4 to 7.4%	(Li, Yu et al. 2007)
	MODIS MOD 17 Net Primary Production Product	Aboveground NPP	Average NPP = 2163 kg ha ⁻¹ (paired t-test, $t = 2.43$, d.f. = 16, $P_{2-sided} = 0.027$).	(De Leeuw, Rizayeva et al. 2019)
	Soil-leaf-canopy radiative transfer model	LAI BIOMASS	$R^2 = 78\%$ & $NRMSE = 30\%$ $R^2 = 90\%$ & $NRMSE = 47\%$	(Schwieder, Buddeberg et al. 2020)
	Plant canopy mortality model	Biomass carbon storage Carbon density	4.95Tg, 4.53Tg, 4.80Tg (1Tg=1×10 ¹² g) in 2002, 2005 and 2009 43.41 g/m ² , 39.69 g/m ² , 41.36 g/m ² respectively in 2002, 2005 and 2009.	(Chen, Wu et al. 2015)
	Canopy height model	Canopy height Aboveground biomass	$R^2 = 0.90$, $RMSE = 19.79$ cm & $rRMSE = 16.5\%$, $p < 0.001$ $R^2 = 0.89$, $RMSE = 91.48$ g/m ² , $rRMSE = 16.11\%$, $p < 0.001$	(Zhang, Sun et al. 2018)
	MODIS GPP	GPP	Mean GPP = 353 and 375 g C m ⁻² for 2000 & 2001 respectively	(Zhang, Wylie et al. 2007)
	Piecewise regression GPP	GPP	$r = 0.82-0.98$ and $d = 0.71-0.97$ cross validation with tower-based GPP mean GPP = 402 and 431 g C m ⁻² for 2001 and 2001	(Zhang, Wylie et al. 2007)
	Biome BGC	GPP	$R^2 = 0.94$ & $RMSE=0.95$ gC/m ² /da $R^2 = 0.83$ & $RMSE=0.48$ gC/m ² /da $R^2 = 0.68$ & $RMSE=1.66$ gC/m ² /da	(You, Wang et al. 2019)
	GLOPEM-CEVSA	NPP	Adjusted $R^2 = 0.80$ ($p < 0.01$).	(Ye, Huang et al. 2019)

Algorithm	Application	Results	Reference
Defoliation formulation model	NPP	Annual NPP predicted between 1982-2011 = 179.41 gC·m ² yr ⁻¹ . Increase rate per time period 1.18 gC·m ² yr ⁻¹ (Adjusted R ² = 0.63, p < 0.01)	(Ye, Huang et al. 2019)
Bayesian model data fusion (MDF)	Biomass Carbon balance	r = 87.5% (biomass harvest) r = 83% (biomass annual yields) r = 0.80 overlap = 90% (grazing intensity)	(Myrgiotis, Harris et al. 2021)
LINGRA	Grass yield	Average normalised error between observed and predicted: 14% for irrigated grass 19% for non-irrigated grass	(Schapendonk, Stol et al. 1998)
Boreal Ecosystem Productivity Simulator (BEPS)	NPP GPP	Total NPP = 2.235 GtC Mean NPP = 235.2 gC m ⁻² yr ⁻¹ Total GPP = 4.418 GtC Mean GPP = 465 gC m ⁻² yr ⁻¹	(Feng, Liu et al. 2007)
Improved Solar-energy efficiency	NPP	Total NPP = 2.9×10 ¹³ gC/a in 2006, with an average of 261.01 gC/m ² ·a.	(Wang and Yang 2012)
Multivariate analysis techniques	Principal Component regression	Biomass R ² = 0.31 & RMSE = 2.48 g/m ²	(Darvishzadeh, Skidmore et al. 2014)
Hydrological models	Soil-vegetation-atmosphere transfer (SVAT)	Canopy evapotranspiration Transpiration Correlation between ET measured from Eddy covariance method and SVAT (r ² = 0.85; ET-SVAT = 0.91 × ET-Eddy + 0.05). 5 July = (0.39 × LAI + 4.3, r ² = 0.64, P < 0.001 31 July = (0.15 × LAI + 4.0, r ² = 0.32, P < 0.001).	(Shimoda and Oikawa 2008)
BROOK90	Evapotranspiration	Explained model variance range R ² = 0.54-0.98 Nash-Sutcliffe model efficiency (E _{NS}) range = 0.53-0.82	(Vetter, Schaffrath et al. 2012)
BROOK90	Evapotranspiration	BROOK90 mean coefficient of variance (CV) range = 25%-75%. Correlation between BROOK 90 and MODIS evapotranspiration data R ² = 0.63, n = 160	(Schaffrath and Bernhofer 2013)
Rangeland Hydrology and Erosion Model (RHEM)	Rainfall run-off	Total run-off volume R ² range = 0.53 to 0.54 & PBIAS % range = -50.33 to -113.27 Peak run-off R ² range = 0.50 to 0.53 & PBIAS % range = -2.71 to -56.56.	(Kautz, Collins et al. 2019)
Two Source Energy Balance Atmosphere Land Exchange Inverse (TSEB ALEXI)	Evapotranspiration	TSEB RMSE = 0.421 mm day ⁻¹ DisALEXI MOD RMSE = 1.877 mm day ⁻¹ DisALEXI MOD vs TSEB RMSE = 1.75 mm day ⁻¹	(Castelli, Anderson et al. 2018)
NOAH Land Surface Model	Soil moisture Evapotranspiration Energy balance components	Predicted soil moisture range = 3-25Vol.% & Root zone moisture = 60-120 mm Predicted ET range = 0 mm-75 mm Predicted energy balance range = -10-150 MJ/m ² /day	(Sridhar and Wedin 2009)
Water cloud model	Soil moisture	RMSE = 4.7 & 7.5 Vol.% Bias = 0.7 & -0.4Vol.%	(El Hajj, Baghdadi et al. 2015)
Water cloud model	Soil moisture	R ² = 0.7075, RMSE = 3.3219 m ² / m ²).	(Xing, He et al. 2014)

Algorithm	Application	Results	Reference
GEOTop Hydrological model	Soil moisture content	$R^2 = 0.2$, RMSE = $0.13 \text{ m}^3/\text{m}^3$ & bias = $-0.02 \text{ m}^3/\text{m}^3$	(Bertoldi, Della Chiesa et al. 2014)
Process based models	Water productivity	R^2 range = 66.5-75.3 & Water productivity estimate range = $11.8\text{-}42.6 \text{ kg ha}^{-1} \text{ mm}^{-1}$.	(Qi, Murray et al. 2017)

4. Land use land cover changes in a typical communal area in Southern Africa

X Zuma, O Mutanga, T Bangira and M Sibanda

4.1. Introduction

Rangelands around the world have become one of the most threatened ecosystems due to human activities and climate variability (Abdulahi, Hashim et al. 2016). These landscapes provide important ecosystem services such as the provision of food, carbon sequestration, biodiversity maintenance, fibre, clean water, recreational space, and wildlife habitat (Sala, Yahdjian et al. 2017, Boone, Conant et al. 2018, Zhao, Liu et al. 2020). The human population highly depends on rangelands for food production considering that several agricultural activities are conducted in grasslands. According to Bedunah and Angerer (2012) about 1.2 billion people who are surviving on less than \$1 per day depend on rangelands. The limited management of rangelands in developing countries makes it difficult to determine the level of grass degradation (Bedunah and Angerer 2012). As the human population increases, food production is also anticipated to increase by about 75% in the next 30 years (Ceballos, Davidson et al. 2010, Bedunah and Angerer 2012). This will exert a lot of pressure on rangelands as they will be converted into croplands to produce more food, similarly development of infrastructure and land use activities such as overgrazing and unmanaged farming practices will cause rangeland fragmentation and biodiversity loss (Palmer and Bennett 2013). Meanwhile, a large population depends on rangelands for livestock production, food and income generation (Abdulahi, Hashim et al. 2016). However, the limited monitoring and management strategies of rangelands in the communal areas of developing countries make it difficult to determine the level of grass degradation (Bedunah and Angerer 2012). In South Africa, about 60% of the grassland biome has been transformed while 25% has been degraded, with approximately 15% remaining unchanged and only 2% being protected (Little et al. 2015). The lack of management of grasses in unprotected areas exacerbates the degradation of rangelands as there are limited comprehensive criteria for assessing their condition and state of fragmentation (McGranahan and Kirkman 2013). Hence there is need for spatially explicit non-invasive techniques for assessing and monitoring the spatial extent and the magnitude of grassland fragmentation for sustainable utilisation of this natural capital.

The advent of earth-observation (EO) facilities has offered fast, efficient and reliable spatially explicit techniques of monitoring the extent of fragmentation and the spatial distribution of grasslands (Jin, Yang et al. 2014). Furthermore, EO facilities offer data that is frequently acquired, with high spatial and spectral resolutions, suitable for monitoring grassland attributes at local to regional scales (Ali, Cawkwell et al. 2016). In this regard, remote sensing

(RS) techniques have been widely used for monitoring rangelands attributes such as biomass (Sibanda, Mutanga et al. 2017), water content (Sibanda, Mutanga et al. 2019) and their phenology (Matongera, Mutanga et al. 2021). Other than monitoring grass attributes, remote sensing techniques have also been widely applied in characterising land use and land cover changes based on a variety of classification algorithms and datasets. The most widely used EO sensors in mapping LULC changes have been from the Landsat mission (Abd El-Kawy, Rød et al. 2011). This is attributed to the fact that Landsat boasts of being the world's longest uninterrupted mission serving remotely sensed data over the land and sea (Ul Din and Mak 2021). Specifically, Landsat 1/2/3 Multi-Spectral Scanner (MSS), Landsat 5 MSS and Thematic Mapper (TM), Landsat 7 Enhanced Thematic Mapper plus (ETM), and Landsat 8 Operational Land Imager (OLI) provide remotely sensed data at a 30 m pixel size, 16 days intervals archived since 1972 to date making it suitable for historical mapping of LULC changes (Loveland and Dwyer 2012, Li, Dong et al. 2020). Subsequently, Landsat datasets offer better prospects of objectively detecting, mapping and monitoring the spatial and temporal variations of grassland fragmentation in communal rangelands (Xie, Phinn et al. 2019).

Literature underscores the importance of integrating multi-temporal datasets with robust algorithms in accurately mapping LULC changes (Ghayour et al. 2021, Kafy et al. 2021). Specifically, machine learning algorithms are the most renowned techniques in image classification for assessing LULC changes due to their greater accuracy and efficiency (Ghayour, Neshat et al. 2021, Kafy, Shuvo et al. 2021). Random forest (RF) classifier is one of the machine learning algorithms that is widely renowned for its robustness in mapping LULC changes, especially in conjunction with multi-spectral and hyperspectral remotely sensed datasets (Talukdar, Singha et al. 2020). Specifically, RF is widely recognised in the community of practice because of its excellent management of outliers and noisy datasets, great performance in dealing with high dimensional and multi-source datasets as well as its attainment of higher accuracies when compared to other classifiers such as the Support Vector Machine (SVM) and Maximum Likelihood Classifier (MLC) (Sheykhmousa, Mahdianpari et al. 2020, Cengiz, Budak et al. 2023). RF uses decision trees during classification, such that the trees with the most selections define the class. To date, the algorithm is the most widely used classifier in conjunction with Landsat data in assessing LULC changes (Rodriguez-Galiano, Ghimire et al. 2012, Thanh Noi and Kappas 2017, Phan, Kuch et al. 2020).

Despite the optimal performance of RF and Landsat data in LULC change assessments for the sustainable management of natural resources, the provision of large-scale land cover

change maps of grasslands is often inhibited by elements such as spectral complexity due to the heterogeneity of the environment as well as the limitation of software/hardware resources to store and process large remotely sensed datasets (Rodriguez-Galiano, Ghimire et al. 2012, Wahap and Shafri 2020). The development of cloud computing platforms such as Google Earth Engine (GEE) has emerged as an invaluable resource for addressing data management challenges in applications such as mapping largescale LULC changes (Wahap and Shafri 2020). GEE is a free cloud-based platform which can be used for large-scale environmental analysis or mapping (Tamiminia, Salehi et al. 2020). GEE, has vastly improved the access and processing of satellite imagery making it possible to conduct assessments on the spatial and temporal variations of community-shared natural resources such as the communal rangelands (Tamiminia, Salehi et al. 2020). The platform provides a large amount of satellite data including Landsat, dating back to the 1970s, while it is capable of administering renowned algorithms such as the RF on the available datasets (Gorelick, Hancher et al. 2017, Wang, Xiao et al. 2017, Kumar and Mutanga 2018). Single date Landsat remotely sensed data sets have been widely used in remote sensing LULC (Langley, Cheshire et al. 2001, Abd El-Kawy, Rød et al. 2011). However, grasslands are highly variable ecosystems which are greatly impacted by situational factors such as seasonality of precipitation, and variations in management practices (Cleland, Collins et al. 2013). This makes it challenging to characterise the spatial and temporal changes of grasslands based on single-date images (Price, Egbert et al. 1997). Considering the relative accessibility of high spatial and temporal Landsat data coverage and the robustness of the RF algorithm, all embedded in GEE, presents opportunities for establishing cheap and reliable grassland monitoring techniques. Therefore, the objective of this study was to assess the spatiotemporal variability of rangelands within a typical southern African communal area from the year 2000 to 2020 using multi-temporal Landsat datasets in conjunction with random forest. The study also sought to assess the magnitude and extent of grassland fragmentation in these communal rangelands using fragmentation statistics.

4.2. Methods and Materials

4.2.1. Study Site

This study was conducted in Inhlazuka (centre coordinates 29° 55' 40" E and 30° 11' 34" S) and Vulindlela (centre coordinates 29° .40' 37.3584" S and 30°. 8' 13.6572" E) communal rangelands located in the uMgungundlovu District Municipality under the uMngeni Catchment in the province of KwaZulu-Natal, South Africa (Figure 4.1). The catchment hosts the country's second largest economic hub and its largest trade port (Hughes, De Winnaar et al. 2018).

Activities such as agriculture and urbanisation are causing immense pressure on the catchment's natural resources (Hughes, De Winnaar et al. 2018). The catchment is mostly covered by grasslands, with much of its grasses being turned into cultivated land (Hughes, De Winnaar et al. 2018). Vulindlela is located in the west of Pietermaritzburg and northwest of the Greater Edendale area, while Inhlazuka is located under the Richmond municipality and is a mountainous area with an elevation of 1313 metres. The areas of Inhlazuka and Vulindlela are rural settings with high levels of poverty. Vulindlela experiences dry winters and hot wet summers and receives on average an annual rainfall of 979 mm (Sibanda, Onesimo et al. 2021). The growing season in Vulindlela starts in October and ends in April, from late April to August frost conditions begin, where the growing season is restricted (Sibanda, Onesimo et al. 2021, Royimani, Mutanga et al. 2022). The average rainfall received by Inhlazuka is 852 mm which starts in October and ends in April (Mncube 2022). Land use activities in Vulindlela include scattered settlements, grazing land, cultivated lands, pockets of indigenous forest and some major timber plantations while Inhlazuka is predominantly characterised by small and large-scale crop farming lands. Vegetation in Inhlazuka is also characterised by bushveld vegetation, which is heavily invaded by alien vegetation, such as bugweed (*Solanum mauritanum*), Lantana camara and bramble (*Rubus spp*) which are often cleared but persisting.

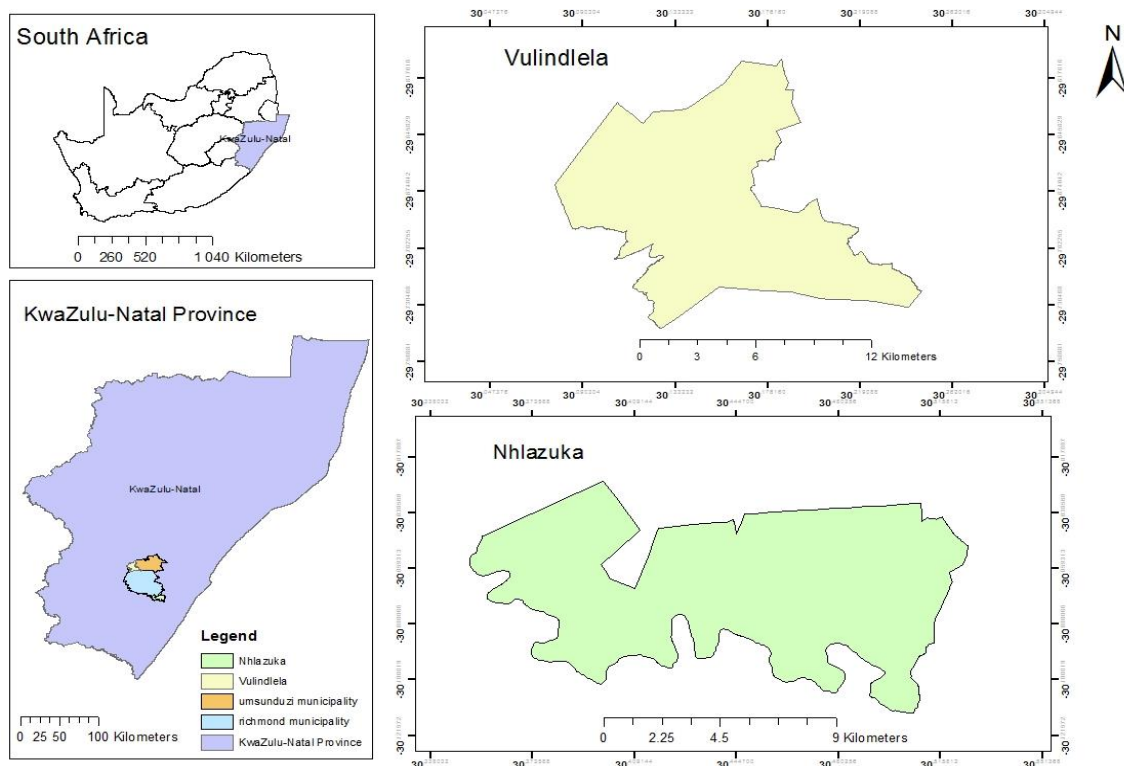


Figure 4.1: Inhlazuka and Vulindlela communal areas In Pietermaritzburg, KwaZulu-Natal South Africa.



Figure 4.2: Typical communal rangeland areas in a) Vulindlela and b) Inhlazuka.

4.2.2. Satellite Data

The study utilised cloud-free and atmospherically corrected multi-temporal Landsat 7 and Landsat 8 Top of atmosphere (TOA) reflectance remotely sensed data to characterise land covers in the years 2000, 2010, and 2020. The GEE platform provides pre-processed images that will have gone through atmospheric correction. These images were selected and used to conduct the classification in the GEE platform (Gorelick, Hancher et al. 2017). The study also used the median reducer for image processing. The median reducer applies a tile by tile processing method where each scene is divided into several tiles, which results in each tile being sent to various Google servers, to be processed (Sidhu, Pebesma et al. 2018). The servers work in parallel and independently to one another and the end result of the processing method is the reduced image(s) which is the outcome of the reconstruction of the tiles (the median reducer produces a single image constructed from the different tiles of satellite images) (Sidhu, Pebesma et al. 2018). All images used in the study were projected to the Universal Transverse Mercator (UTM) coordinate system 1984, zone 36 south.

The dry season/winter images were selected, downloaded, and used to characterise the rangelands. This is because during the summer season the sky is often overcast and there is a lot of crop farming occurring. To avoid the misclassification of the rangelands as croplands, the dry season images (June, July, and August) were. Specifically, available cloud free multi-temporal images covering the dry season were selected and used in this study.

4.2.3. Classification and Change Detection

Classifications were conducted using a stack of multiple images on the GEE platform covering the dry season of each of the years 2000, 2010 and 2020. These images were acquired during dry season months (June, July, and August). A median reducer in the GEE platform was used

to compile and average all the images obtained during the dry season of each year. The GEE median reducer function reduces image collections by calculating the median of all values at each pixel across the stack of all matching bands to produce a single image. In addition, this process does not only reduce image data volume but equally produces high accuracies same as the time series data and improves classification accuracies (Carrasco, O'Neil et al. 2019, Phan, Kuch et al. 2020). The advantage of using the median reducer is that it significantly reduces the volume of data thus making it easier and faster to process and analyse the bulky remotely sensed data (Phan, Kuch et al. 2020). Above all, the utility of multi-temporal images avoids the possible impact of atmospheric influence on the spectral signatures while addressing the spectral variability of grasses induced by the variability of grass species and their management practices (Carrasco, O'Neil et al. 2019). The Random Forest Classifier was then used to discriminate and map rangelands from other LULC types. In utilising the RF, the three hyperparameters, *ntree*, *mtry* and *nodesize* were tuned accordingly (Odebiri, Mutanga et al. 2020). Specifically, the *ntree*, which is the number of regression trees used during observation performance was set to be at 500 (Mutanga, Adam et al. 2012). After iterations, the optimal *ntree* identified and used in this study was 100. The *mtry* which is the number of predictors tested at each node was set to a default value which was the square root of the number of variables considered in this study. Lastly, the node size which is the minimal size of the terminal nodes of the trees was set to 1 (Mutanga, Adam et al. 2012). Sampling points covering various LULC classes were collected during a field survey. However, sampled points for the previous years (2000 and 2010) were verified using Google Earth Pro (Ghorbani and Pakravan 2013, Pu, Sun et al. 2020). Feature classes that were used in the classifications were bare-land (areas that were not covered by any vegetation and were mostly bare soil), grasslands (areas that were covered by grasses only), forests (areas covered by indigenous forests or timber plantations), water (all water bodies such as rivers, and streams) and built-up area (areas where there were buildings and concrete surfaces). Furthermore, vegetation indices were computed and used to characterise the spatial variation of the rangelands. Specifically, the Normalized Difference Vegetation Index (NDVI), the Soil Adjusted Vegetation Index (SAVI), the Green Normalized Difference Vegetation Index (GNDVI), the Normalized Difference Water Index (NDWI), the Infrared Percentage Vegetation Index (IPVI), the Visible Atmospherically Resistant Index (VARI), the Ratio Vegetation Index (RVI), the Difference Vegetation Index (DVI) and the Enhanced Vegetation Index (EVI) were computed and used in this study. These indices were selected and used in this study based on their optimal performance in literature (Xue and Su 2017, Ranjan, Chandel et al. 2019, da Silva, Salami et al. 2020). Vegetation indices were also considered in this study because they have been

proven in literature to improve accuracies while resisting the noise from the sun, topography and clouds, atmospheric changes, and soil background signals (Xue and Su 2017).

4.2.4. Rate of Change

Using the classified image, the spatial extent of each land cover type was computed in a GIS environment. The Rate of change (ROC) in the spatial extent of grassland patches were calculated to understand the magnitude of change in their spatial extent in relation to other land cover types and across different years. The study also sought to assess the extent of grassland cover fragmentation as a measure of rangeland degradation. To conduct this, the classified maps were exported from GEE into ArcMap where the spatial extent (area) of each land cover class was calculated for the three periods. The grassland cover classes were then extracted for fragmentation analysis. Fragstats 4.2 was utilised to compute and characterise the extent of grasslands fragmentation. Fragmentation was calculated at the class level metrics. Specifically, landscape (PLAND), the number of patches (NP), patch density (PD), largest patch index (LPI), patch area (AREA_MN), Euclidean nearest neighbour distance (ENN_MN) and effective mesh size (MESH) were computed and used to assess the extent of fragmentation and as a proxy for rangeland degradation (Figure 4.3). To measure the degree of fragmentation within the rangelands, the NP, PD, LPI were specifically used and the AREA_MN, ENN_MN, PLAND and MESH were utilised to measure extent of grass patches spatial dispersion (Parker and Mac Nally 2002, Midha and Mathur 2010). These Fragmentation metrics were derived from each of the time periods considered in the study and were compared using the analysis of variance test after the data did not significantly deviate from the normal distribution.

Table 4.1: Class level Fragmentation Metrics and their descriptions

Name	Abbreviation	Description
Percentage of Landscape	PLAND	PLAND is described as the 'Area and Edge metric'. It represents the landscape percentage belonging to each class. PLAND is 0 when the proportional class area is decreasing and is equal to 100 when one big patch is present.
Number of Patches	NP	Determines the number of subpopulations in a spatially dispersed population. (Number of patches can be used to determine fragmentation; the higher the number of patches, the more fragmented the class)

Name	Abbreviation	Description
Patch Density	PD	Refers to the number of patches of corresponding patch type divided by total area. (The higher the density of a particular class, the more fragmented it is)
Patch Area	Area MN	Is the average size of patches in a particular of a specific land cover type. It can be computed at the class level, or at the landscape level.
Largest Patch Index	LPI	Quantifies the percentage of the total landscape area compromised by the largest patch.
Effective Mesh Size	MESH	Quantifies the degree of landscape fragmentation. The effective mesh size is based on the probability that two randomly chosen points in a region will be in the same non-fragmented area of land. The higher the mesh size, the less fragmented a particular habitat is.
Euclidean Nearest Neighbor Distance	ENN_MN	The sum of the distance (m) to the nearest neighboring patch of the same type, based on the nearest edge to edge distance, for each patch of the Corresponding patch type, divided by the number of patches of this same type.

The study went on to utilize rainfall data to assess the influence of rainfall on the rangeland spatial distribution changes. Rainfall data was requested from the South African Weather Services (SAWS). The requested data from SAWS was of the years used for classifications (2000, 2010 and 2020) and nine weather stations surrounding the study areas were used by the study to calculate the rainfall patterns in Inhlazuka and Vulindlela by performing Interpolation with the use of ArcMap 10.6. The type of interpolation that was applied by the study was that of the Inverse Distance Weight (IDW). After the application of interpolation, grassland points collected on the field were then overlaid over the study areas to extract the rainfall data. After the extraction of the rainfall data in ArcMap, rainfall averages of the years 2000, 2010 and 2020 in both study areas were calculated with the use of Excel.

4.3. Results

4.3.1. Classifications

The land use land cover changes were classified into five classes which are grasslands, water, forest, built-up area and bareland. In assessing the performance of RF classification models based on spectral bands, vegetation indices independently and the combination of both vegetation indices, the ANOVA test showed that there were no significant difference in the overall accuracies. Subsequently, the classification based on combined datasets were used in this study and all results presented were based on these models. In classifying grasslands from other land cover classes, overall accuracies of 75%, 79% and 83% were obtained in Inhlazuka while accuracies of 89%, 85%, and 89% were obtained in Vulindlela for the years 2000, 2010 and 2020, respectively (Figure 4.3). Meanwhile, kappa accuracy scores of 65%, 68% and 73% were exhibited by the Inhlazuka images classification while Vulindlela exhibited scores of 81%, 75% and 83% for the years 2000, 2010 and 2020, respectively (Figure 4.3). Following a variable importance analysis, the most frequently optimal discrimination spectral features selected by RF across all classifications were Bands 5 and 7, the near infrared (NIR) and the short-wave infrared bands (SWIR), respectively (Figure 4.4)

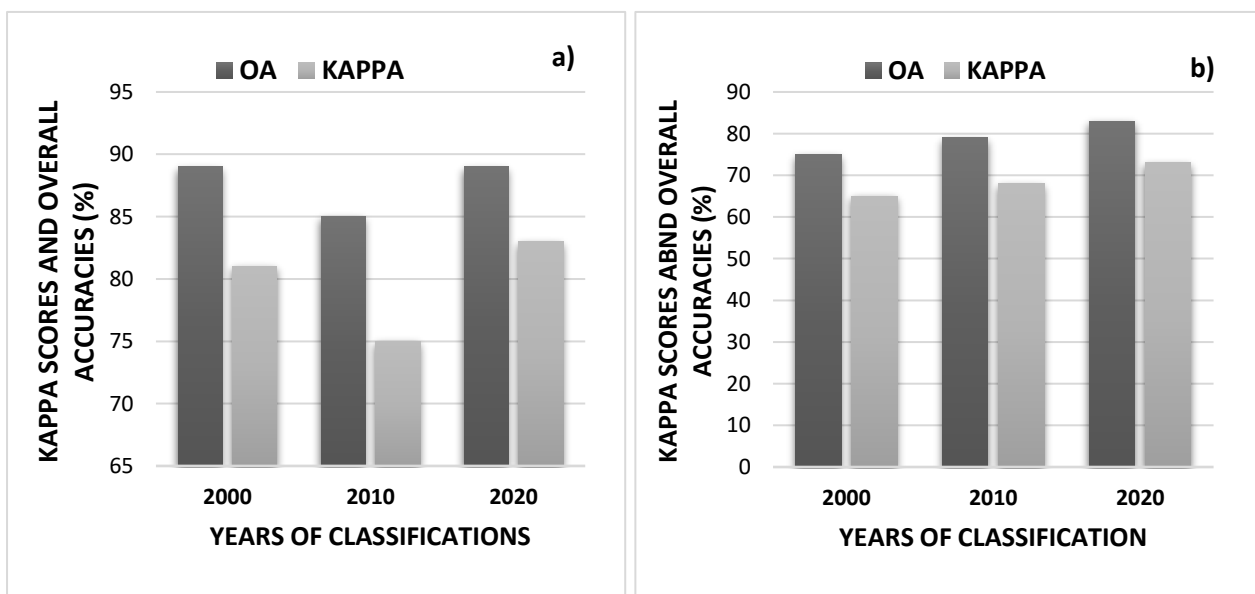
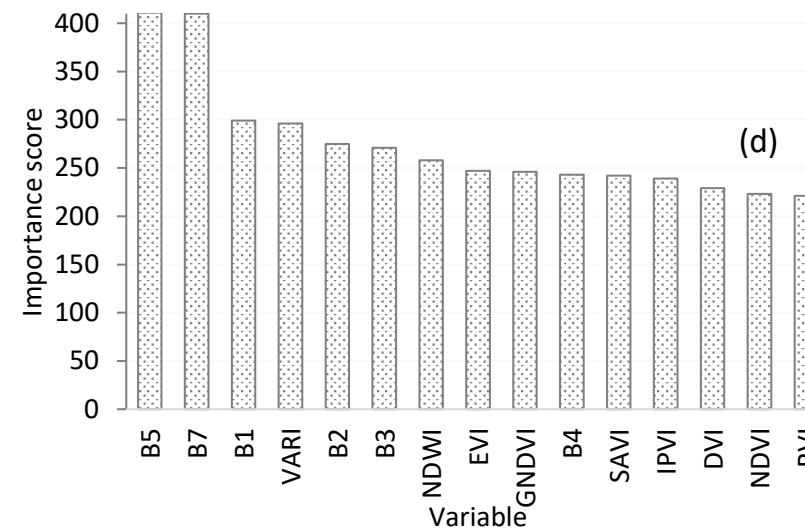
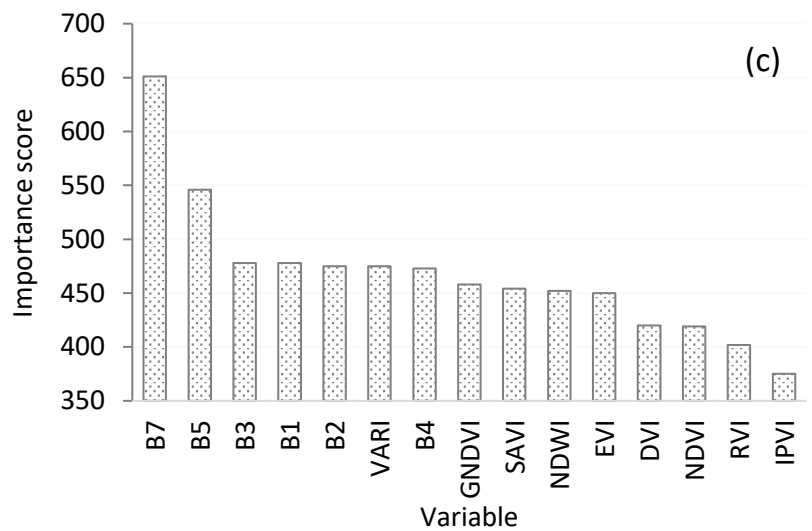
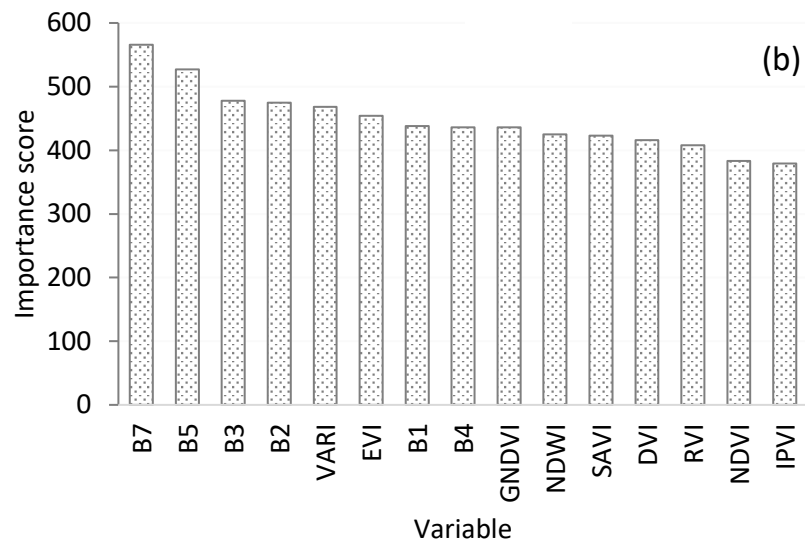
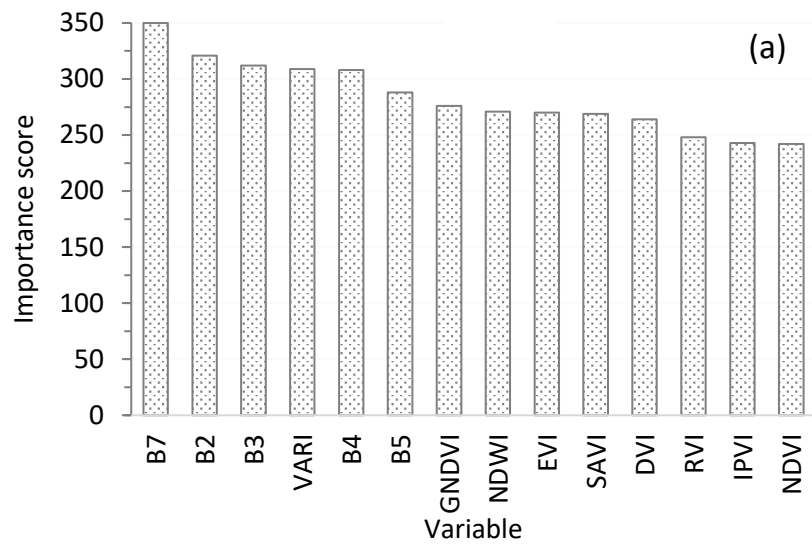


Figure 4.3: Classification overall accuracies and kappa scores in the areas of a) Vulindlela and b) Inhlazuka



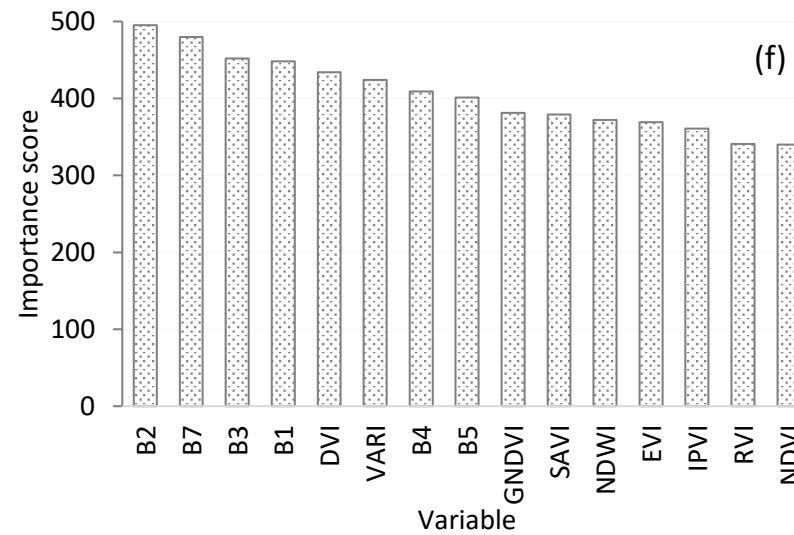
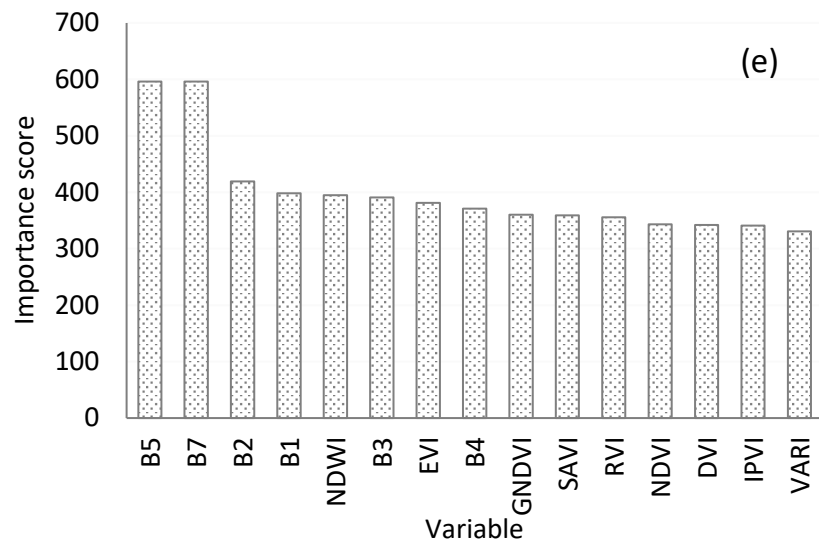


Figure 4.4: Variable importance scores from the image classifications in Vulindlela for the year a) 2000, b) 2010, and c) 2020 as well as Nhlazuka for the year d) 2000, e) 2010, and f) 2020. (NDWI = normalised difference water index, EVI = enhanced vegetation index, GNDVI = green normalised vegetation index, SAVI = soil adjusted vegetation index, RVI = ratio vegetation index, NDVI = normalised vegetation index, DVI = difference vegetation index, IPVI = Integrated Polarization Vegetation Index, and VARI = Visible Atmospherically Resistant Index)

A general decrease in spatial extent of grasslands was observed in Vulindlela from the year 2000 to 2020 while in Inhlazuka, a decrease in the areal extent of rangelands is observed between the years 2000 and 2010 and an increase between the years 2010 to 2020 (Figure 4.5 and 4.6). In Vulindlela, between 2000 to 2020, when grasslands were reduced, built up areas increased rapidly. Specifically, grasslands decreased at a rate of 37.52 hectares per year between the 2000 and 2010. Then from 2010 to 2020, grasslands further decreased at a rate of 76 hectares per year while settlement development continued to increase. Meanwhile, the increase in built-up area from the year 2000 to 2010 was at a rate of 43.15 hectares per year and at a rate of 114.55 ha per year from the year 2010 to 2020. In addition, there was also a relative increase in bareland between these periods, although not at the magnitude of increase in spatial extent of built-up areas.

Inhlazuka was mostly characterised by forests, shrubby vegetation and relatively less grasslands when compared to Vulindlela. The forest class increased between 2000 and 2010 by 86.54 hectares per year thus causing a decline in rangelands. Between 2010 and 2020, there was an increase in rangelands due to a decrease in forests at a rate of 113.84 ha per year. The decrease in rangelands in Inhlazuka between the periods of 2000 to 2010 was at 40.19 ha per year and the increase in rangelands experienced between 2010 and 2020 was at a rate of 45.27ha per year. In addition, in Inhlazuka there was also an increase in built-up areas at a rate of 41.7 ha/per year from 2010 to 2020. However, the increase of built-up area in Inhlazuka did not cause a significant decrease in rangelands when compared to Vulindlela.

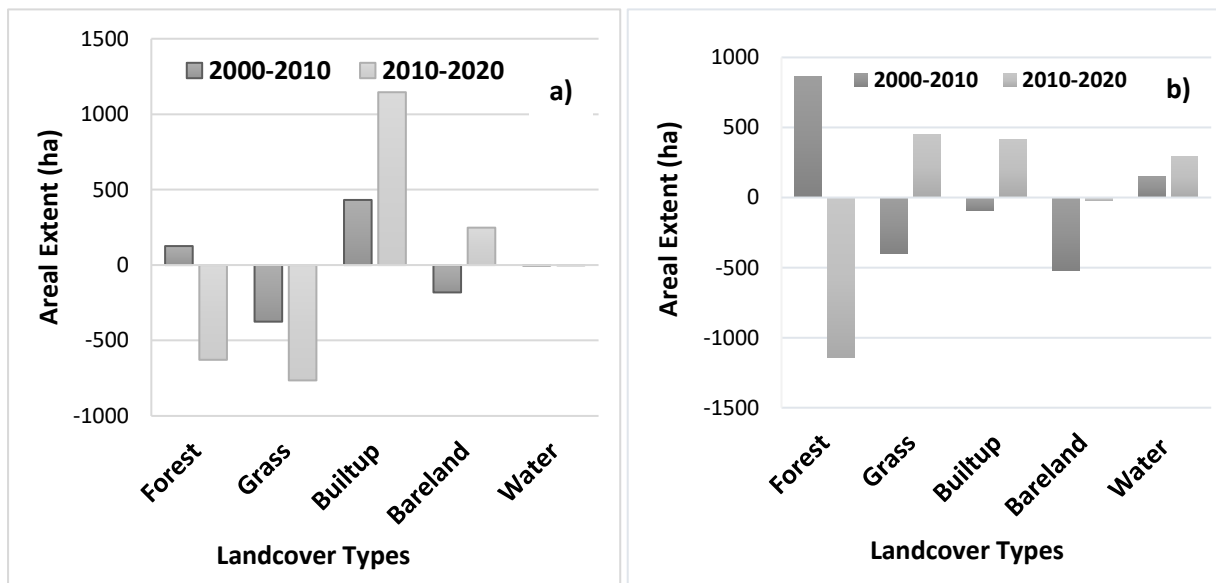


Figure 4.5: Changes in the mapped land cover types in a) Vulindlela and b) Inhlazuka

4.3.2. Changes in the Spatial Extent of Rangelands

The Vulindlela grasslands in 2000 occupied 7799.8 ha, which decreased to 7424.6 ha in 2010 then further decreased to 6660 ha in 2020 while in Inhlazuka, it decreased from 2516.7 ha in 2000, to 2114.7 ha in 2010 then increased to 2567.5 ha in 2020 (Figure 4.6 and Figure 4.7).

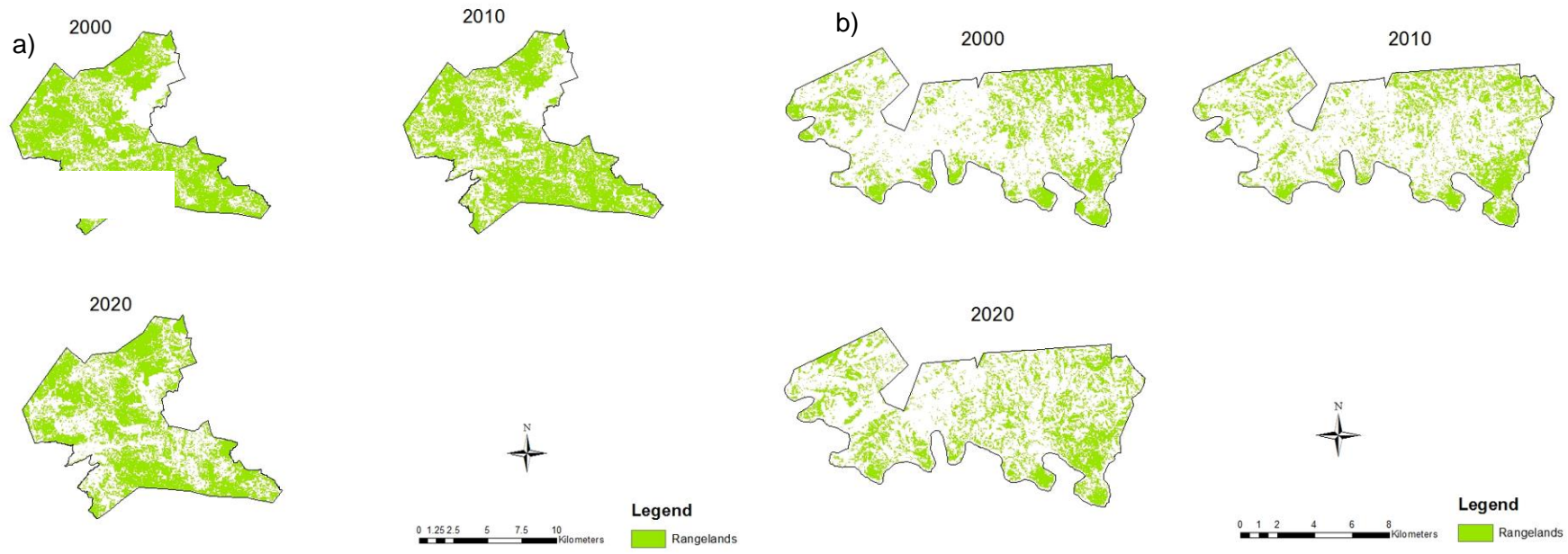


Figure 4.6: Spatial distribution of grasslands in a) Vulindlela and b) Inhlazuka from 2000 to 2020

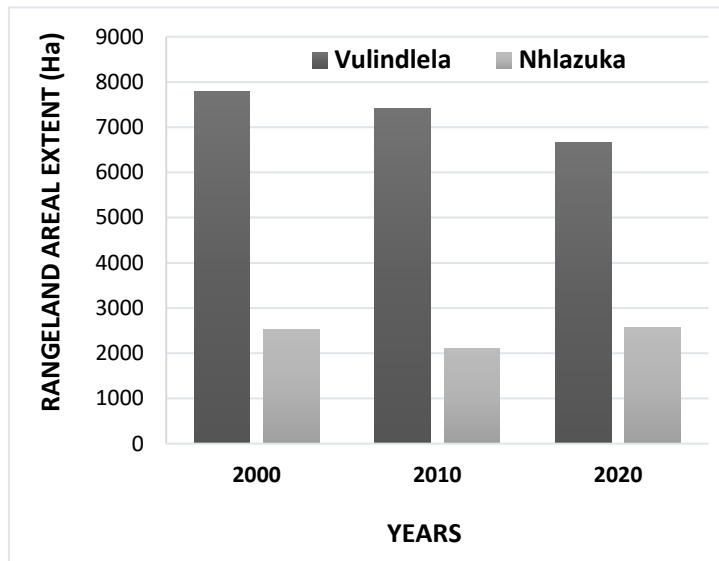


Figure 4.7: Changes in the rangeland spatial extent from 2000 to 2020 in Vulindlela and Nhlazuka.

4.3.3. Patch Analysis at Class Level Metric

Table 4.3 shows fragmentation statistics in Vulindlela and Nhlazuka. Percentage of Landscape (PLAND) decreased from 69.9, 59.6 between 2000, and 2020 indicating an increase in grassland fragmentation. The number of patches (NP) increased from 244 to 342 in 2010 and then it rapidly increased to 780 patches in 2020. The increment in the number of patches therefore is an indication of increased rangeland fragmentation in Vulindlela. Meanwhile, patch density increased from 21 in 2000 to 31.0 in 2010, then increased again to 6.9 ha in 2020 in Vulindlela. The mean patch area (AREA_MN) on the other hand decreased from 31.9 ha in 2000 to 8.5 ha in 2020. The largest patch index (LPI) decreased from 68.3ha in 2000 to 62.6ha in 2010. This further decreased to 43.0ha in 2020. The Euclidean nearest neighbour distance (ENN_MN) is an indicator of isolation within the patches that increased from 71.1 ha in 2000 to 74.7 ha in 2010 and finally increased to 8.5 ha in 2020. Lastly, the effective mesh size (MESH) decreased from 5204.4ha in 2000, to 4380.4 ha and subsequently to 2188.8ha in 2020.

In Nhlazuka, the NP increased from 1392 in 2002 to 1581 in 2010, then declined to 1443 in 2020. The PD was 15.4 in 2000, then it increased to 17.5 in 2010 then decreased in 2020 to 16.0. Meanwhile, the AREA_MN was 1.8 ha in 2000, and then it decreased to 1.3 ha in 2010, and then increased in 2020 to 1.7 ha. On the other hand, the ENN_MN was higher in 2000 and 2010 when compared to 2020, indicating that the grasses were more isolated in 2000 to 2010. The LPI decreased from 7.1 ha in 2000 to 3.5 ha in 2010 then increased to 5.4 ha in

2020, while the PLAND and MESH of grassland were relatively lower in 2010. The MESH size results also show that the rangelands were more fragmented in 2010 and in 2020 as compared to 2000.

Table 4.2: Vulindlela and Inhlazuka grassland patch metrics variations between 2000 and 2020

	GRASS	PLAND	NP	PD	LPI	AREA_MN	ENN_MN	MESH
Vulindlela	2000	69.9	244	2.1	68.3	31.9	71.1	5204.4
	2010	66.6	342	3.0	62.6	21.7	74.7	4380.4
	2020	59.6	780	6.9	43.0	8.5	73.0	2188.8
Inhlazuka	2000	28.0	1392	15.4	7.1	1.8	79.5	55.5
	2010	23.5	1581	17.5	3.5	1.3	79.3	20.8
	2020	28.6	1443	16.0	5.4	1.7	75.0	35.4

4.4. Discussion

This study sought to assess the spatial variation in the areal extent of the rangelands as well as their magnitude of fragmentation using a Landsat time series in conjunction with random forest in a typical communal rangeland of southern Africa between the years 2000, 2010 and 2020. Results of this study showed that the spatial variability of rangelands and other land cover types could be optimally mapped in Vulindlela and Inhlazuka, respectively based on the NIR (Bands 5) and short-wave infrared (SWIR) (Band 7) spectral variables in conjunction with RF in GEE platform. Specifically, overall accuracies (OA) of 75%, 79% and 83% in Inhlazuka as well as OAs 89%, 85%, and 89% in Vulindlela for the years, 2000, 2010, and 2020, respectively, were obtained in this study. The optimal performance of the NIR and short wave infrared (SWIR) bands could be attributed to their sensitivity to grass biochemical and physical properties such as foliar nitrogen, lignin and starch (Ramoelo, Cho et al. 2015, Zhao, Zhu et al. 2022). The NIR section of the electromagnetic spectrum is highly sensitive to the biochemical and biophysical properties of vegetation (Matongera, Mutanga et al. 2017, Mngadi, Odindi et al. 2021). Specifically, the foliar spongy mesophyll facilitates the high reflectance of the NIR energy by plants with a high vigour (Wang, Qu et al. 2008, Kumar, Arya et al. 2022).

The study results also showed that in Vulindlela, rangelands were rapidly being fragmented and converted into built-up and bare areas and a significant change in the spatial configuration of the grasslands was observed. This could be explained by population growth and the

demand for land to develop residential areas as well as increasing agricultural production as the major drivers of rangeland fragmentation in rural areas (Abdulahi, Hashim et al. 2016). According to the Municipality (2016) the population of Vulindlela in 2013 was 161 562 with an estimate of 85 033 structures. The population was estimated to grow at 2% each year to about 183 583, in 2020. The population increase could explain the rapid decrease in grasslands which are being converted into built-up areas (Figure 2.8) to accommodate the burgeoning population. There is growing body of literature which shows that activities such as housing development and overgrazing are the major anthropogenic activities that have extensively degraded rangelands globally (Lu, Kelsey et al. 2017, Dowdy, Ye et al. 2019). Also, the lack of effective livestock management practices, generally results in increased grazing activities with limited breaks given to the grassland ecosystem to self-regulate and recover from over grazing.

Meanwhile, in Inhlazuka, the spatial extent of rangelands decreased while the areal extent of built-up areas increased between 2000 to 2010. The decrease in the spatial extent of forest between 2010 to 2020 could be attributed to the increase in population and demand for residential areas. The increase in rangelands in Inhlazuka in 2020 could be explained by clearance of shrubby and tree like alien invasive species which is a typical exercise in Inhlazuka. Specifically, *Lantana camara* is the most dominant alien invasive plant in the rangelands of Inhlazuka. Lantana is said to be the most widespread alien invasive plant which invades agricultural and natural ecosystems (Parveen, Ravinder et al. 2011). For instance, Dube, Maluleke et al. (2022) makes an example of the Bushbuckridge area where the grasslands have been replaced by the alien plant lantana thus decreasing available forage for livestock and wildlife (Terefe 2015). To circumvent this, uMgungundlovu district municipality implements continuous alien invasive plant removal programmes regulating the variation in the spatial extent of grasslands especially in Inhlazuka. This then explains in the decreases and increases associated with the rangelands in Inhlazuka (Figures 2.7 and 2.6) between 2000, 2010 and 2020. If the alien plant species are not controlled, the communal rangelands of Inhlazuka may be at a risk of being replaced by the Lantana alien plant.

Results also showed that barelands in Vulindlela were increasing. This could be explained by the limited rangeland management interventions which are conducive for unregulated administration of fires. Fire as a management tool in rangelands, is used to improve forage quality and production, to manipulate plant populations (plant composition and structure) and maintain habitats for grazing animals (Little, Hockey et al. 2015). However, if fire is frequently and improperly administered, it becomes destructive. Specifically, it reduces the seedling recruitment of grasses, while burning and depleting the seedbanks on the topsoil

(Ghasempour, Erfanzadeh et al. 2022). Subsequently, the ground is exposed as bareland. Community members in Vulindlela customarily burn grass during the winter season as a tool to promote its growth as feed for livestock (Cho, Onisimo et al. 2021). However, this results in grass failing to recruit seedlings and replenish its populations as the seed banks will be depleted and the topsoil crusted by regular burns (Fidelis, Delgado Cartay et al. 2010, Ghasempour, Erfanzadeh et al. 2022). Literature also illustrates that in the forest and grasslands biomes in Southern Africa, the dominance of grasses or trees (forests) is a function of fire and precipitation (Accatino, De Michele et al. 2010, Baudena, Dekker et al. 2015).

Rainfall plays a significant role in the growth of vegetation (Beier, Beierkuhnlein et al. 2012, Lipiec, Doussan et al. 2013). The lack of rainfall in rangelands results in the decrease of forage and rangeland resources therefore, negatively impacting biomass productivity (Derner and Augustine 2016, Sibanda, Onisimo et al. 2021). This means that the compromised growth of rangelands as a result of the decrease in precipitation causes a decline in the spatial distribution of rangelands, as there is not enough soil moisture to provide conditions for growth, due to rainfall being the main driver of rangeland vegetation dynamics (Palmer and Bennett 2013, Polley, Briske et al. 2013). In Vulindlela, the spatial extent of the rangelands in the year 2000 was 7799.8 ha and the average rainfall received was 61.79 mm. The rainfall received in the year 2000 may have played a role in rangelands in the year 2000. From the year 2000 to the year 2010, the rangeland area decreased to 7424.6 ha and the average rainfall received in 2010 was 61.74 mm, between the year 2000 and 2010 there is not much difference in the average rainfall received, however, there was a decrease of 375.2 ha in the rangelands. Then in 2020, the average rainfall received in Vulindlela was 67.09 mm which is an increase in the rainfall received in 2010. The increase in rainfall in 2020 did not result in the increase of rangelands, instead further decrease was experienced from 7424.6 ha in 2010 to 6660 ha in 2020. Based on the rainfall patterns in Vulindlela, rainfall has limited influence on the declining rate of the communal rangelands. Therefore, the increase of bareland and built-up areas in Vulindlela are the main drivers of the depletion of the rangelands in combination with other land use activities taking place in Vulindlela. In the area of Inhlazuka, the average rainfall of the year 2000 was 65.6 mm, and the area of rangelands was 2516.7 ha. In 2010, rainfall received decreased to 52.34 mm and the spatial extent of rangelands in 2010 also decreased from 2516.7 ha in 2000 to 2114.7 ha in 2010. Rainfall received in the year 2000 in Inhlazuka decreased in 2010. The decrease in rainfall in 2010 may have played a role in the decrease of the spatial extent of rangelands in 2010 as the decrease in rainfall resulted in a decrease in the area of rangelands. In 2020, the average rainfall of 2020 was 69.63 mm, this is an increase from the rainfall received in 2010. The increase in rainfall resulted in an increase in the areal extent of rangelands in 2020 from 2114.7 ha in 2010 to 2567.5 ha in 2020. The

rainfall patterns in Inhlazuka from the year 2000 to 2020 suggest that in Inhlazuka rainfall has an influence in the spatial distribution of rangelands as there was a decrease in rainfall in the year 2010 which resulted in the decrease of rangelands in 2010 and the increase of rainfall in 2020 resulted in the increase of the area of rangelands. However, the alien plants within the area of Inhlazuka may have played an additional role in the decrease of rangelands in the year 2010 especially if there were limited activities of alien removal in 2010. Then in 2020, the removal of the alien plants together with increased rainfall patterns could have created optimal growing conditions for the rangelands in Inhlazuka in the year 2020 therefore, an increase in the areal extent of rangelands.

4.5. Conclusion

The aim of this study was to characterise rangelands and quantify their variability in spatial extent and fragmentation over the period of 20 years in communal areas. Based on the findings of this study, it can be concluded that LULCCs can be optimally characterised using Landsat's bands in combination with the vegetation indices. In addition, the NIR and the SWIR bands were the variables of importance thus, mapping the rangeland changes at high accuracies. Settlement expansion and an increase in crop fields are the main driver of rangeland decline. Fragmentation of rangelands is increasing with time as more grassland patches are getting more isolated and relatively smaller in spatial extent with the increase in built-up area. The findings of this study are a step towards building robust spatially explicit quantitative techniques for monitoring the spatio-temporal variations of grasslands. This is a very important step required if a geospatial Framework for Monitoring grassland ecosystems that will provide actionable information services for grassland assessment and monitoring across different key land management areas is to be realised.

5. Assessing current and future dynamics of landcover using the CA-Markov model in typical communal rangelands Southern Africa

X Zuma, O Mutanga, T Bangira and M Sibanda

5.1. Introduction

Human activities have extensively altered the quality and quantity of grasslands through urbanisation and agricultural activities, exacerbated by climate change, high runoff, and soil erosion amongst others (Hicks, Parks et al. 2008, Clark and Tilman 2017, Mohamed, Anders et al. 2020). The continuous improvements in technology, changes in climate and the increase in human population is an indication that more land use changes are yet occur. This makes a study on LULCCs important to gain a better understanding of their patterns to manage and preserve grasslands as a natural capital (Mondal, Sharma et al. 2016, Hossen, Hossain et al. 2019). Grasslands offer ecosystem services such as erosion control, climate regulation and food provision (Sollenberger, Kohmann et al. 2019, Zhao, Liu et al. 2020). In this regard, the degradation of grasslands results in the loss of these ecosystem services (Wen, Dong et al. 2013, Bengtsson, Bullock et al. 2019). As a result, rangeland degradation urgently requires robust fast and effective frameworks for mapping and monitoring rangelands in a spatially explicit manner. Previously, traditional survey methods were utilised to assess rangeland degradation based on visual assessment at different points.

Considering that traditional field surveys are inefficient and expensive, several researchers have recently resorted to remote sensing techniques that can uncover and analyse near-real time land cover patterns (Lawley, Lewis et al. 2016). RS methods are commonly used in LULC change detection studies due to high revisit frequency and data acquisition, of expansive spatially explicit data (Abd El-Kawy, Rød et al. 2011). Performing change detection studies using RS includes the use of multi-date images to assess the changes occurring between the acquisition dates of the satellite images as a result of environmental conditions and human activities within a specified period (Abd El-Kawy, Rød et al. 2011, Shen, Meng et al. 2016). For instance, Landsat remotely sensed data has been proven to be invaluable in LULCC studies (Alam, Bhat et al. 2020). This is due to their optimal moderate spatial resolution and historical data archives which date back to the 1970s until the current date (Hansen and Loveland 2012, Alam, Bhat et al. 2020).

Landsat data have been widely used in classification studies (Zhu and Woodcock 2014, Phiri and Morgenroth 2017, Cai, Guan et al. 2018, Sawalhah, Al-Kofahi et al. 2018). For instance, DeVries, Pratihast et al. (2016) used Landsat data to characterise forest changes by assessing the use of local expert data in combination with Landsat Time Series to characterize forest

change processes. On the other Parihar, Sarkar et al. (2013) utilised Landsat data in a wetland post classification change detection study of East Kolkata Wetlands. The above-mentioned examples highlight the high prospects associated with Landsat remotely sensed data in detecting and mapping LCCs.

Generally, Landsat is often used in conjunction with robust machine learning algorithms which optimise the classification accuracies. For instance Phan, Kuch et al. (2020) used Landsat data in conjunction with RF to analyse the effect of different composition methods and input images on classification results. RF has been widely engaged by the community of practice because of its simplicity, ability to utilise small sample size using its bagging mechanism and being able to avoid overfitting models (Rodriguez-Galiano, Chica-Olmo et al. 2012, Thanh Noi and Kappas 2017). However, RF does not possess the capability to predict future changes.

Models such as the artificial neural networks (ANN), Markov Chain model (MC), and the Cellular Automata (CA) have been widely used in LULC change predictions (Mondal, Sharma et al. 2016, Liu, Liang et al. 2017, Yirsaw, Wu et al. 2017). However, literature states that these models have limitations when being applied singularly as compared to when they are combined into a hybrid algorithm (Halmy, Gessler et al. 2015, Munthali, Mustak et al. 2020). For example, the Cellular Automata-Markov model (CA-Markov) is an example of a hybrid cellular based model, which is robust and widely used in predicting future Land use changes (Subedi, Subedi et al. 2013, Yirsaw, Wu et al. 2017).

The CA-Markov model is said to be the most suitable model for LULC change prediction as it is a combination of the robust Cellular Automata and the Markov chain model (Yirsaw, Wu et al. 2017, Wu, Li et al. 2019). Furthermore, the model is effective in mapping future land use land cover changes dynamic simulation capability, high efficiency, simple calibration, and ability to simulate multiple land covers and complex patterns spatially and temporally (Sang, Zhang et al. 2011, Gidey, Dikinya et al. 2017, Liping, Yujun et al. 2018, Jalayer, Sharifi et al. 2022), thus making the model appropriate in mapping future rangeland land use land cover changes.

The CA-Markov model has been proven to be robust, efficient and reliable for producing accurate spatio-temporal prediction of land cover types (Wu, Li et al. 2019, Khawaldah, Farhan et al. 2020, Ghalehtemouri, Shamsoddini et al. 2022). In this regard, this study sought to predict the future spatial distribution of grasslands in communal rangelands using the CA-Markov model between the year 2020 and 2040. This study also compared the magnitude of grass fragmentation in the forthcoming 20 years since the same year intervals were considered in generating input maps for modelling. This was aligned with Agenda 2063 goal

number 1, which seeks to achieve a prosperous Africa based on inclusive growth and sustainable development. This goal prioritizes agricultural productivity and production, as well as the sustainable management of natural resources and biodiversity conservation such as land and rangelands. Furthermore, 20-year intervals were chosen and used in this study because they were deemed to be the minimum period when changes could be detected in a landscape. This was deemed to be a step towards assisting the developers in coming up with recommendations to preserve the rangelands within communal areas.

5.2. Methods and Materials

5.2.1. Study Site

Refer to chapter four.

5.2.2. Satellite Data

This study made use of cloud free Landsat 7 & 8 Top of Atmosphere (TOA) reflectance images from Google Earth Engine (GEE). GEE is a cloud-based computing platform which has satellite imagery of over 40 years to the present time. GEE provides images which have been atmospherically corrected, however, original images are provided by the platform. Satellite images available for analysis can be retrieved from the google earth catalogue (<https://developers.google.com/earth-engine/datasets/catalog/>). In this study, pre-processed Landsat images were selected and used to conduct the classification. Then, the median reducer in the GEE platform was utilised to reduce the images into a portable cube. The median reducer reduces bulky images into one image for easier analysis. The reduced image is created through tile reconstruction. Tile reconstruction is a process where each tile for each image is processed by different google servers and the product is a single image made up of the rearranged tiles of the images for better and improved quality of the image (refer to chapter two).

Table 5.1: Image collections used in the study.

Years	Number of Satellite Images which were available	Acquired date of images		Years	Number of Satellite Images which were available	Acquired date of images	
VULINDLELA AREA				NHLAZUKA			
2010	16	1. 2010/06/08	10. 2010/07/26	2010	5	1. 2010/06/08	
		2. 2010/06/08	11. 2010/08/02			2. 2010/06/24	
		3. 2010/06/24	12. 2010/08/02			3. 2010/07/10	
		4. 2010/06/24	13. 2010/08/18			4. 2010/07/26	
		5. 2010/07/10	14. 2010/08/18			5. 2010/08/27	
		6. 2010/07/10	15. 2010/08/27				
		7. 2010/07/17	16. 2010/08/27				
		8. 2010/07/17					
		9. 2010/07/26					
2020	22	1. 2020/06/02	12. 2020/07/13	2020	5	1. 2020/06/11	
		2. 2020/06/02	13. 2020/07/20			2. 2020/06/27	
		3. 2020/06/11	14. 2020/07/20			3. 2020/07/13	
		4. 2020/06/11	15. 2020/07/29			4. 2020/07/29	
		5. 2020/06/18	16. 2020/07/29			5. 2020/08/14	
		6. 2020/06/18	17. 2020/08/05				
		7. 2020/06/27	18. 2020/08/05				
		8. 2020/06/27	19. 2020/08/14				
		9. 2020/07/04	20. 2020/08/14				
		10. 2020/07/04	21. 2020/08/21				
		11. 2020/07/13	22. 2020/08/21				

5.2.3. Projections

The study used already classified images from the years 2010 and 2020 from GEE to predict the spatial distribution of rangelands in the year 2040 (Figure 5.1). Images used for the classification were cloud free. The classified images were a combination of images (temporal images) available between the months of June, July and August reduced to one image by the use of the median reducer in GEE. The median reducer in GEE combines the values of available images, calculates the aggregate of those images, and produces a single image. The use of such an image is important in rangeland studies as rangelands are sensitive to environmental changes. Therefore, using an image that is the result of temporal images is useful in accurately mapping the changes taking place in rangeland ecosystems. In addition, the use of the median reducer improves the quality of an image hence producing high classification accuracies in LULC studies (refer chapter two).

Classifications were performed with the use of the Random Forest (RF) classifier. Feature classes that were selected for the classified images were bare-land areas (which include areas in the study area with no vegetation cover), water bodies (being all water bodies within the study site such as dams, streams and rivers), built-up area (all areas of settlement development), the forest class (all forms of plants within the study site such as alien plant species, indigenous forest, plantations and woodland) and grasslands (being all areas covered with grass). Classifications were performed over a period of 10 years from 2010 to 2020. The study collected sample points for various land cover classes during field observation. Included were the grass points in both the study sites with the use of the handheld Trimble GPS. The study then proceeded to make use of Google Earth Pro for the verification points of the previous years (Cha and Park 2007). The RF makes use of decision trees when performing classifications and in this study 100 decision trees were used which produced accuracies between 79% to 89%. The use of the decision trees, however, does not guarantee an increase in the overall accuracies. Optimal parametrization was set from a range of 10 to 180 decision trees and at a 100-decision trees optimal parametrization was reached with overall accuracy being uniform thereafter (meaning that after 100 decision trees there was not much of a difference in the overall accuracies obtained). Vegetation indices were also computed during the LULCC classification process (refer to chapter two). The vegetation indices were utilized in image classifications in combination with the spectral bands as means to improve classification accuracies (Sinha, Sharma et al. 2015, Koley and Chockalingam 2022).

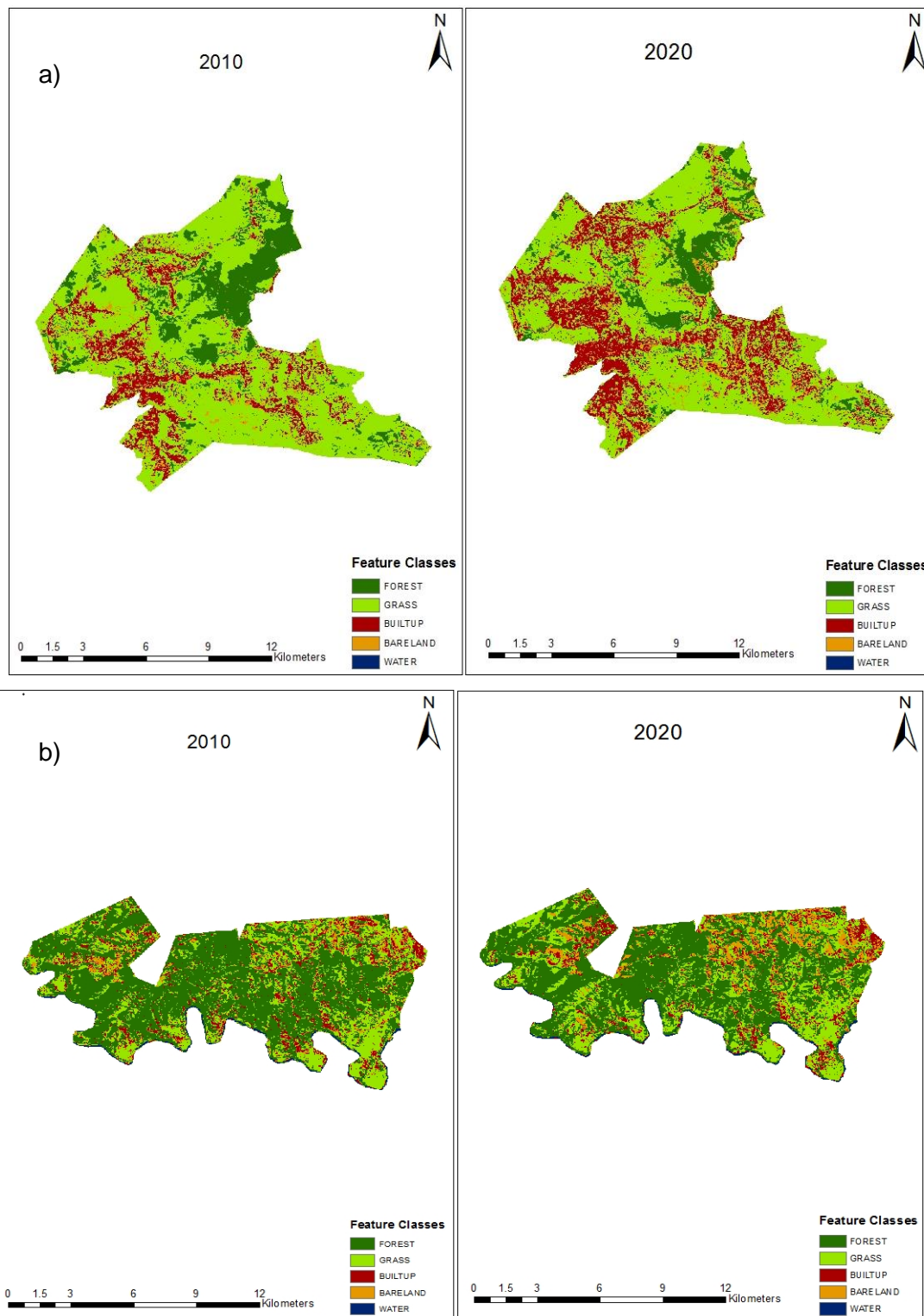


Figure 5.1: The already classified images of land use land cover changes in a) Vulindlela and b) Inhlazuka during the years 2010 and 2022

5.2.4. CA-Markov

The CA-Markov combines the functions of both the CA- and Markov chain analysis to optimize the outcome of the prediction, therefore, creating the opportunity of the model to perform long term predictions of any type of spatial patterns/changes (Mathanraj, Rusli et al. 2021).

The study first calculated the gains and losses for each class by making use of the Land Change Modeler (LCM) Module in TerrSet, performed to get an insight of what was happening in each class from 2010 to 2020. Performing the gains and losses on the LCM in Terrset produced the drivers causing a change in rangelands. The study then used the CA-Markov module in Terrset to perform the predictions. Prior the predictions, transition probabilities were created which gave the percentages/probability of one class transitioning into another. The Markov transition estimator module in Terrset was used to create probability transitions. In creating the transition probabilities, the classified images of 2010 and 2020 were used. The output probabilities from the 2010 and 2020 images in combination with the originally classified image of 2020 was used for the predictions of the year 2040 in the CA-Markov module of Idrisi TerrSet with a contingency filter of 5 and 10 Cellular Automata iterations.

5.2.5. Accuracy assessment

For the accuracy assessment of the CA-Markov model predictions, three indicators were used (i.e. kappa for no ability (K_{no}), kappa for location ($K_{location}$) and kappa for quantity ($K_{quantity}$)). The K_{no} performs the accuracy of the simulation run (Hamad, Balzter et al. 2018), while the $K_{location}$ and $K_{quantity}$ validate the location and quantity between the original classified images and the prediction images (Hamad, Balzter et al. 2018). These indicators are said to be the best indicators for the validation of simulated maps and literature also states that 0.80% is an acceptable accuracy rate for the performance of future prediction maps (Eastman 2015). For further accuracy assessment of the model, the study predicted the year 2020 in both study areas using the classified images of the years 2000 and 2010. The predicted 2020 image was then compared with the originally classified image of 2020. Figure 5.2 shows the procedure followed in simulating future land-use and land cover types in the study area.

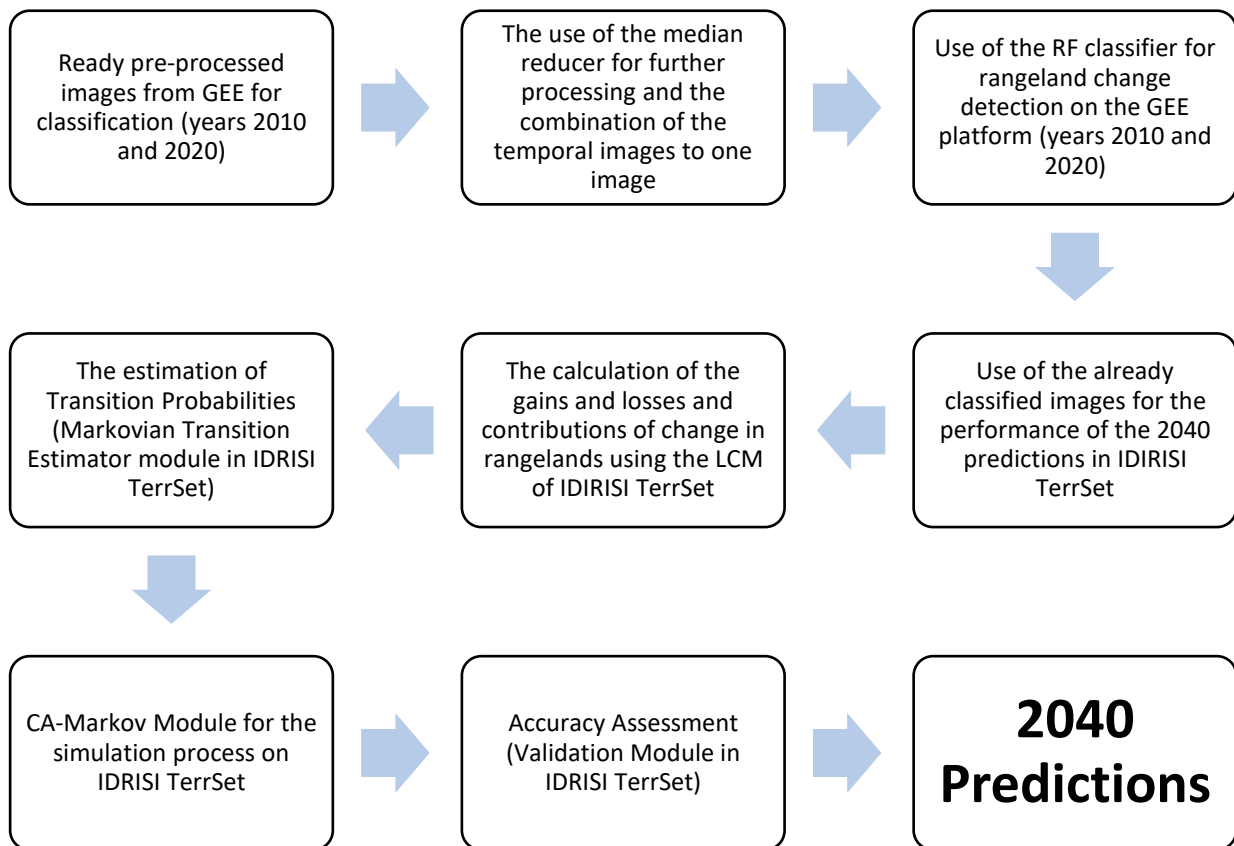


Figure 5.2: A flow chart of the simulation process.

5.2.6. Rangeland Patch Analysis for the projected year 2040

The study calculated fragmentation within the communal rangelands of Inhlazuka and Vulindlela using the Fragstats 4.2 software as a measure of rangeland degradation. To compare the rangeland fragmentation between the year 2020 and the year 2040, the rangeland patch analysis was performed for both years. This was done to compare the extent and level of fragmentation for the current year with that of 2040 to assess the changes in rangeland fragmentation after 20 years. The projected images of 2040 of Vulindlela and Inhlazuka were exported from IDRISI TerrSet to ArcMap 10.6. In ArcMap the projected maps were extracted as GeoTiff images into Fragstats. The 2020 classified image was extracted from Google Earth Engine (GEE) to ArcMap 10.6 then extracted as a GeoTiff image to Fragstats 4.2. The measurement of fragmentation within both study areas was performed at a class level metrics. The class level metrics calculate the fragmentation of each feature class

of the classified map. The metrics used in performing the patch analysis were that of the Percentage of landscape (PLAND), patch area (AREA_MN), the number of patches (NP), largest patch index (LPI), patch density (PD), Euclidean nearest neighbour distance (ENN_MN) and effective mesh size (MESH) were used to measure the extent of fragmentation within the communal rangelands. However, the metrics of NP, PD and LPI were applied by the study to measure the extent of fragmentation within each of the feature classes. Then the metrics of ENN_MN, AREA_MN, PLAND, and MESH, were applied by the study to assess the patch area of each of the feature classes specifically the rangelands. The measurement of fragmentation in the study was performed for the projected year 2040 to be compared with the patch analysis of the year 2020 to compare the level of rangeland degradation between these years.

5.3. Results

5.3.1. Image Classifications

The study performed classifications to monitor the rangelands changes using the Random Forest Classifier (RF). Classifications were performed using the combination of the spectral bands of the Landsat images with vegetation indices. Feature classes that were used during the classification process were that of water, bareland, built-up area, forest, and grasses. The overall accuracies (OAs) achieved during the classification of rangelands were that of 85% and 89% in Vulindlela and OAs of 79% and 83% were obtained in Inhlazuka for the years 2010 and 2020 respectively (Table 5.2, Figure 5.3). The kappa coefficient was applied in the measurement of the classification accuracies and the Kappa scores were that of 75% and 83% in Vulindlela and in Inhlazuka Kappa scores were 68% and 73% for the years 2010 and 2020, respectively (Figure 5.3). The variables of importance obtained from the classifications, selected by the RF were that of bands 5 and 7 which represent the Shortwave Infrared bands (SWIR) and the Near Infrared bands (NIR) (refer to chapter two).

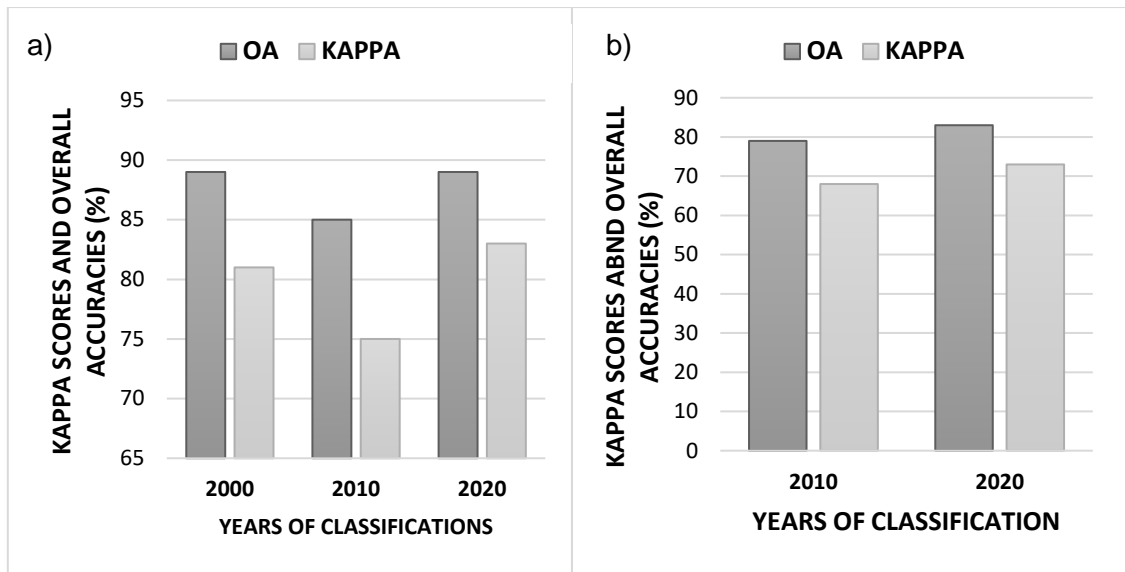


Figure 5.3: Classification overall accuracies and kappa scores in the areas of a) Vulindlela and b) Nhlazuka.

5.3.2. Validation Results

In addition to assessing the CA model prediction accuracy, the year 2020 was predicted using images of the years 2000 and 2010 in both areas of Vulindlela and Nhlazuka. The predicted images of 2020 in both study areas were compared with the original classified images of 2020. The high accuracies in the $K_{location}$ and $K_{quantity}$ of both the study areas presents limited errors meaning the acceptance of the original classified image of 2020 and the validation of the 2040 prediction (Figure 5.4).

Table 5.2: The kappa coefficient scores for quantity and location for the year 2020 prediction.

2020 Projections for Vulindlela		2020 Projections for Nhlazuka	
$K_{no} =$	0.8391	$K_{no} =$	0.7371
$K_{location} =$	0.8562	$K_{location} =$	0.7646
$K_{location\ strata} =$	0.8562	$K_{location\ strata} =$	0.7646
$K_{standard} =$	0.7814	$K_{standard} =$	0.6908

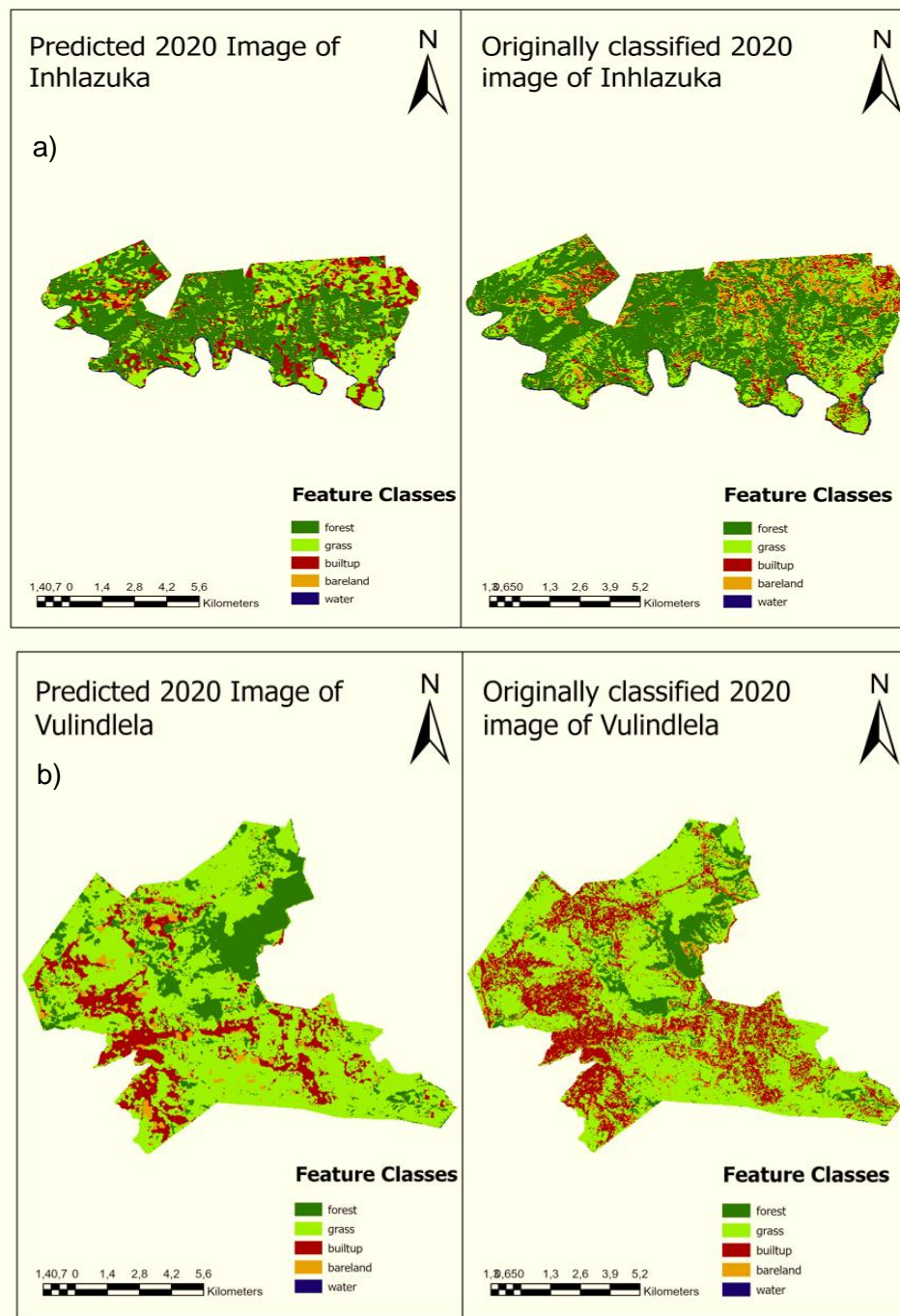


Figure 5.4: Prediction images of 2020 for a) Inhlazuka and b) Vulindlela

5.3.3. Projections

The 2040 projections were performed using the CA-Markov model. Accuracy assessments of the model were performed using the Validation Model of IDRISI TerrSet. The kappa coefficient scores for the projected images are presented below in table form (Table 5.4).

Table 5.3: The kappa coefficient scores for quantity and location for the 2040 prediction.

Projections for Vulindlela	Projections for Inhlazuka
Kno = 0.8741	Kno = 0.8374
Klocation = 0.9208	Klocation = 0.9032
Klocationstrata = 0.9208	Klocationstrata = 0.9032
Kstandard = 0.8308	Kstandard = 0.8087

Figure 5.5 below illustrates the CA-Markov model prediction changes in the areas of Vulindlela and Inhlazuka for the year 2040. In Vulindlela, the rangelands are predicted further decrease while the rangelands in Inhlazuka are predicted to increase. The area of rangelands in Vulindlela for the year 2020 was 6660.04 ha and the projected area of rangelands in 2040 is 5740.30 ha. Therefore, in Vulindlela about 919.74 ha of rangelands are to be lost by the year 2040 thus a loss of 46 ha per year of rangelands. The loss in rangelands will be caused by the further increase in built-up and bareland areas but mostly settlement development as it will increase at a higher rate than the bareland class. In the area of Inhlazuka, the spatial extent of rangelands for 2020 is 2567.55 ha and the projected area of the communal rangelands is 2987.03 ha, meaning that in Inhlazuka an increase of 419.48 ha in rangelands is expected in 2040 with an increase of 21 ha per year in rangelands.

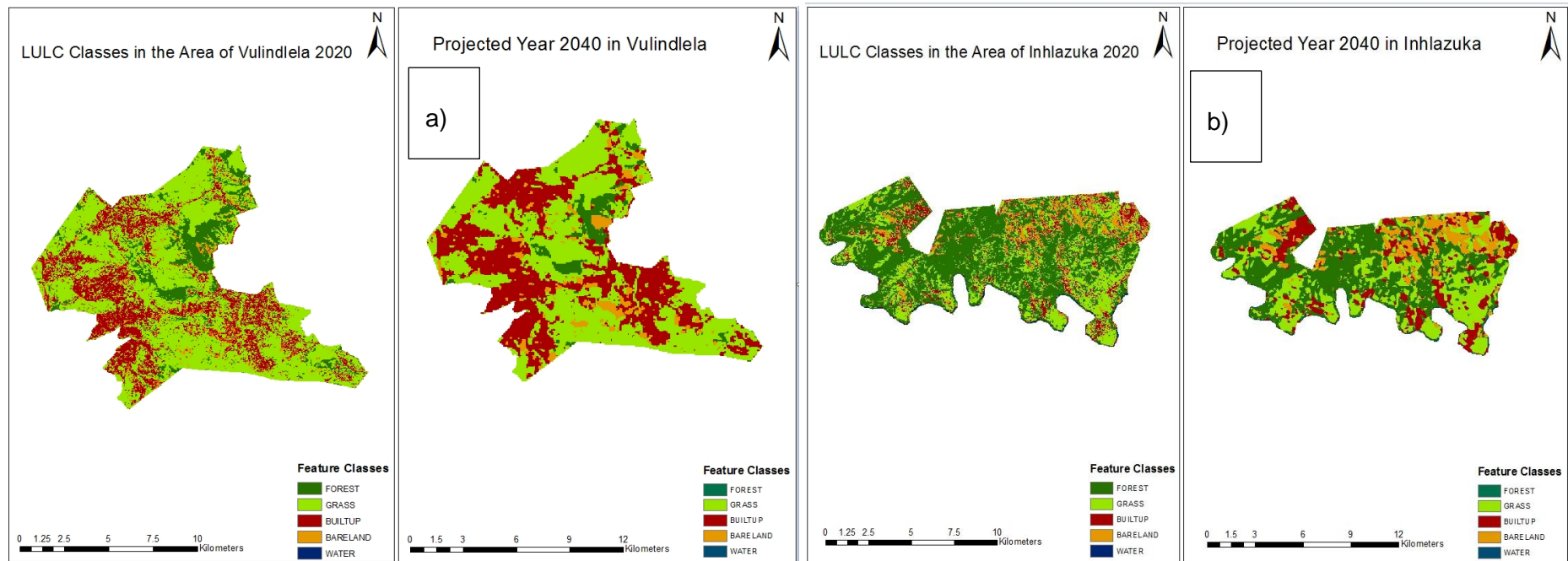


Figure 5.5: The projected changes in a) Vulindlela and b) Inhlazuka for the year 2040.

In Vulindlela rangelands are threatened by the continued increase in built-up area which is projected to increase in 2040 (Figures 5.6 and 5.7). The spatial extent of built-up area in Vulindlela for 2020 is 2821.88 ha and the projected areal extent in 2040 for built-up area is 4157.2 ha, therefore built-up area is expected to have grown by 1335.32 ha by the year 2040 and increase at a rate of 67 ha per year.

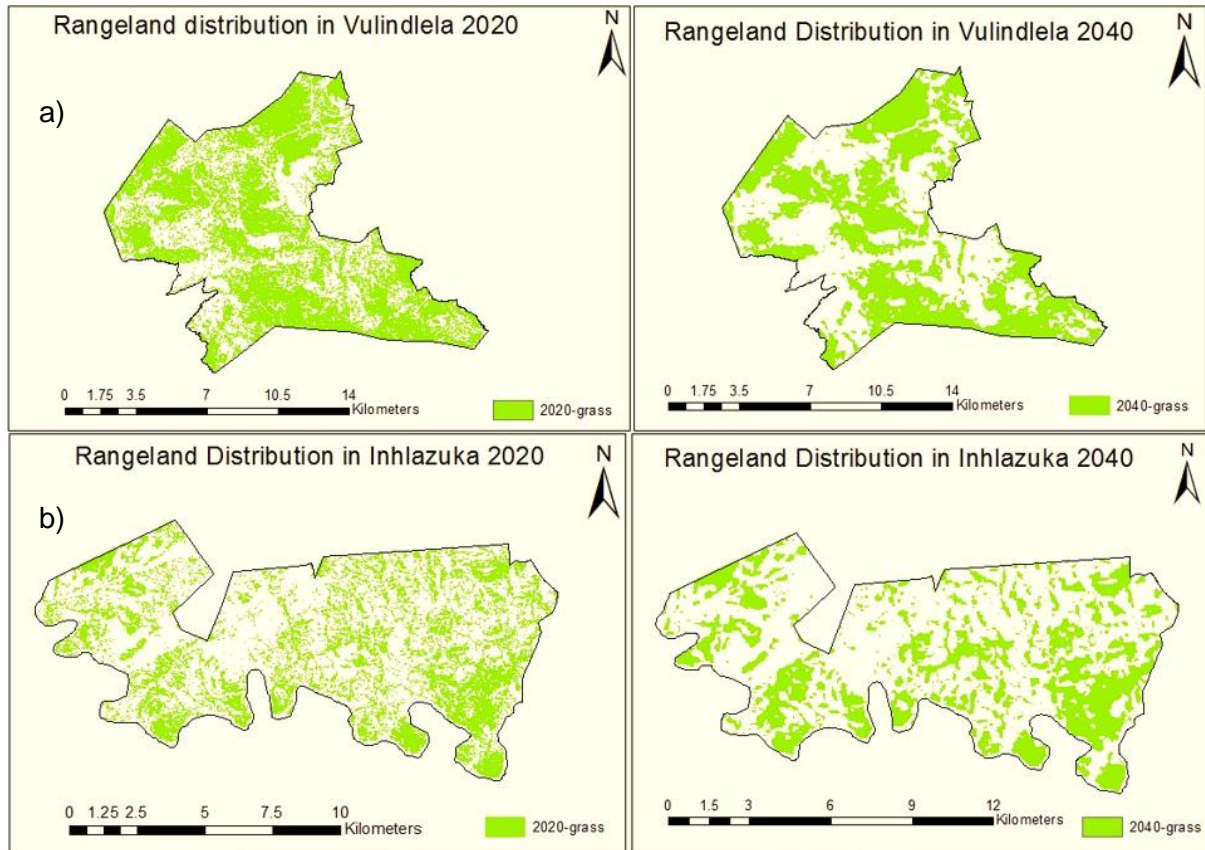


Figure 5.6: A comparison in the rangeland distribution between 2020 and 2040 in (a) Vulindlela and (b) iNhlazuka.

In iNhlazuka, the growth of rangelands and built-up area is causing a decline in the forest class (Figures 5.6 and 5.7). The area of the forest class for 2020 is 4632.09 ha and the projected area for the forest class in 2040 is 3462.18 ha thus, a loss of 1169.91 ha of the forest class by 2040. The forest class shall decrease at a rate of 58.45 ha per year. The built-up area in iNhlazuka for the year 2020 is 2567.55 ha and the project area is 2987.03 ha meaning, by the year 2040, built-up area would have increased by 419.48 ha, therefore increasing at a rate of 21 ha per year.

Hence, the increase in rangelands and built-up area will cause a decrease in the forest class by 2040.

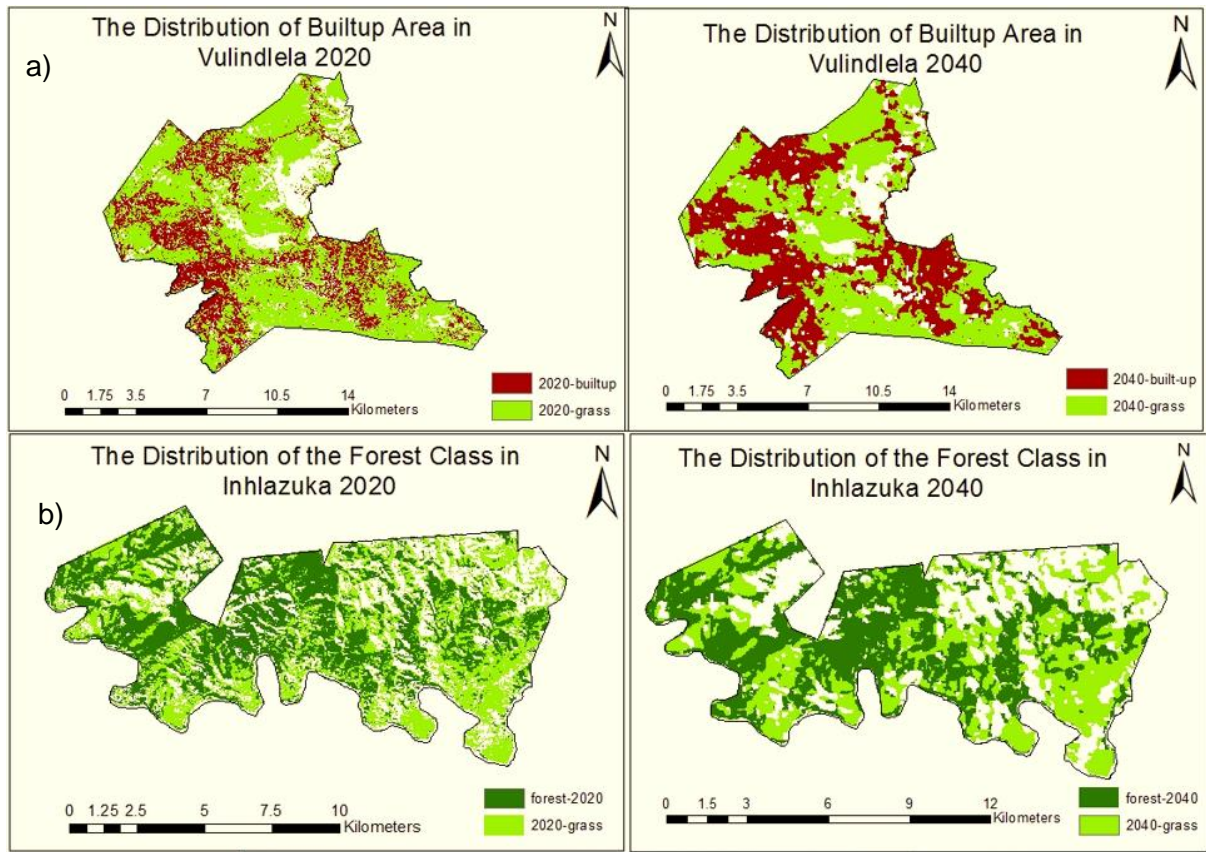


Figure 5.7: The changes in the distribution of rangelands between 2020 and 2040 in (a) Vulindlela and (b) Inhlazuka.

Figure 5.8 presented the LULCCs variations taking place within Vulindlela and Inhlazuka between the years 2010 and 2020. From Figure 5.8, it can be observed that the rangelands are declining as a result of the increasing builtup area in Vulindlela, meaning that the communal rangelands in Vulindlela are declining as a result of the increasing population. In Inhlazuka, the builtup area increased, the forest class decreased and rangelands increased. Furthermore, the gains and losses were calculated using the LCM of TerrSet to present the changes within each class in Vulindlela and Inhlazuka (Figure 5.8) with Figure 5.9 presenting the changes in area of the mapped land cover classes.

Vulindlela

Inhlazuka

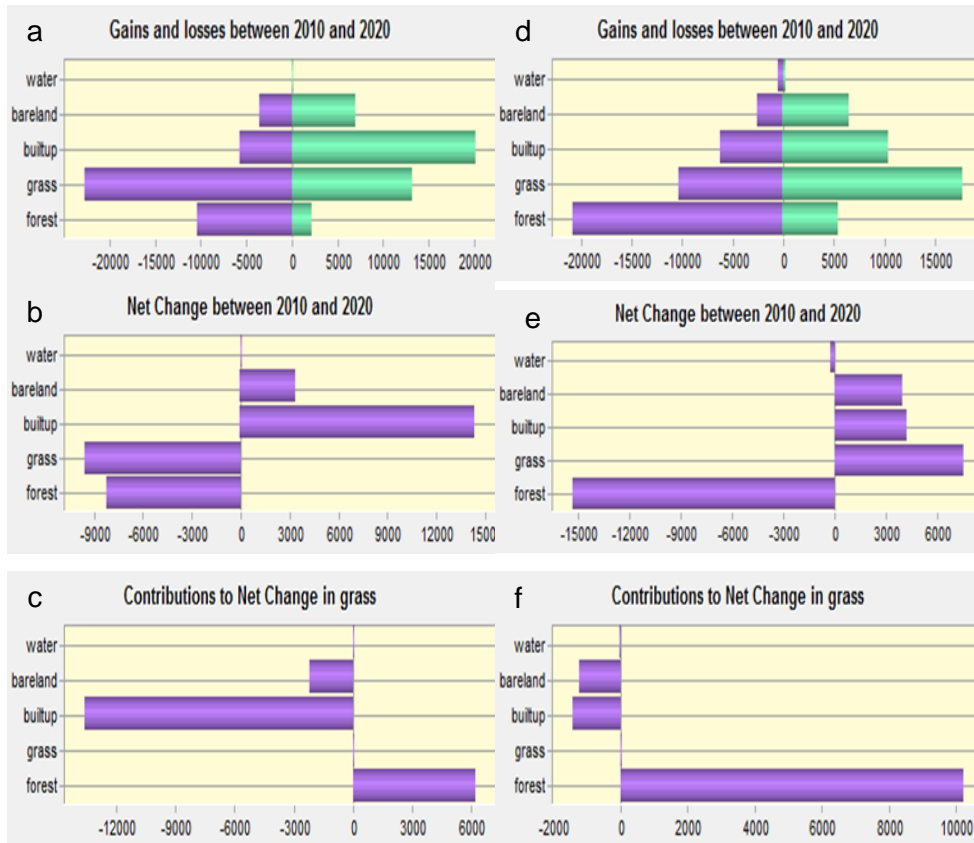


Figure 5.8: (a, b and c) is presenting the gains and losses of each feature class and the Net changes in grasslands in Vulindlela between the years 2010 and 2010 and (d, e and f,) presenting the grassland changes in Inhlazuka, respectively.

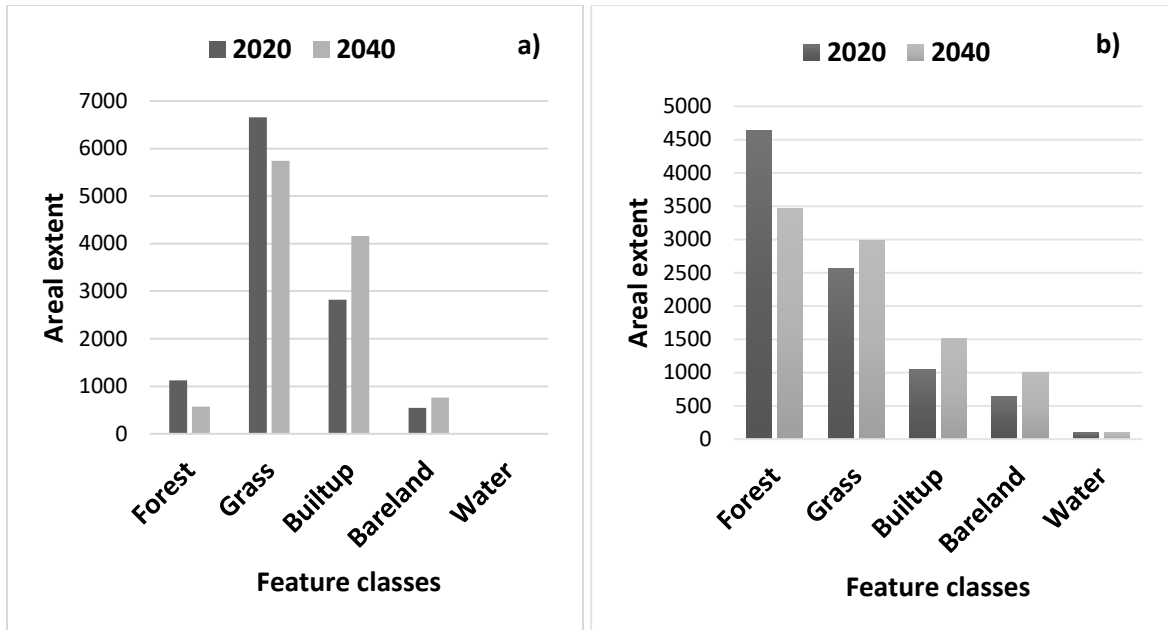


Figure 5.9: The areal difference in the land cover types between 2020 and 2040 in the areas of a) Vulindlela and b) Nhlazuka

5.3.4. Rangeland Patch Analysis 2020 and 2040 comparison

The rangeland patch analysis was performed to measure rangeland degradation comparing the year 2020 with the projected year 2040 (Table 5.7). The results of the Percentage of landscape (PLAND) in Vulindlela suggest that there shall be an increase in the fragmentation of rangelands in the year 2040 as the patch analysis presents a decrease in the PLAND from the year 2020 at 59.6 ha to 51.35 ha. The number of patches (NP) in Vulindlela will decrease from 780 in 2020 to 103 patches in 2040. The patch density (PD) in 2020 will also decrease from 6.9 in 2020 to 0.92 in 2040. The Largest Patch Index (LPI) will decrease from the year 2020 from 43.3 ha to 18.37 ha. The patch area (AREA_MN) shall increase from 8.5 ha to 55.94 ha suggesting an increase in the patch sizes from the year 2020 to the year 2040. The Euclidean nearest neighbour distance (ENN_MN) and the effective mesh size (MESH) propose that there will be an increase in the extent of fragmentation in 2040 due to the increase in the ENN_MN in Vulindlela from the year 2020 from 73.0 ha to 172.20 ha in 2040. This suggests that the isolation of the rangeland patches will increase in 2040. The increase in isolation between the patches is further presented by the MESH as it is expected to decrease from the year 2020 at 2188.8 ha to 743.35 ha in 2040 indicating that the rangeland patches in Vulindlela will lose connectivity. The rangeland patch analysis of Vulindlela therefore, suggests that the rangelands in Vulindlela will become more

isolated in 2040 compared to the year 2020 with larger rangeland patches in 2040 compared to 2020.

In Inhlazuka, the patch metrics results for the PLAND shall increase from 28.6 in 2020 to 32.89 in 2040 therefore a decrease in fragmentation in the year 2040. The NP and PD shall also decrease from the year 2020 to the year 2040. The NP in Inhlazuka will decrease from 1443 to 414 and the PD shall decrease from 16.0 to 6.52. The AREA_MN in 2040 will increase from 1.7 ha to 7.20 ha in 2040 hence larger rangeland patches. However, the increase in the ENN_MN by the year 2040 suggests isolated rangeland patches. The ENN_MN presents an increase from 75.0 ha to 120.60 ha by the year 2040, however the MESH shall increase from 35.4 ha to 58.89 ha in 2040 thus the rangeland patches being more connected in 2040 than in 2020. The results of the patch analysis in Inhlazuka therefore suggests that the rangelands shall increase in patch sizes in the year 2040 however, the rangelands will become more isolated with an increased rangeland patch connectivity when compared to the year 2020.

Table 5.4: Rangeland Patch Analysis of the year 2020 and 2040

	GRASS	PLAND	NP	PD	LPI	AREA_MN	ENN_MN	MESH
Vulindlela	2020	59.6	780	6.9	43.0	8.5	73.0	2188.8
	2040	51.35	103	0.92	18.37	55.94	172.20	743.35
Inhlazuka	2020	28.6	1443	16.0	5.4	1.7	75.0	35.4
	2040	32.89	414	4.57	6.52	7.20	120.60	58.89

5.4. Discussion

The overall aim of this study was to map the future spatio-temporal variations of communal rangelands with the use of Landsat imagery using the CA-Markov model of IDRISI TerrSet. The study used classified Landsat images in Google Earth Engine using the Random Forest classifier to characterise LULC types during the year 2020 based on Near Infrared bands (NIR) (Band 5) and Shortwave Infrared bands (SWIR) Band 7.

The CA-Markov model results showed that rangelands will increase in spatial extent in Inhlazuka in the year 2040 (Figures 3.4 and 3.5) due to the decrease in forested areas whereas in Vulindlela, they were predicted to decrease as a result of the increase in settlement (Figure 3.5). The projected increase in built-up area in Vulindlela implies that there will be an increase in population.

This is supported by the Municipality (2016) which stated that the population is expected to increase in future. In addition, the population growth in the area of Vulindlela could be associated with a possible increase in livestock densities in the grazing lands. The increased number of grazing animals within Vulindlela could result in the rangelands being over grazed and eventually degraded. Furthermore, activities such as unmanaged fire practices for rangeland management and increased agricultural activities in Vulindlela may also contribute to the decline of rangelands in the year 2040. This calls for the practice of sustainable grazing patterns in Vulindlela for the preservation of rangelands.

The increasing barelands in both the areas of Vulindlela and Inhlazuka are due to development which could take place in future alongside the increase in population. In Vulindlela, grasslands are being cleared for residential areas and the development of roads. In addition, activities such as rock mining are also taking place in Vulindlela causing increased bareland areas. In Inhlazuka, bareland could also be caused by the removal of the forest class for development, the construction of roads and the removal of plantations. This suggests that development activities in both study areas are the drivers of increased bareland in conjunction with activities of fire and grazing activities. As a result of the prediction models, the bareland class is projected to increase in Vulindlela and Inhlazuka (Figure 3.9), meaning the increasing barelands shall be as a result of increased development activities. Literature also states that activities of development, unmanaged fire and agricultural practices leave the soil exposed therefore causing an increase in bareland (Tsegaye, Moe et al. 2010, Lehnert, Meyer et al. 2014, Mussa, Teka et al. 2017). However, the changes in temperature and precipitation received could also contribute to the increase in the spatial extent of bareland.

Climate change variabilities in Southern Africa, have brought about a marked seasonality in feed quantity and quality of rangelands which have been deteriorated as a result of the frequent dry seasons in certain parts of the region (Assan 2014). Therefore, the future patterns in temperature and rainfall will influence the growth of grass in these rangelands. The projected decline in rangelands in the areas of Vulindlela may also be attributed to the changing climates through reduced precipitation and increased temperature that restricts growth in rangelands as a result of increased temperatures and decreased rainfall patterns, however, if sufficient rainfall and moderate temperatures are received in the future, then rangelands shall be presented with growing conditions which will not hinder their growth and quality. This also applies to the rangelands of Inhlazuka, with sufficient rainfall and moderate levels of temperature, the communal

rangelands will grow producing quality forage production. However, the increase in the communal rangelands in Inhlazuka depends on both the climatic conditions as well as the maintained and consistent removal of the alien plants, thus creating ideal conditions for growth.

Fragmentation results showed that in both study areas, the grassland patch sizes shall increase meaning that the grassland patches of Vulindlela and Inhlazuka shall be larger compared to the rangeland patches of 2020. In Vulindlela, the patch area is to increase by an average of 32.22 ha by the year 2040 and in Inhlazuka the patch area shall increase by an average of 4.45 ha. Meanwhile the isolation extent (ENN_MN) predicted is to increase by an average of 122.6 ha in Vulindlela and by an average of 97.8 ha in Inhlazuka. However, results also showed a decrease in the of connectivity (The MESH) of patches in Vulindlela by the year 2040. In Inhlazuka rangeland connectivity is to increase by an average size of 47.14 ha by the year 2040 and decrease by an average size of 1466.07 ha in Vulindlela. The drivers behind the future isolation of the rangelands in Vulindlela are as a result the development activities, particularly that of residential development (Figure 3.4 and 3.6). Furthermore, the increase in development in Vulindlela is reducing the connectivity of rangeland therefore, increased fragmentation and loss of rangelands. In Inhlazuka, the increase in the AREA_MN of the rangelands could be caused by the increasing rangelands thus larger grassland patches however, the increase in the isolation of rangelands could be the result of increasing built-up and bareland areas and the decline in the forest class. This is because though the built-up, bareland and forest classes are not affecting the rangeland areal extent, the change in these classes has an influence over the distribution patterns. The increase in the fragmentation in the communal rangelands especially in Vulindlela suggests an urgent need for protecting rangelands due to fragmentation depleting them in Vulindlela. And with continued unmanaged activities of fire, grazing patterns and agriculture, rangeland fragmentation in Vulindlela is to increase causing further degradation and loss of rangelands (Soons, Messelink et al. 2005, Spanowicz and Jaeger 2019).

Rangelands are important ecosystems which regulate our climate, control carbon emissions, produces medicines, fuel wood, is base for wildlife-based tourism and play an important role in water provision meaning that rangeland landscapes are important and should be protected (O'Connor and van Wilgen 2020). Rangelands also play a role of providing income to livestock owners therefore, contributing to the economy. As a result of the lack of management practices in communal rangelands, sustainable development methods within rangelands are important to ensure that the people, economy and the environment are all balanced and with the use of RS in

monitoring rangelands policies to protect rangelands can be put in place to manage the degradation of rangelands. The findings of this study can henceforth, assist the communities residing within these areas and the development planners to perform more sustainable practices of development as well as educate the residents of these areas on sustainable practices of grazing, crop farming and the use of fire as a management tool.

5.5. Conclusion

In conclusion the study successfully performed the 2040 simulations using the CA-Markov model of IDRISI TerrSet with high accuracy. The 2040 predictions illustrate that settlement will increase due to the increase in population. The increase in settlement in Vulindlela is to take place at 67 ha per year and rangelands are to decrease at a rate of 46 ha per year. The patch metrics of Vulindlela and Inhlazuka presented the increase in rangeland fragmentation because of the loss of connectivity in rangelands and increased isolation particularly in Vulindlela as a result of development activities. The increase in settlement development in Vulindlela suggest an urgent need to develop rangeland management plans for the growing rangeland degradation because of rangeland fragmentation. To end off, the study results presented that land use land cover changes are consistently changing and for this reason the use of Remotely Sensed data is important in monitoring LULCC studies to capture all the changes taking place as a result of human or environmental conditions. The use of RS for the spatial monitoring of rangelands and land rehabilitation will also assists in the creation of rangeland conservation policies.

6. Comparing the utility of Artificial Neural Networks (ANN) and Convolutional Neural Networks (CNN) in tandem with Sentinel-2 MSI in estimating dry season aboveground grass biomass

M Vawda, R Lottering, K Peerbay, M Sibanda and O Mutanga

6.1. Introduction

The study and observation of natural phenomena is increasingly becoming more imperative as the world faces unprecedented environmental change (Ali, Greifeneder et al. 2015). The consistent improvements made to both airborne and spaceborne platforms and sensors have resulted in the proliferation of remote sensing research (Mutanga, Dube et al. 2016). Remote sensing has enabled scientists to make earth observations in various facets of the natural world, ranging from weather to vegetation. Vegetation monitoring, in particular, has become an influential research topic in remote sensing academia due to the need for continuous, reliable data to assist in decision-making processes (Mutanga, Dube et al. 2016). The advent of remote sensing, from simple aerial photographs to current high-resolution imagery, has enabled scientists to conduct research at larger spatial and temporal scales (Mutanga, Dube et al. 2016). In recent times, there has been a significant increase of remote sensing data as well as ground data in vegetation studies which has established a solid foundation for vegetation monitoring, presently and in the future (Ali, Greifeneder et al. 2015).

The inundation of remotely sensed data has directed scientists towards finding novel methods for data processing and analysis (Ali, Greifeneder et al. 2015). Remotely sensed data has proven to be voluminous, with data being captured at weekly, monthly and even hourly scales (Das, Ghosh et al. 2022). The heterogeneity of remotely sensed data, with a vast array of sensors with varying spatial, temporal and radiometric resolutions, has produced challenges in data processing and analysis (Ali, Greifeneder et al. 2015, Das, Ghosh et al. 2022). This challenge has ushered scientists into discovering new methodologies at discerning multi-dimensional data, which has resulted in a paradigm shift from conventional statistical methods towards machine learning solutions ((Das, Ghosh et al. 2022). The advancement of artificial intelligence, and subsequently, machine learning technologies has enabled scientists and practitioners alike to address pressing environmental issues due to their real-time processing of data and strong predictive abilities (Das, Ghosh et al. 2022).

Neural networks, which are considered a subset of machine learning, are algorithms that have been designed by mimicking the operation of a biological brain (Mas and Flores 2008). The artificial neural network (ANN), specifically, has been extensively used for remote sensing applications from the inception of the 1990s as they provided promising results (Mas and Flores 2008). Mas and Flores (2008) state that ANNs have been reported to perform much more admirably as compared to traditional statistical methods due to their ability to learn complex patterns, study nonlinear relationships between variables, generalisation abilities and perform various analyses without necessitating the meeting of data assumptions (e.g. Normally distributed data). Jensen, Hardin et al. (2009) acknowledge that ANNs have been used relatively successfully in remote sensing for biophysical estimation and land classification, however, they do have their limitations. These include the complex architectures of ANNs and their demanding computational requirements, the need for large amounts of training data and supervised training of the algorithm to ensure better accuracy and output (Mas and Flores 2008, Jensen, Hardin et al. 2009).

In the last decade, there has been another paradigm shift in the machine learning realm with the focus now being on deep learning approaches (Liu, Han et al. 2019). This is essentially a refinement and improvement on traditional ANNs with the aim of improving predictive accuracy and reducing the complexity of the previous algorithms (Zhu, Tuia et al. 2017). Zhu, Tuia et al. (2017) define deep learning as neural networks characterised by more than two deep layers in the neural network structure and that extract distinct feature patterns from input data. One such example of a deep neural network is the convolutional neural network (CNN), which has been specially engineered for image processing and analysis (Zhu, Tuia et al. 2017, Kattenborn, Leitloff et al. 2021). The increased number of layers and interconnections in CNNs have meant that more complex and intricate patterns and relationships can be deciphered, which is particularly useful for vegetation remote sensing studies (Kattenborn, Leitloff et al. 2021). CNNs have an advantage over ANNs in a sense that they require less computational time and power and produce higher predictive accuracies. However, they require vast amounts of training data to be able to make such accurate predictions and classifications (Brodrick, Davies et al. 2019). Even though the use of CNNs in remote sensing is trend-setting, it is currently only in its inception and has to be tested further to reveal its strengths and weaknesses (Kattenborn, Leitloff et al. 2021).

Grasslands are biomes of high socio-economic and conservational value, particularly in southern Africa (Palmer, Short et al. 2010). Grasslands are highly sensitive to environmental change and are often moderated by biophysical factors such as rainfall and grazing (Vundla, Mutanga et al.

2020). Vegetation parameters are used to assess health and condition and can either be physically measured or remotely estimated by remote sensing (Mutanga, Dube et al. 2016). One such vegetation measure that is used to observe and monitor grassland productivity is aboveground biomass (Ali, Greifeneder et al. 2015). Neural networks, especially ANNs, have been used to assess and predict aboveground vegetation biomass for a considerable time (Ali, Greifeneder et al. 2015). In most cases, ANNs have outperformed typical Bayesian and iterative statistical methods for estimating biomass, as well as other machine learning algorithms such as support vector machines (Ali, Greifeneder et al. 2015). Recent grass biomass studies have gradually incorporated the utilisation of CNNs for biomass predictions, with varying results based on sensor resolutions and platform type (Kattenborn, Leitloff et al. 2021).

There is a substantial lack of grassland biomass studies, in relation to remote sensing, in South African academia, as reported by (Masenyama, Mutanga et al. 2022). Furthermore, from a South African context, no research has attempted at investigating the performance of conventional ANNs and contemporary CNNs in estimating aboveground grass biomass. The study of grasslands are imperative in the face of climate change and hence the use of machine learning techniques to observe and assess grassland health would be inherently useful for both researchers and practitioners (Ali, Greifeneder et al. 2015, Masenyama, Mutanga et al. 2022). Therefore, the objectives of this study were to: 1) compare the predictive performance of shallow ANNs and deep CNNs in estimating aboveground grass biomass using Sentinel 2 MSI and 2) utilise both neural networks in tandem with Sentinel 2 MSI to predict dry season aboveground biomass for Vulindlela.

6.2. Methods

6.2.1. Study Area

The Vulindlela area is situated in the greater Umgeni Catchment of the KwaZulu-Natal province, South Africa. The study area is part of the Umgungundlovu district and falls under the uMsunduzi Municipality (Figure 6.1). The local climate can be classified as a subtropical oceanic climate, with cool and dry winters as well as mild and wet summers (Sibanda, Onesimo et al. 2021). A mean annual rainfall of 979 mm with a median annual rainfall of 850 mm is received in the study area. Annual maximum and minimum temperatures are approximately 22°C and 10°C respectively

within the study area (Sibanda, Onisimo et al. 2021). Vegetation growth in the area is limited primarily by climate, with low precipitation, low temperatures and frost being the major factors (Sibanda, Onisimo et al. 2021). Vulindlela has a mean annual potential evaporation that ranges between 1580 and 1620 mm, which indicates a possible deficit in relation to mean annual rainfall (Sibanda, Onisimo et al. 2021). The edaphic factors of Vulindlela are characterised by shallow soils with moderate to poor drainage; this presents a potential soil erosion risk if not properly managed (Sibanda, Onisimo et al. 2021).

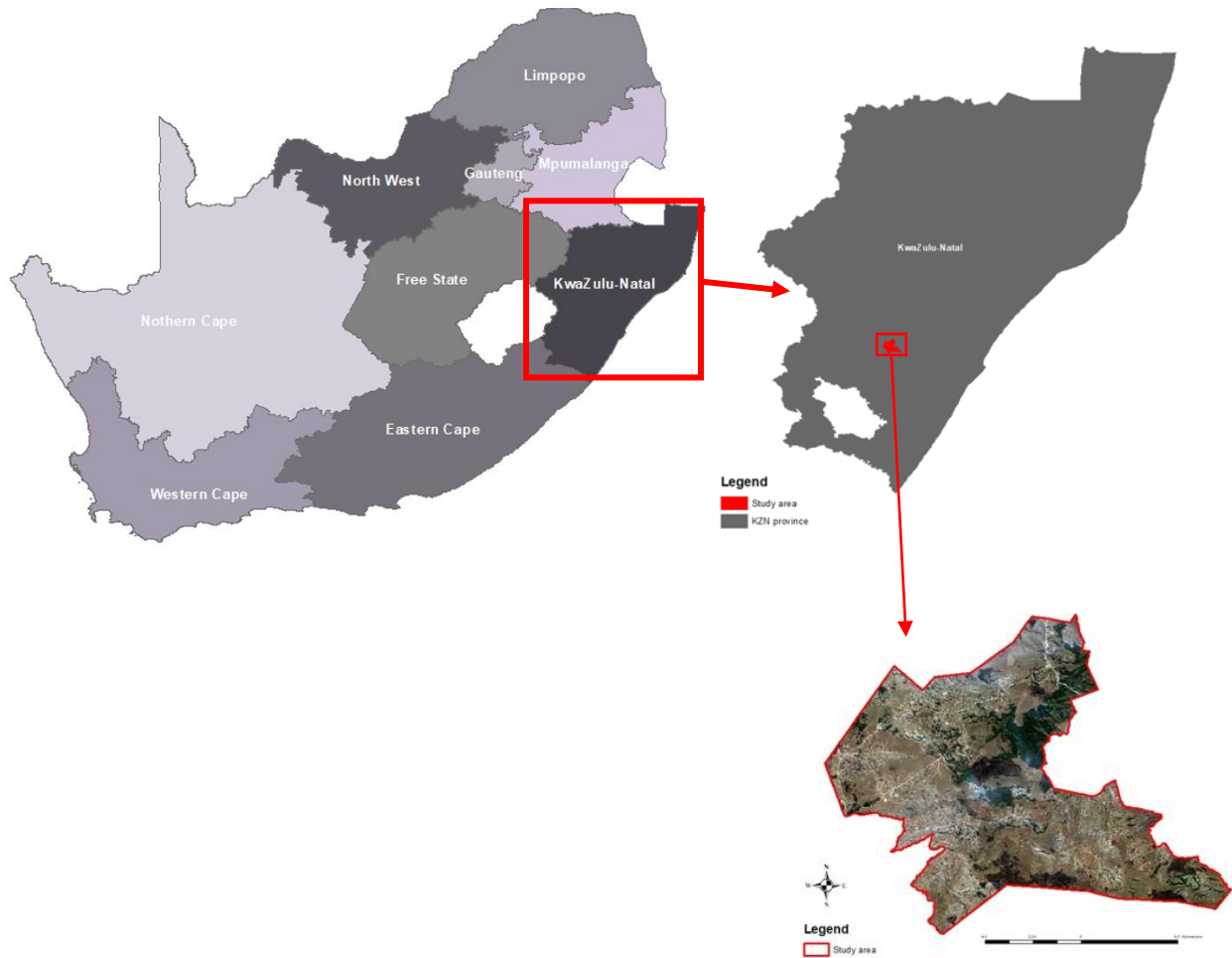


Figure 6.1: Location of Vulindlela area relative to South Africa and KZN.

Grasslands occurring within the study area are characterised as mesic grasslands and typically consist of species such as *Themeda triandra*, *Eragrostis tenuifolia*, *Tristachya leucothrix*, *Paspalum urvillei*, *Sorghum bicolor*, *Panicum maximum*, *Setaria sphacelata*, *Aristida junciformis*

and *Alloteropsis semialata* amongst others (Fynn, Morris et al. 2011) (Figure 6.2). According to Scott-Shaw and Morris (2015), the most palatable species to livestock from the abovementioned grasses are *Themeda triandra*, *Tristachya leucothrix* and *Aristida junciformis*, in order of palatability. Masemola, Cho et al. (2020) state that the dry season in KwaZulu-Natal usually spans between June and July whereas Roffe, Fitchett et al. (2020) state that the wet season in KwaZulu-Natal typically spans between October and March. Grasslands in the study area are not formally managed using scientific management regimes and are considered as communal grasslands. These grasslands are managed using indigenous knowledge systems by the traditional authorities. The grasslands are utilised by locals for rearing livestock, in particular cattle, sheep, and goats. The locals use this as a means of subsistence as well as income generation.

6.2.2. Sentinel 2 MSI satellite imagery

Sentinel 2 is a multispectral imaging sensor operated by the European Space Agency and provides open, freely accessible data. Cloud-free Sentinel 2 data covering the study area was acquired on the 21 October 2021 from Land Viewer (<https://eos.com/products/landviewer/>). The image downloaded was a Sentinel 2B product which is an orthorectified and atmospherically corrected product. The Sen2Cor algorithm is used within the Sentinel Application Platform environment (SNAP) to perform atmospheric corrections and provide bottom of atmosphere reflectance data (Main-Knorn, Pflug et al. 2017). The image was captured on the 22 June 2021 and hence aligns with the days of field data collection. The Sentinel 2 mission acquires 12-bit images with a swath width of 290 km and has a temporal resolution of 5-19 days at spatial resolutions of 10, 20 and 60 m. The ortho-images have a UTM/WGS84 projection.

6.2.3. Field data collection and measurements

Grass biomass samples were collected between the 21 June 2021 and 23 June 2021 in the study area (Figure 6.2). A total of 120 10 m x 10 m quadrats, spaced approximately 100 m apart, were established within Vulindlela using a purposive sampling technique, as conducted by Royimani, Mutanga et al. (2022). A GPS reading was recorded using the Trimble GPS within each plot, which is a highly accurate sub-metre GPS system. Within each plot, two 1 m x 1 m sub-plots were

established and grass clippings were taken, with the dry biomass mass being averaged within each plot (Ma, Li et al. 2019). Grass clippings were being cut approximately 5 cm from the ground and only tufts occurring within the sub-plot were taken. Only grasses were sampled, other vegetation such as forbs and sedges were discarded. Grass samples were placed into labelled brown paper bags and a calibrated digital scale was used to measure the fresh biomass weight on the day of collection, which is known as wet mass. Grass samples were then placed into an oven at 70°C for 48 hours to remove moisture. The samples were then reweighed after being dried to determine dry mass.

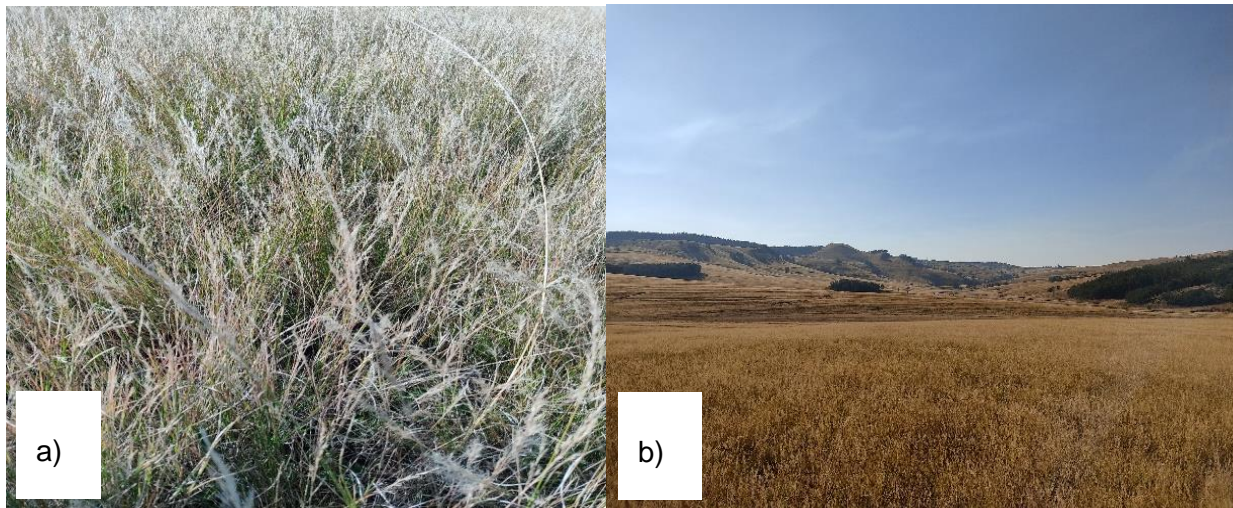


Figure 6.2: (a) *Aristida junciformis* dominated grassland and (b) typical grassland within the study area during the dry season.

6.2.4. Sentinel 2 spectral bands and variables

The Sentinel 2 MSI consists of 13 spectral bands that covers the visible, NIR and SWIR sections. The three bands with a 60 m spatial resolution were excluded from the analysis as they are primarily used for atmospheric monitoring purposes (Shoko, Mutanga et al. 2018) (Table 6.1).

Table 6.1: Sentinel 2B spectral bands (<https://eos.com/find-satellite/sentinel-2/>)

Band Number	Band Name	Central Wavelength (nm)	Bandwidth (nm)	Resolution (m)
1	Coastal aerosol	442.3	20	60
2	Blue	492.1	65	10
3	Green	559	35	10
4	Red	665	30	10
5	Red edge 1	703.8	15	20
6	Red edge 2	739.1	15	20
7	Red edge 3	779.7	20	20
8	NIR	833	115	10
8a	Red edge 8a	864	20	20
9	Water vapour	943.2	20	60
10	SWIR-Cirrus	1376.9	30	60
11	SWIR 1	1610.4	90	20
12	SWIR 2	2185.7	180	20

In addition to the abovementioned spectral bands, various vegetation indices (VIs) were computed utilising the spectral bands to assess aboveground biomass. The VIs used in this study were computed using ArcGIS 10.4 software (www.esri.com) (Table 6.2).

Table 6.2: Various vegetation indices (VIs) used in this study.

Vegetation Index	Abbreviation	Formula	Reference
<i>Broadband VIs</i>			
Enhanced Vegetation Index	EVI	$2.5 \left(\frac{NIR - R}{1 + NIR + 6R - 7.5 \times B} \right)$	(Huete, Didan et al. 2002)
Soil adjusted vegetation index	SAVI	$\frac{(NIR - R) \times (1 + L)}{(NIR + R + L)}$	(Huete 1988)
Normalised difference vegetation index	NDVI	$\frac{(NIR - R)}{(NIR + R)}$	(Huete 1988)
Renormalised difference vegetation index	RDVI	$\frac{(NIR - R)}{\sqrt{(NIR + R)}}$	(Roujean and Breon 1995)
Simple ratio	SR	$\frac{NIR}{R}$	(Chen 1996)
Modified simple ratio	MSR	$\frac{(NIR \div R - 1)}{\sqrt{(NIR \div R) + 1}}$	(Chen 1996)

Vegetation Index	Abbreviation	Formula	Reference
Green normalised difference vegetation index	GNDVI	$\frac{(NIR - Green)}{(NIR + Green)}$	(Fernández-Manso, Fernández-Manso et al. 2016)
Green-blue normalised difference vegetation index	GBNDVI	$\frac{NIR - (G + B)}{NIR + (G + B)}$	(Santoso, Gunawan et al. 2011)
Chlorophyll green index	CGM	$\frac{NIR}{G} - 1$	(Gitelson and Merzlyak 1997)
Red-green ratio	RGR	$\frac{Red}{Green}$	(Gamon and Surfus 1999)
Atmospherically resistance vegetation index	ARVI	$\frac{(NIR - Red)}{(NIR + Blue)}$	(Kaufman and Tanre 1996)
Transformed difference vegetation index	TDVI	$\sqrt{0.5 + \frac{(NIR - Red)}{(NIR + Red)}}$	(Bannari, Asalhi et al. 2002)
Difference vegetation index	DVI	$NIR - Red$	(Tucker 1979)
	<i>Red edge VIs</i>		
Red edge 1 NDVI	NDVIRE1	$\frac{(NIR - RE1)}{(NIR + RE1)}$	
Red edge 2 NDVI	NDVIRE2	$\frac{(NIR - RE2)}{(NIR + RE2)}$	
Red edge 3 NDVI	NDVIRE3	$\frac{(NIR - RE3)}{(NIR + RE3)}$	
Red edge 8a NDVI	NDVIRE8a	$\frac{(NIR - RE8a)}{(NIR + RE8a)}$	(Shoko, Mutanga et al. 2018)
Red edge 1 SR	SRRE1	$\frac{NIR}{RE1}$	
Red edge 2 SR	SRRE2	$\frac{NIR}{RE2}$	
Red edge 3 SR	SRRE3	$\frac{NIR}{RE3}$	
Red edge 8a SR	SRRE8a	$\frac{NIR}{RE8a}$	
Normalised difference red edge 1	NDRE1	$\frac{RE1 - Red}{RE1 + Red}$	
Normalised difference red edge 2	NDRE2	$\frac{RE2 - Red}{RE2 + Red}$	
Normalised difference red edge 3	NDRE3	$\frac{RE3 - Red}{RE3 + Red}$	(Guerini Filho, Kuplich et al. 2020)
Normalised difference red edge 8a	NDRE8a	$\frac{RE8a - Red}{RE8a + Red}$	
Anthocyanin reflectance index	ARI	$\frac{1}{Green} - \frac{1}{RE1}$	(Kobayashi, Tani et al. 2020)
Red edge chlorophyll index	RECI	$\frac{RE3}{RE1} - 1$	(Clevers and Gitelson 2013)
Green chlorophyll index	GCI	$\frac{RE3}{Green} - 1$	(Clevers and Gitelson 2013)
Plant senescence reflective index	PSRI	$\frac{Red - Blue}{RE1}$	(Guerini Filho, Kuplich et al. 2020)

Vegetation Index	Abbreviation	Formula	Reference
Browning reflective index	BRI	$\frac{1}{\frac{Green}{NIR} - \frac{RE1}{NIR}}$	(Kobayashi, Tani et al. 2020)

6.2.5. Statistical analysis and machine learning

This study utilised an artificial neural network (ANN) to predict aboveground biomass using a Sentinel 2 multispectral dataset. The ANN is a machine learning algorithm that has been based on the computational mechanisms of the human brain (Mas and Flores 2008). ANNs can be trained to recognise patterns, perform complex computations and even develop self-organising abilities (Mas and Flores 2008). ANNs are typically comprised of multiple layers (Figure 6.3): an input, output and one or more hidden layers (Yang, Feng et al. 2018). A greater number of layers is associated with a greater complexity of the model (Yang, Feng et al. 2018). In terms of remote sensing applications, ANNs have been utilised extensively and have proven to provide more reliable results as compared to conventional statistical methods (Mas and Flores 2008). In terms of aboveground biomass studies, Deb, Singh et al. (2017) and Yang, Feng et al. (2018) both used ANNs to predict aboveground grass biomass.

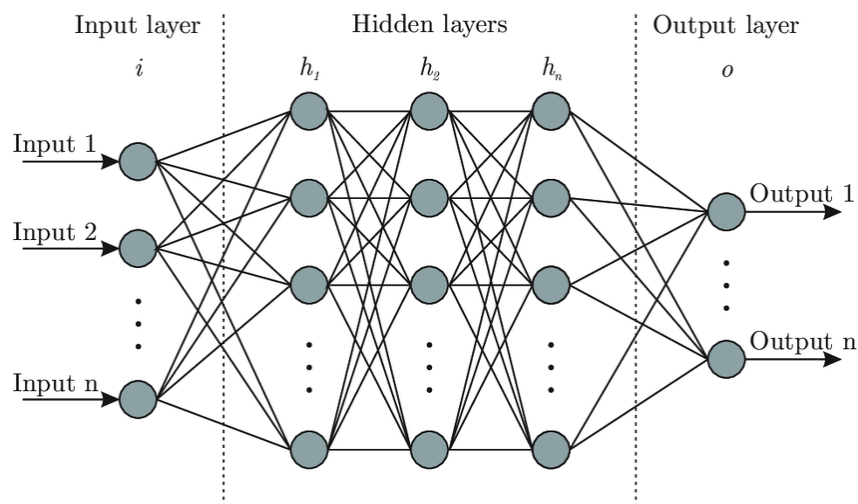


Figure 6.3: The general architecture of an ANN

Meanwhile, CNNs are an advancement to typical ANNs and have been specifically developed for analysing visual imagery (Pires de Lima and Marfurt 2020). CNNs have increasingly become useful and powerful tools in the remote sensing field, especially with image classification (Pires

de Lima and Marfurt 2020). Unlike ANNs that use weights or neurons to “learn” the data, CNNs use multiple layers that are casted on images to analyse them (Pires de Lima and Marfurt 2020). ANNs are more suited to concrete datasets, whereas CNNs are more suited for visual datasets. CNNs also provide a more automated approach to deep learning as it is able to detect important patterns and features in images with minimal human supervision (Ma, Li et al. 2019). Ma, Li et al. (2019) successfully utilised a deep CNN to estimate aboveground biomass for wheat (Figure 6.4).

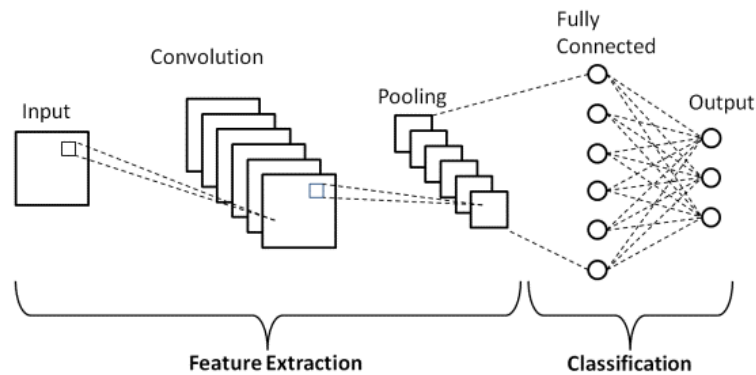


Figure 6.4: The general architecture of a CNN

An ANN and CNN were run to determine the relationship between VIs and spectral data with aboveground biomass. By manually changing the number of nodes in the hidden layer, the model successfully determined the relationship between the variables. Table 6.3 lists the parameters used to train the different models.

Table 6.3: Hyper-parameters used to train the ANN and CNN models.

Model	Hyper-parameters	Value
ANN	Number of hidden layers	4
	Number of epochs	50
	Learning rate	0.001
CNN	Kernel number	32, 64, 128, 256, 512
	Size	1*2
	Stride	2
	Number of epochs	30
	Learning rate	0.001

The models were run a maximum of five times with random initial weights. Model performance was analysed using the coefficient of determination (R^2), root mean square error (RMSE) and RMSE% assessments. The coefficient of determination is a statistical measure of the accuracy of a regression by comparing actual versus predicted data points (Schreiber, Atkinson Amorim et al. 2022). The value of R^2 ranges from 0 to 1 with a higher value insinuating a higher accuracy (Schreiber, Atkinson Amorim et al. 2022). The equation for R^2 is found below (Li, Zhou et al. 2021):

$$R^2 = 1 - \frac{\sum_{j=1}^n (y_j - \bar{y})^2}{\sum_{j=1}^n (y_j - Y)^2} \quad \text{Equation 6-1}$$

Where y_j and y represents measured and estimated biomass values, respectively; Y is the average measured biomass over all samples and n denotes the number of samples (Li, Zhou et al. 2021).

According to Shoko, Mutanga et al. (2018), the RMSE measures the difference between actual and predicted values, in this instance, actual biomass and predicted biomass values. The RMSE was calculated using the following formula as documented by Shoko, Mutanga et al. (2018):

$$RMSE = \sqrt{\frac{\sum_{i=1}^n (\text{measured value} - \text{predicted value})^2}{n}} \quad \text{Equation 6-2}$$

where *measured value* is the measured biomass in the field, *predicted value* is the predicted biomass by the model and i is the predictor variable included. The RMSE% was calculated using the following formula as expressed by Shoko, Mutanga et al. (2018):

$$RMSE\% = \frac{\sqrt{\frac{1}{n} \sum_{i=1}^n (y_i - Y_i)^2}}{y} \quad \text{Equation 6-3}$$

Where n is the number of measured values, y_i is the measured value, Y_i is the estimated value and y is the average of the measured aboveground biomass (Shoko, Mutanga et al. 2018).

Models yielding the highest R^2 and lowest RMSE/RMSE% between predicted and measured levels of biomass, based on an independent test dataset (i.e. 30% of the dataset) were retained for predicting biomass levels. Using the ANN and CNN models with spectral data and VIs, an aboveground biomass distribution map was computed. A sensitivity analysis was also conducted to determine which variables were most important in model development for the ANN and CNN. All statistical analyses were conducted utilising R statistical software package version 3.1.3.

6.3. Results

6.3.1. Descriptive Statistics

Observed grass biomass (g/m^2) during the dry season across 120 sample plots had an average of $47,82 \text{ g/m}^2$ with a standard deviation of $23,38 \text{ g/m}^2$. The highest biomass recorded was $123,8 \text{ g/m}^2$ whereas $8,2 \text{ g/m}^2$ was the lowest (Table 6.4).

Table 6.4: Descriptive statistics of the observed biomass (g/m^2) over the dry season

Period	<i>n</i>	Mean	Std. Dev	Min.	Max.	Range
Dry	120	47.82	23.38	8.2	123.8	115.6

6.3.2. Comparison of the performance of ANN and CNN

Table 6.3 and Figure 6.5 show the training and validation process of both models with their set hyperparameters. The x-axis represents the number of epochs, and the y-axis represents the root mean square error in terms of biomass. An epoch is essentially one cycle of each of the forward- and back-propagation phases. The CNN model was more adept at learning as compared to the ANN, as the CNN required 30 epochs to minimise error whereas the ANN required 50 epochs to minimise error. The error remained more or less constant after the 30th epoch in the CNN and the 50th epoch in the ANN. Determining a suitable number of epochs is essential to preventing the under or overfitting of models (Ali, Greifeneder et al. 2015, Ali, Cawkwell et al. 2016) (Figure 6.5).

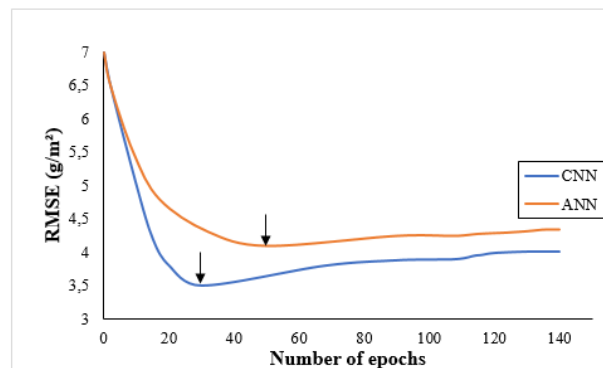


Figure 6.5: Number of epochs for each model. The arrows indicate that for the CNN and ANN models the number of epochs that gave the lowest error was 30 and 50, respectively.

In assessing the predictive performance of both the ANN and CNN machine learning algorithms in estimating aboveground biomass during the dry season, the ANN produced a R^2 value of 0,75 with a RMSE of 5,78 g/m^2 and a RMSE% of 8,90 (Figure 6.6a). In comparison, the CNN produced a R^2 value of 0,83 with a RMSE of 3,36 g/m^2 and a RMSE% of 6,09 (Figure 6.6b).

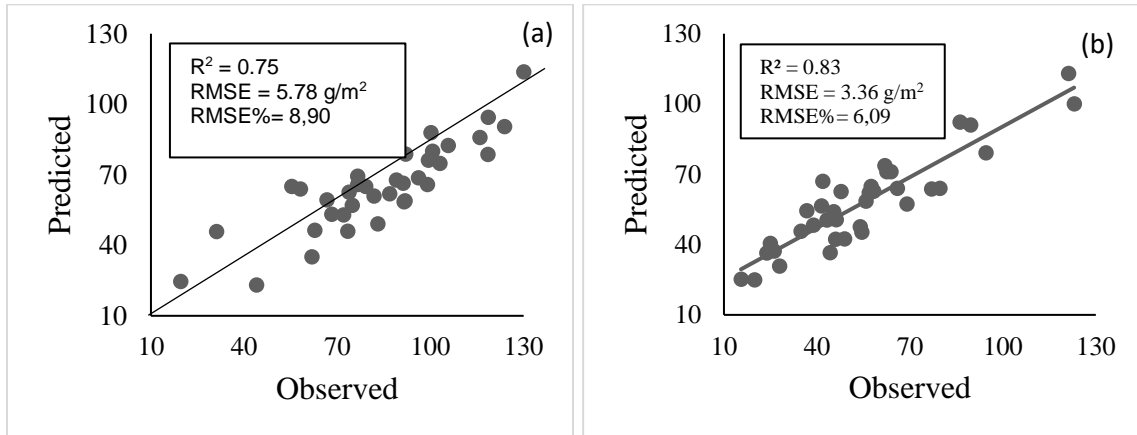


Figure 6.6: Scatterplots showing biomass over the dry season for a. ANN and b. CNN.

Figure 6.7 illustrates the spatial distribution of aboveground grass biomass in the study area during the dry season, as predicted by both the ANN and CNN. It can be observed that the predictive map conjured by the CNN has slightly more accurate aboveground biomass representation as compared to the ANN, especially in the peripheral areas of the study site.

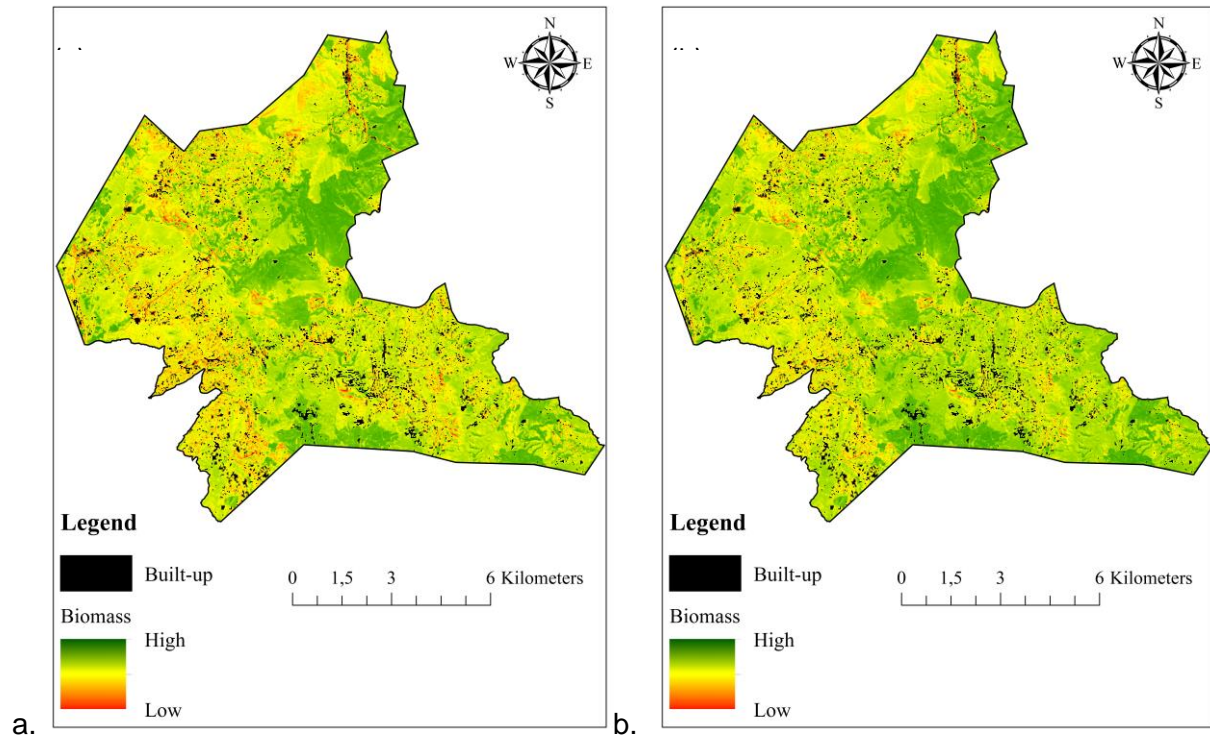


Figure 6.7: Biomass (g/m^2) over the dry season for (a). ANN and (b). CNN

In terms of a sensitivity analysis (Figure 6.8), whereby the importance of spectral bands and VIs are determined and ranked in relation to dry season biomass estimation for each model, the blue band (B02) from Sentinel 2 MSI was the most important band for the ANN, followed by the GCI and the GNDVI. In comparison, the GNDVI was the most important variable for estimating biomass for the CNN, followed closely by the GCI and the blue spectral band (B02) from Sentinel-2. For both models, the GBNDVI was the least significant variable in biomass estimation. Only variables with an average impact of $>0,1$ were included in the models.

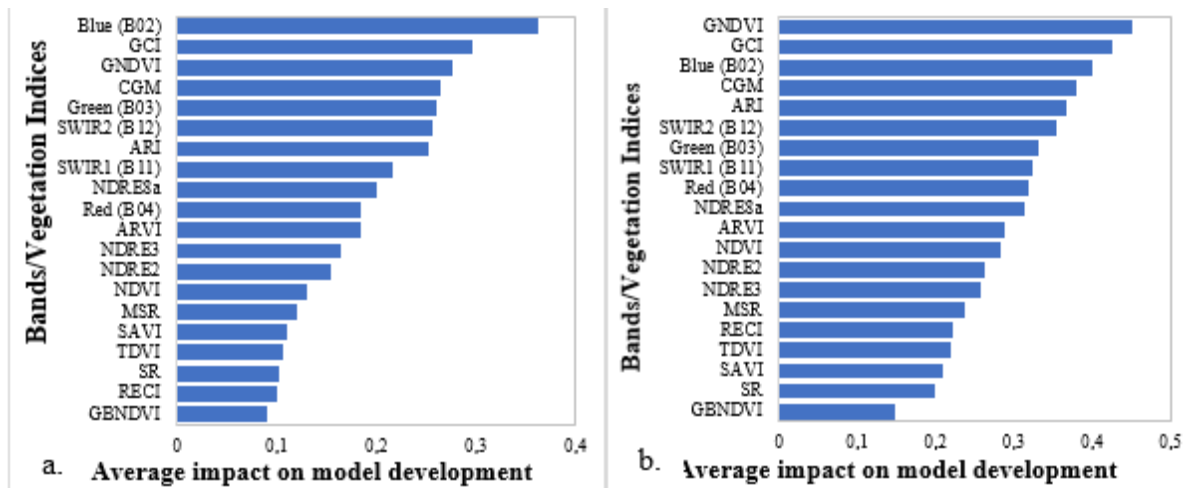


Figure 6.8: Ranking the importance of variables for developing the a. ANN and b. CNN models for biomass detection.

6.4. Discussion

This study has investigated the utilisation of two neural networks in predicting aboveground grass biomass and compared their respective performance in this regard. The advancement in machine learning has provided scientists with numerous opportunities to test their performance in real-world applications, such as in remote sensing and vegetation monitoring (Ali, Greifeneder et al. 2015). Comparing the accuracies of two different neural networks helps reveal the relationships between biomass and remote sensing variables (Dong, Du et al. 2020). To date, machine learning algorithms have proven to be much more complex and dynamic as compared to traditional statistical modelling, allowing for more complex modelling of biophysical parameters and more resounding findings and correlations (Das, Ghosh et al. 2022). This study specifically demonstrated the refinement in neural networks, as the contemporary convolutional neural network ($R^2=0,83$) outperformed the conventional artificial neural network ($R^2=0,75$) in aboveground grass biomass predictions. This is an indication of the onset of deep learning approaches in remote sensing applications (Zhu, Tuia et al. 2017).

There have been numerous recent studies that have conducted a comparative analysis between different machine learning algorithms in remote sensing applications, particularly for vegetation monitoring. The ANN is one of the oldest machine-learning algorithms and has been used extensively for grassland biomass retrieval (Ali, Greifeneder et al. 2015). A study by Xie, Sha et

al. (2009) compared the performance of ANN to multiple linear regression (MLR) in estimating the aboveground biomass of grasslands in Mongolia. This study used Landsat ETM+ (NDVI, bands 1,3,4,5,7) data and results showed that the ANN ($R^2= 0.817$, NRMSE= 42,36%) outperformed the multiple linear regression ($R^2= 0,591$, NRMSE= 53,2%). Similarly, Yang, Feng et al. (2018) found that the ANN ($R^2= 0,75-0,85$) outperforms MLR ($R^2=0,4-0,64$) in estimating grass biomass. Their study utilised normalised difference vegetative index (NDVI), enhanced vegetation index (EVI), modified soil adjusted vegetation index (MSAVI), soil adjusted vegetation index (SAVI) and optimised soil adjusted vegetation index (OSAVI) derived from MODIS data. Xie, Sha et al. (2009) utilised a single date image whereas Yang, Feng et al. (2018) utilised a multi-temporal time series. This proved that machine learning techniques are indeed an improvement to typical regression analyses, even at different spatio-temporal scales (Ali, Greifeneder et al. 2015).

Masenyama, Mutanga et al. (2022) have stated that the average R^2 value for remote sensing-grassland productivity studies ranges between 0,65 (65%) and 0,75 (75%). In comparison, the performance of both the ANN and CNN in this study is commendable with model accuracy of 75% for the ANN and 83% for the CNN. Furthermore, studies by Dong, Du et al. (2020) and Schreiber, Atkinson Amorim et al. (2022) found that ANNs were outperformed by CNNs in aboveground biomass estimation from remotely sensed data. Dong, Du et al. (2020) compared the performance of CNNs against three other machine learning algorithms, namely random forest, support vector regression and ANN, in estimating the aboveground biomass of bamboo. The Worldview-2 platform was used in this study with both spectral bands and vegetation indices being used as input data. Overall, the CNN produced better results than the ANN with a R^2 of 0,94 and RMSE of 23,1% whereas the ANN could only achieve a R^2 of 0,86 and RMSE of 36,1%. The random forest and support vector regression obtained slightly better accuracy than the CNN, however, it must be noted that the CNN had limited input variables in this study, with only spectral bands being used as input data as compared to the other two algorithms that had spectral, VI and texture data (Dong, Du et al. 2020). Similarly, Schreiber, Atkinson Amorim et al. (2022) compared the performance of ANNs and CNNs in predicting aboveground biomass of wheat using UAV-based imagery (RGB imagery with 2,14 cm² pixel size). Their findings show that the CNN reached a R^2 of 0,9065 whereas the ANN reached a R^2 of 0,9056. In this case, the ANN was slightly outperformed by CNN. However, Schreiber, Atkinson Amorim et al. (2022) also acknowledge that the homogeneity of wheat cultivation could be a slight advantage to the ANN, whereas more heterogenous study environments could see the accuracy of ANNs diminish and the accuracy of

CNNs flourish. Furthermore, they also note that the use of hyperspectral data and vegetation indices could greatly improve the accuracy of CNNs, which was absent in their study.

Kattenborn, Leitloff et al. (2021) state that since CNNs have been specialised for image analysis and processing, they are highly suitable for remote sensing applications. CNNs have proven to be extremely useful in extracting biophysical parameters of vegetation from remotely sensed data, such as species composition and biomass (Kattenborn, Leitloff et al. 2021). Deep learning approaches, which include CNNs, are gradually replacing shallow learning techniques such as ANNs, as they analyse, interpret and predict spatial data much more effectively (Zhu, Tuia et al. 2017, Pires de Lima and Marfurt 2020, Kattenborn, Leitloff et al. 2021). There has been a steady influx of biomass estimation studies utilising CNNs and remotely sensed data in academic and research circles.

Ma, Li et al. (2019) utilised a deep CNN in tandem with very high-resolution RGB digital imagery (spatial resolution= 5184 x 3456) to estimate the aboveground biomass of wheat. The CNN had a high coefficient of determination ($R^2= 0,808$) and a low NRMSE (NRMSE= 24,95%) in predicting wheat biomass (Ma, Li et al. 2019). Karila, Alves Oliveira et al. (2022) utilised a drone with RGB and hyperspectral capabilities (pixel size= 1024 x 648, 36 bands in 500-900 nm range) to estimate grass sward quality and quantity. They compared the performance of multiple deep neural networks, a CNN included, to the random forest method. Overall, their findings show that the CNN model (NRMSE= 21%) fared better than the random forest model in estimating aboveground grass biomass, with the CNN being most consistent with hyperspectral data as compared to only RGB data. Varela, Zheng et al. (2022) predicted various key traits, one of them being aboveground biomass, of *Miscanthus* grass using UAV imagery (5 spectral bands – red, blue, green, red edge and near-infrared, spatial resolution= 1,4 cm) and two CNNs. The best R^2 achieved by the 2D CNN, which was multispectral input from a single image, was 0,59 with a RMSE of 180 g whereas the 3D CNN, which was multispectral and multi-temporal (imagery from different days), produced slightly higher R^2 of 0,69 and a RMSE of 149 g.

There have been numerous biomass estimation studies for grasslands using remote sensing and machine learning in a southern African context. However, none of these has attempted at utilising CNNs for biomass prediction (Masenyama, Mutanga et al. 2022). Ramoelo and Cho (2014) attempted to estimate dry season aboveground grass biomass using the random forest algorithm and by comparing Landsat 8 and RapidEye data. They only utilised band reflectance data to

estimate biomass, stating that VIs are not always plausible for biomass estimation during the dry season since there is a lack of “greenness” in vegetation (Ramoelo and Cho 2014). RapidEye yielded better results with random forest, with a R^2 of 0,86, RMSE of 13,42 g/m² and RRMSE of 10,61% whereas Landsat 8 yielded a R^2 of 0,81, RMSE of 15,79 g/m² and RRMSE of 12,49%.

Shoko, Mutanga et al. (2018) utilised the sparse partial least square regression (SPLSR) to estimate grass biomass using three different satellites: Sentinel 2 MSI, Landsat 8 OLI and WorldView 2 in the Drakensberg. They utilised seven spectral bands from Landsat 8, ten from Sentinel 2 and eight from WorldView 2 as well as various VIs. Their findings showed that WorldView 2 derived variables yielded the best predictive accuracies (R^2 between 0,71 and 0,83; RMSE between 6,92% and 9,84%), followed by Sentinel 2 (R^2 between 0,6 and 0,79; RMSE between 7,66% and 14,66%) and lastly Landsat 8 (R^2 between 0,52 and 0,71; RMSE between 9,07% and 19,88%). Vundla, Mutanga et al. (2020) assessed the aboveground biomass of grasslands in the Eastern Cape using Sentinel 2 MSI and the partial least squares regression (PLSR) algorithm. They utilised the visible, red-edge and shortwave infrared bands as well as NDVI and simple ratio (SR) as input data for the PLSR. Their results show that the PLSR performed well in estimating grass biomass, with a R^2 of 0,83 and a RMSE of 19,11 g/m².

The sensitivity analysis for both models was conducted to determine which spectral bands and VIs were most important in estimating aboveground grass biomass. This is discerned by examining the correlation between aboveground biomass values and spectral/VI values (Li, Zhou et al. 2021). For both models, the vegetation indices and spectral bands proved to be relatively accurate proxies for estimating aboveground grass biomass, a finding that also concurs with Pang, Zhang et al. (2020). This contrasts the suggestions of Ramoelo and Cho (2014) that vegetation indices may not be suitable for dry season grass biomass estimation due to grass senescence, with only spectral data yielding better results during the dry season. For both the ANN and CNN models, five bands (blue, green, red, SWIR2, SWIR1), nine VIs (GNDVI, CGM, ARVI, NDVI, MSR, SAVI, TDVI, SR, GBNDVI) and six red edge VIs (GCI, ARI, NDRE8a, NDRE3, NDRE2, RECI) were considered important for model development. Other studies also showed that utilising both spectral data and VIs improved biomass predictions as opposed to using them independently (Shoko, Mutanga et al. 2018, Yang, Feng et al. 2018, Pang, Zhang et al. 2020, Li, Zhou et al. 2021).

By comparing the results of the sensitivity analysis in this study to other similar biomass studies, it is evident that direct comparisons cannot be established due to the diversity in platform and machine learning algorithms used. Shoko, Mutanga et al. (2018), using Sentinel 2 MSI and SPLSR, found that the SWIR1, SWIR2, green, red and red edge 1 were the most important sensor variables, whereas NDRE1 and NDVI were the most important VIs in predicting grass biomass. Parallels can be drawn between the spectral bands for this study and Shoko, Mutanga et al. (2018), however, this study provides substantially more VIs of significance. Vundla, Mutanga et al. (2020), using Sentinel 2 MSI and PLSR, discovered that simple ratio VIs had the highest importance whilst NDVI had the lowest importance in assessing grass biomass. Their findings on the simple ratio VIs contradict the findings in this study, with the simple ratio VI being of smaller importance in both the ANN and CNN models. However, NDVI was shown to have a reduced significance in both studies.

NDVI, a widely used VI in remote sensing, was shown to have a moderate impact on biomass estimation in this study for both models. This concurs with the findings of Deb, Singh et al. (2017) who also found that other VIs produced better biomass estimates than NDVI when paired with neural networks. Ramoelo and Cho (2014) suggest that NDVI is susceptible to grass senescence during the dry season and hence will tend to underestimate biomass. This is due to NDVI essentially measuring vegetation “greenness”, which is primarily absent from grasses during the dry season (Ramoelo and Cho 2014). Deb, Singh et al. (2017) state that NDVI is often subjected to variations in atmospheric conditions, soil elements, plant phenology and external disturbances which hinder its efficacy in estimating biomass. The findings in this study also show a lesser impact of NDVI on biomass estimates as compared to other VIs.

There are no known studies to date that have utilised Sentinel 2 data with CNNs to assess aboveground biomass. Hence, comparing sensitivity analysis results for the CNN is not plausible. Findings in this study come closest to findings by Li, Zhou et al. (2021) who predicted aboveground grass biomass using Sentinel 2 MSI in tandem with RF and XGBoost algorithms. They found that the GNDVI and GCI were the most important variables for developing the RF model. GNDVI and GCI were also highly impacting variables in this study for both the ANN and CNN models. According to Dusseux, Guyet et al. (2022), GNDVI has been well-documented and used in relation to vegetation biomass. GCI, and other red edge-based VIs, have also proven to be particularly useful in biomass studies due to their important relationship with chlorophyll content and nutrients present in plant cells (Vundla, Mutanga et al. 2020, Dusseux, Guyet et al.

2022). Ramoelo and Cho (2014) found that blue, green and red edge spectral data were important for predicting aboveground grass biomass during the dry season, albeit using RapidEye and RF. This study also shows the importance of blue and green spectra; however, shortwave infrared was deemed more significant in this study as compared to red edge spectra.

In comparison to the abovementioned studies, the performance of both NNs in this study is relatively commendable. However, it must be acknowledged that all machine learning algorithms used in remote sensing studies are not comprehensive tools for classifying or predicting biophysical attributes (Dong, Du et al. 2020). They all have their benefits, strengths and limitations based on numerous factors such as sensor type, spatial resolution, temporal resolution and spectral resolution (Das, Ghosh et al. 2022). Dong, Du et al. (2020) state that both CNN and ANN are highly sensitive to the architecture and parameter settings and hence these aspects must be geared appropriately to avoid poor model performance. Model performance can either be too low, whereby the model's predictive ability is poor, or too high, whereby the model begins to overfit the data (Kattenborn, Leitloff et al. 2021). Neural networks are typically known for their tendency to overfit data and hence preventative solutions must be implemented during data processing to mitigate this (Ali, Greifeneder et al. 2015).

Furthermore, both types of neural networks used in this study require high computational power and are time-consuming (Dong, Du et al. 2020). Other machine learning techniques such as random forest are much more compatible with smaller sample sizes or input data as opposed to neural networks, and these factors must be accommodated (Ali, Greifeneder et al. 2015). It must also be noted that CNNs perform better with multi-temporal spatial data (3D CNNs) as compared to single-date imagery (2D CNNs) (Varela, Zheng et al. 2022). The utilisation of CNNs in remote sensing applications is still gaining momentum, and hence there is much need for future research to try and optimise the algorithm for vegetation remote sensing (Kattenborn, Leitloff et al. 2021). Much of the focus of CNNs in vegetation remote sensing has been on object identification and classification, however semantic segmentation applications, such as biomass and LAI predictions, must be explored further (Kattenborn, Leitloff et al. 2021). It is unlikely that CNNs will replace ANNs altogether in the remote sensing field as they both provide advantages and disadvantages, and the practicality of each is case-specific (Ali, Greifeneder et al. 2015). However, CNNs do have great potential for grassland biomass studies in future.

6.5. Conclusion

This study compared the performance of two neural networks in estimating the aboveground biomass of grass, using Sentinel 2 space-borne spectral data and derived vegetation indices. Findings in this study suggest that the deep learning neural network, CNN, outperforms the traditional ANN. However, both algorithms performed satisfactorily in predicting grass biomass. This study can be considered pilot-scale research, particularly in a southern African context, as no known research has attempted to compare the performance of two different neural networks in grassland monitoring. Although each algorithm has pros and cons, with large training datasets and computational time being a common disadvantage of both, this pioneering research establishes a great potential for the utilisation of CNNs in remote sensing research in the future. Future research can improve upon this research by incorporating larger training datasets and utilising multi-temporal and higher-resolution data to enhance the performance of CNNs in biophysical remote sensing studies. The primary objective of this study was to determine which neural network would better predict grass biomass using open-access and freely available satellite data. The CNN model developed in this study can be considered an effective one for the accurate estimation of biomass in grassland monitoring and is evidence of the advancement in applied deep learning.

7. Predicting inter-seasonal grass biomass utilising satellite remote sensing in the Vulindlela area of the Umgeni catchment, KwaZulu-Natal

M Vawda, R Lottering, K Peerbay, and O Mutanga

7.1. Introduction

Grasslands cover approximately 26% of the total land area with the majority of grasslands situated in tropical and sub-tropical developing countries around the world (Boval and Dixon 2012). Grasslands are defined by Mucina and Rutherford (2006) as grass-dominated biomes, with the majority of grasses being C4 plants in low to mid-altitudes and C3 plants being more prominent in higher altitudes. Woody species are controlled by frost, fire or grazing in grasslands which allow grasses to dominate (Mucina and Rutherford 2006). Grasslands are environmentally, socially and economically valuable biomes worldwide as they serve as water catchments, biodiversity reserves, carbon sinks, recreational areas and agricultural practices (Boval and Dixon 2012). The grassland biome is a major biome in South Africa and exists mostly in the eastern parts of the country from altitudes near sea level to around 2800 m above sea level (Mucina and Rutherford 2006).

Grasslands are used extensively in South Africa as a fodder source for livestock rearing in both commercial and rural contexts (Richardson, Hoffman et al. 2010). For livestock production, grasslands are more commonly termed rangelands (Richardson, Hoffman et al. 2010). South Africa consists primarily of two types of grasslands based on environmental factors such as precipitation and altitude: these are the sourveld and sweet veld grasslands (O'Connor, Martindale et al. 2011). The sourveld grasslands have higher fibre content and tend to withdraw nutrients from the leaves during winter or dry periods whereas the sweetveld grasses have lower fibre content and maintain a consistent conglomerate of nutrients during winter or dry periods (Ellery, Scholes et al. 1995). A significant portion of grasslands in South Africa is intensively managed for optimal foraging efficiency in livestock production, which in turn ensures that livestock remains in peak condition to maintain productivity (O'Connor, Martindale et al. 2011).

The livestock and wildlife sectors in South Africa are heavily dependent on the grassland biome for maintaining productivity and functionality (Palmer, Short et al. 2010). Livestock production is essential for meeting the demand for high-quality meat and dairy in South Africa (O'Connor, Martindale et al. 2011). However, livestock is not only economically important but socially

important as well, as many rural communities depend on livestock for a sustainable livelihood (Palmer, Short et al. 2010, Richardson, Hoffman et al. 2010). This is particularly so in a South African context whereby indigenous peoples depend heavily on livestock for food, income, social status and overall well-being (Rasch, Heckelei et al. 2016). Grasslands are a cheap source of stock feed for many rural communities in which natural disasters and socio-economic challenges are prevalent (Sibanda, Mutanga et al. 2017). Hence, rangelands must be managed efficiently to ensure that livestock production remains viable and beneficial.

For grazers like livestock, biomass is the main indicator of the quantity of fodder available to livestock for consumption (Ramoelo and Cho 2014). Biomass varies throughout the year based on seasonal fluctuations: the wet season in the summer months and the dry season in the winter months (Ramoelo and Cho 2014). Livestock is often limited by fodder availability during the dry season. However, in the KZN sourveld grasslands, livestock may be limited by quantity and quality during the dry season (Ramoelo, Cho et al. 2015). Rust and Rust (2013) emphasise that climate change poses a significant threat to rangelands and livestock production as increased variability in climatic conditions provides rangeland managers with a stern challenge to predict future fodder availability. Other threats to grassland productivity include infrastructural development, crop farming and overgrazing (Sibanda, Mutanga et al. 2017). On the contrary, O'Mara (2012) suggests that grasslands may play a significant role in food security and carbon sequestration in the future, despite the many threats. Therefore, the prediction of fluxes in seasonal fodder biomass is essential to inform planning and management strategies in grasslands (Ramoelo and Cho 2014).

The technological advancements in remote sensing enable scientists to successfully predict and estimate biomass in both natural and agricultural contexts (Ramoelo and Cho 2014). Remote sensing allows managers to monitor the quantity and quality of fodder throughout the year to inform decision-making and maintain rangeland productivity (Ramoelo, Cho et al. 2015). Ramoelo, Cho et al. (2015) state that conventional methods of predicting biomass are time-consuming and energy intensive. Mutanga, Dube et al. (2016) have documented how remote sensing has been applied to vegetation monitoring in South Africa with readily available and easily accessible satellite data. Remote sensing, also termed earth observation, has been used extensively to facilitate biomass monitoring at various spatio-temporal scales with satisfactory results of accuracy and precision (Sibanda, Mutanga et al. 2017). However, earth observation is a complex process and often produces varying degrees of success based on the different

methodologies used as well as the diverse biophysical and environmental traits in vegetation (Sibanda, Mutanga et al. 2017).

The number of biomass estimation studies using remote sensing data is ever-growing. However, such studies are still limited in data-scarce countries such as those in southern Africa (Sibanda, Mutanga et al. 2017). The majority of historical biomass studies have focused on forests and have used Landsat data due to it being freely available (Samimi and Kraus 2004, Sibanda, Mutanga et al. 2017). However, Landsat data has its limitations with restricted spatial and radiometric capabilities (Shoko, Mutanga et al. 2018). Recent studies have gradually progressed to more high-resolution data, such as Sentinel 2 (Shoko, Mutanga et al. 2018), WorldView 2 (Shoko, Mutanga et al. 2018) and WorldView 3 (Sibanda, Mutanga et al. 2017). These satellites provide higher spatial and spectral resolution with faster revisit times and hence allow for much more refined biomass monitoring and estimation studies (Shoko, Mutanga et al. 2018).

Furthermore, the complexity and multi-dimensionality of remote sensing data have proved to be a challenge in terms of data processing and analysis, especially when using traditional statistical methods (Ali, Greifeneder et al. 2015). Scientists have successfully applied the use of machine learning to remote sensing studies over the years for the classification, object identification or prediction of biophysical variables (Mas and Flores 2008). However, the ongoing improvement and refinement of machine learning techniques have resulted in numerous types of algorithms that can be applied to remote sensing (Ali, Greifeneder et al. 2015). Currently, there is a growing shift towards deep learning approaches, which have the potential to yield much more accurate results in remote sensing studies (Zhu, Tuia et al. 2017). One such example of a deep learning technique is convolutional neural networks (CNNs) which have been specifically geared for imagery (Kattenborn, Leitloff et al. 2021). The utility of CNNs for vegetation biomass has been investigated before by Ma, Li et al. (2019), Dong, Du et al. (2020) and Varela, Zheng et al. (2022). However, the practicality of CNNs for assessing aboveground grass biomass has yet to be determined.

The advancement in multispectral scanners such as the introduction of Sentinel-2 provides great opportunities to build on and improve biomass studies in southern Africa (Sibanda, Mutanga et al. 2017). There is a lack of studies with regard to inter-seasonal changes in grasslands (Masenyama, Mutanga et al. 2022), particularly at larger spatial scales in both South Africa (Dingaana and Tsubo 2019) and Africa (Hunter, Mitchard et al. 2020). In this regard, this study

aims to fulfilling this research gap in the academic literature as well as in an applicational sense, that can assist rangeland managers and rural communities in making more informed decisions. This study sought to predict inter-seasonal variations of grass biomass in using Sentinel 2 MSI remotely sensed data in conjunction with convolutional neural networks (CNNs). It also explored potential measures that can be used to improve grassland management.

7.2. Methods

7.2.1. Study Area

Vulindlela is located within the UMgungundlovu district and is considered a part of the greater Umgeni river catchment in the KwaZulu-Natal province (Figure 7.1). Sibanda, Onisimo et al. (2021) describe the local climate as sub-tropical, typical of cool, dry winters and mild, wet summers. The area receives a mean annual rainfall of approximately 980 mm and a median annual rainfall of around 850 mm. Recorded annual maximum and minimum temperatures are 22°C and 10°C respectively (Sibanda, Onisimo et al. 2021). Soil factors within the area are shallow with moderate to poor drainage (Sibanda, Onisimo et al. 2021). Climatic factors such as temperature and precipitation are the main driving factors for vegetation in this area (Sibanda, Onisimo et al. 2021).

Fynn, Morris et al. (2011) state that grasslands within the study area are categorised as mesic grasslands and are usually dominated by a few species, depending on grassland conditions. The grasslands were initially dominated by *Themeda triandra* grass (Royimani, Mutanga et al. 2022). However, due to anthropogenic transformation, the grasslands are now characterised by species such as *Aristida junciformis*, *Panicum maximum* and *Paspalum urvillei*, amongst others (Royimani, Mutanga et al. 2022). The study area experiences the dry season in June/July (Masemola, Cho et al. 2020) whereas the wet season usually stretches from October to March (Roffe, Fitchett et al. 2020) (Figure 7.1). Local communities utilise the communal grasslands as rangelands for their livestock as well as for cultural purposes. Livestock is a significant source of income for the locals and hence rangeland productivity affects them directly.

7.2.2. Sentinel 2 MSI satellite imagery

Two Sentinel-2 Multi-Spectral Instrument (MSI) seasonal scenes were freely acquired from Land Viewer (<https://eos.com/products/landviewer/>). The images were downloaded on 21 October 2021 and 14 April 2022 respectively. Both images were downloaded as cloud-free Sentinel 2B products which are orthorectified and atmospherically corrected products that are pre-processed in the Sentinel Application Platform (SNAP) using the Sen2Cor algorithm (Main-Knorn, Pflug et al. 2017). The dry season image was captured on 22 June 2021 whereas the wet season image was captured on 29 March 2022. The image acquisition dates, therefore, align with the field data collection periods. Sentinel-2 MSI acquires 12-bit images with a swath width of 290 km, a revisit time of 5-19 days and spatial resolutions ranging from 10 to 60 m. Sentinel-2 MSI has been highly recommended for grassland monitoring mainly due to its extensive coverage, high spatial and temporal resolutions and its ability to capture data in the Red Edge section of the electromagnetic spectrum (Royimani, Mutanga et al. 2022).

7.2.3. Field data collection and measurements

Dry season data collection was conducted between 21 June 2021 and 23 June 2021. Wet season data collection was conducted between 28 March 2022 and 1 April 2022. The sampling strategy remained uniform between the two seasons. In each data collection period, a total of 120 plots of 10 m x 10 m in size at a distance of 100 m apart were established using the purposive sampling technique (Royimani, Mutanga et al. 2022). Within each plot, a GPS reading was recorded using a Trimble GPS which outputs coordinates at a sub-metre level. Within each plot, two sub-plots of 1 m x 1 m in size were sampled for aboveground biomass, with the mean dry biomass being recorded for each plot (Ma, Li et al. 2019). Ma, Li et al. (2019) state that 1 m x 1 m quadrats are suitable for grasslands that are heterogenous, such as natural grasslands. Grass clippings were initially weighed using a calibrated scale and wet mass was recorded. The samples were then oven-dried for 48 hours at 70°C and were thereafter reweighed to determine dry mass.

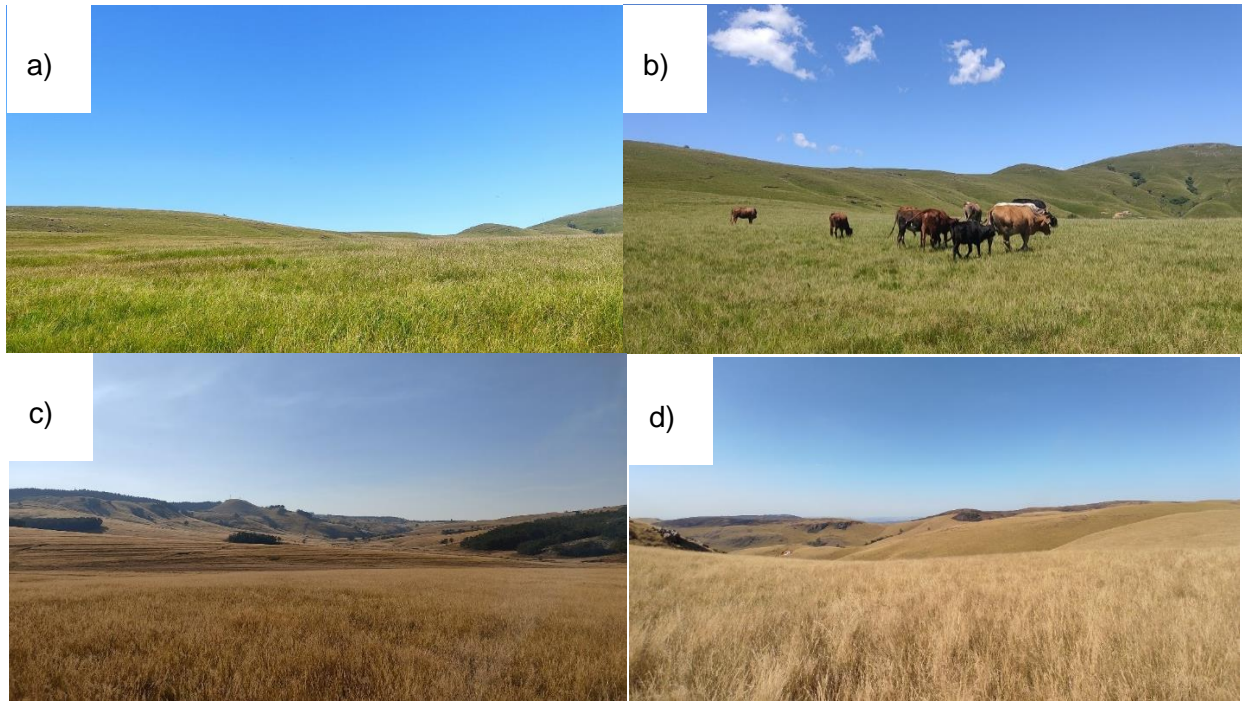


Figure 7.1: Images of the study area (a) during the wet season (b) in the context of grazing, (c and d). during the dry season (March 2022).

7.2.4. Sentinel 2 spectral bands and variables

Sentinel 2 MSI provides spectral data in 13 bands that range from visible to shortwave infrared. Blue, green, red and NIR have a spatial resolution of 10 m, whereas Red Edge and SWIR bands have a spatial resolution of 20 m. Coastal aerosol, SWIR Cirrus and water vapour have a spatial resolution of 60 m, however, these were excluded from this study as they are mainly used for atmospheric monitoring (Shoko, Mutanga et al. 2018).

Numerous vegetation indices (VIs) were computed from the Sentinel 2 spectral data. All VIs were calculated in ArcGIS 10.4 (www.esri.com). A detailed description of all VIs and their associated formulas is given in the table below (Table 7.1).

Table 7.1: Vegetation indices used in this study derived from Sentinel 2 spectral data.

Vegetation Index	Abbreviation	Formula	Reference
<i>Broadband VIs</i>			
Enhanced Vegetation Index	EVI	$2.5 \left(\frac{NIR - R}{1 + NIR + 6R - 7.5 \times B} \right)$	(Huete, Didan et al. 2002)
Soil-adjusted vegetation index	SAVI	$\frac{(NIR - R) \times (1 + L)}{(NIR + R + L)}$	(Huete 1988)
Normalised difference vegetation index	NDVI	$\frac{(NIR - R)}{(NIR + R)}$	(Huete 1988)
Renormalised difference vegetation index	RDVI	$\frac{(NIR - R)}{\text{Sqrt}(NIR + R)}$	(Roujean and Breon 1995)
Simple ratio	SR	$\frac{NIR}{R}$	(Chen 1996)
Modified simple ratio	MSR	$\frac{(NIR \div R - 1)}{\text{Sqrt}(NIR \div R) + 1}$	(Chen 1996)
Green normalised difference vegetation index	GNDVI	$\frac{(NIR - Green)}{(NIR + Green)}$	(Fernández-Manso, Fernández-Manso et al. 2016)
Green-blue normalised difference vegetation index	GBNDVI	$\frac{NIR - (G + B)}{NIR + (G + B)}$	(Santoso, Gunawan et al. 2011)
Chlorophyll green index	CGM	$\frac{NIR}{G} - 1$	(Gitelson and Merzlyak 1997)
Red-green ratio	RGR	$\frac{Red}{Green}$	(Gamon and Surfus 1999)
Atmospherically resistance vegetation index	ARVI	$\frac{(NIR - Red)}{(NIR + Blue)}$	(Kaufman and Tanre 1996)

Vegetation Index	Abbreviation	Formula	Reference
Transformed difference vegetation index	TDVI	$\sqrt{0.5 + \frac{(NIR - Red)}{(NIR + Red)}}$	(Bannari, Asalhi et al. 2002)
Difference vegetation index	DVI	$NIR - Red$	(Tucker 1979)
<i>Red edge VIs</i>			
Red edge 1 NDVI	NDVIRE1	$\frac{(NIR - RE1)}{(NIR + RE1)}$	(Shoko, Mutanga et al. 2018)
Red edge 2 NDVI	NDVIRE2	$\frac{(NIR - RE2)}{(NIR + RE2)}$	
Red edge 3 NDVI	NDVIRE3	$\frac{(NIR - RE3)}{(NIR + RE3)}$	
Red edge 8a NDVI	NDVIRE8a	$\frac{(NIR - RE8a)}{(NIR + RE8a)}$	
Red edge 1 SR	SRRE1	$\frac{NIR}{RE1}$	
Red edge 2 SR	SRRE2	$\frac{NIR}{RE2}$	
Red edge 3 SR	SRRE3	$\frac{NIR}{RE3}$	
Red edge 8a SR	SRRE8a	$\frac{NIR}{RE8a}$	
Normalised difference red edge 1	NDRE1	$\frac{RE1 - Red}{RE1 + Red}$	(Guerini Filho, Kuplich et al. 2020)
Normalised difference red edge 2	NDRE2	$\frac{RE2 - Red}{RE2 + Red}$	
Normalised difference red edge 3	NDRE3	$\frac{RE3 - Red}{RE3 + Red}$	
Normalised difference red edge 8a	NDRE8a	$\frac{RE8a - Red}{RE8a + Red}$	

Vegetation Index	Abbreviation	Formula	Reference
Anthocyanin reflectance index	ARI	$\frac{1}{Green} - \frac{1}{RE1}$	(Kobayashi, Tani et al. 2020)
Red edge chlorophyll index	RECI	$\frac{RE3}{RE1} - 1$	(Clevers and Gitelson 2013)
Green chlorophyll index	GCI	$\frac{RE3}{Green} - 1$	(Clevers and Gitelson 2013)
Plant senescence reflective index	PSRI	$\frac{Red - Blue}{RE1}$	(Guerini Filho, Kuplich et al. 2020)
Browning reflective index	BRI	$\frac{1}{Green} - \frac{1}{RE1}$ NIR	(Kobayashi, Tani et al. 2020)

7.2.5. Statistical analysis and machine learning

Convolutional Neural Networks are an emerging class of machine learning algorithms that have been used to interpret geospatial information in primarily two ways: object detection and semantic segmentation (Brodrick, Davies et al. 2019). Object detection is characterised as the identification of key components in an image and semantic segmentation is the classification of each pixel individually in an image (Brodrick, Davies et al. 2019). CNNs are a subset of deep learning models and are viewed as an advancement to typical ANNs (Brodrick, Davies et al. 2019). In the application of remote sensing for vegetation monitoring, input data in the form of spectral indices and texture metrics are the cornerstone of modelling (Kattenborn, Leitloff et al. 2021). However, these predictors are endless and it is difficult to define the most appropriate predictors for vegetation analysis as they are influenced by the biochemical and structural properties of plants as well as other environmental factors (Kattenborn, Leitloff et al. 2021). With deep learning, the CNN has the ability to learn and decipher which input variables are the best for analysis based on learning spatial features present in the data (Kattenborn, Leitloff et al. 2021).

CNNs are made up of neurons that are organised in layers, with three main layers: input, hidden and output layers (Kattenborn, Leitloff et al. 2021). Neurons within the same layer and between different layers are connected by weights and biases (Kattenborn, Leitloff et al. 2021). CNNs contain at least one convolutional layer within the hidden layers. These convolutional layers

exploit patterns in the data using filters by convolving, which is the sliding of the filter over the layer and calculating the dot-product of the filter and layer values (Kattenborn, Leitloff et al. 2021). The product of convolving is called a feature map. The feature maps are simplified in a pooling layer which assists in data reduction, simpler model parameters, lower computational load and a reduction in overfitting (Kattenborn, Leitloff et al. 2021). Biomass prediction would be performed using a semantic segmentation variation of a CNN. Encoding layers within the convolutional layer cluster and aggregate information from the entire dataset. Decoding layers follow encoding layers, and these are responsible for increasing spatial resolution and decreasing convolution depth. In simple terms, this allows the CNN to make pixel-by-pixel predictions at the same spatial resolution as the input data. This would ensure that model predictions and ground truthing data can be compared directly (Brodrick, Davies et al. 2019). A typical structure of a CNN, known as CNN architecture, is depicted below (Figure 7.2):

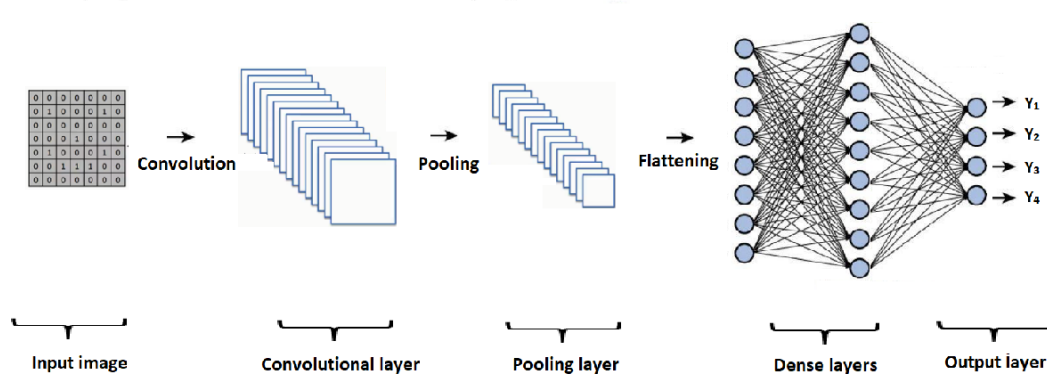


Figure 7.2: A general structure of a CNN.

Dong, Du et al. (2020) give the formula of convolution as:

$$map_{l,j}^{x,y} = f \left[\sum_m \sum_{h=0}^{H_i-1} \sum_{w=0}^{W_i-1} k_{l,j,m}^{h,w} map_{(l-1),m}^{(x+h),(y+w)} + b_{l,j} \right] \quad \text{Equation 7-1}$$

where $k_{l,j,m}^{h,w}$ represents the value at the position (h,w) of the kernel connected to the m th feature map in the $(l-1)$ th layer, H_i and W_i are the height and width of the kernel, $b_{l,j}$ is the bias of the j th feature map in the l th layer and f is the activation function (Dong, Du et al. 2020). The CNN model was constructed and run using R statistical software version 3.1.3. The hyper-parameters of the CNN in this study can be found below in Table 7.2:

Table 7.2: Hyper-parameters used to train the CNN model.

Model	Hyper-parameters	Value
CNN-Dry	Kernel number	32, 64, 128, 256, 512
	Size	1*2
	Stride	2
	Number of epochs	30
	Learning rate	0.001
CNN-Wet	Kernel number	32, 64, 128, 256, 512
	Size	1*2
	Stride	2
	Number of epochs	30
	Learning rate	0.001

7.2.6. Accuracy Assessment

Accuracy assessments are essential for understanding model performance and determining model practicality. Three standardised error metrics were used to assess model performance: coefficient of determination (R^2), root mean square error (RMSE) and root mean square error percentage (RMSE%). Schreiber, Atkinson Amorim et al. (2022) define R^2 as a statistical measure of accuracy by comparing observed versus predicted data points. R^2 values tend to range from 0 to 1 with a higher value translating into higher model accuracy and vice-versa. The equation for R^2 is found below (Li, Zhou et al. 2021):

$$R^2 = 1 - \frac{\sum_{j=1}^n (y_j - \hat{y})^2}{\sum_{j=1}^n (y_j - Y)^2} \quad \text{Equation 7-2}$$

Where y_j represents measured biomass, \hat{y} is estimated biomass, Y is mean biomass across all samples and n is the sample number (Li, Zhou et al. 2021).

The RMSE measures the difference between actual and predicted values and is calculated by:

$$RMSE = \sqrt{\frac{\sum_{i=1}^n (\text{measured value} - \text{predicted value})^2}{n}} \quad \text{Equation 7-3}$$

as documented by Shoko, Mutanga et al. (2018). The *measured value* and *predicted value* is the actual biomass in the field and the predicted biomass, respectively.

The RMSE% provides a magnitude of error in relation to actual values and can be expressed by the following formula (Shoko, Mutanga et al. 2018):

$$RMSE\% = \frac{\sqrt{\frac{1}{n} \sum_{i=1}^n (y_i - Y_i)^2}}{y} \quad \text{Equation 7-4}$$

Where n is the number of samples, y_i and Y_i are measured and predicted values, respectively; and y is the average of the measured values.

Following the general training/test rule, 70% of the dataset was used to train the CNN model whereas 30% was used to test the model. Models with the highest R^2 and lowest RMSE/RMSE% were retained for predicting aboveground biomass in both seasons. Using Sentinel 2 spectral bands and derived VIs as input data, predictive biomass distribution maps were constructed for both seasons. A sensitivity analysis was also run to determine which input variables were the most significant in developing the CNN model.

7.3. Results

7.3.1. Descriptive Statistics

The mean aboveground biomass recorded during the dry season was 47,82 g/m² with a standard deviation of 23,38 g/m². The range observed during the same period was 115,6 g/m² with 123,8 g/m² and 8,2 g/m² being the highest and lowest biomass values recorded, respectively. Aboveground biomass recorded during the wet season differed substantially, with average biomass of 195,67 g/m² and a standard deviation of 72,04 g/m². The wet season had a range of 403,5 g/m² with 477,3 g/m² and 73,8 g/m² being the highest and lowest biomass values recorded, respectively (Table 7.3).

Table 7.3: Descriptive statistics of the observed biomass (g/m^2) over the wet and dry season

Period	<i>n</i>	Mean	Std. Dev	Min.	Max.	Range
Dry	120	47.82	23.38	8.2	123.8	115.6
Wet	120	195.67	72.04	73.8	477.3	403.5

7.3.2. CNN Training History

The CNN models for both seasons were run with a maximum of 140 epochs, however, this was stopped after 30 epochs as this was when model performance was optimal (Figure 7.3). An epoch can be defined as one complete cycle of the forward and back-propagation phases. The loss function for the models was RMSE.

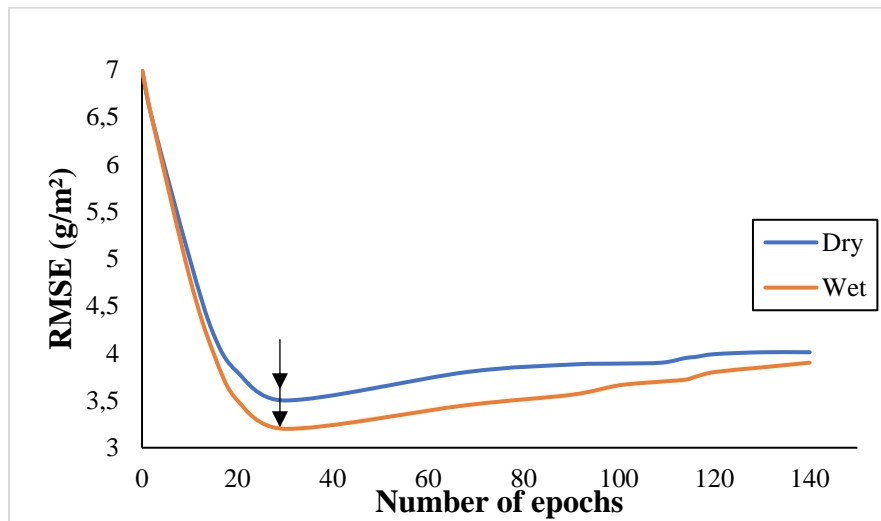


Figure 7.3: Number of epochs for each model. The arrows indicate that for the CNN-Dry and CNN-Wet models the number of epochs that gave the lowest error was both 30.

7.3.3. Dry season vs Wet season

The CNN algorithm used to predict aboveground biomass produced an R^2 of 0,83 with a RMSE of 3,36 g/m^2 and an RMSE% of 6,09 in the dry season (Figure 7.4(a)). Comparatively, the CNN produced a R^2 of 0,85, RMSE of 2,41 g/m^2 and RMSE% of 3,71 in the wet season (Figure 7.4(b)).

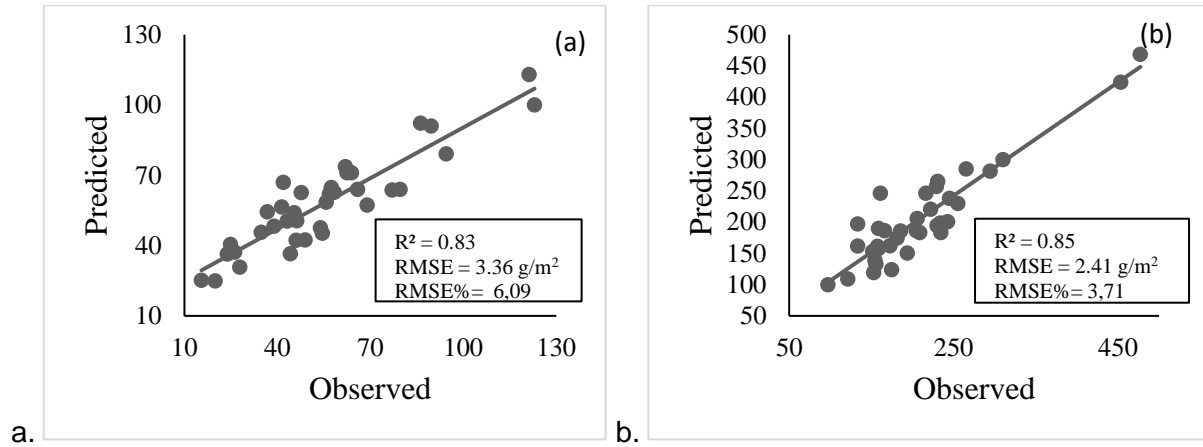


Figure 7.4: Scatterplots showing observed and predicted biomass over the a. dry season and b. wet season using CNN.

Figure 7.5 illustrates the spatial distribution of aboveground grass biomass during the dry and wet seasons. The difference in aboveground grass biomass can be observed between the two seasons with higher biomass indicated in the wet season as compared to the dry season. Although higher biomass was predicted in some areas of the study site during the dry season, these areas of high biomass are concentrated in certain parts of the study area. Overall, the wet season depicts higher biomass over a greater spatial scale, with biomass being more evenly distributed across the study area.

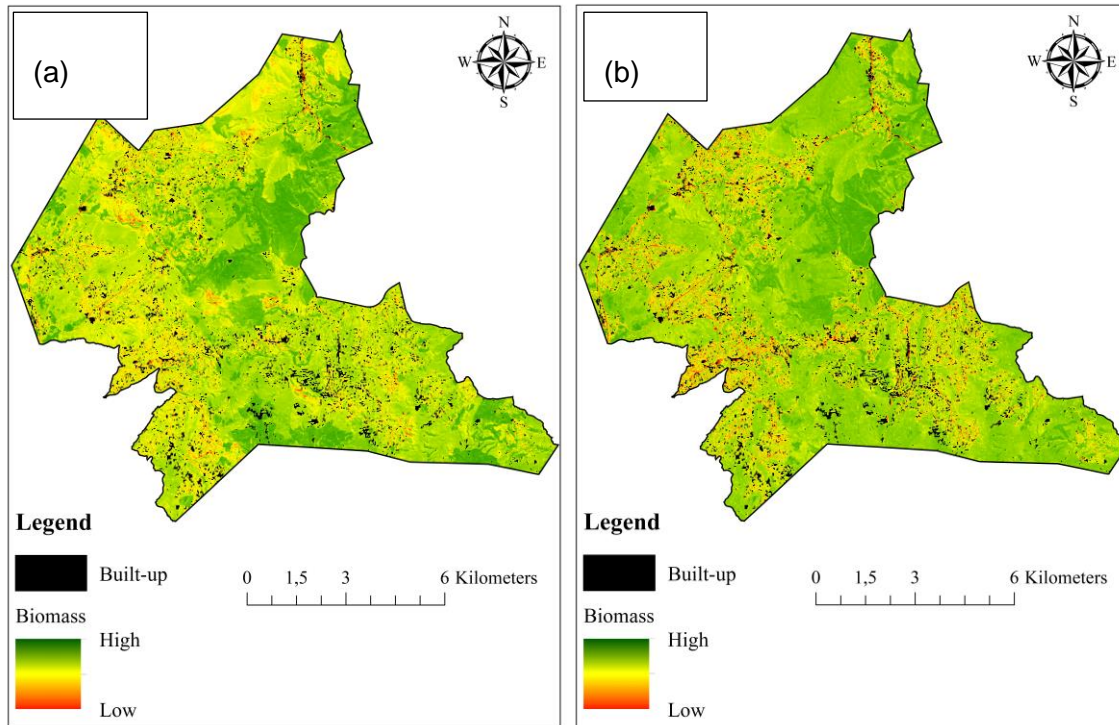


Figure 7.5: Predicted biomass (g/m²) over the a. dry and b. wet season using CNN.

7.3.4. Sensitivity Analysis

Deciphering which input variables are the most significant for model development is especially critical in ensuring respectable model performance. Figure 7.6 depicts which input variables, from Sentinel 2 spectral bands and derived VIs, were most important for model development in both seasons. It must be noted that only variables with an average impact of >0.1 were included in the model. The top three variables for the dry season included the GNDVI, GCI and the blue band whereas GCI, GNDVI and blue band were the three most important for the wet season.

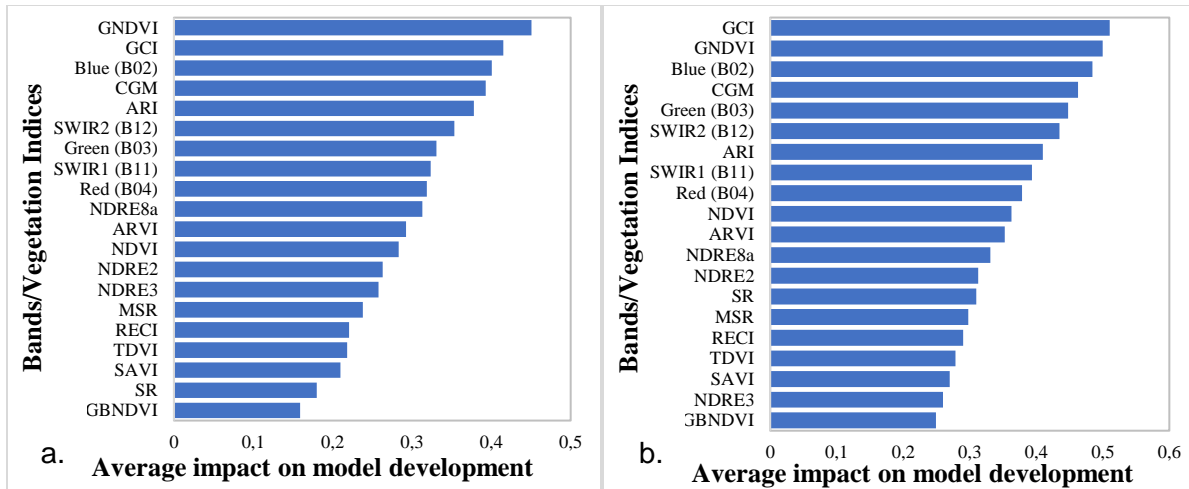


Figure 7.6: Ranking the importance of variables for developing the CNN model for biomass detection in the (a) dry season and (b) wet season.

7.4. Discussion

This study has estimated and compared aboveground grass biomass between the dry season (April-July) and the wet season (November-March) in the greater UMngeni catchment. Overall, recorded grass biomass increased from $\pm 48 \text{ g/m}^2$ in the dry season to $\pm 196 \text{ g/m}^2$ in the wet season. The predicted biomass maps also depict a significant increase in aboveground biomass across the study area during the wet season, whereas biomass is primarily concentrated in small patches across the study area during the dry season.

Grasslands are driven by external factors such as precipitation, temperature and fire (Masenyama, Mutanga et al. 2022). These factors maintain the ecological functionality of the grassland, however, these factors also fluctuate spatiotemporally (Shoko, Mutanga et al. 2018). It has been widely agreed that grassland productivity is directly and significantly related to changes in both rainfall and temperature (Shoko, Mutanga et al. 2018, Dinga and Tsubo 2019, Magandana, Hassen et al. 2020). Both rainfall and temperature variables fluctuate based on seasonal variations and hence play a significant role in influencing grassland productivity, particularly aboveground biomass (Magandana, Hassen et al. 2020). Van den Hoof, Verstraete et al. (2018) found that there is a statistically significant relationship between rainfall variability and grassland productivity. Furthermore, Magandana, Hassen et al. (2020) found statistically

significant relationships between changes in rainfall and temperature with changes in aboveground grass biomass.

The findings in this study seem to concur with both Van den Hoof, Verstraete et al. (2018) and Magandana, Hassen et al. (2020), albeit this study originates from a remote sensing background. Average total rainfall from April 2021 to July 2021 had a downward trend with an average total rainfall of approximately 16,5 mm for the dry period (Figure 7.7(a)). Average rainfall across the wet season, from November 2021 to March 2021, had an overall increasing trend with average total rainfall for the wet period estimated to be 96,84 mm (Figure 7.7(b)). This indicates an almost six-fold increase in rainfall received in the wet season as opposed to the dry season. Furthermore, temperature data from the dry and wet seasons appear to follow the same trend, with average daily maximum temperature decreasing gradually during the dry months and increasing steeply during the wet months (Figure 7.8(a) and Figure 7.8(b)). Average daily maximum temperature across the dry and wet period was approximately 20,44°C and 27.42°C, respectively. Therefore, the increase in aboveground grass biomass can be linked to an increase in both rainfall and temperature, as also suggested by Van den Hoof, Verstraete et al. (2018) and Magandana, Hassen et al. (2020).

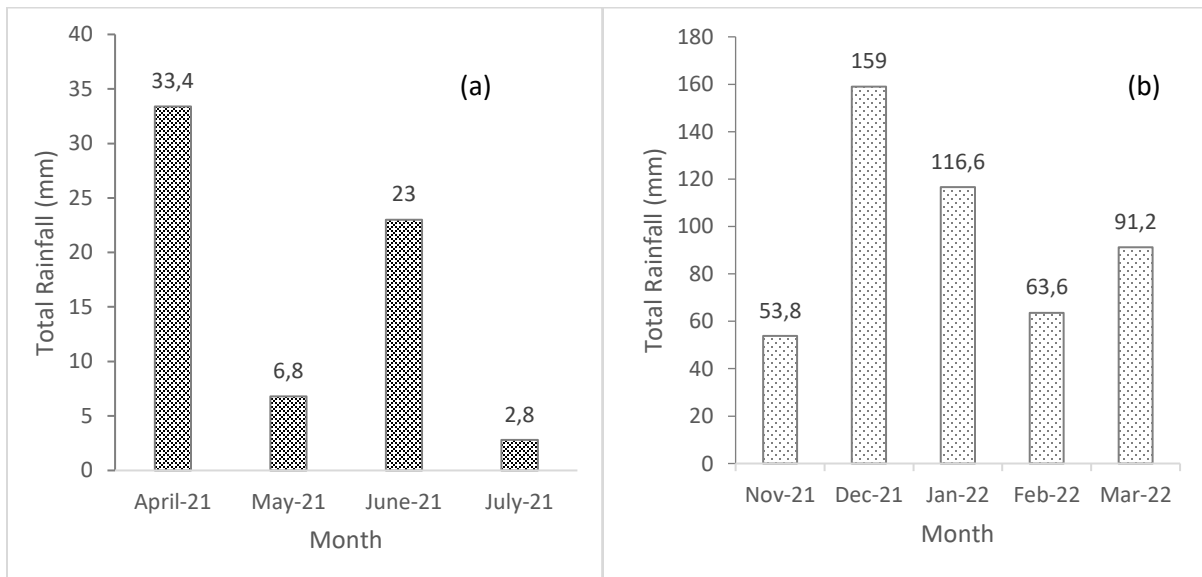


Figure 7.7: Total monthly rainfall in Vulindlela during the (a) dry season and (b) wet season (Data provided by South African Weather Services)

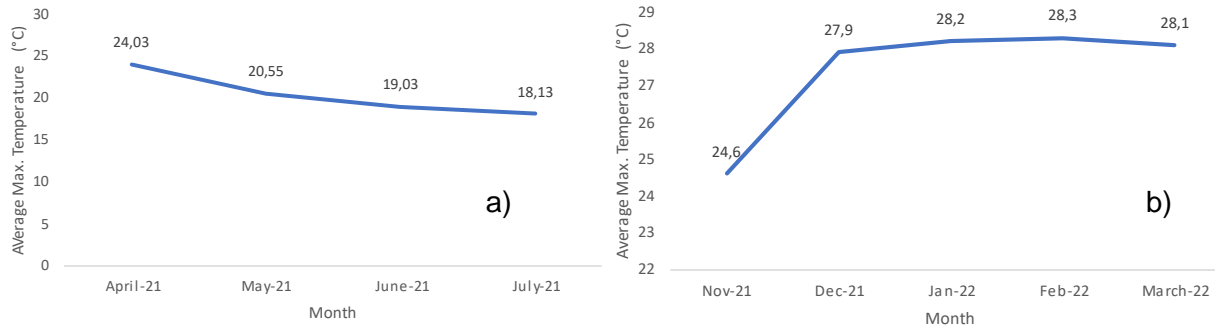


Figure 7.8: Average maximum daily temperature in Vulindlela over the a. dry season and b. wet season (Data provided by South African Weather Services)

Although rainfall and temperature are the major drivers of grassland productivity, the influence of other biophysical factors such as soil and rainfall type cannot be omitted (Van den Hoof, Verstraete et al. 2018). The type of rainfall received is as important as the quantity of rainfall received over time (Roffe, Fitchett et al. 2019). Gradual rainfall events allow for better water absorption into the soil column as opposed to erratic rainfall events, in which most of the rainfall is lost as surface run-off (Van den Hoof, Verstraete et al. 2018, Roffe, Fitchett et al. 2019). The edaphic factors of the grassland also play a significant role in productivity, particularly soil pH, texture and organic matter content (Van den Hoof, Verstraete et al. 2018). An increase in precipitation brings about an increase in plant production, which in turn increases soil organic matter (Van den Hoof, Verstraete et al. 2018). Soil type is also influential in plant productivity, with fine clay-like soils being more suitable for optimal production than coarse sandy soils (Van den Hoof, Verstraete et al. 2018). This is due to clay-like soils being more adept at nutrient exchange, holding organic content, better bulk density and higher soil organic carbon than sandy soils (Van den Hoof, Verstraete et al. 2018).

The study area consists mainly of two soil types, Acrisols and Ferralsols, as deduced from Fey (2010). Acrisols are defined as brownish-reddish soils with fine granular structure and sandy-loamy texture (Podwojewski, Janeau et al. 2011). Acrisols are generally unproductive soils that lack sufficient plant nutrients, have a high pH and usually form a substrate for grasslands or savannah (Podwojewski, Janeau et al. 2011). Acrisols are also highly porous soils and are especially susceptible to soil erosion (Podwojewski, Janeau et al. 2011). Ferralsols are characterised by reddish-yellow soils that have a high clay content (Mukangango, Nduwamungu et al. 2020). Ferralsols are structurally sound soils with good infiltration and drainage. However,

they are chemically poor soils with the majority of plant nutrients being stored in the biomass and can only be recycled back into the soil column by moribund (Mukangango, Nduwamungu et al. 2020). Acrisols and Ferralsols are similar and can often be found together, with both soils being susceptible to dry periods and drought (Mukangango, Nduwamungu et al. 2020). Since both soils are well drained and are poor at water retention, they cannot provide enough moisture for grasses and vegetation, particularly on slopes (Mukangango, Nduwamungu et al. 2020). The lack of precipitation during the dry season can possibly account for changes in edaphic factors, which inherently affects biomass availability.

Grasslands are naturally maintained by grazing and fire, two non-climatic factors that also influence plant productivity (Koerner and Collins 2014). The grassland in this study is utilised as a communal rangeland by the locals for their livestock (Cho, Onisimo et al. 2021). However, the lack of a formal rangeland management plan has resulted in adverse conditions within the grassland, and this mainly due to fire and overgrazing (Cho, Onisimo et al. 2021). Fire is administered by locals whenever deemed fit, even though it may be contrary to scientific guidelines. This not only affects the ability of grasses to regenerate, it affects the soil characteristics (nutrients, moisture content, organic content) which severely reduces productivity (Reinhart, Dangi et al. 2016). Furthermore, livestock are allowed to graze freely which has resulted in uneven forage distribution and soil erosion in some areas. This was evident and observed within the study area during data collection visits (Figure 7.1(a) and (b)). Continuous grazing by livestock hinders grass productivity as the grass does not have the ability to regrow, particularly in the dry season when stored nutrients are scarce (Koerner and Collins 2014). Grazing factors such as stocking rates are significant in maintaining grassland productivity, as high stocking rates affect grasslands negatively if not conducted in a controlled manner (O'Connor, Martindale et al. 2011). Cho, Onisimo et al. (2021) states that locals are facing challenges with effective rangeland management, which has resulted in a shortfall of forage, especially during the dry season. The need for an effective and collaborative rangeland management plan, with appropriate stocking rates and rotational grazing, is imperative to improve grassland productivity in Vulindlela (Cho, Onisimo et al. 2021).

This study can be considered a pilot study as it is one of the first studies, to the best of the authors' knowledge, to predict vegetation biomass using deep learning and Sentinel 2 MSI. Remote sensing has been extensively used in biomass studies, with relatively good levels of success (Mutanga, Dube et al. 2016). The advent of machine learning has enabled extensive and complex

data analysis in remote sensing, often producing more reliable and accurate results as compared to traditional statistical methods (Ali, Greifeneder et al. 2015). Machine learning, it itself, has advanced through time and contemporary deep learning approaches to data analysis appears to be the outlook for the foreseeable future (Zhu, Tuia et al. 2017). Neural networks are the foundation of deep learning approaches, and the CNN is one of the most promising deep learning algorithms for vegetation remote sensing applications (Kattenborn, Leitloff et al. 2021). Deep learning differs from typical shallow learning mainly by the way the algorithm processes data. In typical machine learning, a human has to ensure that structured data has to be organised and pre-processed in order for learning to take place, also termed as supervised machine learning (Yuan, Shen et al. 2020). However, with deep learning, the algorithm has the ability to learn and decipher which data components should be used for feature extraction, resulting in less dependency on supervised learning and pre-processed data (Zhu, Tuia et al. 2017).

The use of deep CNNs for vegetation biomass studies are sparse, however, they are gaining momentum in academia (Yuan, Shen et al. 2020). Most of the studies utilising CNNs have an agricultural background and have used unmanned aerial vehicles (UAVs) data in small-scale spatial contexts. This study utilised a CNN to estimate grass biomass using open-access and readily available satellite data at a larger spatial scale. Karila, Alves Oliveira et al. (2022) state that there are two broad types of CNNs that can be used for vegetation monitoring: 2D and 3D CNNs. 2D CNNs are simple CNNs that only utilise a single image (mono-temporal) as an input whereas 3D CNNs have multiple images as input data (Karila, Alves Oliveira et al. 2022, Varela, Zheng et al. 2022). This study made use of a simple 2D CNN as only single images from respective dry and wet seasons were used.

Karila, Alves Oliveira et al. (2022) used an UAV with a RGB and hyperspectral sensor (1024 x 648-pixel size and 36 bands between 500-900 nm) to estimate grass biomass, amongst other variables. Their 2D CNN model recorded a NRMSE of 21% whereas their 3D CNN yielded a NRMSE of 10%. Karila, Alves Oliveira et al. (2022) only used NRMSE for model accuracy assessments hence R^2 and RMSE values are not included. Similarly, Varela, Zheng et al. (2022) predicted aboveground biomass of *Miscanthus* grass using UAV imagery with RGB, near infrared and red edge bands (1,4 cm spatial resolution) using 2D and 3D CNNs. Their 2D CNN recorded a R^2 of 0,59 and RMSE of 180 g whereas their 3D CNN produced a R^2 of 0,69 and RMSE of 149 g. Alves Oliveira, Marcato Junior et al. (2022) utilised UAV RGB data and 3D CNNs of different architectures to estimate aboveground grass biomass. Their best model recorded a R^2 of 0,88

and RMSE of 482,12 kg/ha, with model performance being significantly influenced by the type of architecture. In comparison, the simple CNN model in this study performed well with $R^2=0,83$ /RMSE%= 6,09 and $R^2= 0,85$ / in the dry and wet seasons, respectively. Taking into consideration that Sentinel 2 imagery was used in this study as opposed to high resolution UAV data, this study shows that CNNs have the potential to be used with freely available satellite data and can be used at regional spatial contexts.

Chen, Guerschman et al. (2021) is arguably a study that can be directly compared to the findings in this study. Chen, Guerschman et al. (2021) used Sentinel 2 imagery paired with a deep sequential neural network (SNN), which is a subset of Recurrent Neural Networks (RNN), to estimate pasture biomass. Their study only used the ten applicable spectral bands, used in this study as well, and NDVI. However, they also included climate data in their models which could not be included in the CNN models in this study due to the lack of complete climate datasets for our study area, with data from the SAWS being relatively disjointed and incomplete to be able to be included in model development. According to Lakhal, Çevikalp et al. (2018), the main difference between CNNs and RNNs is that the latter is specialised in processing temporal information or information that follows a set sequence. This was apt for Chen, Guerschman et al. (2021) as they utilised time series Sentinel 2 data from 2017 to 2018 to study pasture biomass, albeit at a paddock-level spatial scale. Their SNN model performed adequately with a R^2 of 0,6 and a RMSE of 356 kg/ha. Furthermore, their study also observed that seasonal patterns in aboveground pasture biomass were distinct, with biomass increasing in the wet season and decreasing in the dry season. They also associate this with changes in climatic conditions, with water availability being highly influential to pasture biomass (Chen, Guerschman et al. 2021).

Jin, Li et al. (2020) utilised mono-temporal Sentinel 2 imagery with a deep neural network to estimate maize biomass. Their study used fifteen VIs and leaf area index (LAI) data as input data to predict maize biomass. Their model performed well with best R^2 of 0,91, RMSE of 1,49 t/ha and RRMSE of 20,05%. In terms of a sensitivity analysis, Jin, Li et al. (2020) found that the three band water index (TBWI), normalised difference infrared index (NDII) and normalised difference moisture index (NDMI) were the most important VIs for biomass estimation. In this study, the most important VIs for model development for both seasons were GNDVI, GCI and CGM. Théau, Lauzier-Hudon et al. (2021) study found that GNDVI has a high correlation with grass biomass, particularly in grasslands with low vegetation levels of $<0,5$ kg/m², which was the case in our study particularly in the dry season. Hamada, Zumpf et al. (2021), also using Sentinel 2 for grass

biomass predictions, found that CGM, GCI and GNDVI all had a high correlation with biomass. Jin, Li et al. (2020), Chen, Guerschman et al. (2021) and Hamada, Zumpf et al. (2021) all found that NDVI was moderately to poorly correlated to biomass and hence was not a relatively important variable in model development. Findings in this study seem to concur as NDVI was moderately significant for both dry and wet seasons. Both Théau, Lauzier-Hudon et al. (2021) and Hamada, Zumpf et al. (2021) found that green and blue spectral bands were more important for biomass predictions than the red band, which was also found in this study.

Many authors agree that the use of CNN models for biomass estimation are preliminary, novel and pioneering (Ma, Li et al. 2019, Dong, Du et al. 2020, Alves Oliveira, Marcato Junior et al. 2022). The same sentiment can be iterated in this study as no known studies have attempted to use CNNs and satellite imagery for biomass predictions. CNNs require large amounts of training data to be able to operate accurately, and this may prove to be a limitation as large datasets are not always available (Kattenborn, Leitloff et al. 2021). Using CNNs for small datasets has been done before, as recorded by Narayanan, Saadeldin et al. (2021), however they may require some pre-training and transfer learning to ensure that they are optimised for biomass estimation (Narayanan, Saadeldin et al. 2021). Furthermore, the architecture and hyperparameters of CNNs are highly influential in model performance and these must be further studied to improve the generalizability of CNNs (Alves Oliveira, Marcato Junior et al. 2022). This study also was limited in using only single image as inputs for model training. Studies show that using multi-temporal imagery significantly improves CNN model accuracy (Karila, Alves Oliveira et al. 2022, Varela, Zheng et al. 2022). Future studies can perhaps attempt to improve on model performance using multi-temporal satellite data.

7.5. Conclusion

This study evaluated the change in aboveground biomass from the dry season to the wet season using Sentinel 2 remotely sensed imagery and simple convolutional neural networks. Sentinel 2 MSI bands and derived VIs were used as input proxy data to train the CNN model for both seasons while ground data was used as a benchmark to assess model accuracy. A significant difference between dry and wet season grass biomass was discovered, with the wet season biomass increasing four times of dry season biomass. These changes can be primarily related to significant changes in rainfall and temperature which also bring about influential changes in other biophysical

factors such as soil. Overall, findings in this study concur with previous studies studying seasonal biomass changes.

This study can also be considered a pilot study as it attempted to utilise a deep learning approach to predict grass biomass. Model performance produced promising results, albeit with a simple CNN and a limited dataset. This research could prove useful to farmers and rangeland managers in planning and decision-making as remote sensing allows for fast and accurate estimation of grassland productivity. However, future research can improve the reliability and practicality of CNN modelling by incorporating multi-temporal data and utilising larger datasets. Using more complex and intricate CNN models in future may also improve predictive performance.

8. Inter-seasonal estimation of grass water content indicators using multisource remotely sensed data metrics and cloud-computing Google Earth Engine platform

A Masenyama, O Mutanga, T Dube, M Sibanda, O Odebiri and T Mabhaudhi

8.1. Introduction

Plant water content (PWC) is one of the critical parameters of the land surface-atmosphere interactions, which considerably affects the seasonal terrestrial water cycle (KOIKE, NAKAMURA et al. 2004). This is because the quantity of water contained in vegetation canopy structure has profound effects on physiological processes such as evapotranspiration, and photosynthesis which directly affect an ecosystem's water balance (Bonan 2008, Osakabe, Osakabe et al. 2014). Thus, vegetation water-related properties are critical for understanding key components of the hydrological cycle to derive insights on catchment water variation.

Several interrelated physiological indicators have been used to assess vegetation water conditions at different structural levels. The commonly used indicators include relative water content (Cervena, Lhotakova et al. 2014), leaf water potential (Browne, Yardimci et al. 2020), equivalent water thickness (Ferreira, Asner et al. 2011), live fuel moisture content (Zhu, Webb et al. 2021), canopy water content (Ustin, Riaño et al. 2012), canopy storage capacity and stomatal conductance (Zhou, Duursma et al. 2013). Amongst these, canopy storage capacity (CSC) is the volume of water that can be retained in plant canopies (Bulcock and Jewitt 2010). The CSC directly influences hydrology through rainfall interception and altering infiltration, thus affecting water redistribution (Sibanda, Mutanga et al. 2019). Canopy water content (CWC) is the total amount of water content per unit area of a ground surface which depends on the balance between water losses from transpiration and water uptake from the soil (Ustin, Riaño et al. 2012). Equivalent water thickness (EWT) is the quantity of water content per unit leaf area. It plays a critical role in eco-hydrological processes such as evaporation and transpiration (Sibanda, Onesimo et al. 2021). The reflectance of vegetation water content is affected by many biophysical parameters, and it is challenging to separate the contribution of leaf area index (LAI) and water content from remotely sensed data at the leaf level (Pan, Chen et al. 2018). In this regard, LAI and the above-explained water content indicators are of interest in this study.

In the past decades, water content indicators have been utilized as a proxy for crop water stress or drought assessment and monitoring (Gao, Wang et al. 2014, Zhang and Zhou 2019, Ndlovu,

Odindi et al. 2021), prediction of ecosystems susceptibility to wild-fire (Chuvieco, Riaño et al. 2002, Danson and Bowyer 2004) and in forestry studies (Oumar and Mutanga 2010, Sibanda, Mutanga et al. 2019). However, more effort needs to be made to study the seasonal variability of vegetation water content indicators specifically in the context of grassland ecosystems. By virtue of their location mostly in catchment areas, GWC significantly impact on various hydrological processes since vegetation water content can be assumed to reflect the hydrological conditions of the antecedent hydrological year (Gómez-Giráldez, Aguilar et al. 2014). Moreso, since GWC indicators are closely related to hydrological variables, their estimation can be helpful for the hydrological modelling of surface run-off, recharge and groundwater processes, and soil moisture budget.

Remote sensing has been widely recognized to be invaluable in providing effective, non-invasive, and reliable techniques for assessing water content indicators (Zhang, Xu et al. 2010). Remote sensing sensors including multispectral (Rubio, Riaño et al. 2006, Yilmaz, Hunt Jr et al. 2008, Wang, Wang et al. 2011) and hyperspectral (Clevers, Kooistra et al. 2007, Bulcock and Jewitt 2010, Neinavaz, Skidmore et al. 2017) sensors have been applied for vegetation water content monitoring. However, multispectral sensors such as Landsat and MODIS are associated with low spectral resolution, thus posing a challenge to optimally exploit the comprehensive water absorption features in the short-wave infrared region (SWIR) (Roberto, Lorenzo et al. 2016). Although hyperspectral sensors are renowned for their high accuracy in monitoring vegetation water conditions, they are coupled with exorbitant prices, yet they cover a small spatial extent (Zhang and Zhou 2018).

Recent advancement in earth observation sensors has seen the advent of freely available data from Sentinel-2, equipped with a multi-spectral imager (MSI) and providing an opportunity for robust estimation of vegetation-water-related properties (Sibanda, Mutanga et al. 2019). Sentinel-2 MSI offers the best combination of high spatial (i.e. up to 10 m pixel resolution), spectral (i.e. 13 bands covering the critical red edge section), and an optimal temporal sampling resolution of 5 days, making it suitable for characterizing the spatiotemporal variations of vegetation attributes (Zhang, Su et al. 2017). Specifically, Sentinel-2 MSI red-edge (RE) wavebands are critical in mapping vegetation attributes because they are sensitive to photosynthetic attributes such as chlorophyll, leaf area index, and foliar moisture content (Bramich, Bolch et al. 2021, Ndlovu, Odindi et al. 2021).

Meanwhile, literature underscores the performance of spectral derivatives such as vegetation indices in estimating vegetation attributes such as water content amongst others (Zhang and Zhou 2019, Zhou, Zhou et al. 2022). The most widely used vegetation indices in literature are derived from the visible and near-infrared region (NIR) wavelengths (Zhang and Zhou 2019, Zhou, Zhou et al. 2022). Meanwhile, the SWIR which is heavily influenced by water in plant tissues also plays a significant role in mapping and monitoring moisture content (Ceccato, Flasse et al. 2001). Thus, the use of moisture-sensitive indices derived from longer wavelengths such as the NIR and SWIR reflectance could be more viable for monitoring vegetation water content (Ghulam, Li et al. 2007). Other than optical spatial data, site-specific spatial data such as topographic and climate-related data are critical and required to improve the accuracy of optical models.

Topographic variables derived from digital elevation models such as the Shuttle Radar Topographic Mission (SRTM) can effectively increase the accuracy of vegetation monitoring (Zeng, Ren et al. 2019, Zhou, Li et al. 2021). Specifically, variations in topographic metrics such as the slope, topographic position index, state of curvature, and aspect are directly linked to vegetation aspects such as sunlight, temperature while indirectly linked to other aspects such as soil moisture, soil quality (Emran, Roy et al. 2018, Odebiri, Mutanga et al. 2020). For instance, Sibanda, Onesimo et al. (2021) showed that topographic variables such as slope, aspect, and altitude play a significant role in the spatial variability of GWC parameters. Furthermore, climatic variables such as rainfall and temperature are critical factors controlling photosynthetic activities in vegetation as well as foliar water content variation (Mouillot, Rambal et al. 2002). Specifically, seasonal precipitation and temperature result in soil moisture content variations which affect vegetation water content despite the impact of topographic variations (Zeppel, Wilks et al. 2014). However, the interacting influence of seasonal precipitation and temperature with topographic variations on GWC indicators has not been extensively researched, especially in communal grazing lands. Since topographic and climatic factors have been proven to be important variables in facilitating the spatial distribution of vegetation water content, there is a need to assess and understand the interacting influence of seasonality and topo-climatic variables on spatial variability of grassland water content indicators.

This study sought to test the utility of multi-source data in estimating LAI, CSC, CWC, and EWT within communal grasslands across wet and dry seasons. It was hypothesized that integrating multi-source data with a robust machine learning algorithm would improve the prediction

accuracies of GWC indicators as a step towards building spatially explicit communal rangeland monitoring frameworks.

8.2. Materials and methods

Study site description

This study was conducted in Vulindlela, a communal area located in Kwa-Zulu Natal province, on east coast of South Africa (Figure 8.1). The mean annual rainfall of the area is 979 mm. The maximum monthly rainfall occurs in January (Rouault and Richard 2003). Annual minimum and maximum mean temperatures are 10.3°C and 21.9°C respectively (Sibanda, Onisimo et al. 2021). The driest month with the lowest temperatures is July. The study site is located in a subtropical climate, characterized by a standard Southern Africa bimodal climate. The wet season occurs from September to March and the dry season from April to August (Ndlovu and Demlie 2020, Royimani, Mutanga et al. 2022). The study site is mainly a mesic subtropical grassland biome characterized by *Aristida junciformis*, *Tristachya leucothrix*, *Eragrostis tenuifolia*, *Themeda triandra*, *Sorghum bicolor*, *Paspalum urvillei*, *Alloteropsis semialata*, *Panicum maximum* and *Setaria sphacelata* grass species amongst others (Fynn, Morris et al. 2011). However, the dominant grass species are *Aristida junciformis*. The optimal growing period of these species occurs from October to April (Tsvuura and Kirkman 2013). Vulindlela is a good example of a predominantly rural community, in which land is managed using the communal ownership approach (Cho, Onisimo et al. 2021). The primary source of livelihood in Vulindlela is livestock farming and communities depend on grasslands as grazing grounds for their livestock. This highlights the need to provide an efficient and cost-effective strategy for managing this natural resource.

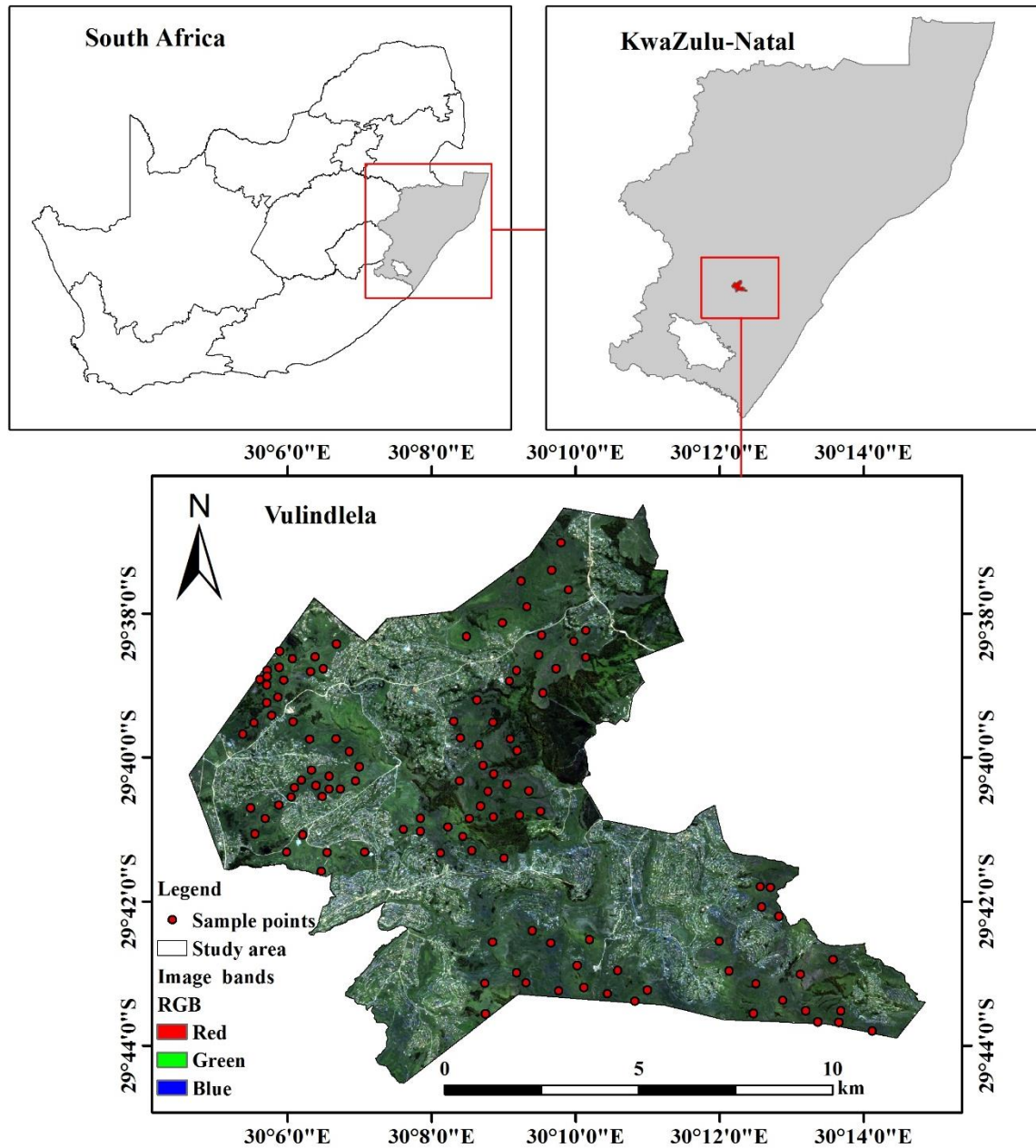


Figure 8.1: Location of the study area

Field sampling strategy and water content indicators measurements

Field data for the wet season was conducted between 27 and 31 March 2022. This was meant to capture the peak water content period after the grass had responded to maximum rainfall occurring in January. The dry season data was collected between 16 and 20 June when the GWC

was low due to senescence. Although the driest month with the lowest temperatures is July, the communities in Vulindlela initiate seasonal burning of grass in June to stimulate new growth for livestock, making it impossible for data collection to be conducted in July.

Hundred and thirteen, 10 m × 10 m quadrats were established at 150 m distance apart using a purposive sampling strategy. A plot size of 10 m by 10 m was chosen in this study to ensure that all sampled areas are within the confines of Sentinel-2 MSI bands. Consequently, the 150 m distance was chosen to account for possible ground-truth-satellite image geolocation errors. Within each plot, two 1 m × 1 m sub-quadrats were randomly established within the 10 m plots for clipping grass. A handheld Trimble Global Positioning System (GPS) with a sub-meter accuracy was used to collect the centre co-ordinates of the sub-quadrats. The co-ordinate points were stored as waypoints and later used for navigation in the dry season data collection. Grass was clipped within each sub-quadrat, placed in brown paper bags, and correctly labelled. The fresh weight (FW) of sampled biomass was instantly weighed using a calibrated scale with a 0.5 g measurement error. The samples were taken to the laboratory and placed in the oven at 105°C. For dry weight (DW), the samples were weighed consistently until a constant dry weight was reached (48-72 hrs).

LAI was also measured within each sub-plot using a portable handheld ground-based and non-destructive LAI 2200 plant canopy analyzer (Li-Cor, USA). Specifically, in measuring LAI five readings were conducted, one above the grass canopy and four below the grass canopy. Field measurements for LAI was conducted between 12:00 noon and 14:00 as this is the most optimal period of the day for vegetation photosynthetic activity (Yan, Hu et al. 2019).

Measurement of grass water content elements

The LAI (A), FW and DW were used as input variables to compute GWC indicators. CSC was computed using the von Hoyningen-huene (1981) model as follows:

$$S_{\max}^c \text{ (mm)} = 0.935 + 0.498 \text{ (LAI)} - 0.00575 \text{ (LAI}^2\text{)} \quad \text{Equation 8-1}$$

The von Hoyningen-huene (1981) model is an accurate, non-species-specific model for the estimation of maximum storage capacity (Kozak, Ahuja et al. 2007). The model was chosen for

this study following its successful application within South Africa (Bulcock and Jewitt 2009, Bulcock and Jewitt 2010, Sibanda, Mutanga et al. 2019, Sibanda, Onesimo et al. 2021).

CWC was calculated based on the following equation:

$$\text{CWC (g/m}^{-2}\text{)} = \text{FW} - \text{DW} \quad \text{Equation 8-2}$$

EWT was calculated as follows:

$$\text{EWT (g/m}^{-2}\text{)} = \frac{(\text{FW} - \text{DW})}{A} \quad \text{Equation 8-3}$$

After retrieving all the GWC variables, they were averaged and integrated with the GPS points on an Excel spreadsheet. The data was then converted into separate point map shapefiles using ArcMap. The shape files were then uploaded on Google Earth Engine (GEE) platform for overlaying them with spectral data for further analysis.

Sentinel 2 MSI data acquisition

Sentinel 2 MSI, Level 2A remotely sensed data was imported from Copernicus in GEE data catalogue. Sentinel 2 is a combination of twin satellites (Sentinel-2A and Sentinel-2B) in the same orbit, phased 180° apart, operating at an altitude of 786 km and designed to provide high spatial resolution imagery in global environmental monitoring (Wang, Shi et al. 2016). Both satellites are equipped with MSI deriving data in 13 spectral channels along a 290-km sun-synchronous orbital path (Gascon, Bouzinac et al. 2017). The two-satellite constellation provides a temporal resolution of 5 days (Jin, Azzari et al. 2019) which makes it suitable for detecting seasonal changes in grass productivity. Specifically, GEE provides Level 2A products derived from Sentinel-2A which are readily processed by Sentinel-2 atmospheric correction processor (Sen2Cor) as a default configuration to provide orthorectified atmospherically corrected surface reflectance (Sola, García-Martín et al. 2018).

Remotely sensed imagery with dates which coincided with the field data collection dates for both seasons were acquired. The *ee.filterDate* function was used to acquire images in the date range which coincided with the time when field surveys were conducted. This is necessary since changes in atmospheric conditions between on-site data collection and satellite data acquisition may affect grass properties and might alter model accuracy (Gao 2006). Prior to image

downloading, the cloud pixel percentage was set to 10% to filter out Sentinel-2 scenes with a cloud cover that was more than 10%. Subsequently, the *ee.Reducer.median* function was applied to create a single image by calculating the median of all values at each pixel across the stack of all matching bands. The study area shapefile was imported and the *ee.filterBounds* filter was applied to narrow the image at the location of the region of interest. The ground sampling distance (GSD) of Sentinel-2 MSI is divided into spectral bands with 4 bands at 10 m, 6 bands (20 m) and 3 bands (60 m). Bands acquired at 60 m GSD (1, 9 and 10) were not included in this study because they are designed for detecting atmospheric characteristics and are unsuitable for vegetation analysis (Drusch, Del Bello et al. 2012). As a result, only 10 bands were selected using the *ee.Feature.select* a filter and utilized it in this study. The Sentinel-2 MSI bands were resampled to a spectral resolution of 10 m to give all the bands the same pixel size.

Selection of spectral indices

The prediction of water content in vegetation using spectral indices mostly depends on the reflectance behaviour of water molecules in the leaves to various sections of the electromagnetic spectrum (Wijewardana, Alsajri et al. 2019). For instance, the high foliar water content in vegetation is highly sensitive to water absorption features in the SWIR section which explains the reflectance of vegetation in these regions (Sims and Gamon 2003). Additionally, the RE region is sensitive to vegetation chlorophyll absorption which is directly related to water content (Adamczyk and Osberger 2015, Dong, Liu et al. 2019). In comparison to other indices, water-sensitive as well as RE-based vegetation indices may have an advantage of accurate estimation of grass leaf water-related elements. In this regard, this study specifically evaluates the potential of water-sensitive spectral vegetation indices which provide the absolute measure of plant water content as well as the RE region-based spectral vegetation indices. The vegetation indices formulas were identified and selected from literature whereas the formulas were derived from an online Index Database (<https://www.indexdatabase.de/>) and computed in GEE platform (Table 8.1).

Table 8.1: Spectral vegetation indices used in this study.

VI	VI formula	Sentinel-2 Bands	References
Normalized Difference Water Index (NDWI)	$\frac{NIR - SWIR}{NIR + SWIR}$	B8, B12	(Gao 1996)
Modified Normalized Difference Water Index (MNDWI)	$\frac{Green - SWIR}{Green + SWIR}$	B3, B11	(Xu 2006)
Normalized Difference Infrared Index (NDII)	$\frac{NIR - SWIR}{NIR + SWIR}$	B8, B11	(Klemas and Smart 1983)
Moisture Stress Index (MSI)	$\frac{SWIR}{NIR}$	B11, B8	(Hunt Jr and Rock 1989)
Normalized Difference Red-Edge (NDRE)	$\frac{NIR - RE}{NIR + RE}$	B8, B5	(Barnes, Clarke et al. 2000)
Red-edge Ratio Index 1 (RRI1)	$\frac{NIR}{RE}$	B8, B5	(Ehammer, Fritsch et al. 2010)
Red edge 1 (Rededge1)	$\frac{RE}{RED}$	B5, B4	(Cloutis, Connery et al. 1996)
Red edge 2 (Rededge2)	$\frac{RE - RED}{RE + RED}$	B5, B4	(Cloutis, Connery et al. 1996)
Red edge Normalized Difference Vegetation index (NDVI ₇₀₅)	$\frac{RE2 - RE1}{RE2 + RE1}$	B6, B5	(Gamon and Surfus 1999)

Topo-climatic variables

Topographic variables are classified into three main groups: local (elevation, slope, land surface curvature) which examine surface geometry specific to a point on the land surface, non-local (flow accumulation, catchment area, relief) influenced by the relative location of a specific point on the land surface and combined topographic metrics (topographic wetness index) which integrate both the local and nonlocal topographic metrics (Speight 1968, Young 1972, Shary, Kuryakova et al. 1991, Moore, Gessler et al. 1993, Gumede, Mutanga et al. 2022). Twenty-three topographic variables (Table 8.2) were derived from a 30 m x 30 m DEM created from SRTM data in SAGA QGIS (2.3.2) and ArcGIS 10.6 software. The rainfall and temperature datasets were acquired from South African Weather Services (SAWS). The climatic datasets were averaged per season and resampled to 10 m spatial resolution to give them the same pixel size as the remotely sensed

imagery. The topo-climatic variables shapefiles were then imported into GEE as shapefiles for further analysis.

Table 8.2: Topographic variables used in this study as explained in Odebiri, Mutanga et al. (2020).

Topographic Variable	Description
Slope	Degree of inclination of land surface
Elevation	Height above sea level
Aspect	Compass direction of a slope
Minimum curvature	Lowest deviation from slope curve
Maximum curvature	Highest deviation from slope curve
Longitudinal curvature	Explains the flowing speed of a substance downslope
Cross-section curvature	Explains the divergence or convergence of a flowing substance
Profile curvature	Represents morphology of the topography
General curvature	Total curvature of the surface
Plan curvature	Horizontal curvature of contour lines
Catchment area	Run-off water flow, forming a waterway
Positive openness	Dominance of a landscape location
Negative openness	Enclosure of a landscape location
Standardized height	Slope position and height
Normalized height	Slope position and height
Valley depth	Relative height of a valley
Convergence index	Calculates valleys and ridges
Wind effect	Effects of the direction and speed of wind on the surface
Direct insolation	Incoming solar radiation
Terrain roughness index	Surface heterogeneity
Topographic wetness index	Quantifies topographic control on hydrological processes
Skyview factor	Visible sky
Mass balance index	Terrain morphometry

8.2.1. Spatial analyses

All statistical analyses in this study were performed using the GEE platform. A random forest (RF) ensemble was used to predict grass water content elements. RF is an ensemble learning technique first proposed by Breiman (2001). It is considered a robust regression technique that uses multiple decision trees to make predictions (Duro, Franklin et al. 2012). In RF, a large number of decision trees are randomly created (with replacement) from the original training data and variables (Rodriguez-Galiano, Sanchez-Castillo et al. 2015). Each node per regression tree is grown with a randomized subset of input variables considered for binary spitting (Wang, Zhou et al. 2016). The final output of RF regression is based on averaging the outputs of all decision trees to produce accurate predictions that do not overfit the data (LI, XIN et al. 2017). Generally, two user-defined parameters need to be optimized in RF regression namely *Ntree* which is the number of regression trees. The default value for *Ntree* is always set on 500. However, in this study, hyper parameter tuning was done and a *Ntree* of 400 was selected as being optimal. The second parameter is the *Mtry* which is the number of input predictor variables per node. In the case of RF regression, the default value of *Mtry* is that all variables are divided by 3 (Odebiri, Mutanga et al. 2020).

RF was chosen and used in this study because it is fast, insensitive to overfitting, and effective in handling data multicollinearity and dimensionality (Belgiu and Drăguț 2016). RF has been renowned for being more accurate and outperforming other regression algorithms (Shataee, Kalbi et al. 2012, Lu and He 2019, Yuan, Li et al. 2019, Elmahdy, Ali et al. 2020, Shen, Ding et al. 2022). Above all, it offers variable importance matrices in its computation which provide valuable insights to explore the effects of each predictor variable on the response variable (Oshiro, Perez et al. 2012). RF variable importance scores are derived from assessing the lowest Gini Index (a variable selection measure which measures the error of a variable with respect to the output model) (Wang, Zhou et al. 2016, Singh, Sihag et al. 2017). In this regard, the variable importance from RF was used to select the most influential predictor variables with the high predictive power. In predicting the grass water content, RF regression models were built in 4 stages of analysis which are:

1. Stand-alone Sentinel 2 MSI bands (Analysis stage 1)
2. Vegetation indices only (Analysis stage 2)
3. Environmental variables only (Analysis stage 3)
4. Combined variables (Analysis stage 4)

Prior to each analysis, the sampled data was randomly split into 70% for training and 30% for assessing the accuracy of predictive models.

8.2.2. Accuracy assessment

An accuracy assessment was conducted to evaluate the performance of regression models in predicting grass water content indicators. The derived RF models were assessed for accuracy based on the coefficient of determination (R^2), root mean square error (RMSE), and root means square error percentage (RMSE%). Specifically, the R^2 was used to measure the variation between measured and predicted grass water content indicators. The RMSE was used to assess the prediction error between the actual field measurements and the modelled grass water content variables. The RMSE% was used to estimate the magnitude of error from the measured values, expressed as a percentage. To compute RMSE%, the RMSEs from each model were normalized using the mean of each field-measured variable and then expressed as a percentage (Richter, Hank et al. 2012). Based on the testing datasets, the model with the lowest RMSE and RMSE% across all models was selected as the most ideal model that explains more significant variables in predicting the GWC elements. These models were used to generate maps illustrating the spatial distribution of the estimated GWC elements within the study site.

8.3. Results

8.3.1. Estimating grass water content variables using spectral and topo-climatic variables

Table 8.3 shows the predictive accuracies exhibited in estimating LAI, CSC, CWC and EWT based on the 4 levels of analysis across wet and dry seasons. For the wet season, the spectral bands and vegetation indices models for estimating LAI showed high variations between the observed and predicted but both models exhibited the same RMSE. For instance, when estimating LAI, the spectral bands model yielded an RMSE of $0.03 \text{ m}^{-2}/ \text{m}^{-2}$ and R^2 of 0.78. The vegetation indices model had an increased R^2 of 0.86 but exhibited a similar RMSE of $0.03 \text{ m}^{-2}/ \text{m}^{-2}$. On the other hand, results showed that there were insignificant differences between the spectral bands and vegetation indices predictive models for estimating CSC. When estimating

CWC and EWT, the spectral bands models yielded considerable high accuracies of RMSE = 20.42 g/m² and R² of 0.68, RMSE = 10.98 g/m² and R² of 0.69 respectively. The vegetation indices models for these water content variables showed a decrease in the accuracy to an RMSE = 21.5 g/m² and R² = 0.55, RMSE of 11.4 g/m² and R² = 0.55, respectively. The topo-climatic variables produced the lowest model accuracies across all GWC indicators.

Meanwhile, RF regression results obtained in the dry season indicated that the spectral bands model for estimating LAI yielded a RMSE accuracy of 0.05 m² and R² = 0.91. Results of the dry season also showed that the vegetation indices and topo-climatic models for estimating LAI retained the same RMSE of 0.09 m². The results obtained using bands and combined data models for estimating CSC yielded the same accuracies (RMSE = 0.03 mm and R² = 0.93). Although the vegetation indices and the topo-climatic models for estimating CSC had significant variations of about 14% in terms of the R², the two models still produced the same RMSE of 0.05 mm. For CWC, the dry season results indicated that Sentinel-2 MSI bands and vegetation indices models yielded the same RMSE of 1.63 g/m², although the model's R² values had a slight difference of 2%. The topo-climatic variables model performed poorly in estimating CWC. In terms of estimating EWT, dry season results showed significant variations amongst the spectral bands, vegetation indices and topo-climatic variables models.

Overall, the models that integrated bands, vegetation indices and topo-climatic variables exhibited the highest accuracies for estimating GWC indicators across both seasons except for LAI in a wet season where the vegetation indices model had a higher co-efficient of determination across all stages of analysis and CSC in the dry season where bands and combined data exhibited the same accuracies. Nevertheless, these differences were insignificant since the models yielded the same RMSE accuracies.

Table 8.3: Estimation accuracies of LAI, CSC, CWC, and EWT derived using spectral data and topo-climatic variables.

Water content variable	Explanatory variable	R ²	Wet season		Dry season		
			RMSE	RMSE%	R ²	RMSE	RMSE%
LAI (m ⁻²)	Bands	0.78	0.03	1.8	0.91	0.05	3.2
	Vegetation indices	0.86	0.03	1.8	0.57	0.09	5.7
	Topo-climatic	0.77	0.04	2.4	0.59	0.09	5.7
	Combined	0.83	0.03	1.8	0.90	0.04	2.6
CSC (mm)	Bands	0.80	0.01	0.6	0.93	0.03	1.8
	Vegetation indices	0.79	0.01	0.6	0.57	0.05	2.9
	Topo-climatic	0.36	0.02	1.1	0.71	0.05	2.9
	Combined	0.86	0.01	0.6	0.93	0.03	1.8
CWC (g/m ⁻²)	Bands	0.68	20.42	10.6	0.77	1.63	1.8
	Vegetation indices	0.55	21.5	11.2	0.75	1.63	1.8
	Topo-climatic	0.34	24.52	13.2	0.09	3.07	3.4
	Combined	0.76	19.42	10.1	0.87	1.35	1.5
EWT (g/m ⁻²)	Bands	0.69	10.98	9.6	0.89	2.21	3.6
	Vegetation indices	0.55	11.4	10	0.31	5.37	8.9
	Topo-climatic	0.22	14.29	12.5	0.56	4.65	7.7
	Combined	0.65	10.75	9.4	0.91	2.01	3.3

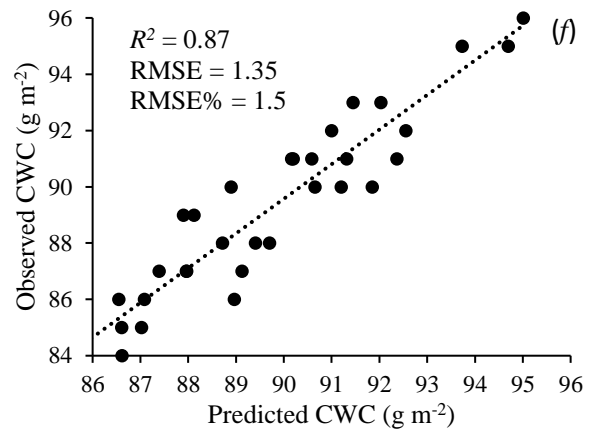
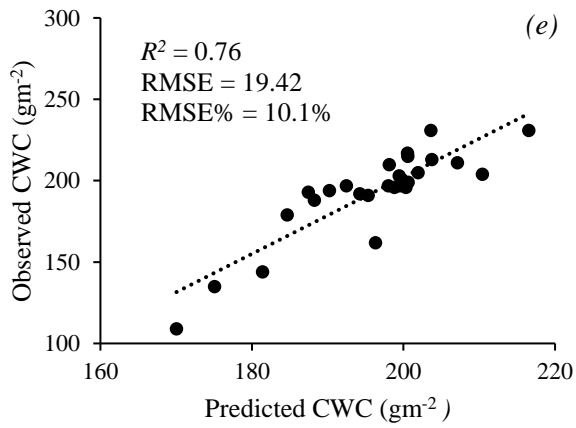
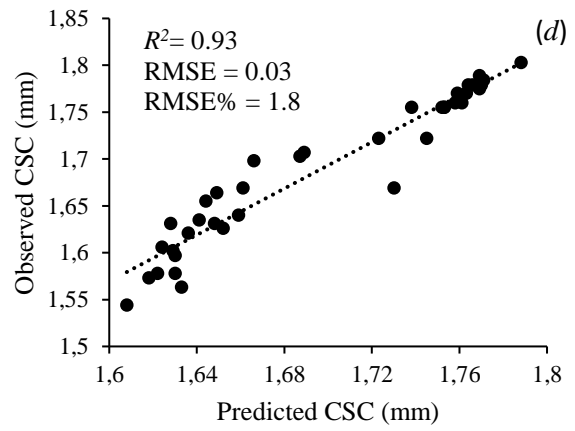
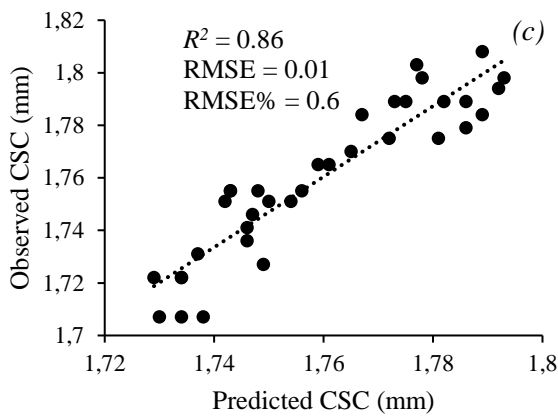
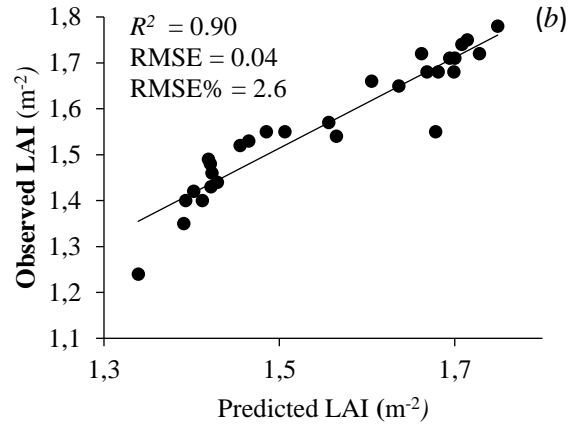
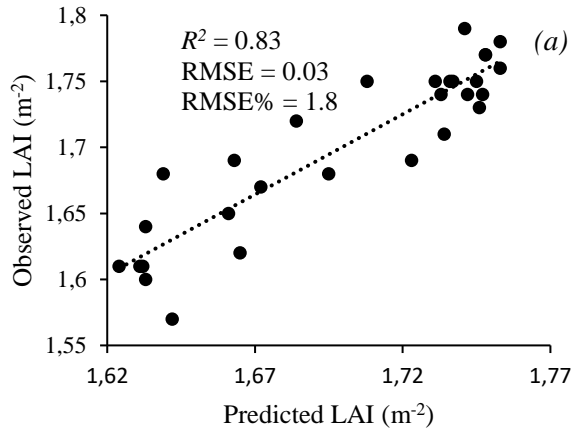
8.3.2. Comparing the optimal seasonal models of grass water content elements between the dry and the wet seasons.

LAI was better estimated during the wet season to a RMSE of 0.03 m^{-2} and R^2 of 0.83 based on MNDWI, B7, B6, B11, B8A, B8, NDWI, Minimum curvature, Rainfall, Positive openness, Temperature and Direct insolation in their order of importance (Figure 8.2(a) and Figure 8.3(a)). During the dry season LAI was estimated to RMSE = 0.04 m^{-2} and $R^2 = 0.90$ based on B2, B4, B12, B3, B11, B5 NDII, RRI, NDRE, NDVI705, MSI, Wind effect, Temperature, Elevation, Negative openness, Rainfall and Standardized height in order of importance (Figure 8.2(b) and Figure 8.3(b)).

Similarly, CSC was also optimally estimated during the wet season than the dry season. Specifically, CSC was predicted with a RMSE of 0.01 mm and R^2 of 0.86 based on MNDWI, B6, B11, B8A, B7, NDVI705, Rainfall, Elevation, Aspect, Temperature and Positive openness (Figure 8.2(c) and Figure 8.3(c)) in the wet season. It was then estimated to a RMSE = 0.03 mm and $R^2 = 0.93$ with B12, B2, B4, B3, B11, NDII, RR1, B5, MSI, Rainfall, Wind effect, Positive openness, Temperature, Direct insolation, and Negative openness being the most influential variables in the dry season (Figure 8.2(d) and Figure 8.3(d)).

Contrary to the CSC and LAI, CWC was optimally estimated during the dry season to a RMSE = 1.35 g/m^{-2} and $R^2 = 0.87$ using B8, B6, B7, NDWI, B8A, MSI, NDII, NDVI705, RRI1, NDRE, Aspect, Wind effect, Slope, Rainfall, Skyview factor, Temperature, Positive openness as the best optimal predictor variables, also in order of importance (Figure 8.2(f) and Figure 8.3(f)). The wet season yielded relatively lower estimation accuracies of CWC of a RMSE of 19.42 g/m^{-2} and R^2 of 0.76 based on NDWI, NDRE, NDVI705, B4, RRI1, B2, Cross section, Maximum curvature, Elevation, Red edge2, B5, Negative openness, Red edge1, MSI, B8, B3, Rainfall, Temperature (Figure 8.2(e) and Figure 8.3(e)).

Also, dry season EWT exhibited high accuracy of RMSE = 2.01 g/m^{-2} and $R^2 = 0.91$ based on B3, B5, B6, B12, B4, B2, B11, B8A, B7, Aspect, Rainfall, Longitudinal curvature, MSI, Temperature, NDII and Skyview factor as optimal predictor variables in order of importance (Figure 8.2(h) and Figure 8.3(h)). During the wet season, EWT was to RMSE = 10.75 g/m^{-2} and $R^2 = 0.65$ based on NDRE, NDWI, B8, NDVI705, B4, Negative openness, RRI1, Rainfall, Red edge 1, B8A, Elevation, B7 and Temperature (Figure 8.2(g) and Figure 8.3(g)). Overall, CSC was optimally estimated with high accuracies across both seasons as compared to other grass water content indicators.



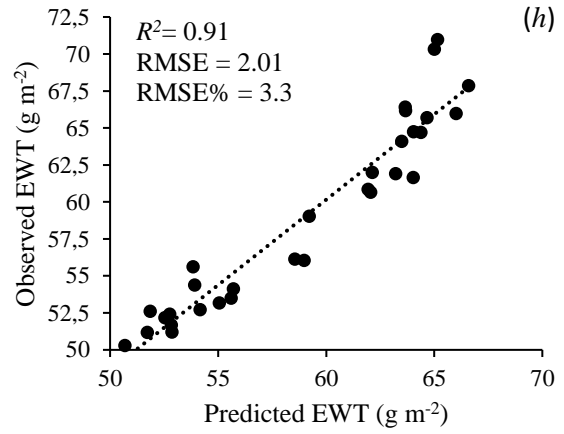
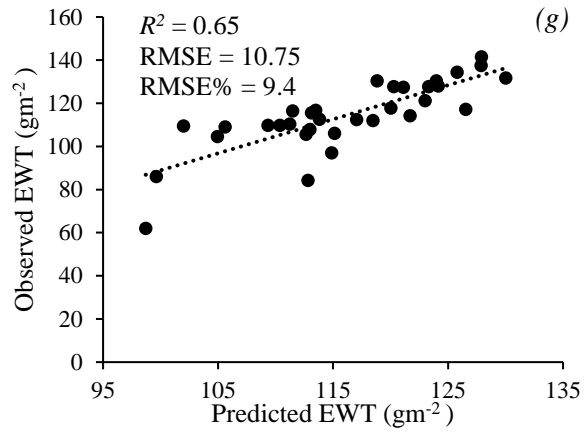
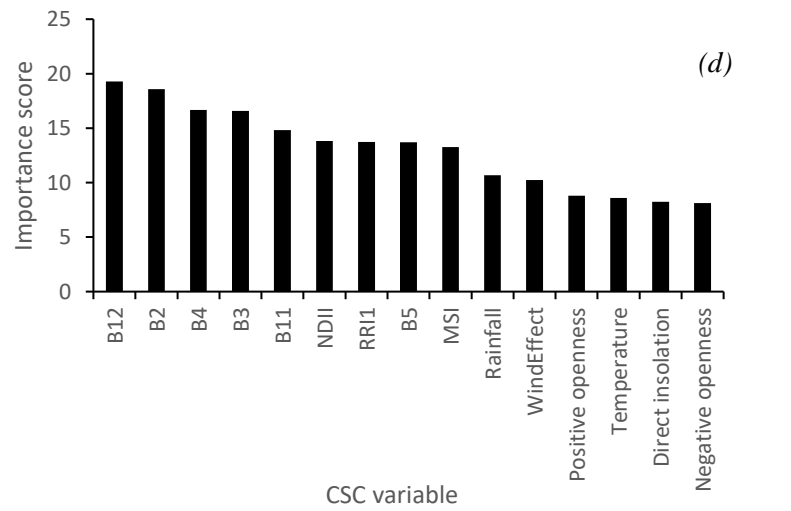
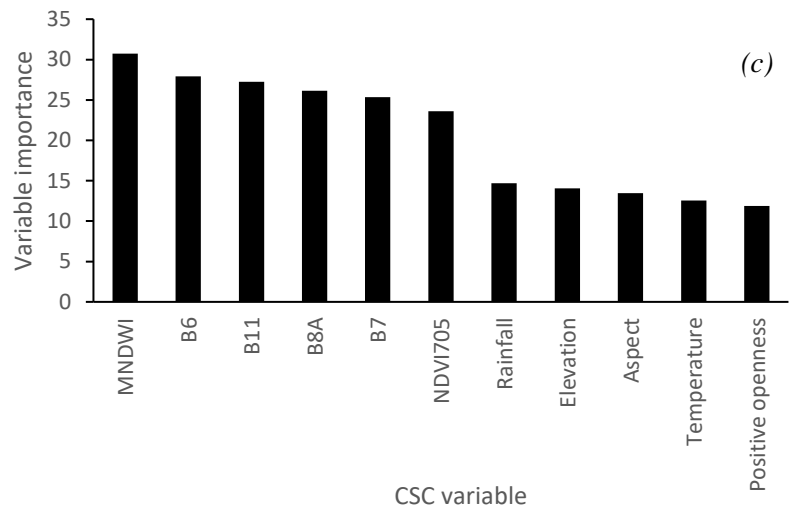
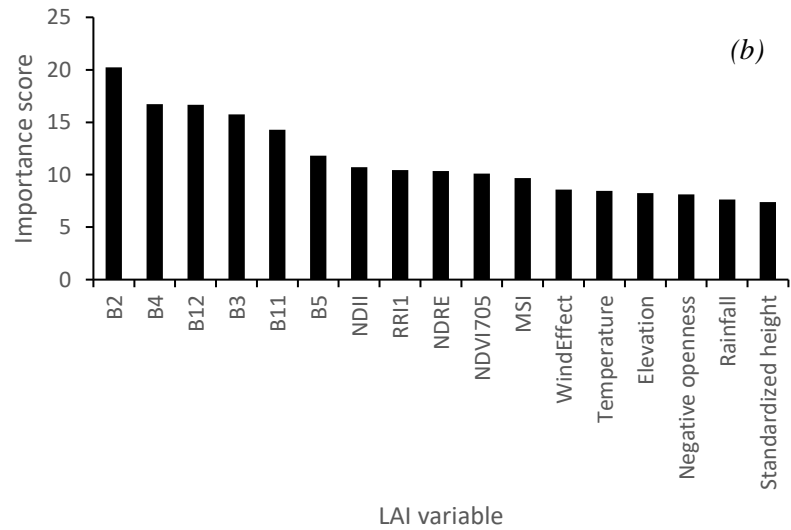
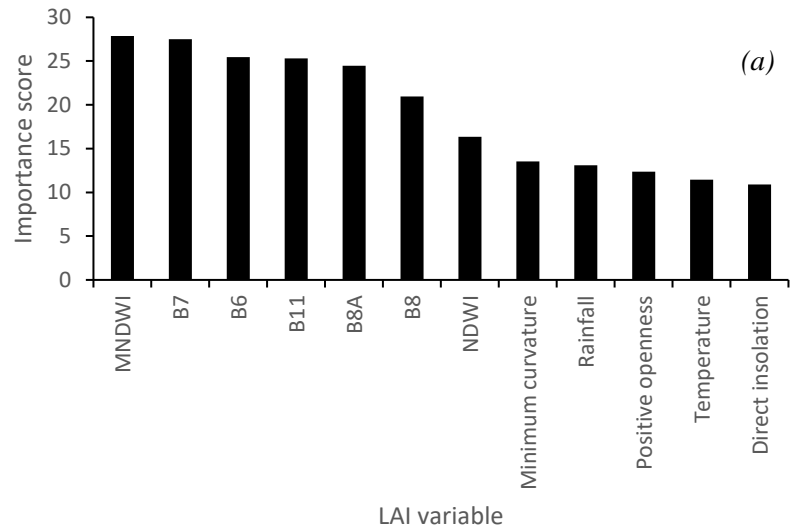


Figure 8.2: Relationship between observed and predicted grass LAI (a and b), CSC (c and d), CWC (e and f) and EWT (g and h) derived using optimally selected predictor variables for the wet and dry seasons respectively.



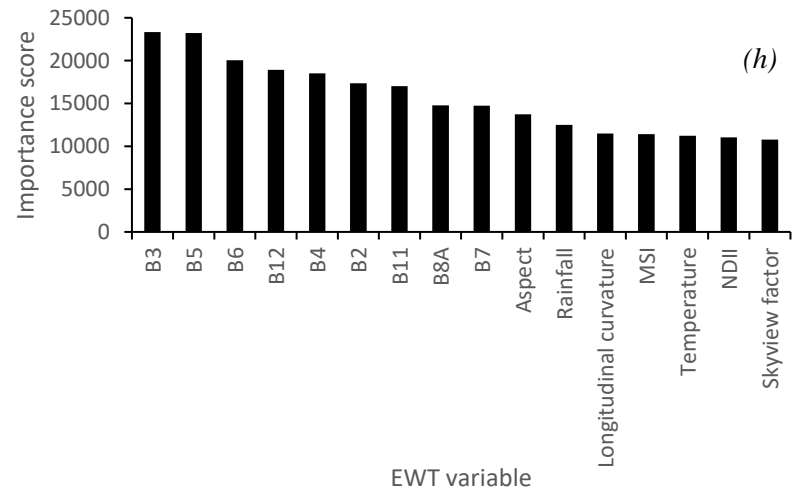
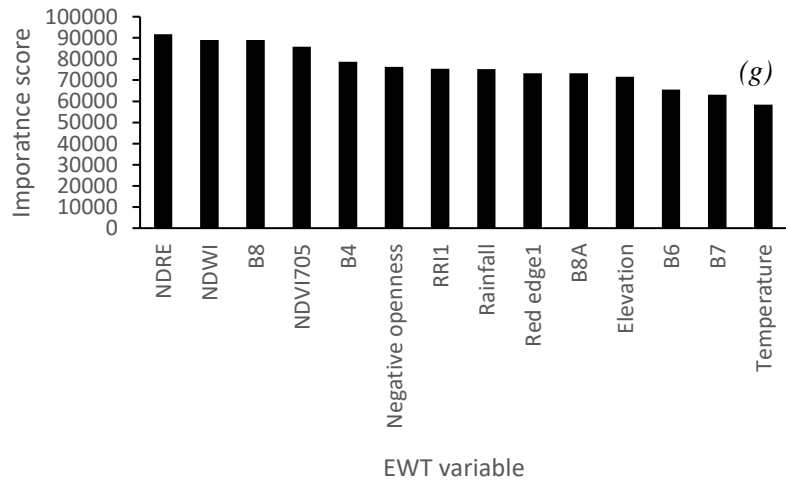
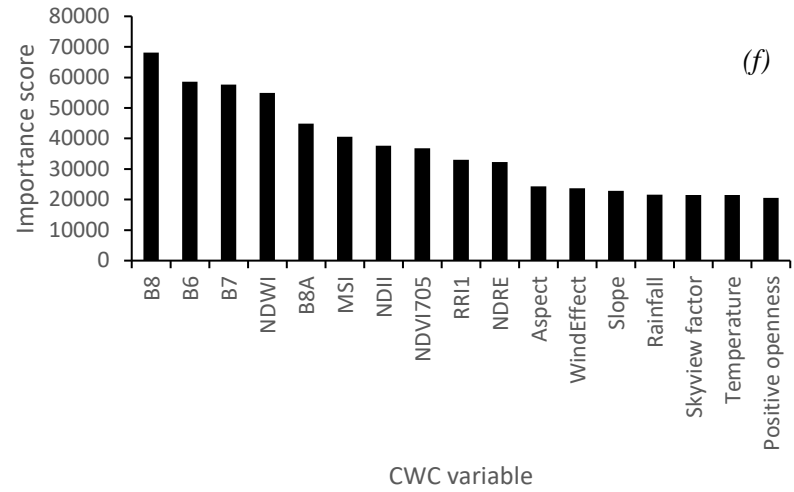
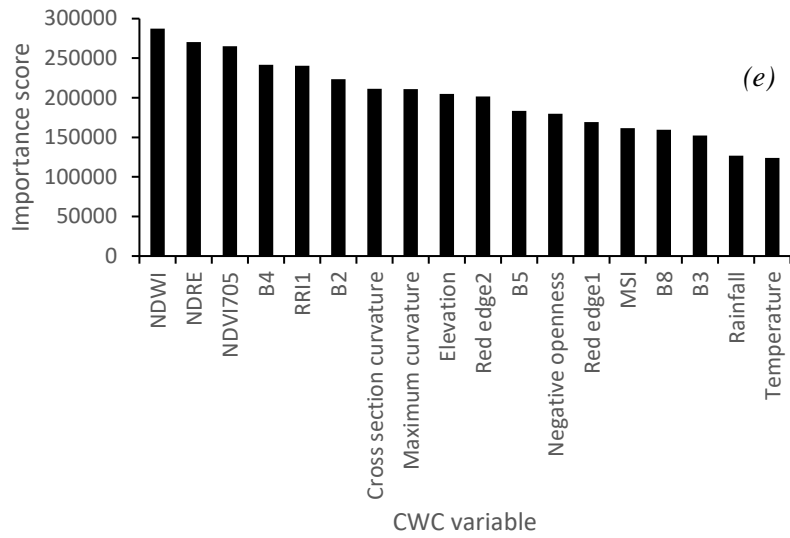


Figure 8.3: Variable importance scores of selected variables in estimating (a and b) LAI, (c and d) CSC, (e and f) CWC and (g and h) EWT for the wet season and dry seasons respectively.

8.3.3. Spatial distribution of modelled grass water content variables

The spatial distribution of GWC indicators was estimated based on the optimal models for each grass water content indicator. Figure 8.4 depicts the spatial distribution of estimated GWC for the wet season and dry seasons. Interestingly, the spatial distribution of LAI appears to correspond with that of CSC for both seasons. Again, the spatial distribution of CWC seems to coincide with that of EWT for both seasons. Overall, the GWC range values are relatively high for the wet season, and it can be observed that there is a decrease in the spatial variation ranges for all GWC variables in the dry season. Specifically, a drastic decrease of more than 50% in CWC and EWT spatial variations can be noted. Interestingly, the spatial distribution of LAI does not correspond to that of CWC and EWT for both seasons. For instance, areas with high leaf area index are not corresponding to high CWC and EWT.

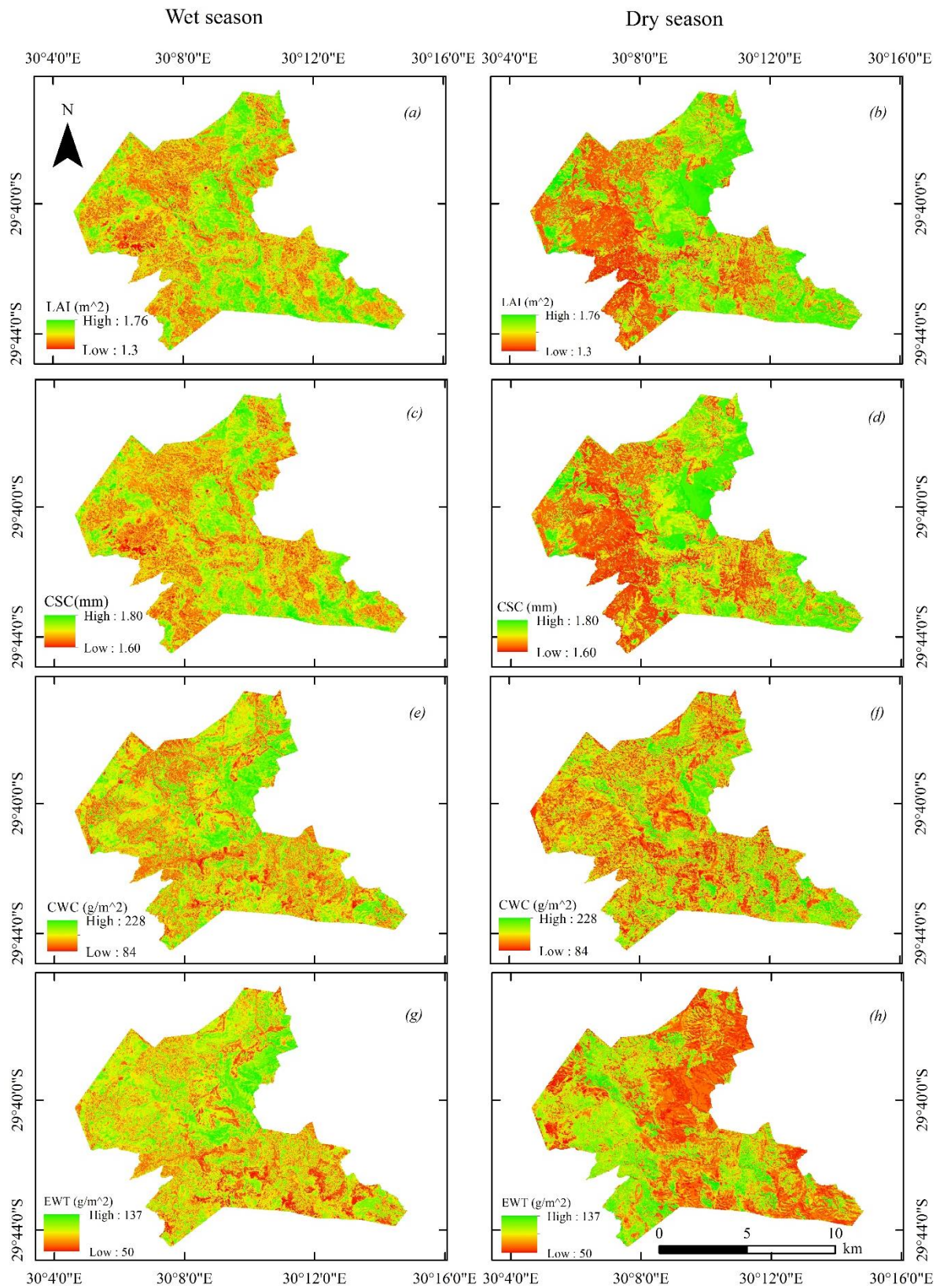


Figure 8.4: Spatial distribution of modelled LAI (a and b), CSC (c and d), CWC (e and f) and EWT (g and h) for the wet and dry seasons respectively.

8.4. Discussion

The objective of this study was to test the utility of multi-source data in estimating GWC indicators across wet and dry seasons. In this study, RF was used to model GWC indicators based on remotely sensed data and topo-climatic variables.

8.4.1. Predictive performance of spectral and environmental variables in determining grass water content indicators

Results of this study showed that Sentinel-2 MSI bands performed better than all the variables in estimating different grass foliar water elements across all seasons based on visible, NIR and SWIR bands 5, 6, 7, 8, 8a, 11 and 12. This could be explained by the fact that Sentinel-2 MSI data is characterized by high spatial resolution bands (i.e. 10 m) which can capture distinct and discrete interaction between grass canopy and the reflected radiation (Sakowska, Juszczak et al. 2016). More so, the MSI sensor operates on a 12 bit radiometric resolution with a radiometric accuracy of less than 5% which enables the distinction of differences in the reflected electromagnetic energy within the same band, making each band more sensitive especially in mapping and monitoring vegetation attributes such as foliar moisture content (Frampton, Dash et al. 2013, Ose, Corpetti et al. 2016). Furthermore, the sensor is equipped with high spectral variability spanning from the VIS to the SWIR which are suitable for monitoring moisture content of grass. Specifically, the results showed that the red-edge, NIR and the SWIR bands were more influential in estimating LAI, CSC, CWC and EWT.

Although comparing bands and vegetation indices was not the key component of this study, results showed that spectral bands models yielded high accuracies as comparable to those derived based on vegetation indices models for all GWC indicators across both seasons. This is an interesting finding which is contrary to what is documented in literature. For instance, related studies (Datt 1999, Ceccato, Flasse et al. 2001, Gao, Walker et al. 2015, Sibanda, Mutanga et al. 2019, Sibanda, Onisimo et al. 2021) which utilized spectral indices in estimating vegetation water-related properties illustrated that vegetation indices outperform conventional bands. Spectral indices tend to effectively deal with scattering effects of single bands as well as noise such as that from the soil background, angle of the sun and angle of the sensor, and topographic effects (Zhang, Xu et al. 2010). The optimal performance of bands which was comparable to vegetation in this study could be explained by the fact that the grass covered much of the ground surface hence there was limited background effect to influence the spectra. Also, the terrain was generally flat where most of the sampling points were located

such that there was also minimal impact of angle of the sun and angle of the sensor, and topographic effects.

Results illustrates that topo-climatic variables exhibited low accuracies across all models. The results of this study concur with those of Sibanda, Onesimo et al. (2021) who reported that environmental variables yielded poor model accuracies when estimating grass foliar moisture content as standalone variables. This could be explained by the notion that topographic indices are derived from digital elevation models which only represents the height above sea level. In this regard, they are not directly related to physical foliar moisture content such as the spectral reflection measured shown by Sentinel-2 MSI spectral bands. Furthermore, the SRTM DEM used to derive topographic variables in this study is characterized by a relatively coarse spatial resolution of about 30 m. This could further explain the low performance exhibited by the topographic variables.

8.4.2. Comparing predictor variables for estimating grass water content indicators

Results of this study illustrates that different set of predictor variables could be noted for estimating each GWC indicator across both seasons. This was expected as variations in GWC as a result of wet and dry season variations tends to affect the spectral properties of vegetation. For instance, when estimating GWC indicators in the wet season, most optimal predictor variables were based on spectral variables derived from NIR and the red-edge. Similar results were obtained by Clevers, Kooistra et al. (2008) and Serrano, Ustin et al. (2000) who reported that spectral variables derived from the NIR were the best indicators for estimating vegetation with high water content. During the wet season, grass has a lot of moisture available to facilitate and optimize their photosynthetic activities as they draw more moisture and produce more chlorophyll content. Subsequently, the grass moisture elements become sensitive and optimally estimated using the NIR. It has widely been proven that healthy vegetation reflects highly in the NIR as a result of cellulose structure of vegetation leaves (Sims and Gamon 2003). Meanwhile the RE (680-780nm) spectral information has been widely proven to be sensitive to chlorophyll content variations which has been generalized to be directly proportional to the quantity of water present in vegetation (Gao, Wang et al. 2014, Lin, Li et al. 2019). As the amount of vegetation chlorophyll increases, major chlorophyll absorption features around 680nm are broadened, causing a shift in the slope and RE position towards longer wavelengths (Gholizadeh, Mišurec et al. 2016). The chlorophyll concentration changes with the changes in moisture content required to optimize photosynthetic activities. Subsequently, the RE is one of the optimal estimation variables of foliar content associated with the wet season.

Meanwhile for dry season, most optimal spectral variables were derived from the visible, SWIR and the RE. The importance of the blue (B2) and red (B4) bands can be attributed to the lack of pigmentation and photosynthetic activities of vegetation in the dry season (Roy 1989). A study by Caturegli, Matteoli et al. (2020) illustrates that the SWIR is effective in characterizing water stress in vegetation water attributes due to higher reflectance of dry vegetation when its water content decreases along spectral wavelengths of 1400nm and 2500nm (Ceccato, Flasse et al. 2001). More so, the RE portion is also considered useful in studying dry vegetation because water deficit changes vegetation foliar chlorophyll composition, resulting in a shift of RE reflectance toward shorter wavelengths. In this regard, RE can detect plant pigment changes and has been correlated with water stress variations in leaf photosynthetic rates, therefore could be used in assessing foliar moisture variability (Easterday, Kislik et al. 2019). The strength of RE in estimating vegetation when it is in the condition of water stress was demonstrated by Easterday, Kislik et al. (2019) and Eitel, Vierling et al. (2011) who illustrated that it can effectively detect changes in plant stress as indicated by changes in chlorophyll content. This could possibly explain the importance of the visible, SWIR and RE based spectral variables in determining GWC in the dry season.

Overall, results showed that the combination of bands, vegetation indices and topo-climatic variables improved prediction accuracies and yielded the best models for estimating GWC indicators in the two seasons. Spectral bands offer data that can accurately provide the near real time state of the amount of water in vegetation, vegetation indices tend to surpass the influence of atmospheric and soil background noise (Zhao, Huang et al. 2007) while topographic indices bring forth the eco-hydrological attributes which facilitate the distribution of vegetation water content (Alexander, Deák et al. 2016). Although topographic variables yielded poor model accuracies as standalone estimation variables, it is important to note that they played a critical role in combined data estimation models. This could be explained by the fact that they are important in characterizing spatial heterogeneity of a landscape which affects nutrient resources and moisture availability for plants (Lukyanchuk, Kovalchuk et al. 2020). For instance, topographic indices such as slope and those related to terrain curvatures play an important role in catchment-related hydrological responses, driving soil moisture availability which influence the amount of water found in vegetation canopies (Amatulli, Domisch et al. 2018). Also, the seasonal climate variations either facilitate plant root water uptake, leading to high GWC or cause water deficit within grasses which in turn influence its reflectance in the electromagnetic spectrum. Therefore, the use of multi-source data with various strengths tends to result in a more accurate estimation of parameters describing the amount of water in vegetation, hence the high overall accuracies obtained in this study. The models attained in

this study underscores the importance of combining variables in the estimation of GWC indicators.

8.4.3. Relevance of the study

The findings of this study demonstrated the unprecedented opportunity for deriving reliable near real time information pertaining parameters describing the amount of water content in grasslands, presented by the interacting influence of environmental variables in concert with Sentinel-2 MSI data and the RF algorithm in GEE. Such information is crucial for rangeland managers in understanding GWC variations across different seasons as well as different ecological gradients. Since grasslands in Vulindlela are utilized specifically for livestock farming, the findings of this study are a step towards generating spatially explicit information that could be used in understanding the spatial variability of rangelands through the two seasons so as to inform sustainable grazing management strategies. Furthermore, the seasonal estimations obtained in this study could also offer water resource managers information and insight pertaining to catchment variation of hydrological elements such as CSC which are directly linked to hydrological system of these rangelands. This may be useful in understanding the hydrological cycle particularly surface water resource systems critical for management planning, while contributing towards the achievement of sustainable goals 1, 2, 6 and 12 which advocate for the provision of clean water, responsible consumption and production as well as addressing hunger, prevent climate change through carbon sequestration.

In conducting this study, the winter data collection was done earlier before the driest month. This might have an impact on depicting GWC variability across the two seasons. The grass species in the study area are mixed, although the dominant species is *Aristida juncifomis*. The canopy geometry of these species is a critical component which could have affected the spectral reflectance of the GWC variables. This could probably explain the mismatch of LAI spatial distribution to that of CWC and EWT obtained in this study. Additionally, the varying pixel size from the different data sources used might have an impact on the accuracy estimates obtained in this study. However, all GWC variables were estimated with acceptable accuracies regardless the influence of field conditions such as differences in canopy structure from the grass species in the study area.

8.5. Conclusion

This study sought to test the utility of multi-source data in estimating GWC variables across wet and dry seasons. Based on the finding of this study, it can be concluded that:

- The use of multi-source data in conjunction with RF in GEE can model LAI, CSC, CWC and EWT with acceptable accuracies. LAI was best estimated in the wet season with an accuracy of RMSE = 0.03 m⁻² and R² = 0.83 as compared to the dry season (RMSE = 0.04 m⁻² and R² = 0.90). Similarly, CSC was estimated with a high accuracy in the wet seasons yielding a RMSE of 0.01 mm and R² of 0.86 comparable to the dry season (RMSE = 0.03 mm and R² = 0.93). For CWC the wet season results yielded RMSE of 19.42 g/m⁻² and R² of 0.76 which was lower than the dry season results (RMSE = 1.35 g/m⁻² and R² = 0.87). Finally, EWT was best estimated in the dry season (RMSE = 2.01 g/m⁻² and R² = 0.91) as compared to the wet season (RMSE = 10.75 g/m⁻² and R² = 0.65).
- The optimal model for estimating LAI (RMSE of 0.03 m⁻² and R² of 0.83) had MNDWI, B7, B6, B11, B8A, B8, NDWI, Minimum curvature, Rainfall, Positive openness, Temperature and Direct insolation as the optimal predictor variables.
- Overall, CSC performed optimally as an indicator of grass water content across both seasons based on MNDWI, B6, B11, B8A, B7, NDVI705, Rainfall, Elevation, Aspect, Temperature, Positive openness in the wet season and B12, B2, B4, B3, B11, NDII, RR1, B5, MSI, Rainfall, Wind effect, Positive openness, Temperature, Direct insolation, and Negative openness in the dry season.
- CWC was best estimated in the dry season based on B8, B6, B7, NDWI, B8A, MSI, NDII, NDVI705, RR11, NDRE, Aspect, Wind effect, Slope, Rainfall, Skyview factor, Temperature, Positive openness as the best optimal predictor variables, also in order of importance.
- EWT was estimated with high accuracies in the dry season using B3, B5, B6, B12, B4, B2, B11, B8A, B7, Aspect, Rainfall, Longitudinal curvature, MSI, Temperature, NDII and Skyview factor as optimal predictor variables.

9. General discussion, conclusions and recommendations

M Sibanda, O Mutanga, T Bangira, T Mabhaudhi, T Dube, and R Lottering

9.1. General Discussion

Grasslands constitute one of the most widely distributed terrestrial biomes globally, covering 52.54 million km² and 40.5% of land area (Zhao, Liu et al. 2020). Meanwhile, in South Africa, grasslands are the second largest biome. Communal rangelands cover approximately 13% of the country's agricultural land, supporting 13 million people, in South Africa (Vetter 2013). These grasslands are important because they sustain livelihoods, provide ecosystem services while preserving biological diversity. However, communal grasslands are mainly utilised as grazing lands which are managed based on a communal tenure system. This tenure system has raised concerns relating to the degradation of these grasslands threatening their role of sustaining livelihoods, preserving biodiversity, and providing ecosystem services. Despite the tragedy of the commons in these grasslands, they still have not received sufficient recognition within the ecosystem services framework and received less attention in the ecosystem services global policy discussion (Bengtsson, Bullock et al. 2019). Following these unfortunate circumstances, the current extent and magnitude of productivity of these grasslands had not been extensively researched and remains unknown. This has been mainly due to the limited spatial explicit monitoring frameworks. Therefore, there has been an urgent need to develop spatially explicit frame works for monitoring grassland ecosystems especially in communal areas. This project aimed to contribute to the development of a framework that will provide actionable information services for grassland assessment and monitoring across different key land management areas. Recent advances in remote sensing technologies, data provision as well as big data cloud computing and storage capabilities have availed possibilities for spatially quantifying and mapping grassland ecosystem services. Specifically, the project aimed,

- (i) to conduct a comprehensive and state of the art literature review on the potential use of remote sensing-based models for grassland productivity monitoring in the light of climate change,
- (ii) to review the importance of grasslands as an ecosystem service, particularly the contribution of leaf area index (LAI), canopy storage capacity and biomass in water management,
- (iii) to characterise and model communal grassland productivity status in a changing climate at three sites within the uMgungundlovu District Municipality and

- (iv) to assess intra- and interannual changes in grassland productivity and proportionate land use change within the catchment and explain the changes thereof.

To address these objectives, seven specific objectives were drawn as follows;

- To conducting a comprehensive and state of the art literature review on the potential use of remote sensing-based models for grassland productivity (GP) monitoring in the light of climate change.
- To systematically review the literature on the remote sensing of grassland ecosystem services, with a particular focus on the contribution of leaf area index (LAI), canopy storage capacity and biomass in water management services.
- To assess the spatiotemporal variability of rangelands within a typical southern African communal area from the year 2000 to 2020 using multi-temporal Landsat datasets in conjunction with random forest.
- To predict the future spatial distribution of grasslands in communal rangelands using the CA-Markov model between the year 2020 and 2040.
- To compare the predictive performance of shallow artificial neural networks (ANNs) and deep convolutional neural networks (CNNs) in estimating aboveground grass biomass using Sentinel 2 MSI during the dry season.
- To predict inter-seasonal variations of grass biomass in using Sentinel 2 MSI remotely sensed data in conjunction with convolutional neural networks (CNNs).
- To test the utility of multi-source data in estimating LAI, CSC, CWC, and EWT within communal grasslands across wet and dry seasons.

In conducting the systematic literature reviews After conducting two literature reviews to understand remote sensing of grass productivity and grassland ecosystem services, the following lessons were drawn. It was noted that in the southern African context, much of the studies used above ground biomass, LAI, and chlorophyll content as proxies for evaluating and monitoring grass productivity and ecosystem services. Also, it was concluded that there is need for more research efforts in characterising grassland senescence as it is linked to the availability and variations of all ecosystem services derived from grasslands. Results of the reviews also suggested that there is no clear-cut algorithm and specific vegetation indices that can be used to characterise grass productivity as a proxy for understanding grassland ecosystem services as optimal ones differed across different studies. The findings of the reviews underscored that the most suitable remotely sensed data sets for understanding changes in health, productivity, spatial extent, and quantitatively enumerating ecosystem

services at a landscape scale were the freely available sensors, including Landsat 8 OLI, and Sentinel-2 MSI. Meanwhile, deep machine learning algorithms such as CNN, and ANN as well as the GEE-based algorithms such as Random Forest and support vector machines, were amongst the most widely used robust and accurate procedures for developing grassland monitoring models. The findings of the reviews implied that the Integration of robust non-parametric machine learning algorithms, freely available multispectral datasets, topographic metrics and UAVS derived datasets in GEE could yield an opportunity for designing an objective framework for mapping and monitoring rangeland productivity and other ecosystem services. Although very few studies have been conducted based on remote sensing-based models to characterise grass land ecosystem services, there are high prospects from the available advanced and robust computation infrastructure (i.e. GEE) and the freely available sensors covering critical sections of the electromagnetic spectrum in vegetation mapping and monitoring. These findings informed the methodological approaches used to address the contractual objectives and the projects specific objectives.

In characterising and quantifying the variability in spatial extent and fragmentation of communal grasslands over the period of 20 years in the study area, the findings led to a conclusion that LULCCs can be optimally characterised using Landsat's bands in combination with the vegetation indices. In addition, the NIR and the SWIR bands were the most influential variables for mapping the rangeland changes with high accuracies. Settlement expansion and an increase in crop fields were identified as the main drivers of rangeland decline and degradation. Fragmentation of rangelands was increasing with time as more grassland patches were getting more isolated and relatively smaller in spatial extent as built-up area increased.

In assessing current and future dynamics of the spatial extent of grassland using the CA-Markov model in typical communal rangeland of Southern Africa, the 2040 predictions showed that settlements (built-up areas) will increase due to an increase in population. In Vulindlela, built-up areas were predicted to increase by 67 ha per year while rangelands decrease at a rate of 46 ha per year. The patch metrics of grasslands in Vulindlela and Inhlazuka predicted an increase in rangeland fragmentation as a result of the loss of connectivity in rangelands and increased isolation, especially in Vulindlela as a result of development activities. The increase in settlement development suggests that there is an urgent need to develop rangeland management plans for the accelerating rangeland degradation through fragmentation.

In comparing the performance of deep convolutional (CNNs) and artificial neural networks (ANNs) in estimating the aboveground biomass of grass using Sentinel-2 MSI remotely sensed data, findings demonstrated that the CNNs outperformed the traditional ANN even though both algorithms performed satisfactorily in predicting grass biomass. This section of the project could be considered to be pilot-scale research, particularly in a southern African context of utilising the robust deep learning machine algorithms in monitoring grassland.

Following its optimal performance, the CNN was then used to predict inter-seasonal grass biomass variations in conjunction with Sentinel-2 MSI. The findings demonstrated that there was a significant difference between dry and wet season grass biomass in the study area, with the wet season biomass being four times higher than that from the dry season. These changes were noted to be primarily related to significant changes in rainfall and temperature that in turn influenced changes in other biophysical factors such as soil. These findings demonstrated that deep neural network approaches are very robust to facilitate an accurate time-effective assessment of grasslands.

Findings from this study also showed that geospatial technologies and can be optimally used to map and monitor the inter- and-intra-seasonal variability of communal grass productivity as well as water-related ecosystem services attributes. Specifically, grassland productivity elements, which include biomass, leaf area index, equivalent moisture thickness, canopy storage capacity, foliar moisture content, and canopy water content, as well as the variations in the extent and magnitude of fragmentation, were all optimally estimated using the readily accessible Landsat and Sentinel 2 MSI remotely sensed data in conjunction with robust machine learning techniques.

9.2. Limitations of The Study

In the context of systematic literature reviews, it is common that not all articles in their entirety are included in the analysis. This is attributed to language bias, exorbitant article accessing charges and the perpetual advancement in earth observation facilities and technologies used to monitor grasslands. This suggest that more research efforts are required to comprehensively enhance our understanding of the existing works on the remote sensing of grassland productivity and associated ecosystem services.

In Inhlazuka, there may have been some misclassifications between the rangelands and forest classes, making it difficult to discriminate these classes in certain areas using the Landsat remotely sensed data. This could be explained by the rapid emergence and clearance

activities of alien invasive species in the area, as well as the topographic variations which could have affected the spectral data through the shadow effect. Additionally, the impact of fire that was not extensively considered in this study could have impacted on the accuracies of models derived in this study. This suggests that a holistic model approach is still required to comprehensively monitor the productivity and ecosystem services elements of communal grasslands.

The occurrence of various grass species entails that the resultant spectral information detected from the canopy was a function of variations in species specific canopy geometries. This could have relatively impacted the models derived from such mixed signals, suggesting the need to consider species specific quantifications when assessing and understanding grass productivity and water-related ecosystem services elements. Given the spatial and spectral variability of grass species, finding the correct dataset, with the optimal spectral and spatial resolution, remains a crucial drawback for estimating GP using RS data. Currently, GP estimates in light of climate change are required at the regional or national scale. These sensors must have the optimum spectral and spatial resolution sufficient to provide very-high spatial resolution data. However, the spatial resolution of current multispectral data products acquired in wide swaths have a low temporal resolution (10 days at the equator with one satellite), negatively affecting the performance of techniques for explicitly estimating GP.

Also, given the time and resources constraints, the destructive sampling intervals of grass were limited to selected areas of uMngeni catchment and in terms of replication. This implies that there is need for more spatiotemporally intensive sampling strategies to building a robust database that could be used in generating site-specific models, considering the variability in terms of land use within the grasslands.

9.3. Conclusion

Based on this study's findings, it can be concluded that geospatial technologies can be optimally used to map and monitor the inter- and-intra-seasonal variability of communal grass productivity and water-related ecosystem services attributes. Specifically, grassland productivity elements, which include biomass, leaf area index, equivalent moisture thickness, canopy storage capacity, foliar moisture content, and canopy water content, as well as the variations in the extent and magnitude of fragmentation, were all optimally estimated using the readily accessible Landsat and Sentinel 2 MSI remotely sensed data in conjunction with robust machine learning techniques. Since, the project merely identified the optimal data and tools that could be effectively used as proxies to map the variability of grassland productivity in

communal areas, this project is a pathway towards the development of a geospatial system for monitoring grassland ecosystems. The system will provide actionable information services for grassland assessment and monitoring across different key land management areas. Specifically, the assessment and monitoring service will deliver satellite-based Earth observation spatiotemporal models that will assist users in their operational grassland management as well as policy and decision making in the target areas.

9.4. Recommendations

Several research gaps remain regarding the utility of geospatial technologies and data in mapping and monitoring the spatiotemporal dynamics of grassland productivity, especially in communal rangelands.

- There is still a need to assess the utility of integrating deep Machine learning geospatial technologies and multi-source data in mapping and monitoring grass physiological attributes.
- The varying pixel size and radiometric resolutions of different earth observation sensors utilised in this project could have impacted on the accurate estimation of grass productivity and water-related ecosystem services elements. In this regard, future research needs to test and compare the utility of various sensors including the newly launched Landsat-9 OLI-2 and EnMAP.
- Research efforts should also be exerted towards understanding the general distribution, productivity, water-related ecosystem services and forage quality attributes of specifically the sourveld and sweetveld grasses in uMngeni catchment to improve and inform the sustainable utilisation of communal grasslands.
- There is an urgent need to increase research efforts on rangeland management strategies that can be implemented in communal areas to create awareness on the vital importance of protecting the ecosystems. Future studies could also assess the impact of activities such as livestock production and grazing intensity/patterns as well as fire administration in communal areas as individual agents impacting on the quality and quantity rangelands.
- Above all, there is still an urgent need to design and implement a Geospatial system for monitoring grassland ecosystems. This system will facilitate the smooth interpretation and simplification of the generated spatially explicit information on grassland productivity dynamics. The simplified information could assist the farmers to

fully exploit the generated information, thereby assisting them in reinforcing decision-making processes for sustainable utilisation of the grasslands. In the long run, this will enhance the provision of ecosystem services and livestock production based on grassland productivity.

- There is need for development of comprehensive rangeland management plans, tailored to the unique characteristics and challenges of communal grasslands in southern Africa. These plans should prioritise sustainable land management practices, including rotational grazing systems, controlled burning and restoration initiatives, to prevent further degradation and fragmentation of communal rangelands.
- There is a need to strengthen existing land-use policies and regulatory frameworks to promote the conservation and sustainable utilisation of communal grasslands. This should integrate measures for addressing the drivers of rangeland degradation, including settlement expansion and agricultural intensification, through zoning regulations, land use planning, and enforcement mechanism. This could be strengthened by fostering community participation and collaboration in rangeland management decision-making processes.

REFERENCES

- Abd El-Kawy, O., J. Rød, H. Ismail and A. Suliman (2011). "Land use and land cover change detection in the western Nile delta of Egypt using remote sensing data." Applied geography **31**(2): 483-494.
- Abdel-Hamid, A., O. Dubovyk and K. Greve (2021). "The potential of sentinel-1 InSAR coherence for grasslands monitoring in Eastern Cape, South Africa." International Journal of Applied Earth Observation and Geoinformation **98**.
- Abdulahi, M. M., H. Hashim and M. Teha (2016). "Rangeland degradation: Extent, impacts, and alternative restoration techniques in the rangelands of Ethiopia." Tropical and Subtropical Agroecosystems **19**(3).
- Accatino, F., C. De Michele, R. Vezzoli, D. Donzelli and R. J. Scholes (2010). "Tree-grass co-existence in savanna: interactions of rain and fire." Journal of theoretical biology **267**(2): 235-242.
- Adamczyk, J. and A. Osberger (2015). "Red-edge vegetation indices for detecting and assessing disturbances in Norway spruce dominated mountain forests." International Journal of Applied Earth Observation and Geoinformation **37**: 90-99.
- Agapiou, A., D. G. Hadjimitsis and D. D. J. R. s. Alexakis (2012). "Evaluation of broadband and narrowband vegetation indices for the identification of archaeological crop marks." **4**(12): 3892-3919.
- Alam, A., M. S. Bhat and M. Maheen (2020). "Using Landsat satellite data for assessing the land use and land cover change in Kashmir valley." GeoJournal **85**(6): 1529-1543.
- Alexander, C., B. Deák and H. J. E. i. Heilmeyer (2016). "Micro-topography driven vegetation patterns in open mosaic landscapes." **60**: 906-920.
- Ali, I., B. Barrett, F. Cawkwell, S. Green, E. Dwyer and M. Neumann (2017). "Application of Repeat-Pass TerraSAR-X Staring Spotlight Interferometric Coherence to Monitor Pasture Biophysical Parameters: Limitations and Sensitivity Analysis." Ieee Journal of Selected Topics in Applied Earth Observations and Remote Sensing **10**(7): 3225-3231.
- Ali, I., F. Cawkwell, E. Dwyer, B. Barrett and S. Green (2016). "Satellite remote sensing of grasslands: from observation to management." Journal of Plant Ecology **9**(6): 649-671.
- Ali, I., F. Cawkwell, E. Dwyer and S. Green (2016). "Modeling managed grassland biomass estimation by using multitemporal remote sensing data – A machine learning approach." IEEE Journal of Selected Topics in Applied Earth Observations and Remote Sensing **10**(7): 3254-3264.
- Ali, I., F. Cawkwell, S. Green and N. Dwyer (2014). Application of statistical and machine learning models for grassland yield estimation based on a hypertemporal satellite remote sensing time series. 2014 IEEE geoscience and remote sensing symposium, IEEE.
- Ali, I., F. Greifeneder, J. Stamenkovic, M. Neumann and C. Notarnicola (2015). "Review of machine learning approaches for biomass and soil moisture retrievals from remote sensing data." Remote Sensing **7**(12): 16398-16421.

Alkemade, R., R. S. Reid, M. van den Berg, J. de Leeuw and M. Jeuken (2013). "Assessing the impacts of livestock production on biodiversity in rangeland ecosystems." Proceedings of the National Academy of Sciences **110**(52): 20900-20905.

Alves Oliveira, R., J. Marcato Junior, C. Soares Costa, R. Näsi, N. Koivumäki, O. Niemeläinen, J. Kaivosoja, L. Nyholm, H. Pistori and E. Honkavaara (2022). "Silage Grass Sward Nitrogen Concentration and Dry Matter Yield Estimation Using Deep Regression and RGB Images Captured by UAV." Agronomy **12**(6): 1352.

Amatulli, G., S. Domisch, M.-N. Tuanmu, B. Parmentier, A. Ranipeta, J. Malczyk and W. Jetz (2018). "A suite of global, cross-scale topographic variables for environmental and biodiversity modeling." Scientific data **5**(1): 1-15.

Anderson, G. L., J. D. Hanson and R. H. Haas (1993). "Evaluating landsat thematic mapper derived vegetation indices for estimating above-ground biomass on semiarid rangelands." Remote Sensing of Environment **45**(2): 165-175.

Anderson, M. C., J. M. Norman, T. P. Meyers and G. R. Diak (2000). "An analytical model for estimating canopy transpiration and carbon assimilation fluxes based on canopy light-use efficiency." Agricultural and Forest Meteorology **101**(4): 265-289.

Andrew, M. E., M. A. Wulder and T. A. Nelson (2014). "Potential contributions of remote sensing to ecosystem service assessments." Progress in Physical Geography **38**(3): 328-353.

Ardö, J., T. Tagesson, S. Jamali and A. Khatir (2018). "MODIS EVI-based net primary production in the Sahel 2000-2014." International Journal of Applied Earth Observation and Geoinformation **65**: 35-45.

Arjasakusuma, S., S. Swahyu Kusuma and S. Phinn (2020). "Evaluating variable selection and machine learning algorithms for estimating forest heights by combining lidar and hyperspectral data." ISPRS International Journal of Geo-Information **9**(9): 507.

Assan, N. (2014). "Possible impact and adaptation to climate change in livestock production in Southern Africa." IOSR J Environ Sci Toxicol Food Technol **8**(2): 104-112.

Atzberger, C., A. Klisch, M. Mattiuzzi and F. Vuolo (2014). "Phenological Metrics Derived over the European Continent from NDVI3g Data and MODIS Time Series." Remote Sensing **6**(1): 257-284.

Baghdadi, N. N., M. El Hajj, M. Zribi and I. Fayad (2015). "Coupling SAR C-band and optical data for soil moisture and leaf area index retrieval over irrigated grasslands." IEEE Journal of Selected Topics in Applied Earth Observations and Remote Sensing **9**(3): 1229-1243.

Bannari, A., H. Asalhi and P. M. Teillet (2002). Transformed difference vegetation index (TDVI) for vegetation cover mapping. IEEE International geoscience and remote sensing symposium, IEEE.

Bardgett, R. D., J. M. Bullock, S. Lavorel, P. Manning, U. Schaffner, N. Ostle, M. Chomel, G. Durigan, E. L Fry and D. Johnson (2021). "Combatting global grassland degradation." Nature Reviews Earth & Environment: 1-16.

Barnes, E., T. Clarke, S. Richards, P. Colaizzi, J. Haberland, M. Kostrzewski, P. Waller, C. Choi, E. Riley and T. Thompson (2000). Coincident detection of crop water stress, nitrogen

status and canopy density using ground based multispectral data. Proceedings of the fifth international conference on precision agriculture, Bloomington, MN, USA.

Barrett, B., I. Nitze, S. Green and F. Cawkwell (2014). "Assessment of multi-temporal, multi-sensor radar and ancillary spatial data for grasslands monitoring in Ireland using machine learning approaches." Remote sensing of environment **152**: 109-124.

Baudena, M., S. C. Dekker, P. M. van Bodegom, B. Cuesta, S. I. Higgins, V. Lehsten, C. H. Reick, M. Rietkerk, S. Scheiter and Z. Yin (2015). "Forests, savannas, and grasslands: bridging the knowledge gap between ecology and Dynamic Global Vegetation Models." Biogeosciences **12**(6): 1833-1848.

Bédard, F., S. Crump and J. Gaudreau (2006). "A comparison between Terra MODIS and NOAA AVHRR NDVI satellite image composites for the monitoring of natural grassland conditions in Alberta, Canada." Canadian Journal of Remote Sensing **32**(1): 44-50.

Bedunah, D. J. and J. P. Angerer (2012). "Rangeland degradation, poverty, and conflict: how can rangeland scientists contribute to effective responses and solutions?" Rangeland Ecology & Management **65**(6): 606-612.

Beier, C., C. Beierkuhnlein, T. Wohlgemuth, J. Penuelas, B. Emmett, C. Körner, H. de Boeck, J. H. Christensen, S. Leuzinger and I. A. Janssens (2012). "Precipitation manipulation experiments – challenges and recommendations for the future." Ecology letters **15**(8): 899-911.

Belgiu, M. and L. Drăguț (2016). "Random forest in remote sensing: A review of applications and future directions." ISPRS journal of photogrammetry and remote sensing **114**: 24-31.

Bella, D., R. Faivre, F. Ruget, B. Seguin, M. Guerif, B. Combal, M. Weiss and C. Rebella (2004). "Remote sensing capabilities to estimate pasture production in France." International Journal of Remote Sensing **25**(23): 5359-5372.

Bellocchi, G. and C. Picon-Cochard (2021). Effects of Climate Change on Grassland Biodiversity and Productivity, Multidisciplinary Digital Publishing Institute.

Bengtsson, J., J. Bullock, B. Egoh, C. Everson, T. Everson, T. O'Connor, P. O'Farrell, H. Smith and R. Lindborg (2019). "Grasslands – more important for ecosystem services than you might think." Ecosphere **10**(2): e02582.

Bengtsson, J., J. M. Bullock, B. Egoh, C. Everson, T. Everson, T. O'Connor, P. J. O'Farrell, H. G. Smith and R. Lindborg (2019). "Grasslands – more important for ecosystem services than you might think." Ecosphere **10**(2): e02582.

Berger, K., C. Atzberger, M. Danner, G. D'Urso, W. Mauser, F. Vuolo and T. Hank (2018). "Evaluation of the PROSAIL Model Capabilities for Future Hyperspectral Model Environments: A Review Study." Remote Sensing **10**(1): 85.

Bertoldi, G., S. Della Chiesa, C. Notarnicola, L. Pasolli, G. Niedrist and U. Tappeiner (2014). "Estimation of soil moisture patterns in mountain grasslands by means of SAR RADARSAT2 images and hydrological modeling." Journal of Hydrology **516**: 245-257.

Bonan, G. B. (2008). "Forests and climate change: forcings, feedbacks, and the climate benefits of forests." science **320**(5882): 1444-1449.

- Boochs, F., G. Kupfer, K. Dockter and W. Kühbauch (1990). "Shape of the red edge as vitality indicator for plants." Remote Sensing **11**(10): 1741-1753.
- Boone, R. B., R. T. Conant, J. Sircely, P. K. Thornton and M. Herrero (2018). "Climate change impacts on selected global rangeland ecosystem services." Global change biology **24**(3): 1382-1393.
- Boschetti, M., S. Bocchi and P. A. Brivio (2007). "Assessment of pasture production in the Italian Alps using spectrometric and remote sensing information." Agriculture, ecosystems & environment **118**(1-4): 267-272.
- Boussetta, S., G. Balsamo, A. Beljaars, T. Kral and L. Jarlan (2013). "Impact of a satellite-derived leaf area index monthly climatology in a global numerical weather prediction model." International journal of remote sensing **34**(9-10): 3520-3542.
- Boval, M. and R. Dixon (2012). "The importance of grasslands for animal production and other functions: a review on management and methodological progress in the tropics." Animal **6**(5): 748-762.
- Bramich, J., C. J. Bolch and A. Fischer (2021). "Improved red-edge chlorophyll-a detection for Sentinel 2." Ecological Indicators **120**: 106876.
- Breiman, L. (2001). "Random forests." Machine learning **45**(1): 5-32.
- Briske, D. D. (2017). Rangeland systems: processes, management and challenges, Springer Nature.
- Brodrick, P. G., A. B. Davies and G. P. Asner (2019). "Uncovering ecological patterns with convolutional neural networks." Trends in ecology & evolution **34**(8): 734-745.
- Brown, G., J. M. Montag and K. Lyon (2012). "Public participation GIS: a method for identifying ecosystem services." Society & natural resources **25**(7): 633-651.
- Browne, M., N. T. Yardimci, C. Scoffoni, M. Jarrahi and L. Sack (2020). "Prediction of leaf water potential and relative water content using terahertz radiation spectroscopy." Plant direct **4**(4): e00197.
- Buckley, J. R. and A. M. Smith (2010). Monitoring grasslands with radarsat 2 quad-pol imagery. 2010 IEEE International Geoscience and Remote Sensing Symposium.
- Bulcock, H. and G. Jewitt (2009). "Improved spatial mapping of leaf area index using hyperspectral remote sensing for hydrological applications with a particular focus on canopy interception." Hydrology & Earth System Sciences Discussions **6**(5).
- Bulcock, H. and G. Jewitt (2010). "Spatial mapping of leaf area index using hyperspectral remote sensing for hydrological applications with a particular focus on canopy interception." Hydrology and Earth System Sciences **14**(2): 383-392.
- Cadman, M., C. De Villiers and R. Lechmere-Oertel (2013). Grassland ecosystem guidelines: landscape interpretation for planners and managers.
- Cai, Y., K. Guan, J. Peng, S. Wang, C. Seifert, B. Wardlow and Z. Li (2018). "A high-performance and in-season classification system of field-level crop types using time-series Landsat data and a machine learning approach." Remote sensing of environment **210**: 35-47.

Cameron, A. C. and F. A. Windmeijer (1997). "An R-squared measure of goodness of fit for some common nonlinear regression models." Journal of econometrics **77**(2): 329-342.

Carlberg, C. (2014). Statistical analysis: Microsoft excel 2013, Que Publishing.

Carlier, L., I. Rotar, M. Vlahova and R. Vidican (2009). "Importance and functions of grasslands." Notulae Botanicae Horti Agrobotanici Cluj-Napoca **37**(1): 25.

Carrasco, L., A. W. O'Neil, R. D. Morton and C. S. Rowland (2019). "Evaluating combinations of temporally aggregated Sentinel-1, Sentinel-2 and Landsat 8 for land cover mapping with Google Earth Engine." Remote Sensing **11**(3): 288.

Castelli, M., M. Anderson, Y. Yang, G. Wohlfahrt, G. Bertoldi, G. Niedrist, A. Hammerle, P. Zhao, M. Zebisch and C. Notarnicola (2018). "Two-source energy balance modeling of evapotranspiration in Alpine grasslands." Remote Sensing of Environment **209**: 327-342.

Caturegli, L., S. Matteoli, M. Gaetani, N. Grossi, S. Magni, A. Minelli, G. Corsini, D. Remorini and M. Volterrani (2020). "Effects of water stress on spectral reflectance of bermudagrass." Scientific Reports **10**(1): 1-12.

Cawley, G. C. and N. L. Talbot (2010). "On over-fitting in model selection and subsequent selection bias in performance evaluation." The Journal of Machine Learning Research **11**: 2079-2107.

Ceballos, G., A. Davidson, R. List, J. Pacheco, P. Manzano-Fischer, G. Santos-Barrera and J. Cruzado (2010). "Rapid decline of a grassland system and its ecological and conservation implications." PloS one **5**(1): e8562.

Ceccato, P., S. Flasse, S. Tarantola, S. Jacquemoud and J.-M. Grégoire (2001). "Detecting vegetation leaf water content using reflectance in the optical domain." Remote sensing of environment **77**(1): 22-33.

Cengiz, A., M. Budak, N. YAĞMUR and F. BALÇIK (2023). "Comparison between random forest and support vector machine algorithms for LULC classification." International Journal of Engineering and Geosciences **8**(1): 1-10.

Ceotto, E. (2008). "Grasslands for bioenergy production. A review." Agronomy for Sustainable Development **28**(1): 47-55.

Cerasoli, S., M. Campagnolo, J. Faria, C. Nogueira and M. d. C. Caldeira (2018). "On estimating the gross primary productivity of Mediterranean grasslands under different fertilization regimes using vegetation indices and hyperspectral reflectance." Biogeosciences **15**(17): 5455-5471.

Cervena, L., Z. Lhotakova, L. Kupkova, M. Kovarova and J. Albrechtova (2014). Models for estimating leaf pigments and relative water content in three vertical canopy levels of Norway spruce based on laboratory spectroscopy. EARSeL 34th Symposium Proceedings, Proceedings of the 34th EARSeL Symposium.

Cha, S.-y. and C.-h. Park (2007). "The utilization of Google Earth images as reference data for the multitemporal land cover classification with MODIS data of North Korea." Korean Journal of Remote Sensing **23**(5): 483-491.

- Chen, J. M. (1996). "Evaluation of vegetation indices and a modified simple ratio for boreal applications." Canadian Journal of Remote Sensing **22**(3): 229-242.
- Chen, Y., J. Guerschman, Y. Shendryk, D. Henry and M. T. Harrison (2021). "Estimating pasture biomass using Sentinel-2 imagery and machine learning." Remote Sensing **13**(4): 603.
- Chen, Z.-x., W.-b. Wu and H. Qing (2015). Estimation of above-ground biomass carbon storage in Hulunbeier grassland based on remotely sensed data. 2015 Fourth International Conference on Agro-Geoinformatics (Agro-geoinformatics), IEEE.
- Chiarito, E., F. Cigna, G. Cuzzo, G. Fontanelli, A. M. Aguilar, S. Paloscia, M. Rossi, E. Santi, D. Tapete and C. Notarnicola (2021). "Biomass retrieval based on genetic algorithm feature selection and support vector regression in Alpine grassland using ground-based hyperspectral and Sentinel-1 SAR data." European Journal of Remote Sensing **54**(1): 209-225.
- Chicco, D., M. J. Warrens and G. Jurman (2021). "The coefficient of determination R-squared is more informative than SMAPE, MAE, MAPE, MSE and RMSE in regression analysis evaluation." PeerJ Computer Science **7**: e623.
- Cho, M. A., M. Onesimo and T. Mabhaudhi (2021). "Using participatory GIS and collaborative management approaches to enhance local actors' participation in rangeland management: the case of Vulindlela, South Africa." Journal of Environmental Planning and Management: 1-20.
- Chuvieco, E., D. Riaño, I. Aguado and D. Cocero (2002). "Estimation of fuel moisture content from multitemporal analysis of Landsat Thematic Mapper reflectance data: applications in fire danger assessment." International journal of remote sensing **23**(11): 2145-2162.
- Clark, M. and D. Tilman (2017). "Comparative analysis of environmental impacts of agricultural production systems, agricultural input efficiency, and food choice." Environmental Research Letters **12**(6): 064016.
- Cleland, E. E., S. L. Collins, T. L. Dickson, E. C. Farrer, K. L. Gross, L. A. Gherardi, L. M. Hallett, R. J. Hobbs, J. S. Hsu and L. Turnbull (2013). "Sensitivity of grassland plant community composition to spatial vs. temporal variation in precipitation." Ecology **94**(8): 1687-1696.
- Clevers, J. G. and A. A. Gitelson (2013). "Remote estimation of crop and grass chlorophyll and nitrogen content using red-edge bands on Sentinel-2 and -3." International Journal of Applied Earth Observation and Geoinformation **23**: 344-351.
- Clevers, J. G., L. Kooistra and M. E. Schaepman (2008). "Using spectral information from the NIR water absorption features for the retrieval of canopy water content." International Journal of Applied Earth Observation and Geoinformation **10**(3): 388-397.
- Clevers, J. G., L. Kooistra, M. E. Schaepman, S. Liang, N. E. Groot and M. Kneubühler (2007). Canopy water content retrieval from hyperspectral remote sensing, ISPRS.
- Clevers, J. G. P. W. and A. A. Gitelson (2013). "Remote estimation of crop and grass chlorophyll and nitrogen content using red-edge bands on Sentinel-2 and -3." International Journal of Applied Earth Observation and Geoinformation **23**: 344-351.

- Cloutis, E., D. Connery, D. Major and F. Dover (1996). "Airborne multi-spectral monitoring of agricultural crop status: effect of time of year, crop type and crop condition parameter." Remote Sensing **17**(13): 2579-2601.
- Conant, R. T., C. E. P. Cerri, B. B. Osborne and K. Paustian (2017). "Grassland management impacts on soil carbon stocks: a new synthesis." Ecological Applications **27**(2): 662-668.
- Curran, P. J., J. L. Dungan and H. L. Gholz (1990). "Exploring the relationship between reflectance red edge and chlorophyll content in slash pine." Tree physiology **7**(1-2-3-4): 33-48.
- da Silva, V. S., G. Salami, M. I. O. da Silva, E. A. Silva, J. J. Monteiro Junior and E. Alba (2020). "Methodological evaluation of vegetation indexes in land use and land cover (LULC) classification." Geology, Ecology, and Landscapes **4**(2): 159-169.
- Dai, E., Y. Huang, Z. Wu and D. Zhao (2016). "Analysis of spatio-temporal features of a carbon source/sink and its relationship to climatic factors in the Inner Mongolia grassland ecosystem." Journal of Geographical Sciences **26**(3): 297-312.
- Dancy, K., R. Webster and N. Abel (1986). "Estimating and mapping grass cover and biomass from low-level photographic sampling." International Journal of Remote Sensing **7**(12): 1679-1704.
- Danson, F. M. and P. Bowyer (2004). "Estimating live fuel moisture content from remotely sensed reflectance." Remote Sensing of Environment **92**(3): 309-321.
- Darvishzadeh, R., A. Skidmore, M. Schlerf and C. Atzberger (2008). "Inversion of a radiative transfer model for estimating vegetation LAI and chlorophyll in a heterogeneous grassland." Remote Sensing of Environment **112**(5): 2592-2604.
- Darvishzadeh, R., A. Skidmore, M. Schlerf, C. Atzberger, F. Corsi and M. Cho (2008). "LAI and chlorophyll estimation for a heterogeneous grassland using hyperspectral measurements." ISPRS Journal of Photogrammetry and Remote Sensing **63**(4): 409-426.
- Darvishzadeh, R., A. K. Skidmore, M. Mirzaie, C. Atzberger and M. Schlerf (2014). Fresh biomass estimation in heterogeneous grassland using hyperspectral measurements and multivariate statistical analysis. In AGU Fall Meeting Abstracts.
- Das, M., S. K. Ghosh, V. M. Chowdary, P. Mitra and S. Rijal (2022). Statistical and Machine Learning Models for Remote Sensing Data Mining – Recent Advancements, MDPI. **14**: 1906.
- Datt, B. (1999). "Remote sensing of water content in Eucalyptus leaves." Australian Journal of botany **47**(6): 909-923.
- Davidson, A., S. Wang and J. Wilmshurst (2006). "Remote sensing of grassland-shrubland vegetation water content in the shortwave domain." International Journal of Applied Earth Observation and Geoinformation **8**(4): 225-236.
- de Araujo Barbosa, C. C., P. M. Atkinson and J. A. Dearing (2015). "Remote sensing of ecosystem services: A systematic review." Ecological Indicators **52**: 430-443.
- De Leeuw, J., A. Rizayeva, E. Namazov, E. Bayramov, M. T. Marshall, J. Etzold and R. Neudert (2019). "Application of the MODIS MOD 17 Net Primary Production product in

grassland carrying capacity assessment." International Journal of Applied Earth Observation and Geoinformation **78**: 66-76.

De Simone, W., M. Allegranza, A. R. Frattaroli, S. Montecchiari, G. Tessei, V. Zuccarello and M. Di Musciano (2021). "From Remote Sensing to Species Distribution Modelling: An Integrated Workflow to Monitor Spreading Species in Key Grassland Habitats." Remote Sensing **13**(10): 1904.

de Wit, M., J. Blignaut and F. Nazare (2006). "Monetary Valuation of the Grasslands in South Africa. 2006. Available online: http://biodiversityadvisor.sanbi.org/wp-content/uploads/2014/07/2006deWit_Background-InfoRep5_Strategic-Monetary-valuation.pdf (accessed on 6 January 2017)."

De Witt, M. and J. Blignaut (2006). "Using monetary valuation results with specific reference to grasslands in South Africa." Report prepared for SANBI as part of the project "Making the case for the value of ecosystem goods and services provided by the Grassland Biome". Report No. SO6002. De Witt Sustainable Options (Pty) Ltd.

Deb, D., J. Singh, S. Deb, D. Datta, A. Ghosh and R. Chaurasia (2017). "An alternative approach for estimating above ground biomass using Resourcesat-2 satellite data and artificial neural network in Bundelkhand region of India." Environmental monitoring and assessment **189**(11): 1-12.

del Río-Mena, T., L. Willemen, G. T. Tesfamariam, O. Beukes and A. Nelson (2020). "Remote sensing for mapping ecosystem services to support evaluation of ecological restoration interventions in an arid landscape." Ecological indicators **113**: 106182.

Derner, J. D. and D. J. Augustine (2016). "Adaptive management for drought on rangelands." Rangelands **38**(4): 211-215.

DeVries, B., A. K. Pratihast, J. Verbesselt, L. Kooistra and M. Herold (2016). "Characterizing forest change using community-based monitoring data and Landsat time series." PLOS ONE **11**(3): e0147121.

Dingaen, M. N. and M. Tsubo (2019). "Improved assessment of pasture availability in semi-arid grassland of South Africa." Environmental monitoring and assessment **191**(12): 1-12.

Dixon, A. P., D. Faber-Langendoen, C. Josse, J. Morrison and C. J. Loucks (2014). "Distribution mapping of world grassland types." Journal of Biogeography **41**(11): 2003-2019.

Dong, L., H. Du, N. Han, X. Li, D. e. Zhu, F. Mao, M. Zhang, J. Zheng, H. Liu and Z. Huang (2020). "Application of convolutional neural network on lei bamboo above-ground-biomass (AGB) estimation using Worldview-2." Remote Sensing **12**(6): 958.

Dong, T., J. Liu, J. Shang, B. Qian, B. Ma, J. M. Kovacs, D. Walters, X. Jiao, X. Geng and Y. Shi (2019). "Assessment of red-edge vegetation indices for crop leaf area index estimation." Remote Sensing of Environment **222**: 133-143.

Dowdy, A. J., H. Ye, A. Pepler, M. Thatcher, S. L. Osbrough, J. P. Evans, G. Di Virgilio and N. McCarthy (2019). "Future changes in extreme weather and pyroconvection risk factors for Australian wildfires." Scientific reports **9**(1): 10073.

Drusch, M., U. Del Bello, S. Carlier, O. Colin, V. Fernandez, F. Gascon, B. Hoersch, C. Isola, P. Laberinti and P. J. R. s. o. E. Martimort (2012). "Sentinel-2: ESA's optical high-resolution mission for GMES operational services." **120**: 25-36.

Dube, T., X. G. Maluleke and O. Mutanga (2022). "Mapping rangeland ecosystems vulnerability to Lantana camara invasion in semi-arid savannahs in South Africa." *African Journal of Ecology*.

Dube, T., O. Mutanga and R. Ismail (2016). "Quantifying aboveground biomass in African environments: A review of the trade-offs between sensor estimation accuracy and costs." *Tropical Ecology* **57**(3): 393-405.

Dube, T., S. Pandit, C. Shoko, A. Ramoelo, D. Mazvimavi and T. Dalu (2019). "Numerical Assessments of Leaf Area Index in Tropical Savanna Rangelands, South Africa Using Landsat 8 OLI Derived Metrics and In-Situ Measurements." *Remote Sensing* **11**(7).

Dube, T., C. Shoko and T. W. Gara (2021). "Remote sensing of aboveground grass biomass between protected and non-protected areas in savannah rangelands." *African Journal of Ecology* **59**(3): 687-695.

Duley, F. and C. E. Domingo (1949). "Effect of grass on intake of water."

Duro, D. C., S. E. Franklin and M. G. Dubé (2012). "Multi-scale object-based image analysis and feature selection of multi-sensor earth observation imagery using random forests." *International Journal of Remote Sensing* **33**(14): 4502-4526.

Dusseux, P., T. Corpetti, L. Hubert-Moy and S. Corgne (2014). "Combined Use of Multi-Temporal Optical and Radar Satellite Images for Grassland Monitoring." *Remote Sensing* **6**(7): 6163-6182.

Dusseux, P., T. Guyet, P. Pattier, V. Barbier and H. Nicolas (2022). "Monitoring of grassland productivity using Sentinel-2 remote sensing data." *International Journal of Applied Earth Observation and Geoinformation* **111**: 102843.

Easterday, K., C. Kislik, T. E. Dawson, S. Hogan and M. Kelly (2019). "Remotely sensed water limitation in vegetation: insights from an experiment with unmanned aerial vehicles (UAVs)." *Remote Sensing* **11**(16): 1853.

Eastman, J. R. (2015). "TerrSet manual." *Accessed in TerrSet version* **18**(1).

Egoh, B. N., B. Reyers, M. Rouget and D. M. Richardson (2011). "Identifying priority areas for ecosystem service management in South African grasslands." *Journal of Environmental Management* **92**(6): 1642-1650.

Ehammer, A., S. Fritsch, C. Conrad, J. Lamers and S. Dech (2010). *Statistical derivation of fPAR and LAI for irrigated cotton and rice in arid Uzbekistan by combining multi-temporal RapidEye data and ground measurements*. Remote Sensing for Agriculture, Ecosystems, and Hydrology XII, International Society for Optics and Photonics.

Eitel, J. U., L. A. Vierling, M. E. Litvak, D. S. Long, U. Schulthess, A. A. Ager, D. J. Krofcheck and L. Stoscheck (2011). "Broadband, red-edge information from satellites improves early stress detection in a New Mexico conifer woodland." *Remote Sensing of Environment* **115**(12): 3640-3646.

- El Hajj, M., N. Baghdadi, H. Bazzi and M. Zribi (2019). "Penetration analysis of SAR signals in the C and L bands for wheat, maize, and grasslands." Remote Sensing **11**(1): 31.
- El Hajj, M., N. Baghdadi, M. Zribi, G. Belaud, B. Cheviron, D. Courault and F. Charron (2015). Soil moisture retrieval over irrigated grasslands using X-band SAR data combined with optical data acquired at high resolution. 2015 IEEE International Geoscience and Remote Sensing Symposium (IGARSS), IEEE.
- Ellery, W., R. Scholes and M. Scholes (1995). "The distribution of sweetveld and sourveld in South Africa's grassland biome in relation to environmental factors." African Journal of Range & Forage Science **12**(1): 38-45.
- Elmahdy, S. I., T. A. Ali, M. M. Mohamed, F. M. Howari, M. Abouleish and D. Simonet (2020). "Spatiotemporal mapping and monitoring of mangrove forests changes from 1990 to 2019 in the Northern Emirates, UAE using random forest, Kernel logistic regression and Naive Bayes Tree models." Frontiers in Environmental Science **8**: 102.
- Emran, A., S. Roy, M. S. H. Bagmar and C. Mitra (2018). "Assessing topographic controls on vegetation characteristics in Chittagong Hill Tracts (CHT) from remotely sensed data." Remote Sensing Applications: Society and Environment **11**: 198-208.
- Feng, X., B. Fu, X. Yang and Y. Lü (2010). "Remote sensing of ecosystem services: An opportunity for spatially explicit assessment." Chinese Geographical Science **20**(6): 522-535.
- Feng, X., G. Liu, J. Chen, M. Chen, J. Liu, W. Ju, R. Sun and W. Zhou (2007). "Net primary productivity of China's terrestrial ecosystems from a process model driven by remote sensing." Journal of environmental management **85**(3): 563-573.
- Fernández-Manso, A., O. Fernández-Manso and C. Quintano (2016). "Sentinel-2A red-edge spectral indices suitability for discriminating burn severity." International Journal of Applied Earth Observation and Geoinformation **50**: 170-175.
- Ferreira, L. G., G. P. Asner, D. E. Knapp, E. A. Davidson, M. Coe, M. M. Bustamante and E. L. de Oliveira (2011). "Equivalent water thickness in savanna ecosystems: MODIS estimates based on ground and EO-1 Hyperion data." International Journal of Remote Sensing **32**(22): 7423-7440.
- Fey, M. (2010). A short guide to the soils of South Africa, their distribution and correlation with World Reference Base soil groups. Proceedings.
- Fidelis, A. T., M. D. Delgado Cartay, C. C. Blanco, S. C. Muller, V. d. P. Pillar and J. S. Pfadenhauer (2010). "Fire intensity and severity in Brazilian campos grasslands." Interciencia: revista de ciencia y tecnologia de america. Caracas. Vol. 35, n. 10 (Oct. 2010), p. 739-745.
- Finch, H. (2005). "Comparison of the performance of nonparametric and parametric MANOVA test statistics when assumptions are violated." Methodology **1**(1): 27-38.
- Frampton, W. J., J. Dash, G. Watmough and E. J. Milton (2013). "Evaluating the capabilities of Sentinel-2 for quantitative estimation of biophysical variables in vegetation." ISPRS journal of photogrammetry and remote sensing **82**: 83-92.
- Franke, J., V. Keuck and F. Siegert (2012). "Assessment of grassland use intensity by remote sensing to support conservation schemes." Journal for Nature Conservation **20**(3): 125-134.

Friedl, M. A., J. Michaelsen, F. W. Davis, H. Walker and D. S. Schimel (1994). "Estimating Grassland Biomass and Leaf-Area Index Using Ground and Satellite Data." International Journal of Remote Sensing **15**(7): 1401-1420.

Fu, X., C. Tang, X. Zhang, J. Fu and D. Jiang (2014). "An improved indicator of simulated grassland production based on MODIS NDVI and GPP data: A case study in the Sichuan province, China." Ecological indicators **40**: 102-108.

Fynn, R., C. Morris, D. Ward and K. Kirkman (2011). "Trait-environment relations for dominant grasses in South African mesic grassland support a general leaf economic model." Journal of Vegetation Science **22**(3): 528-540.

Gamon, J. and J. Surfus (1999). "Assessing leaf pigment content and activity with a reflectometer." The New Phytologist **143**(1): 105-117.

Gan, R., Y. Zhang, H. Shi, Y. Yang, D. Eamus, L. Cheng, F. H. Chiew and Q. Yu (2018). "Use of satellite leaf area index estimating evapotranspiration and gross assimilation for Australian ecosystems." Ecohydrology **11**(5): e1974.

Gao, A., S. Wu, F. Wang, X. Wu, P. Xu, L. Yu and S. Zhu (2019). "A Newly Developed Unmanned Aerial Vehicle (UAV) Imagery Based Technology for Field Measurement of Water Level." Water **11**(1).

Gao, B.-C. (1996). "NDWI-A normalized difference index for remote sensing of vegetation liquid water from space." Remote Sens. Environ. **52**: 155-162.

Gao, J. (2006). "Quantification of grassland properties: how it can benefit from geoinformatic technologies?" International Journal of Remote Sensing **27**(7): 1351-1365.

Gao, S., Z. Niu, N. Huang and X. Hou (2013). "Estimating the Leaf Area Index, height and biomass of maize using HJ-1 and RADARSAT-2." International Journal of Applied Earth Observation and Geoinformation **24**: 1-8.

Gao, T., B. Xu, X. Yang, Y. Jin, H. Ma, J. Li and H. Yu (2013). "Using MODIS time series data to estimate aboveground biomass and its spatio-temporal variation in Inner Mongolia's grassland between 2001 and 2011." International Journal of Remote Sensing **34**(21): 7796-7810.

Gao, X., S. Dong, S. Li, Y. Xu, S. Liu, H. Zhao, J. Yeomans, Y. Li, H. Shen and S. Wu (2020). "Using the random forest model and validated MODIS with the field spectrometer measurement promote the accuracy of estimating aboveground biomass and coverage of alpine grasslands on the Qinghai-Tibetan Plateau." Ecological Indicators **112**: 106114.

Gao, X., S. Dong, S. Li, Y. Xu, S. Liu, H. Zhao, J. Yeomans, Y. Li, H. Shen, S. Wu and Y. Zhi (2020). "Using the random forest model and validated MODIS with the field spectrometer measurement promote the accuracy of estimating aboveground biomass and coverage of alpine grasslands on the Qinghai-Tibetan Plateau." Ecological Indicators **112**.

Gao, Y., J. P. Walker, M. Allahmoradi, A. Monerris, D. Ryu and T. J. Jackson (2015). "Optical sensing of vegetation water content: A synthesis study." IEEE Journal of Selected Topics in Applied Earth Observations and Remote Sensing **8**(4): 1456-1464.

Gao, Z., Q. Wang, X. Cao and W. Gao (2014). "The responses of vegetation water content (EWT) and assessment of drought monitoring along a coastal region using remote sensing." GIScience & remote sensing **51**(1): 1-16.

Gascon, F., C. Bouzinac, O. Thépaut, M. Jung, B. Francesconi, J. Louis, V. Lonjou, B. Lafrance, S. Massera and A. J. R. S. Gaudel-Vacaresse (2017). "Copernicus Sentinel-2A calibration and products validation status." **9**(6): 584.

Ge, Q., X. Yang, Z. Qiao, H. Liu and J. Liu (2014). "Monitoring Grassland Tourist Season of Inner Mongolia, China Using Remote Sensing Data." Advances in Meteorology **2014**.

Ghalehtemouri, K. J., A. Shamsoddini, M. N. Mousavi, F. B. C. Ros and A. Khedmatzadeh (2022). "Predicting spatial and decadal of land use and land cover change using integrated cellular automata Markov chain model based scenarios (2019-2049) Zarriné-Rūd River Basin in Iran." Environmental Challenges **6**: 100399.

Ghasempour, M., R. Erfanzadeh and P. Török (2022). "Fire effects on soil seed banks under different woody plant species in Mazandaran province, Iran." Ecological Engineering **183**: 106762.

Ghayour, L., A. Neshat, S. Paryani, H. Shahabi, A. Shirzadi, W. Chen, N. Al-Ansari, M. Geertsema, M. Pourmehdi Amiri and M. Gholamnia (2021). "Performance evaluation of sentinel-2 and landsat 8 OLI data for land cover/use classification using a comparison between machine learning algorithms." Remote Sensing **13**(7): 1349.

Gholizadeh, A., J. Mišurec, V. Kopačková, C. Mielke and C. Rogass (2016). "Assessment of red-edge position extraction techniques: A case study for norway spruce forests using hmap and simulated sentinel-2 data." Forests **7**(10): 226.

Ghorbani, A., F. Dadjou, M. Moameri and A. Biswas (2020). "Estimating Aboveground Net Primary Production (ANPP) Using Landsat 8-Based Indices: A Case Study From Hir-Neur Rangelands, Iran." Rangeland Ecology & Management **73**(5): 649-657.

Ghorbani, A. and M. Pakravan (2013). "Land use mapping using visual vs. digital image interpretation of TM and Google earth derived imagery in Shrivani-Darasi watershed (Northwest of Iran)." European Journal of Experimental Biology **3**(1): 576-582.

Ghulam, A., Z.-L. Li, Q. Qin, Q. Tong, J. Wang, A. Kasimu and L. Zhu (2007). "A method for canopy water content estimation for highly vegetated surfaces-shortwave infrared perpendicular water stress index." Science in China Series D: Earth Sciences **50**(9): 1359-1368.

Gidey, E., O. Dikinya, R. Sebego, E. Segosebe and A. Zenebe (2017). "Cellular automata and Markov Chain (CA_Markov) model-based predictions of future land use and land cover scenarios (2015-2033) in Raya, northern Ethiopia." Modeling Earth Systems and Environment **3**: 1245-1262.

Gitelson, A. A. and M. N. Merzlyak (1997). "Remote estimation of chlorophyll content in higher plant leaves." International Journal of Remote Sensing **18**(12): 2691-2697.

Gómez-Giráldez, P. J., C. Aguilar and M. J. Polo (2014). "Natural vegetation covers as indicators of the soil water content in a semiarid mountainous watershed." Ecological indicators **46**: 524-535.

Gorelick, N., M. Hancher, M. Dixon, S. Ilyushchenko, D. Thau and R. Moore (2017). "Google Earth Engine: Planetary-scale geospatial analysis for everyone." Remote Sensing of Environment **202**: 18-27.

Gough, D., S. Oliver and J. Thomas (2017). An introduction to systematic reviews, Sage.

Grant, K. M., D. L. Johnson, D. V. Hildebrand and D. R. Peddle (2014). "Quantifying biomass production on rangeland in southern Alberta using SPOT imagery." Canadian Journal of Remote Sensing **38**(6): 695-708.

Gu, Y. X., B. K. Wylie and N. B. Bliss (2013). "Mapping grassland productivity with 250-m eMODIS NDVI and SSURGO database over the Greater Platte River Basin, USA." Ecological Indicators **24**: 31-36.

Guerini Filho, M., T. M. Kuplich and F. L. D. Quadros (2020). "Estimating natural grassland biomass by vegetation indices using Sentinel 2 remote sensing data." International Journal of Remote Sensing **41**(8): 2861-2876.

Guerini Filho, M., T. M. Kuplich and F. L. F. D. Quadros (2020). "Estimating natural grassland biomass by vegetation indices using Sentinel 2 remote sensing data." International Journal of Remote Sensing **41**(8): 2861-2876.

Gumede, N., O. Mutanga and M. Sibanda (2022). "Mapping leaf area index of the Yellowwood tree species in an Afromontane mistbelt forest of southern Africa using topographic variables." Remote Sensing Applications: Society and Environment **27**: 100778.

Gupta, R., D. Vijayan and T. Prasad (2003). "Comparative analysis of red-edge hyperspectral indices." Advances in Space Research **32**(11): 2217-2222.

Habel, J. C., J. Dengler, M. Janišová, P. Török, C. Wellstein and M. Wiezik (2013). "European grassland ecosystems: threatened hotspots of biodiversity." Biodiversity and Conservation **22**(10): 2131-2138.

Hajj, M. E., N. Baghdadi, G. Belaud, M. Zribi, B. Cheviron, D. Courault, O. Hagolle and F. Charron (2014). "Irrigated grassland monitoring using a time series of TerraSAR-X and COSMO-skyMed X-Band SAR Data." Remote Sensing **6**(10): 10002-10032.

Halmy, M. W. A., P. E. Gessler, J. A. Hicke and B. B. Salem (2015). "Land use/land cover change detection and prediction in the north-western coastal desert of Egypt using Markov-CA." Applied Geography **63**: 101-112.

Hamad, R., H. Balzter and K. Kolo (2018). "Predicting land use/land cover changes using a CA-Markov model under two different scenarios." Sustainability **10**(10): 3421.

Hamada, Y., C. R. Zumpf, J. F. Cacho, D. Lee, C.-H. Lin, A. Boe, E. Heaton, R. Mitchell and M. C. Negri (2021). "Remote Sensing-Based Estimation of Advanced Perennial Grass Biomass Yields for Bioenergy." Land **10**(11): 1221.

Han, J., H.-J. Kang, M. Kim and G. H. Kwon (2020). "Mapping the intellectual structure of research on surgery with mixed reality: Bibliometric network analysis (2000-2019)." Journal of Biomedical Informatics: 103516.

Hansen, M. C. and T. R. Loveland (2012). "A review of large area monitoring of land cover change using Landsat data." Remote Sensing of Environment **122**: 66-74.

Havstad, K. M., D. P. Peters, R. Skaggs, J. Brown, B. Bestelmeyer, E. Fredrickson, J. Herrick and J. Wright (2007). "Ecological services to and from rangelands of the United States." Ecological Economics **64**(2): 261-268.

He, B., M. Xing and X. Bai (2014). "A synergistic methodology for soil moisture estimation in an alpine prairie using radar and optical satellite data." Remote Sensing **6**(11): 10966-10985.

Hicks, R. L., B. C. Parks, J. T. Roberts and M. J. Tierney (2008). Greening aid?: Understanding the environmental impact of development assistance, OUP Oxford.

Holmes, M. (1992). "Monitoring vegetation in the future: radar." Botanical journal of the Linnean Society **108**(2): 93-109.

Horsley, T., O. Dingwall and M. Sampson (2011). "Checking reference lists to find additional studies for systematic reviews." Cochrane Database of Systematic Reviews(8).

Hossen, S., M. Hossain and M. Uddin (2019). "Land cover and land use change detection by using remote sensing and GIS in Himchari National Park (HNP), Cox's Bazar." Bangladesh. J. Sci. Technol. Environ. Inform **7**(02): 544-554.

Huete, A., K. Didan, T. Miura, E. P. Rodriguez, X. Gao and L. G. Ferreira (2002). "Overview of the radiometric and biophysical performance of the MODIS vegetation indices." Remote sensing of environment **83**(1-2): 195-213.

Huete, A. R. (1988). "A soil-adjusted vegetation index (SAVI)." Remote sensing of environment **25**(3): 295-309.

Hughes, C., G. De Winnaar, R. Schulze, M. Mander and G. Jewitt (2018). "Mapping of water-related ecosystem services in the uMngeni catchment using a daily time-step hydrological model for prioritisation of ecological infrastructure investment – Part 2: Outputs." Water SA **44**(4): 590-600.

Hunt Jr, E. R. and B. N. Rock (1989). "Detection of changes in leaf water content using near- and middle-infrared reflectances." Remote sensing of environment **30**(1): 43-54.

Hunter, F. D., E. T. Mitchard, P. Tyrrell and S. Russell (2020). "Inter-seasonal time series imagery enhances classification accuracy of grazing resource and land degradation maps in a savanna ecosystem." Remote Sensing **12**(1): 198.

Imran, H. A., D. Gianelle, D. Rocchini, M. Dalponte, M. P. Martín, K. Sakowska, G. Wohlfahrt and L. Vescovo (2020). "VIS-NIR, Red-Edge and NIR-Shoulder Based Normalized Vegetation Indices Response to Co-Varying Leaf and Canopy Structural Traits in Heterogeneous Grasslands." Remote Sensing **12**(14): 2254.

Inoue, Y., T. Kurosui, H. Maeno, S. Uratsuka, T. Kozu, K. Dabrowska-Zielinska and J. Qi (2002). "Season-long daily measurements of multifrequency (Ka, Ku, X, C, and L) and full-polarization backscatter signatures over paddy rice field and their relationship with biological variables." Remote Sensing of Environment **81**(2): 194-204.

Jalayer, S., A. Sharifi, D. Abbasi-Moghadam, A. Tariq and S. Qin (2022). "Modeling and predicting land use land cover spatiotemporal changes: a case study in chalus watershed, Iran." IEEE Journal of Selected Topics in Applied Earth Observations and Remote Sensing **15**: 5496-5513.

- Jansen, B. V. S., C. A. Kolden, H. E. Greaves and J. U. H. Eitel (2019). "Lidar provides novel insights into the effect of pixel size and grazing intensity on measures of spatial heterogeneity in a native bunchgrass ecosystem." Remote Sensing of Environment **235**.
- Jarchow, C. J., K. Didan, A. Barreto-Muñoz, P. L. Nagler and E. P. Glenn (2018). "Application and comparison of the MODIS-derived enhanced vegetation index to VIIRS, landsat 5 TM and landsat 8 OLI platforms: A case study in the arid colorado river delta, Mexico." Sensors **18**(5): 1546.
- Jensen, R. R., P. J. Hardin and G. Yu (2009). "Artificial neural networks and remote sensing." Geography Compass **3**(2): 630-646.
- Jia, X., B. Xie, M. a. Shao and C. Zhao (2015). "Primary productivity and precipitation-use efficiency in temperate grassland in the Loess Plateau of China." PLoS One **10**(8): e0135490.
- Jiang, L., Z. Qin, W. Xie, R. Wang, B. Xu and Q. Lu (2007). "Estimation of grassland ecosystem services value of China using remote sensing data." Journal of Natural Resources **22**(2): 161-170.
- Jiang, Z., A. R. Huete, Y. Kim and K. Didan (2007). 2-band enhanced vegetation index without a blue band and its application to AVHRR data. Remote Sensing and Modeling of Ecosystems for Sustainability IV, International Society for Optics and Photonics.
- Jin, X., Z. Li, H. Feng, Z. Ren and S. Li (2020). "Deep neural network algorithm for estimating maize biomass based on simulated Sentinel 2A vegetation indices and leaf area index." The Crop Journal **8**(1): 87-97.
- Jin, Y., X. Yang, J. Qiu, J. Li, T. Gao, Q. Wu, F. Zhao, H. Ma, H. Yu and B. Xu (2014). "Remote sensing-based biomass estimation and its spatio-temporal variations in temperate grassland, Northern China." Remote Sensing **6**(2): 1496-1513.
- Jin, Z., G. Azzari, C. You, S. Di Tommaso, S. Aston, M. Burke and D. B. Lobell (2019). "Smallholder maize area and yield mapping at national scales with Google Earth Engine." Remote Sensing of Environment **228**: 115-128.
- John, R., J. Chen, V. Giannico, H. Park, J. Xiao, G. Shirkey, Z. Ouyang, C. Shao, R. Laforteza and J. Qi (2018). "Grassland canopy cover and aboveground biomass in Mongolia and Inner Mongolia: Spatiotemporal estimates and controlling factors." Remote Sensing of Environment **213**: 34-48.
- Jones, M. B. and A. Donnelly (2004). "Carbon sequestration in temperate grassland ecosystems and the influence of management, climate and elevated CO₂." New Phytologist **164**(3): 423-439.
- Jordan, C. F. (1969). "Derivation of leaf-area index from quality of light on the forest floor." Ecology **50**(4): 663-666.
- Kafy, A.-A., R. M. Shuvo, M. N. H. Naim, M. S. Sikdar, R. R. Chowdhury, M. A. Islam, M. H. S. Sarker, M. H. H. Khan and M. A. Kona (2021). "Remote sensing approach to simulate the land use/land cover and seasonal land surface temperature change using machine learning algorithms in a fastest-growing megacity of Bangladesh." Remote Sensing Applications: Society and Environment **21**: 100463.

- Karila, K., R. Alves Oliveira, J. Ek, J. Kaivosoja, N. Koivumäki, P. Korhonen, O. Niemeläinen, L. Nyholm, R. Näsi and I. Pölönen (2022). "Estimating Grass Sward Quality and Quantity Parameters Using Drone Remote Sensing with Deep Neural Networks." Remote Sensing **14**(11): 2692.
- Kattenborn, T., J. Leitloff, F. Schiefer and S. Hinz (2021). "Review on Convolutional Neural Networks (CNN) in vegetation remote sensing." ISPRS Journal of Photogrammetry and Remote Sensing **173**: 24-49.
- Kaufman, Y. J. and D. Tanre (1996). "Strategy for direct and indirect methods for correcting the aerosol effect on remote sensing: from AVHRR to EOS-MODIS." Remote sensing of Environment **55**(1): 65-79.
- Kautz, M. A., C. D. H. Collins, D. P. Guertin, D. C. Goodrich, W. J. van Leeuwen and C. J. Williams (2019). "Hydrologic model parameterization using dynamic Landsat-based vegetative estimates within a semiarid grassland." Journal of Hydrology **575**: 1073-1086.
- Kawamura, K., T. Akiyama, H. o. Yokota, M. Tsutsumi, T. Yasuda, O. Watanabe and S. Wang (2005). "Comparing MODIS vegetation indices with AVHRR NDVI for monitoring the forage quantity and quality in Inner Mongolia grassland, China." Grassland Science **51**(1): 33-40.
- Kawamura, K., T. Akiyama, H. o. Yokota, M. Tsutsumi, T. Yasuda, O. Watanabe and S. J. G. S. Wang (2005). "Comparing MODIS vegetation indices with AVHRR NDVI for monitoring the forage quantity and quality in Inner Mongolia grassland, China." **51**(1): 33-40.
- Khawaldah, H., I. Farhan and N. Alzboun (2020). "Simulation and prediction of land use and land cover change using GIS, remote sensing and CA-Markov model." Global Journal of Environmental Science and Management **6**(2): 215-232.
- Kiala, Z., J. Odindi and O. Mutanga (2017). "Potential of interval partial least square regression in estimating leaf area index." South African Journal of Science **113**(9-10): 1-9.
- Kiala, Z., J. Odindi, O. Mutanga and K. Peerbhay (2016). "Comparison of partial least squares and support vector regressions for predicting leaf area index on a tropical grassland using hyperspectral data." Journal of Applied Remote Sensing **10**(3): 036015.
- Kim, Y., A. R. Huete, T. Miura and Z. Jiang (2010). "Spectral compatibility of vegetation indices across sensors: band decomposition analysis with Hyperion data." Journal of Applied Remote Sensing **4**(1): 043520.
- Klemas, V. and R. Smart (1983). "The influence of soil salinity, growth form, and leaf moisture on-the spectral radiance of." Photogramm. Eng. Remote Sens **49**: 77-83.
- Kobayashi, N., H. Tani, X. Wang and R. Sonobe (2020). "Crop classification using spectral indices derived from Sentinel-2A imagery." Journal of Information and Telecommunication **4**(1): 67-90.
- Koerner, S. E. and S. L. Collins (2014). "Interactive effects of grazing, drought, and fire on grassland plant communities in North America and South Africa." Ecology **95**(1): 98-109.
- KOIKE, T., Y. NAKAMURA, I. KAIHOTSU, G. DAVAA, N. MATSUURA, K. TAMAGAWA and H. FUJII (2004). "Development of an advanced microwave scanning radiometer (AMSR-E) algorithm for soil moisture and vegetation water content." Proceedings of Hydraulic Engineering **48**: 217-222.

- Koley, S. and J. Chockalingam (2022). "Sentinel 1 and Sentinel 2 for cropland mapping with special emphasis on the usability of textural and vegetation indices." Advances in Space Research **69**(4): 1768-1785.
- Kong, B., H. Yu, R. Du and Q. Wang (2019). "Quantitative estimation of biomass of alpine grasslands using hyperspectral remote sensing." Rangeland Ecology & Management **72**(2): 336-346.
- Kozak, J. A., L. R. Ahuja, T. R. Green and L. Ma (2007). "Modelling crop canopy and residue rainfall interception effects on soil hydrological components for semi-arid agriculture." Hydrological Processes: An International Journal **21**(2): 229-241.
- Kumar, L. and O. Mutanga (2018). "Google Earth Engine applications since inception: Usage, trends, and potential." Remote Sensing **10**(10): 1509.
- Kumar, S., S. Arya and K. Jain (2022). "A SWIR-based vegetation index for change detection in land cover using multi-temporal Landsat satellite dataset." International Journal of Information Technology **14**(4): 2035-2048.
- Lakhal, M. I., H. Çevikalp, S. Escalera and F. Ofli (2018). "Recurrent neural networks for remote sensing image classification." IET Computer Vision **12**(7): 1040-1045.
- Lamb, D. W., M. Steyn-Ross, P. Schaare, M. M. Hanna, W. Silvester and A. Steyn-Ross (2002). "Estimating leaf nitrogen concentration in ryegrass (*Lolium* spp.) pasture using the chlorophyll red-edge: theoretical modelling and experimental observations." International Journal of Remote Sensing **23**(18): 3619-3648.
- Langley, S. K., H. M. Cheshire and K. S. Humes (2001). "A comparison of single date and multitemporal satellite image classifications in a semi-arid grassland." Journal of Arid Environments **49**(2): 401-411.
- Latham, J., R. Cumani, I. Rosati and M. Bloise (2014). "Global land cover share (GLC-SHARE) database beta-release version 1.0-2014." FAO: Rome, Italy.
- Lavorel, S., K. Grigulis, P. Lamarque, M. P. Colace, D. Garden, J. Girel, G. Pellet and R. Douzet (2011). "Using plant functional traits to understand the landscape distribution of multiple ecosystem services." Journal of Ecology **99**(1): 135-147.
- Law, B. E., A. Cescatti and D. D. Baldocchi (2001). "Leaf area distribution and radiative transfer in open-canopy forests: implications for mass and energy exchange." Tree Physiology **21**(12-13): 777-787.
- Lawley, V., M. Lewis, K. Clarke and B. Ostendorf (2016). "Site-based and remote sensing methods for monitoring indicators of vegetation condition: An Australian review." Ecological Indicators **60**: 1273-1283.
- Leemans, R. and R. De Groot (2003). "Millennium Ecosystem Assessment: Ecosystems and human well-being: a framework for assessment."
- Lehmann, C. E., S. A. Archibald, W. A. Hoffmann and W. J. Bond (2011). "Deciphering the distribution of the savanna biome." New Phytologist **191**(1): 197-209.

Lehnert, L. W., H. Meyer, N. Meyer, C. Reudenbach and J. Bendix (2014). "A hyperspectral indicator system for rangeland degradation on the Tibetan Plateau: A case study towards spaceborne monitoring." Ecological Indicators **39**: 54-64.

Lehnert, L. W., H. Meyer, Y. Wang, G. Miehe, B. Thies, C. Reudenbach and J. Bendix (2015). "Retrieval of grassland plant coverage on the Tibetan Plateau based on a multi-scale, multi-sensor and multi-method approach." Remote sensing of Environment **164**: 197-207.

Lemaire, G., J. Hodgson and A. Chabbi (2011). Grassland productivity and ecosystem services, Cabi.

Li, C., L. Zhou and W. Xu (2021). "Estimating aboveground biomass using Sentinel-2 MSI data and ensemble algorithms for grassland in the Shengjin Lake Wetland, China." Remote Sensing **13**(8): 1595.

Li, F., X. Wang, J. Zhao, X. Zhang and Q. Zhao (2013). "A method for estimating the gross primary production of alpine meadows using MODIS and climate data in China." International journal of remote sensing **34**(23): 8280-8300.

Li, J., Y. Pei, S. Zhao, R. Xiao, X. Sang and C. Zhang (2020). "A review of remote sensing for environmental monitoring in China." Remote Sensing **12**(7): 1130.

Li, T., L. Cui, Z. Xu, R. Hu, P. K. Joshi, X. Song, L. Tang, A. Xia, Y. Wang and D. Guo (2021). "Quantitative analysis of the research trends and areas in grassland remote sensing: A scientometrics analysis of web of science from 1980 to 2020." Remote Sensing **13**(7): 1279.

Li, W., R. Dong, H. Fu, J. Wang, L. Yu and P. Gong (2020). "Integrating Google Earth imagery with Landsat data to improve 30-m resolution land cover mapping." Remote Sensing of Environment **237**: 111563.

Li, Z.-w., X.-p. XIN, T. Huan, Y. Fan, B.-r. CHEN and B.-h. ZHANG (2017). "Estimating grassland LAI using the Random Forests approach and Landsat imagery in the meadow steppe of Hulunber, China." Journal of Integrative Agriculture **16**(2): 286-297.

Li, Z.-w., X.-p. Xin, H. Tang, F. Yang, B.-r. Chen and B.-h. Zhang (2017). "Estimating grassland LAI using the Random Forests approach and Landsat imagery in the meadow steppe of Hulunber, China." Journal of Integrative Agriculture **16**(2): 286-297.

Li, Z., T. Huffman, B. McConkey and L. Townley-Smith (2013). "Monitoring and modeling spatial and temporal patterns of grassland dynamics using time-series MODIS NDVI with climate and stocking data." Remote Sensing of Environment **138**: 232-244.

Li, Z., J. Wang, H. Tang, C. Huang, F. Yang, B. Chen, X. Wang, X. Xin and Y. Ge (2016). "Predicting grassland leaf area index in the Meadow Steppes of Northern China: A comparative study of regression approaches and hybrid geostatistical methods." Remote Sensing **8**(8): 632.

Li, Z., G. Yu, X. Xiao, Y. Li, X. Zhao, C. Ren, L. Zhang and Y. Fu (2007). "Modeling gross primary production of alpine ecosystems in the Tibetan Plateau using MODIS images and climate data." Remote Sensing of Environment **107**(3): 510-519.

Lin, S., J. Li, Q. Liu, L. Li, J. Zhao and W. Yu (2019). "Evaluating the effectiveness of using vegetation indices based on red-edge reflectance from Sentinel-2 to estimate gross primary productivity." Remote Sensing **11**(11): 1303.

- Lipiec, J., C. Doussan, A. Nosalewicz and K. Kondracka (2013). "Effect of drought and heat stresses on plant growth and yield: a review." International Agrophysics **27**(4): 463-477.
- Liping, C., S. Yujun and S. Saeed (2018). "Monitoring and predicting land use and land cover changes using remote sensing and GIS techniques – A case study of a hilly area, Jiangle, China." PloS one **13**(7): e0200493.
- Little, I. T., P. A. Hockey and R. Jansen (2015). "Impacts of fire and grazing management on South Africa's moist highland grasslands: A case study of the Steenkampsberg Plateau, Mpumalanga, South Africa." Bothalia-African Biodiversity & Conservation **45**(1): 1-15.
- Liu, H. Q. and A. Huete (1995). "A feedback based modification of the NDVI to minimize canopy background and atmospheric noise." IEEE transactions on geoscience and remote sensing **33**(2): 457-465.
- Liu, J. H., C. Atzberger, X. Huang, K. J. Shen, Y. M. Liu and L. Wang (2020). "Modeling grass yields in Qinghai Province, China, based on MODIS NDVI data-an empirical comparison." Frontiers of Earth Science **14**(2): 413-429.
- Liu, M., T. Wang, A. K. Skidmore and X. Liu (2018). "Heavy metal-induced stress in rice crops detected using multi-temporal Sentinel-2 satellite images." Science of the total environment **637**: 18-29.
- Liu, S., F. Cheng, S. Dong, H. Zhao, X. Hou and X. Wu (2017). "Spatiotemporal dynamics of grassland aboveground biomass on the Qinghai-Tibet Plateau based on validated MODIS NDVI." Scientific reports **7**(1): 1-10.
- Liu, X., F. Han, K. H. Ghazali, I. I. Mohamed and Y. Zhao (2019). A review of convolutional neural networks in remote sensing image. Proceedings of the 2019 8th International Conference on Software and Computer Applications.
- Liu, X., X. Liang, X. Li, X. Xu, J. Ou, Y. Chen, S. Li, S. Wang and F. Pei (2017). "A future land use simulation model (FLUS) for simulating multiple land use scenarios by coupling human and natural effects." Landscape and Urban Planning **168**: 94-116.
- Liu, Z.-Y., J.-F. Huang, X.-H. Wu and Y.-P. Dong (2007). "Comparison of Vegetation Indices and Red-edge Parameters for Estimating Grassland Cover from Canopy Reflectance Data." Journal of Integrative Plant Biology **49**(3): 299-306.
- Loc, H. H., E. Park, T. N. Thu, N. T. H. Diep and N. T. Can (2021). "An enhanced analytical framework of participatory GIS for ecosystem services assessment applied to a Ramsar wetland site in the Vietnam Mekong Delta." Ecosystem Services **48**: 101245.
- Loris, V. and G. Damiano (2006). "Mapping the green herbage ratio of grasslands using both aerial and satellite-derived spectral reflectance." Agriculture, ecosystems & environment **115**(1-4): 141-149.
- Loveland, T. R. and J. L. Dwyer (2012). "Landsat: Building a strong future." Remote Sensing of Environment **122**: 22-29.
- Lu, B. and Y. He (2019). "Evaluating empirical regression, machine learning, and radiative transfer modelling for estimating vegetation chlorophyll content using bi-seasonal hyperspectral images." Remote Sensing **11**(17): 1979.

- Lu, B. and Y. He (2019). "Leaf area index estimation in a heterogeneous grassland using optical, SAR, and DEM data." Canadian Journal of Remote Sensing **45**(5): 618-633.
- Lu, X., K. C. Kelsey, Y. Yan, J. Sun, X. Wang, G. Cheng and J. C. Neff (2017). "Effects of grazing on ecosystem structure and function of alpine grasslands in Qinghai-Tibetan Plateau: A synthesis." Ecosphere **8**(1): e01656.
- Lukyanchuk, K., I. Kovalchuk and O. Pidkova (2020). Application of a remote sensing in monitoring of erosion processes. Geoinformatics: Theoretical and Applied Aspects 2020, European Association of Geoscientists & Engineers.
- Ma, J., Y. Li, Y. Chen, K. Du, F. Zheng, L. Zhang and Z. Sun (2019). "Estimating above ground biomass of winter wheat at early growth stages using digital images and deep convolutional neural network." European Journal of Agronomy **103**: 117-129.
- MA, M. E. A. (2005). "Millennium ecosystem assessment. Ecosystems and human well-being: synthesis." World Resources Institute, Washington, DC.
- Magandana, T. P., A. Hassen and E. H. Tesfamariam (2020). "Seasonal herbaceous structure and biomass production response to rainfall reduction and resting period in the semi-arid grassland area of South Africa." Agronomy **10**(11): 1807.
- Main-Knorn, M., B. Pflug, J. Louis, V. Debaecker, U. Müller-Wilm and F. Gascon (2017). Sen2Cor for sentinel-2. Image and Signal Processing for Remote Sensing XXIII, International Society for Optics and Photonics.
- Mas, J. F. and J. J. Flores (2008). "The application of artificial neural networks to the analysis of remotely sensed data." International Journal of Remote Sensing **29**(3): 617-663.
- Masemola, C., M. A. Cho and A. Ramoelo (2020). "Sentinel-2 time series based optimal features and time window for mapping invasive Australian native Acacia species in KwaZulu-Natal, South Africa." International Journal of Applied Earth Observation and Geoinformation **93**: 102207.
- Masenyama, A., O. Mutanga, T. Dube, T. Bangira, M. Sibanda and T. Mabhaudhi (2022). "A systematic review on the use of remote sensing technologies in quantifying grasslands ecosystem services." GIScience & Remote Sensing **59**(1): 1000-1025.
- Mathanraj, S., N. Rusli and G. Ling (2021). Applicability of the CA-Markov Model in Land-use/Land cover Change Prediction for Urban Sprawling in Batticaloa Municipal Council, Sri Lanka. IOP Conference Series: Earth and Environmental Science, IOP Publishing.
- Matongera, T. N., O. Mutanga, T. Dube and M. Sibanda (2017). "Detection and mapping the spatial distribution of bracken fern weeds using the Landsat 8 OLI new generation sensor." International journal of applied earth observation and geoinformation **57**: 93-103.
- Matongera, T. N., O. Mutanga, M. Sibanda and J. Odindi (2021). "Estimating and Monitoring Land Surface Phenology in Rangelands: A Review of Progress and Challenges." Remote Sensing **13**(11): 2060.
- McCallum, I., W. Wagner, C. Schmulius, A. Shvidenko, M. Obersteiner, S. Fritz and S. Nilsson (2009). "Satellite-based terrestrial production efficiency modeling." Carbon balance and management **4**(1): 1-14.

- McGranahan, D. A. and K. P. Kirkman (2013). "Multifunctional rangeland in Southern Africa: Managing for production, conservation, and resilience with fire and grazing." Land **2**(2): 176-193.
- McNairn, H. and B. Brisco (2004). "The application of C-band polarimetric SAR for agriculture: A review." Canadian Journal of Remote Sensing **30**(3): 525-542.
- Meng, B., J. Ge, T. Liang, S. Yang, J. Gao, Q. Feng, X. Cui, X. Huang and H. Xie (2017). "Evaluation of remote sensing inversion error for the above-ground biomass of alpine meadow grassland based on multi-source satellite data." Remote Sensing **9**(4): 372.
- Meshesha, D. T., M. M. Ahmed, D. Y. Abdi and N. Haregeweyn (2020). "Prediction of grass biomass from satellite imagery in Somali regional state, eastern Ethiopia." Heliyon **6**(10): e05272.
- Mncube, N. L. (2022). Investigating the contribution of social cash transfers to the food security situation of agricultural-based rural households of Nhlazuka, Richmond Municipality, South Africa.
- Mngadi, M., J. Odindi, K. Peerbhay and O. Mutanga (2021). "Examining the effectiveness of Sentinel-1 and 2 imagery for commercial forest species mapping." Geocarto International **36**(1): 1-12.
- Modernel, P., W. A. Rossing, M. Corbeels, S. Dogliotti, V. Picasso and P. Tittonell (2016). "Land use change and ecosystem service provision in Pampas and Campos grasslands of southern South America." Environmental Research Letters **11**(11): 113002.
- Mohamed, M. A., J. Anders and C. Schneider (2020). "Monitoring of changes in land use/land cover in Syria from 2010 to 2018 using multitemporal Landsat imagery and GIS." Land **9**(7): 226.
- Moher, D., A. Liberati, J. Tetzlaff, D. G. Altman and P. Group (2009). "Preferred reporting items for systematic reviews and meta-analyses: the PRISMA statement." PLoS medicine **6**(7): e1000097.
- Mondal, M. S., N. Sharma, P. K. Garg and M. Kappas (2016). "Statistical independence test and validation of CA Markov land use land cover (LULC) prediction results." The Egyptian Journal of Remote Sensing and Space Science **19**(2): 259-272.
- Monteith, J. (1972). "Solar radiation and productivity in tropical ecosystems." Journal of applied ecology **9**(3): 747-766.
- Moore, I. D., P. E. Gessler, G. Nielsen and G. J. S. s. o. a. j. Peterson (1993). "Soil attribute prediction using terrain analysis." **57**(2): 443-452.
- Mouillot, F., S. Rambal and R. Joffre (2002). "Simulating climate change impacts on fire frequency and vegetation dynamics in a Mediterranean-type ecosystem." Global Change Biology **8**(5): 423-437.
- Mountrakis, G., J. Im and C. Ogole (2011). "Support vector machines in remote sensing: A review." ISPRS Journal of Photogrammetry and Remote Sensing **66**(3): 247-259.
- Mucina, L. and M. C. Rutherford (2006). The vegetation of South Africa, Lesotho and Swaziland, South African National Biodiversity Institute.

- Mukangango, M., J. Nduwamungu, F. X. Naramabuye, G. Nyberg and A. S. Dahlin (2020). "Supplementing grass-based cattle feeds with legume leaves and its effects on manure quality and value as a soil improver for an Anthropic Ferralsol in Rwanda." Experimental Agriculture **56**(4): 483-494.
- Municipality, M. "Vulindlela Local Area Plan: Spatial Framework. 2016." Pietermaritzburg, KwaZulu-Natal.
- Munthali, M., S. Mustak, A. Adeola, J. Botai, S. Singh and N. Davis (2020). "Modelling land use and land cover dynamics of Dedza district of Malawi using hybrid Cellular Automata and Markov model." Remote Sensing Applications: Society and Environment **17**: 100276.
- Munyati, C., H. Balzter and E. Economon (2020). "Correlating Sentinel-2 MSI-derived vegetation indices with in-situ reflectance and tissue macronutrients in savannah grass." International Journal of Remote Sensing **41**(10): 3820-3844.
- Muraoka, H. and H. Koizumi (2009). "Satellite Ecology (SATECO) – linking ecology, remote sensing and micrometeorology, from plot to regional scale, for the study of ecosystem structure and function." Journal of plant research **122**(1): 3-20.
- Mussa, M., H. Teka and Y. Mesfin (2017). "Land use/cover change analysis and local community perception towards land cover change in the lowland of Bale rangelands, Southeast Ethiopia." International Journal of Biodiversity and Conservation **9**(12): 363-372.
- Mutanga, O., E. Adam and M. A. Cho (2012). "High density biomass estimation for wetland vegetation using WorldView-2 imagery and random forest regression algorithm." International Journal of Applied Earth Observation and Geoinformation **18**: 399-406.
- Mutanga, O., T. Dube and F. Ahmed (2016). "Progress in remote sensing: vegetation monitoring in South Africa." South African Geographical Journal **98**(3): 461-471.
- Mutanga, O. and A. Skidmore (2004). "Integrating imaging spectroscopy and neural networks to map grass quality in the Kruger National Park, South Africa." Remote sensing of environment **90**(1): 104-115.
- Mutanga, O. and A. K. Skidmore (2004). "Narrow band vegetation indices overcome the saturation problem in biomass estimation." International Journal of Remote Sensing **25**(19): 3999-4014.
- Mutanga, O. and A. K. Skidmore (2007). "Red edge shift and biochemical content in grass canopies." ISPRS Journal of Photogrammetry and Remote Sensing **62**(1): 34-42.
- Mutanga, O., A. K. Skidmore, L. Kumar and J. Ferwerda (2005). "Estimating tropical pasture quality at canopy level using band depth analysis with continuum removal in the visible domain." International Journal of Remote Sensing **26**(6): 1093-1108.
- Myrriotis, V., P. Harris, A. Revill, H. Sint and M. Williams (2021). "Inferring management and predicting sub-field scale C dynamics in UK grasslands using biogeochemical modelling and satellite-derived leaf area data." Agricultural and Forest Meteorology **307**: 108466.
- Naidoo, L., H. van Deventer, A. Ramoelo, R. Mathieu, B. Nondlazi and R. Gangat (2019). "Estimating above ground biomass as an indicator of carbon storage in vegetated wetlands of the grassland biome of South Africa." International Journal of Applied Earth Observation and Geoinformation **78**: 118-129.

Narayanan, B., M. Saadeldin, P. Albert, K. McGuinness and B. Mac Namee (2021). "Extracting pasture phenotype and biomass percentages using weakly supervised multi-target deep learning on a small dataset." arXiv preprint arXiv:2101.03198.

Ndlovu, H. S., J. Odindi, M. Sibanda, O. Mutanga, A. Clulow, V. G. Chimonyo and T. Mabhaudhi (2021). "A comparative estimation of maize leaf water content using machine learning techniques and unmanned aerial vehicle (UAV)-based proximal and remotely sensed data." Remote Sensing **13**(20): 4091.

Ndlovu, H. S., J. Odindi, M. Sibanda, O. Mutanga, A. Clulow, V. G. P. Chimonyo and T. Mabhaudhi (2021). "A Comparative Estimation of Maize Leaf Water Content Using Machine Learning Techniques and Unmanned Aerial Vehicle (UAV)-Based Proximal and Remotely Sensed Data." Remote Sensing **13**(20): 4091.

Ndlovu, M. S. and M. Demlie (2020). "Assessment of meteorological drought and wet conditions using two drought indices across KwaZulu-Natal Province, South Africa." Atmosphere **11**(6): 623.

Neinavaz, E., A. K. Skidmore, R. Darvishzadeh and T. A. Groen (2017). "Retrieving vegetation canopy water content from hyperspectral thermal measurements." Agricultural and forest meteorology **247**: 365-375.

Nestola, E., C. Calfapietra, C. Emmerton, C. Wong, D. Thayer and J. Gamon (2016). "Monitoring Grassland Seasonal Carbon Dynamics, by Integrating MODIS NDVI, Proximal Optical Sampling, and Eddy Covariance Measurements." Remote Sensing **8**(3).

Niu, Z., H. He, S. Peng, X. Ren, L. Zhang, F. Gu, G. Zhu, C. Peng, P. Li and J. Wang (2021). "A Process-Based Model Integrating Remote Sensing Data for Evaluating Ecosystem Services." Journal of Advances in Modeling Earth Systems **13**(6): e2020MS002451.

Nouvellon, Y., M. S. Moran, D. L. Seen, R. Bryant, S. Rambal, W. Ni, A. Bégué, A. Chehbouni, W. E. Emmerich and P. Heilman (2001). "Coupling a grassland ecosystem model with Landsat imagery for a 10-year simulation of carbon and water budgets." Remote Sensing of Environment **78**(1-2): 131-149.

O'Mara, F. P. (2012). "The role of grasslands in food security and climate change." Annals of botany **110**(6): 1263-1270.

O'Connor, T. G., G. Martindale, C. D. Morris, A. Short, T. Witkowski and R. Scott-Shaw (2011). "Influence of grazing management on plant diversity of highland sourveld grassland, KwaZulu-Natal, South Africa." Rangeland Ecology & Management **64**(2): 196-207.

O'Connor, T. G. and B. W. van Wilgen (2020). "The impact of invasive alien plants on rangelands in South Africa." Biological Invasions in South Africa **14**: 459-487.

Ochoa-Sánchez, A., P. Crespo and R. Célleri (2018). "Quantification of rainfall interception in the high Andean tussock grasslands." Ecohydrology **11**(3): e1946.

Odebiri, O., O. Mutanga, J. Odindi, K. Peerbhay and S. Dovey (2020). "Predicting soil organic carbon stocks under commercial forest plantations in KwaZulu-Natal province, South Africa using remotely sensed data." GIScience & Remote Sensing **57**(4): 450-463.

Odebiri, O., O. Mutanga, J. Odindi, K. Peerbhay, S. Dovey and R. Ismail (2020). "Estimating soil organic carbon stocks under commercial forestry using topo-climate variables in KwaZulu-Natal, South Africa." South African Journal of Science **116**(3-4): 1-8.

Osakabe, Y., K. Osakabe, K. Shinozaki and L.-S. P. Tran (2014). "Response of plants to water stress." Frontiers in plant science **5**: 86.

Ose, K., T. Corpetti and L. Demagistri (2016). Multispectral satellite image processing. Optical remote sensing of land surface, Elsevier: 57-124.

Oshiro, T. M., P. S. Perez and J. A. Baranauskas (2012). How many trees in a random forest? International workshop on machine learning and data mining in pattern recognition, Springer.

Oumar, Z. and O. Mutanga (2010). "Predicting plant water content in Eucalyptus grandis forest stands in KwaZulu-Natal, South Africa using field spectra resampled to the Sumbandila Satellite Sensor." International Journal of Applied Earth Observation and Geoinformation **12**(3): 158-164.

Page, M. J., J. E. McKenzie, P. M. Bossuyt, I. Boutron, T. C. Hoffmann, C. D. Mulrow, L. Shamseer, J. M. Tetzlaff, E. A. Akl and S. E. Brennan (2021). "The PRISMA 2020 statement: an updated guideline for reporting systematic reviews." Bmj **372**.

Pairman, D., S. McNeill, S. Belliss, D. Dalley and R. Dynes (2008). Pasture Monitoring from Polarimetric TerraSAR-X Data. IGARSS 2008-2008 IEEE International Geoscience and Remote Sensing Symposium.

Palmer, A., A. Short and I. A. Yunusa (2010). "Biomass production and water use efficiency of grassland in KwaZulu-Natal, South Africa." African Journal of Range & Forage Science **27**(3): 163-169.

Palmer, A. R. and J. E. Bennett (2013). "Degradation of communal rangelands in South Africa: towards an improved understanding to inform policy." African Journal of Range & Forage Science **30**(1-2): 57-63.

Palmer, A. R., I. Samuels, C. Cupido, A. Finca, W. F. Kangombe, I. A. M. Yunusa, S. Vetter and I. Mapaure (2016). "Aboveground biomass production of a semi-arid southern African savanna: towards a new model." African Journal of Range & Forage Science **33**(1): 43-51.

Pan, C. and Z. Shangguan (2006). "Runoff hydraulic characteristics and sediment generation in sloped grassplots under simulated rainfall conditions." Journal of Hydrology **331**(1-2): 178-185.

Pan, H., Z. Chen, J. Ren, H. Li and S. Wu (2018). "Modeling winter wheat leaf area index and canopy water content with three different approaches using Sentinel-2 multispectral instrument data." IEEE Journal of Selected Topics in Applied Earth Observations and Remote Sensing **12**(2): 482-492.

Pang, H., A. Zhang, X. Kang, N. He and G. Dong (2020). "Estimation of the Grassland Aboveground Biomass of the Inner Mongolia Plateau Using the Simulated Spectra of Sentinel-2 Images." Remote Sensing **12**(24): 4155.

Pang, H., A. Zhang, X. Kang, N. He and G. Dong (2020). "Estimation of the Grassland Aboveground Biomass of the Inner Mongolia Plateau Using the Simulated Spectra of Sentinel-2 Images." Remote Sensing **12**(24).

- Parihar, S. M., S. Sarkar, A. Dutta, S. Sharma and T. Dutta (2013). "Characterizing wetland dynamics: a post-classification change detection analysis of the East Kolkata Wetlands using open source satellite data." Geocarto International **28**(3): 273-287.
- Paruelo, J. M., W. K. Lauenroth, I. C. Burke and O. E. Sala (1999). "Grassland precipitation-use efficiency varies across a resource gradient." Ecosystems **2**(1): 64-68.
- Parveen, K. D., K. K. Ravinder and R. B. Daizy (2011). "Impact of Lantana camara L. invasion on riparian vegetation of Nayar region in Garhwal Himalayas (Uttarakhand, India)." Journal of Ecology and the Natural Environment **3**(1): 11-22.
- Pearson, R. L., C. J. Tucker and L. D. Miller (1976). "Spectral Mapping of Shortgrass Prairie Biomass." Photogrammetric Engineering and Remote Sensing **42**(3): 317-&.
- Peng, W. T., W. Q. Liu, W. B. Cai, X. Wang, Z. Huang and C. Z. Wu (2019). "Evaluation of ecosystem cultural services of urban protected areas based on public participation GIS (PPGIS): A case study of Gongqing Forest Park in Shanghai, China." Ying Yong Sheng tai xue bao= The Journal of Applied Ecology **30**(2): 439-448.
- Phan, T. N., V. Kuch and L. W. Lehnert (2020). "Land Cover Classification using Google Earth Engine and Random Forest Classifier – The Role of Image Composition." Remote Sensing **12**(15): 2411.
- Phiri, D. and J. Morgenroth (2017). "Developments in Landsat land cover classification methods: A review." Remote Sensing **9**(9): 967.
- Piao, S. L., A. Mohammat, J. Y. Fang, Q. Cai and J. M. Feng (2006). "NDVI-based increase in growth of temperate grasslands and its responses to climate changes in China." Global Environmental Change-Human and Policy Dimensions **16**(4): 340-348.
- Pires de Lima, R. and K. Marfurt (2020). "Convolutional neural network for remote-sensing scene classification: Transfer learning analysis." Remote Sensing **12**(1): 86.
- Podwojewski, P., J. L. Janeau, S. Grellier, C. Valentin, S. Lorentz and V. Chaplot (2011). "Influence of grass soil cover on water runoff and soil detachment under rainfall simulation in a sub-humid South African degraded rangeland." Earth Surface Processes and Landforms **36**(7): 911-922.
- Polley, H. W., D. D. Briske, J. A. Morgan, K. Wolter, D. W. Bailey and J. R. Brown (2013). "Climate change and North American rangelands: trends, projections, and implications." Rangeland Ecology & Management **66**(5): 493-511.
- Price, K. P., S. L. Egbert, M. D. Nellis, R.-Y. Lee and R. Boyce (1997). "Mapping land cover in a high plains agro-ecosystem using a multirate Landsat thematic mapper modeling approach." Transactions of the Kansas Academy of Science (1903): 21-33.
- Pritchard, A. (1969). "Statistical bibliography or bibliometrics." Journal of documentation **25**(4): 348-349.
- Prochnow, A., M. Heiermann, M. Plöchl, T. Amon and P. Hobbs (2009). "Bioenergy from permanent grassland – A review: 2. Combustion." Bioresource technology **100**(21): 4945-4954.

- Prochnow, A., M. Heiermann, M. Plöchl, B. Linke, C. Idler, T. Amon and P. Hobbs (2009). "Bioenergy from permanent grassland – A review: 1. Biogas." Bioresource technology **100**(21): 4931-4944.
- Propastin, P. A., M. W. Kappas, S. M. Herrmann and C. J. Tucker (2012). "Modified light use efficiency model for assessment of carbon sequestration in grasslands of Kazakhstan: combining ground biomass data and remote-sensing." International Journal of Remote Sensing **33**(5): 1465-1487.
- Psomas, A., M. Kneubühler, S. Huber, K. Itten and N. E. Zimmermann (2011). "Hyperspectral remote sensing for estimating aboveground biomass and for exploring species richness patterns of grassland habitats." International Journal of Remote Sensing **32**(24): 9007-9031.
- Pu, D., J. Sun, Q. Ding, Q. Zheng, T. Li and X. Niu (2020). "Mapping urban areas using dense time series of landsat images and google earth engine." The International Archives of Photogrammetry, Remote Sensing and Spatial Information Sciences **42**: 403-409.
- Pu, R., P. Gong, G. S. Biging and M. R. Larrieu (2003). "Extraction of red edge optical parameters from Hyperion data for estimation of forest leaf area index." IEEE Transactions on Geoscience and Remote Sensing **41**(4): 916-921.
- Punalekar, S. M., A. Verhoef, T. L. Quaife, D. Humphries, L. Bermingham and C. K. Reynolds (2018). "Application of Sentinel-2A data for pasture biomass monitoring using a physically based radiative transfer model." Remote Sensing of Environment **218**: 207-220.
- Qi, A., P. J. Murray and G. M. Richter (2017). "Modelling productivity and resource use efficiency for grassland ecosystems in the UK." European Journal of Agronomy **89**: 148-158.
- Quan, X. W., B. B. He, M. Yebra, C. M. Yin, Z. M. Liao, X. T. Zhang and X. Li (2017). "A radiative transfer model-based method for the estimation of grassland aboveground biomass." International Journal of Applied Earth Observation and Geoinformation **54**: 159-168.
- Ramoelo, A., M. Cho, R. Mathieu and A. K. Skidmore (2015). "Potential of Sentinel-2 spectral configuration to assess rangeland quality." Journal of Applied Remote Sensing **9**(1): 094096-094096.
- Ramoelo, A. and M. A. Cho (2014). "Dry season biomass estimation as an indicator of rangeland quantity using multi-scale remote sensing data."
- Ramoelo, A., M. A. Cho, R. Mathieu, S. Madonsela, R. Van De Kerchove, Z. Kaszta and E. Wolff (2015). "Monitoring grass nutrients and biomass as indicators of rangeland quality and quantity using random forest modelling and WorldView-2 data." International journal of applied earth observation and geoinformation **43**: 43-54.
- Ranjan, R., A. K. Chandel, L. R. Khot, H. Y. Bahlol, J. Zhou, R. A. Boydston and P. N. Miklas (2019). "Irrigated pinto bean crop stress and yield assessment using ground based low altitude remote sensing technology." Information Processing in Agriculture **6**(4): 502-514.
- Rasch, S., T. Heckelei and R. J. Oomen (2016). "Reorganizing resource use in a communal livestock production socio-ecological system in South Africa." Land use policy **52**: 221-231.
- Reichstein, M., P. Ciais, D. Papale, R. Valentini, S. Running, N. Viogy, W. Cramer, A. Granier, J. Ogee and V. Allard (2007). "Reduction of ecosystem productivity and respiration during the

European summer 2003 climate anomaly: a joint flux tower, remote sensing and modelling analysis." Global Change Biology **13**(3): 634-651.

Reinermann, S., S. Asam and C. Kuenzer (2020). "Remote Sensing of Grassland Production and Management-A Review." Remote Sensing **12**(12): 32.

Reinhart, K. O., S. R. Dangi and L. T. Vermeire (2016). "The effect of fire intensity, nutrients, soil microbes, and spatial distance on grassland productivity." Plant and Soil **409**(1): 203-216.

Richardson, F., M. T. Hoffman and L. Gillson (2010). "Modelling the complex dynamics of vegetation, livestock and rainfall in a semi-arid rangeland in South Africa." African Journal of Range & Forage Science **27**(3): 125-142.

Richter, K., T. B. Hank, W. Mauser and C. Atzberger (2012). "Derivation of biophysical variables from Earth observation data: validation and statistical measures." Journal of Applied Remote Sensing **6**(1): 063557.

Roberto, C., B. Lorenzo, M. Michele, R. Micol and P. Cinzia (2016). "10 Optical Remote Sensing of Vegetation Water Content." Hyperspectral remote sensing of vegetation: 227.

Rodriguez-Galiano, V., M. Chica-Olmo, F. Abarca-Hernandez, P. M. Atkinson and C. Jeganathan (2012). "Random Forest classification of Mediterranean land cover using multi-seasonal imagery and multi-seasonal texture." Remote Sensing of Environment **121**: 93-107.

Rodriguez-Galiano, V., M. Sanchez-Castillo, M. Chica-Olmo and M. Chica-Rivas (2015). "Machine learning predictive models for mineral prospectivity: An evaluation of neural networks, random forest, regression trees and support vector machines." Ore Geology Reviews **71**: 804-818.

Rodriguez-Galiano, V. F., B. Ghimire, J. Rogan, M. Chica-Olmo and J. P. Rigol-Sanchez (2012). "An assessment of the effectiveness of a random forest classifier for land-cover classification." ISPRS journal of photogrammetry and remote sensing **67**: 93-104.

Roffe, S., J. Fitchett and C. Curtis (2019). "Classifying and mapping rainfall seasonality in South Africa: a review." South African Geographical Journal= Suid-Afrikaanse Geografiese Tydskrif **101**(2): 158-174.

Roffe, S. J., J. M. Fitchett and C. J. Curtis (2020). "Determining the utility of a percentile-based wet-season start- and end-date metrics across South Africa." Theoretical & Applied Climatology **140**.

Rouault, M. and Y. Richard (2003). "Intensity and spatial extension of drought in South Africa at different time scales." Water Sa **29**(4): 489-500.

Roujean, J.-L. and F.-M. Breon (1995). "Estimating PAR absorbed by vegetation from bidirectional reflectance measurements." Remote sensing of Environment **51**(3): 375-384.

Rouse, J., R. Haas, J. Schell and D. Deering (1974). "Monitoring Vegetation Systems in the Great Plains with ERTS, NASA Special Publication."

Roy, D. P., V. Kovalevskiy, H. K. Zhang, E. F. Vermote, L. Yan, S. S. Kumar and A. Egorov (2016). "Characterization of Landsat-7 to Landsat-8 reflective wavelength and normalized difference vegetation index continuity." Remote Sensing of Environment **185**: 57-70.

Roy, P. (1989). Spectral reflectance characteristics of vegetation and their use in estimating productive potential. Proceedings/Indian Academy of Sciences, Springer.

Royimani, L., O. Mutanga, J. Odindi, M. Sibanda and S. Chamane (2022). "Determining the onset of autumn grass senescence in subtropical sour-veld grasslands using remote sensing proxies and the breakpoint approach." Ecological Informatics **69**: 101651.

Rubio, M., D. Riaño, Y. Cheng and S. Ustin (2006). Estimation of canopy water content from MODIS using artificial neural networks trained with radiative transfer models. Proceedings of 6th Annual Meeting of the European Meteorological Society & 6th European Conference on Applied Climatology, Ljubljana, Slovenia.

Rust, J. and T. Rust (2013). "Climate change and livestock production: A review with emphasis on Africa." South African Journal of Animal Science **43**(3): 256-267.

Rust, J. and T. Rust (2013). "Climate change and livestock production: A review with emphasis on Africa." South African Journal of Animal Science **43**(3): 255-267.

Saatchi, S. S., J. J. van Zyl and G. Asrar (1995). "Estimation of canopy water content in Konza Prairie grasslands using synthetic aperture radar measurements during FIFE." Journal of Geophysical Research: Atmospheres **100**(D12): 25481-25496.

Sakowska, K., R. Juszczak and D. Gianelle (2016). "Remote sensing of grassland biophysical parameters in the context of the Sentinel-2 satellite mission." Journal of Sensors **2016**.

Sala, O. E., L. Yahdjian, K. Havstad and M. R. Aguiar (2017). Rangeland ecosystem services: nature's supply and humans' demand. Rangeland systems, Springer, Cham: 467-489.

Sala, O. E., L. Yahdjian, K. Havstad and M. R. Aguiar (2017). "Rangeland ecosystem services: Nature's supply and humans' demand." Rangeland systems: Processes, management and challenges: 467-489.

Samimi, C. and T. Kraus (2004). "Biomass estimation using Landsat-TM and-ETM+. Towards a regional model for Southern Africa?" GeoJournal **59**(3): 177-187.

Sang, L., C. Zhang, J. Yang, D. Zhu and W. Yun (2011). "Simulation of land use spatial pattern of towns and villages based on CA-Markov model." Mathematical and Computer Modelling **54**(3-4): 938-943.

Santoso, H., T. Gunawan, R. H. Jatmiko, W. Darnosarkoro and B. Minasny (2011). "Mapping and identifying basal stem rot disease in oil palms in North Sumatra with QuickBird imagery." Precision Agriculture **12**(2): 233-248.

Sawalhah, M. N., S. D. Al-Kofahi, Y. A. Othman and A. F. Cibils (2018). "Assessing rangeland cover conversion in Jordan after the Arab spring using a remote sensing approach." Journal of Arid Environments **157**: 97-102.

Schaffrath, D. and C. Bernhofer (2013). "Variability and distribution of spatial evapotranspiration in semi arid Inner Mongolian grasslands from 2002 to 2011." SpringerPlus **2**(1): 1-17.

Schapendonk, A., W. Stol, D. Van Kraalingen and B. Bouman (1998). "LINGRA, a sink/source model to simulate grassland productivity in Europe." European Journal of Agronomy **9**(2-3): 87-100.

Schino, G., F. Borfecchia, L. De Cecco, C. Dibari, M. Iannetta, S. Martini and F. Pedrotti (2003). "Satellite estimate of grass biomass in a mountainous range in central Italy." Agroforestry Systems **59**(2): 157-162.

Schreiber, L. V., J. G. Atkinson Amorim, L. Guimarães, D. Motta Matos, C. Maciel da Costa and A. Parraga (2022). "Above-ground Biomass Wheat Estimation: Deep Learning with UAV-based RGB Images." Applied Artificial Intelligence: 1-15.

Schwieder, M., M. Buddeberg, K. Kowalski, K. Pfoch, J. Bartsch, H. Bach, J. Pickert and P. Hostert (2020). "Estimating grassland parameters from Sentinel-2: A model comparison study." PGF-Journal of Photogrammetry, Remote Sensing and Geoinformation Science **88**(5): 379-390.

Scott-Shaw, R. and C. D. Morris (2015). "Grazing depletes forb species diversity in the mesic grasslands of KwaZulu-Natal, South Africa." African Journal of Range & Forage Science **32**(1): 21-31.

Seastedt, T. and P. Pyšek (2011). "Mechanisms of plant invasions of North American and European grasslands." Annual Review of Ecology, Evolution, and Systematics **42**: 133-153.

Serrano, L., S. L. Ustin, D. A. Roberts, J. A. Gamon and J. Penuelas (2000). "Deriving water content of chaparral vegetation from AVIRIS data." Remote sensing of Environment **74**(3): 570-581.

Shary, P., G. Kuryakova and I. J. T. h. G. o. t. E. S. S. Florinsky (1991). "On the international experience of topographic methods employment in landscape researches (the concise review)." 15-29.

Shataee, S., S. Kalbi, A. Fallah and D. Pelz (2012). "Forest attribute imputation using machine-learning methods and ASTER data: comparison of k-NN, SVR and random forest regression algorithms." International journal of remote sensing **33**(19): 6254-6280.

Shen, B., L. Ding, L. Ma, Z. Li, A. Pulatov, Z. Kulenbekov, J. Chen, S. Mambetova, L. Hou and D. Xu (2022). "Modeling the Leaf Area Index of Inner Mongolia Grassland Based on Machine Learning Regression Algorithms Incorporating Empirical Knowledge." Remote Sensing **14**(17): 4196.

Shen, H., X. Meng and L. Zhang (2016). "An integrated framework for the spatio-temporal-spectral fusion of remote sensing images." IEEE Transactions on Geoscience and Remote Sensing **54**(12): 7135-7148.

Sheykhmousa, M., M. Mahdianpari, H. Ghanbari, F. Mohammadimanesh, P. Ghamisi and S. Homayouni (2020). "Support vector machine versus random forest for remote sensing image classification: A meta-analysis and systematic review." IEEE Journal of Selected Topics in Applied Earth Observations and Remote Sensing **13**: 6308-6325.

Shimoda, S. and T. Oikawa (2008). "Characteristics of canopy evapotranspiration from a small heterogeneous grassland using thermal imaging." Environmental and experimental botany **63**(1-3): 102-112.

Shoko, C., O. Mutanga and T. Dube (2016). "Progress in the remote sensing of C3 and C4 grass species aboveground biomass over time and space." ISPRS Journal of Photogrammetry and Remote Sensing **120**: 13-24.

Shoko, C., O. Mutanga and T. Dube (2019). "Remotely sensed C3 and C4 grass species aboveground biomass variability in response to seasonal climate and topography." African Journal of Ecology **57**(4): 477-489.

Shoko, C., O. Mutanga, T. Dube and R. Slotow (2018). "Characterizing the spatio-temporal variations of C3 and C4 dominated grasslands aboveground biomass in the Drakensberg, South Africa." International Journal of Applied Earth Observation and Geoinformation **68**: 51-60.

Sibanda, M., O. Mutanga, T. Dube, T. S Vundla and P. L Mafongoya (2019). "Estimating LAI and mapping canopy storage capacity for hydrological applications in wattle infested ecosystems using Sentinel-2 MSI derived red edge bands." GIScience & remote sensing **56**(1): 68-86.

Sibanda, M., O. Mutanga and M. Rouget (2015). "Examining the potential of Sentinel-2 MSI spectral resolution in quantifying above ground biomass across different fertilizer treatments." ISPRS Journal of Photogrammetry and Remote Sensing **110**: 55-65.

Sibanda, M., O. Mutanga and M. Rouget (2016). "Comparing the spectral settings of the new generation broad and narrow band sensors in estimating biomass of native grasses grown under different management practices." GIScience & remote sensing **53**(5): 614-633.

Sibanda, M., O. Mutanga and M. Rouget (2016). "Testing the capabilities of the new WorldView-3 space-borne sensor's red-edge spectral band in discriminating and mapping complex grassland management treatments." International Journal of Remote Sensing **38**(1): 1-22.

Sibanda, M., O. Mutanga, M. Rouget and L. Kumar (2017). "Estimating biomass of native grass grown under complex management treatments using worldview-3 spectral derivatives." Remote Sensing **9**(1): 55.

Sibanda, M., M. Onisimo, T. Dube and T. Mabhaudhi (2021). "Quantitative assessment of grassland foliar moisture parameters as an inference on rangeland condition in the mesic rangelands of southern Africa." International Journal of Remote Sensing **42**(4): 1474-1491.

Sidhu, N., E. Pebesma and G. Câmara (2018). "Using Google Earth Engine to detect land cover change: Singapore as a use case." European Journal of Remote Sensing **51**(1): 486-500.

Sims, D. A. and J. A. Gamon (2003). "Estimation of vegetation water content and photosynthetic tissue area from spectral reflectance: a comparison of indices based on liquid water and chlorophyll absorption features." Remote sensing of environment **84**(4): 526-537.

Singh, B., P. Sihag and K. Singh (2017). "Modelling of impact of water quality on infiltration rate of soil by random forest regression." Modeling Earth Systems and Environment **3**(3): 999-1004.

Singh, L., O. Mutanga, P. Mafongoya and K. Peerbhay (2017). "Remote sensing of key grassland nutrients using hyperspectral techniques in KwaZulu-Natal, South Africa." Journal of Applied Remote Sensing **11**(3): 036005.

Singh, L., O. Mutanga, P. Mafongoya and K. Y. Peerbhay (2018). "Multispectral mapping of key grassland nutrients in KwaZulu-Natal, South Africa." Journal of Spatial Science **63**(1): 155-172.

Sinha, S., L. K. Sharma and M. S. Nathawat (2015). "Improved land-use/land-cover classification of semi-arid deciduous forest landscape using thermal remote sensing." The Egyptian Journal of Remote Sensing and Space Science **18**(2): 217-233.

Smallman, T. L. and M. Williams (2019). "Description and validation of an intermediate complexity model for ecosystem photosynthesis and evapotranspiration: ACM-GPP-ETv1." Geoscientific Model Development **12**(6): 2227-2253.

Smith, P., D. Powlson, M. Glendining and J. O. Smith (1997). "Potential for carbon sequestration in European soils: preliminary estimates for five scenarios using results from long-term experiments." Global Change Biology **3**(1): 67-79.

Sola, I., A. García-Martín, L. Sardonís-Pozo, J. Álvarez-Mozos, F. Pérez-Cabello, M. González-Audicana and R. M. Llovería (2018). "Assessment of atmospheric correction methods for Sentinel-2 images in Mediterranean landscapes." International journal of applied earth observation and geoinformation **73**: 63-76.

Sollenberger, L. E., M. M. Kohmann, J. C. Dubeux Jr and M. L. Silveira (2019). "Grassland management affects delivery of regulating and supporting ecosystem services." Crop Science **59**(2): 441-459.

Soons, M., J. Messelink, E. Jongejans and G. Heil (2005). "Habitat fragmentation reduces grassland connectivity for both short-distance and long-distance wind-dispersed forbs." Journal of Ecology **93**(6): 1214-1225.

Soubry, I., T. Doan, T. Chu and X. Guo (2021). "A Systematic Review on the Integration of Remote Sensing and GIS to Forest and Grassland Ecosystem Health Attributes, Indicators, and Measures." Remote Sensing **13**(16): 3262.

Spanowicz, A. G. and J. A. Jaeger (2019). "Measuring landscape connectivity: On the importance of within-patch connectivity." Landscape Ecology **34**: 2261-2278.

Speight, J. G. J. L. e. (1968). "Parametric description of land form." 239-250.

Sridhar, V. and D. A. Wedin (2009). "Hydrological behaviour of grasslands of the Sandhills of Nebraska: water and energy-balance assessment from measurements, treatments, and modelling." Ecohydrology: Ecosystems, Land and Water Process Interactions, Ecohydrogeomorphology **2**(2): 195-212.

Subedi, P., K. Subedi and B. Thapa (2013). "Application of a hybrid cellular automaton-Markov (CA-Markov) model in land-use change prediction: a case study of Saddle Creek Drainage Basin, Florida." Applied Ecology and Environmental Sciences **1**(6): 126-132.

Svoray, T. and M. Shoshany (2002). "SAR-based estimation of areal aboveground biomass (AAB) of herbaceous vegetation in the semi-arid zone: a modification of the water-cloud model." International Journal of Remote Sensing **23**(19): 4089-4100.

Tagesson, T., J. Ardö, B. Cappelaere, L. Kergoat, A. Abdi, S. Horion and R. Fensholt (2017). "Modelling spatial and temporal dynamics of gross primary production in the Sahel from earth-observation-based photosynthetic capacity and quantum efficiency." Biogeosciences **14**(5): 1333-1348.

Talukdar, S., P. Singha, S. Mahato, S. Pal, Y.-A. Liou and A. Rahman (2020). "Land-use land-cover classification by machine learning classifiers for satellite observations – A review." Remote Sensing **12**(7): 1135.

Tamiminia, H., B. Salehi, M. Mahdianpari, L. Quackenbush, S. Adeli and B. Brisco (2020). "Google Earth Engine for geo-big data applications: A meta-analysis and systematic review." ISPRS Journal of Photogrammetry and Remote Sensing **164**: 152-170.

Terefe, D. (2015). Impacts of invasive plants (Lantana camara and Parthenium hysterophorus) on livestock and rangeland production in pastoral and agro pastoral areas of Somali Region, Ethiopia. 32nd annual research and extension workshop. Haramaya University, Alemaya.

Tesemma, Z., Y. Wei, M. Peel and A. Western (2015). "The effect of year-to-year variability of leaf area index on Variable Infiltration Capacity model performance and simulation of runoff." Advances in Water Resources **83**: 310-322.

Thanh Noi, P. and M. Kappas (2017). "Comparison of random forest, k-nearest neighbor, and support vector machine classifiers for land cover classification using Sentinel-2 imagery." Sensors **18**(1): 18.

Théau, J., É. Lauzier-Hudon, L. Aubé and N. Devillers (2021). "Estimation of forage biomass and vegetation cover in grasslands using UAV imagery." PLOS ONE **16**(1): e0245784.

Thenkabail, P. S., R. B. Smith and E. De Pauw (2000). "Hyperspectral vegetation indices and their relationships with agricultural crop characteristics." Remote sensing of Environment **71**(2): 158-182.

Thenkabail, P. S., R. B. Smith and E. De Pauw (2002). "Evaluation of narrowband and broadband vegetation indices for determining optimal hyperspectral wavebands for agricultural crop characterization." Photogrammetric engineering and remote sensing **68**(6): 607-622.

Tong, A. and Y. He (2017). "Estimating and mapping chlorophyll content for a heterogeneous grassland: Comparing prediction power of a suite of vegetation indices across scales between years." ISPRS Journal of Photogrammetry and Remote Sensing **126**: 146-167.

Tong, A. and Y. H. He (2017). "Estimating and mapping chlorophyll content for a heterogeneous grassland: Comparing prediction power of a suite of vegetation indices across scales between years." Isprs Journal of Photogrammetry and Remote Sensing **126**: 146-167.

Tsegaye, D., S. R. Moe, P. Vedeld and E. Aynekulu (2010). "Land-use/cover dynamics in Northern Afar rangelands, Ethiopia." Agriculture, ecosystems & environment **139**(1-2): 174-180.

Tsiko, C., H. Makurira, A. Gerrits and H. Savenije (2012). "Measuring forest floor and canopy interception in a savannah ecosystem." Physics and Chemistry of the Earth, Parts A/B/C **47**: 122-127.

Tsvuura, Z. and K. P. Kirkman (2013). "Yield and species composition of a mesic grassland savanna in South Africa are influenced by long-term nutrient addition." Austral Ecology **38**(8): 959-970.

Tucker, C. J. (1979). "Red and photographic infrared linear combinations for monitoring vegetation." Remote sensing of Environment **8**(2): 127-150.

- Tucker, C. J., L. Miller and R. L. Pearson (1976). "Shortgrass prairie spectral measurements." Photogrammetric Engineering and Remote Sensing **42**(3): 317-323.
- Ul Din, S. and H. W. L. Mak (2021). "Retrieval of Land-Use/Land Cover Change (LUCC) Maps and Urban Expansion Dynamics of Hyderabad, Pakistan via Landsat Datasets and Support Vector Machine Framework." Remote Sensing **13**(16): 3337.
- Ullah, S., Y. Si, M. Schlerf, A. K. Skidmore, M. Shafique and I. A. Iqbal (2012). "Estimation of grassland biomass and nitrogen using MERIS data." International Journal of Applied Earth Observation and Geoinformation **19**: 196-204.
- Ustin, S. L., D. Darling, S. Kefauver, J. Greenberg, Y.-B. Cheng and M. L. Whiting (2004). Remotely sensed estimates of crop water demand. Remote Sensing and Modeling of Ecosystems for Sustainability, International Society for Optics and Photonics.
- Ustin, S. L., D. Riaño and E. R. Hunt (2012). "Estimating canopy water content from spectroscopy." Israel Journal of Plant Sciences **60**(1-2): 9-23.
- Van den Hoof, C., M. Verstraete and R. J. Scholes (2018). "Differing responses to rainfall suggest more than one functional type of grassland in South Africa." Remote Sensing **10**(12): 2055.
- van Eck, N. J. and L. Waltman (2010). "Software survey: VOSviewer, a computer program for bibliometric mapping." Scientometrics **84**(2): 523-538.
- Varela, S., X.-y. Zheng, J. Njuguna, E. Sacks, D. Allen, J. Ruhter and A. D. Leakey (2022). "Deep convolutional neural networks exploit high spatial and temporal resolution aerial imagery to predict key traits in miscanthus." AgriRxiv(2022): 20220405560.
- Vargas, L., L. Willemsen and L. Hein (2019). "Assessing the capacity of ecosystems to supply ecosystem services using remote sensing and an ecosystem accounting approach." Environmental management **63**(1): 1-15.
- Verrelst, J., G. Camps-Valls, J. Muñoz-Marí, J. P. Rivera, F. Veroustraete, J. G. Clevers and J. Moreno (2015). "Optical remote sensing and the retrieval of terrestrial vegetation biogeophysical properties – A review." ISPRS Journal of Photogrammetry and Remote Sensing **108**: 273-290.
- Verrelst, J., Z. Malenovský, C. Van der Tol, G. Camps-Valls, J.-P. Gastellu-Etchegorry, P. Lewis, P. North and J. Moreno (2019). "Quantifying vegetation biophysical variables from imaging spectroscopy data: a review on retrieval methods." Surveys in Geophysics **40**(3): 589-629.
- Vescovo, L., G. Wohlfahrt, M. Balzarolo, S. Pilloni, M. Sottocornola, M. Rodeghiero and D. Gianelle (2012). "New spectral vegetation indices based on the near-infrared shoulder wavelengths for remote detection of grassland phytomass." International journal of remote sensing **33**(7): 10.1080/01431161.01432011.01607195.
- Vetter, S. (2013). "Development and sustainable management of rangeland commons – aligning policy with the realities of South Africa's rural landscape." African journal of range & forage science **30**(1-2): 1-9.

Vetter, S. H., D. Schaffrath and C. Bernhofer (2012). "Spatial simulation of evapotranspiration of semi-arid Inner Mongolian grassland based on MODIS and eddy covariance data." Environmental Earth Sciences **65**(5): 1567-1574.

Villoslada Peciña, M., T. F. Bergamo, R. D. Ward, C. B. Joyce and K. Sepp (2021). "A novel UAV-based approach for biomass prediction and grassland structure assessment in coastal meadows." Ecological Indicators **122**.

Vohland, M. and T. Jarmer (2010). "Estimating structural and biochemical parameters for grassland from spectroradiometer data by radiative transfer modelling (PROSPECT+SAIL)." International Journal of Remote Sensing **29**(1): 191-209.

Vundla, T., O. Mutanga and M. Sibanda (2020). "Quantifying grass productivity using remotely sensed data: an assessment of grassland restoration benefits." African Journal of Range & Forage Science **37**(4): 247-256.

Wachendorf, M., T. Fricke and T. Möckel (2018). "Remote sensing as a tool to assess botanical composition, structure, quantity and quality of temperate grasslands." Grass and Forage Science **73**(1): 1-14.

Wahap, N. and H. Z. Shafri (2020). Utilization of Google earth engine (GEE) for land cover monitoring over Klang Valley, Malaysia. IOP Conference Series: Earth and Environmental Science, IOP Publishing.

Wang, G., S. Liu, T. Liu, Z. Fu, J. Yu and B. Xue (2018). "Modelling above-ground biomass based on vegetation indexes: a modified approach for biomass estimation in semi-arid grasslands." International Journal of Remote Sensing **40**(10): 3835-3854.

Wang, G., S. Liu, T. Liu, Z. Fu, J. Yu and B. Xue (2019). "Modelling above-ground biomass based on vegetation indexes: a modified approach for biomass estimation in semi-arid grasslands." International Journal of Remote Sensing **40**(10): 3835-3854.

Wang, J., X. Xiao, R. Bajgain, P. Starks, J. Steiner, R. B. Doughty and Q. Chang (2019). "Estimating leaf area index and aboveground biomass of grazing pastures using Sentinel-1, Sentinel-2 and Landsat images." ISPRS Journal of Photogrammetry and Remote Sensing **154**: 189-201.

Wang, J., X. Xiao, Y. Qin, J. Dong, G. Geissler, G. Zhang, N. Cejda, B. Alikhani and R. B. Doughty (2017). "Mapping the dynamics of eastern redcedar encroachment into grasslands during 1984-2010 through PALSAR and time series Landsat images." Remote Sensing of Environment **190**: 233-246.

Wang, L.-T., S.-X. Wang, Y. Zhou, W.-L. Liu and F.-T. Wang (2011). "Vegetation water content retrieval and application of drought monitoring using multi-spectral remote sensing." Guang pu xue yu Guang pu fen xi= Guang pu **31**(10): 2804-2808.

Wang, L., C. Chen, Z. Zhang, W. Gan, J. Yu and H. Chen (2021). "Approach for estimation of ecosystem services value using multitemporal remote sensing images." Journal of Applied Remote Sensing **16**(1): 012010.

Wang, L., J. J. Qu, X. Hao and Q. Zhu (2008). "Sensitivity studies of the moisture effects on MODIS SWIR reflectance and vegetation water indices." International Journal of Remote Sensing **29**(24): 7065-7075.

- Wang, L. a., X. Zhou, X. Zhu, Z. Dong and W. Guo (2016). "Estimation of biomass in wheat using random forest regression algorithm and remote sensing data." The Crop Journal **4**(3): 212-219.
- Wang, Q., W. Shi, Z. Li and P. M. J. R. s. o. e. Atkinson (2016). "Fusion of Sentinel-2 images." **187**: 241-252.
- Wang, R., J. A. Gamon, C. A. Emmerton, K. R. Springer, R. Yu and G. Hmimina (2020). "Detecting intra- and inter-annual variability in gross primary productivity of a North American grassland using MODIS MAIAC data." Agricultural and Forest Meteorology **281**.
- Wang, R. J. and L. W. Yang (2012). Using RS technology to estimate net primary production of rangeland ecosystem in hulunbuir of china. Advanced Materials Research, Trans Tech Publ.
- Wang, X., L. Ge and X. Li (2013). "Pasture Monitoring Using SAR with COSMO-SkyMed, ENVISAT ASAR, and ALOS PALSAR in Otway, Australia." Remote Sensing **5**(7): 3611-3636.
- Wang, Z., X. Deng, W. Song, Z. Li and J. Chen (2017). "What is the main cause of grassland degradation? A case study of grassland ecosystem service in the middle-south Inner Mongolia." Catena **150**: 100-107.
- Wen, L., S. Dong, Y. Li, X. Li, J. Shi, Y. Wang, D. Liu and Y. Ma (2013). "Effect of degradation intensity on grassland ecosystem services in the alpine region of Qinghai-Tibetan Plateau, China." PloS one **8**(3): e58432.
- Wigley-Coetsee, C. and A. C. Staver (2020). "Grass community responses to drought in an African savanna." African Journal of Range & Forage Science **37**(1): 43-52.
- Wijewardana, C., F. A. Alsajri, J. T. Irby, L. J. Krutz, B. Golden, W. B. Henry, W. Gao and K. R. Reddy (2019). "Physiological assessment of water deficit in soybean using midday leaf water potential and spectral features." Journal of Plant Interactions **14**(1): 533-543.
- Wu, H., Z. Li, K. C. Clarke, W. Shi, L. Fang, A. Lin and J. Zhou (2019). "Examining the sensitivity of spatial scale in cellular automata Markov chain simulation of land use change." International Journal of Geographical Information Science **33**(5): 1040-1061.
- Xia, J., S. Liu, S. Liang, Y. Chen, W. Xu and W. Yuan (2014). "Spatio-Temporal Patterns and Climate Variables Controlling of Biomass Carbon Stock of Global Grassland Ecosystems from 1982 to 2006." Remote Sensing **6**(3): 1783-1802.
- Xie, Y., Z. Sha, M. Yu, Y. Bai and L. Zhang (2009). "A comparison of two models with Landsat data for estimating above ground grassland biomass in Inner Mongolia, China." Ecological Modelling **220**(15): 1810-1818.
- Xie, Z., S. R. Phinn, E. T. Game, D. J. Pannell, R. J. Hobbs, P. R. Briggs and E. McDonald-Madden (2019). "Using Landsat observations (1988-2017) and Google Earth Engine to detect vegetation cover changes in rangelands - A first step towards identifying degraded lands for conservation." Remote Sensing of Environment **232**: 111317.
- Xing, M., B. He, X. Li and X. Quan (2014). Soil moisture retrieval using RADARSAT-2 and HJ-1 CCD data in grassland. 2014 IEEE Geoscience and Remote Sensing Symposium, IEEE.

Xiong, P., Z. Chen, J. Zhou, S. Lai, C. Jian, Z. Wang and B. Xu (2021). "Aboveground biomass production and dominant species type determined canopy storage capacity of abandoned grassland communities on semiarid Loess Plateau." Ecohydrology **14**(2): e2265.

Xu, B., P. Gichuki, L. Shan and F. Li (2006). "Aboveground biomass production and soil water dynamics of four leguminous forages in semiarid region, northwest China." South African Journal of Botany **72**(4): 507-516.

Xu, B., X. Yang, W. Tao, Z. Qin, H. Liu and J. Miao (2007). "Remote sensing monitoring upon the grass production in China." Acta Ecologica Sinica **27**(2): 405-413.

Xu, B., X. Yang, W. Tao, Z. Qin, H. Liu, J. Miao and Y. Bi (2008). "MODIS-based remote sensing monitoring of grass production in China." International Journal of Remote Sensing **29**(17-18): 5313-5327.

Xu, B., X. C. Yang, W. G. Tao, Z. H. Qin, H. Q. Liu, J. M. Miao and Y. Y. Bi (2008). "MODIS-based remote sensing monitoring of grass production in China." International Journal of Remote Sensing **29**(17-18): 5313-5327.

Xu, B., X. C. Yang, W. G. Tao, Z. H. Qin, H. Q. Liu, J. M. Miao and Y. Y. Bi (2010). "MODIS-based remote sensing monitoring of grass production in China." International Journal of Remote Sensing **29**(17-18): 5313-5327.

Xu, D. and X. Guo (2015). "Some Insights on Grassland Health Assessment Based on Remote Sensing." Sensors **15**(2): 3070-3089.

Xu, H. (2006). "Modification of normalised difference water index (NDWI) to enhance open water features in remotely sensed imagery." International journal of remote sensing **27**(14): 3025-3033.

Xu, H., X. Hu, H. Guan, B. Zhang, M. Wang, S. Chen and M. Chen (2019). "A remote sensing based method to detect soil erosion in forests." Remote Sensing **11**(5): 513.

Xue, J. and B. Su (2017). "Significant remote sensing vegetation indices: A review of developments and applications." Journal of Sensors **2017**.

Yan, G., R. Hu, J. Luo, M. Weiss, H. Jiang, X. Mu, D. Xie and W. Zhang (2019). "Review of indirect optical measurements of leaf area index: Recent advances, challenges, and perspectives." Agricultural and forest meteorology **265**: 390-411.

Yang, S., Q. Feng, T. Liang, B. Liu, W. Zhang and H. Xie (2018). "Modeling grassland above-ground biomass based on artificial neural network and remote sensing in the Three-River Headwaters Region." Remote Sensing of Environment **204**: 448-455.

Yang, S., Q. Hao, H. Liu, X. Zhang, C. Yu, X. Yang, S. Xia, W. Yang, J. Li and Z. Song (2019). "Impact of grassland degradation on the distribution and bioavailability of soil silicon: Implications for the Si cycle in grasslands." Science of the Total Environment **657**: 811-818.

Yang, Y., Z. Wang, J. Li, C. Gang, Y. Zhang, I. Odeh and J. Qi (2017). "Assessing the spatiotemporal dynamic of global grassland carbon use efficiency in response to climate change from 2000 to 2013." Acta Oecologica **81**: 22-31.

Yang, Y. H., J. Y. Fang, Y. D. Pan and C. J. Ji (2009). "Aboveground biomass in Tibetan grasslands." Journal of Arid Environments **73**(1): 91-95.

- Ye, H., X.-t. Huang, G.-p. Luo, J.-b. Wang, M. Zhang and X.-x. Wang (2019). "Improving remote sensing-based net primary production estimation in the grazed land with defoliation formulation model." Journal of Mountain Science **16**(2): 323-336.
- Yilmaz, M. T., E. R. Hunt Jr, L. D. Goins, S. L. Ustin, V. C. Vanderbilt and T. J. Jackson (2008). "Vegetation water content during SMEX04 from ground data and Landsat 5 Thematic Mapper imagery." Remote Sensing of Environment **112**(2): 350-362.
- Yin, C., B. He, X. Quan and Z. Liao (2016). "Chlorophyll content estimation in arid grasslands from Landsat-8 OLI data." International Journal of Remote Sensing **37**(3): 615-632.
- Yirsaw, E., W. Wu, X. Shi, H. Temesgen and B. Bekele (2017). "Land use/land cover change modeling and the prediction of subsequent changes in ecosystem service values in a coastal area of China, the Su-Xi-Chang Region." Sustainability **9**(7): 1204.
- You, Y., S. Wang, Y. Ma, X. Wang and W. Liu (2019). "Improved modeling of gross primary productivity of Alpine Grasslands on the Tibetan Plateau using the biome-BGC model." Remote Sensing **11**(11): 1287.
- Young, A. (1972). Slopes, Oliver and Boyd, Edinburgh, Wetenschappen.
- Yu, H., Y. Wu, L. Niu, Y. Chai, Q. Feng, W. Wang and T. Liang (2021). "A method to avoid spatial overfitting in estimation of grassland above-ground biomass on the Tibetan Plateau." Ecological Indicators **125**: 107450.
- Yu, H., Y. F. Wu, L. T. Niu, Y. F. Chai, Q. S. Feng, W. Wang and T. G. Liang (2021). "A method to avoid spatial overfitting in estimation of grassland above-ground biomass on the Tibetan Plateau." Ecological Indicators **125**: 107450.
- Yu, K., T. G. Pypker, R. F. Keim, N. Chen, Y. Yang, S. Guo, W. Li and G. Wang (2012). "Canopy rainfall storage capacity as affected by sub-alpine grassland degradation in the Qinghai-Tibetan Plateau, China." Hydrological Processes **26**(20): 3114-3123.
- Yu, R. Y., Y. J. Yao, Q. Wang, H. W. Wan, Z. J. Xie, W. J. Tang, Z. P. Zhang, J. M. Yang, K. Shang, X. Z. Guo and X. Y. Bei (2021). "Satellite-Derived Estimation of Grassland Aboveground Biomass in the Three-River Headwaters Region of China during 1982-2018." Remote Sensing **13**(15): 2993.
- Yuan, Q., S. Li, L. Yue, T. Li, H. Shen and L. Zhang (2019). "Monitoring the variation of vegetation water content with machine learning methods: Point-surface fusion of MODIS products and GNSS-IR observations." Remote Sensing **11**(12): 1440.
- Yuan, Q., H. Shen, T. Li, Z. Li, S. Li, Y. Jiang, H. Xu, W. Tan, Q. Yang and J. Wang (2020). "Deep learning in environmental remote sensing: Achievements and challenges." Remote Sensing of Environment **241**: 111716.
- Zeng, N., X. Ren, H. He, L. Zhang, D. Zhao, R. Ge, P. Li and Z. Niu (2019). "Estimating grassland aboveground biomass on the Tibetan Plateau using a random forest algorithm." Ecological Indicators **102**: 479-487.
- Zeppel, M., J. V. Wilks and J. D. Lewis (2014). "Impacts of extreme precipitation and seasonal changes in precipitation on plants." Biogeosciences **11**(11): 3083-3093.

- Zerga, B. (2015). "Rangeland degradation and restoration: A global perspective." Point Journal of Agriculture and Biotechnology Research **1**(2): 37-54.
- Zhang, B., I. Valentine, P. Kemp and G. Lambert (2006). "Predictive modelling of hill-pasture productivity: integration of a decision tree and a geographical information system." Agricultural Systems **87**(1): 1-17.
- Zhang, C., Y. Zhang, Z. Wang, J. Li and I. Odeh (2019). "Monitoring Phenology in the Temperate Grasslands of China from 1982 to 2015 and Its Relation to Net Primary Productivity." Sustainability **12**(1).
- Zhang, F. and G. Zhou (2018). "Research progress on monitoring vegetation water content by using hyperspectral remote sensing." Chinese Journal of Plant Ecology **42**(5): 517-525.
- Zhang, F. and G. Zhou (2019). "Estimation of vegetation water content using hyperspectral vegetation indices: A comparison of crop water indicators in response to water stress treatments for summer maize." BMC ecology **19**(1): 1-12.
- Zhang, H., M. Huang, X. Qing, G. Li and C. Tian (2017). "Bibliometric analysis of global remote sensing research during 2010-2015." ISPRS International Journal of Geo-Information **6**(11): 332.
- Zhang, H., Y. Sun, L. Chang, Y. Qin, J. Chen, Y. Qin, J. Du, S. Yi and Y. Wang (2018). "Estimation of grassland canopy height and aboveground biomass at the quadrat scale using unmanned aerial vehicle." Remote sensing **10**(6): 851.
- Zhang, J., Y. Xu, F. Yao, P. Wang, W. Guo, L. Li and L. Yang (2010). "Advances in estimation methods of vegetation water content based on optical remote sensing techniques." Science China Technological Sciences **53**(5): 1159-1167.
- Zhang, L., B. Wylie, T. Loveland, E. Fosnight, L. L. Tieszen, L. Ji and T. Gilmanov (2007). "Evaluation and comparison of gross primary production estimates for the Northern Great Plains grasslands." Remote Sensing of Environment **106**(2): 173-189.
- Zhang, M., R. Lal, Y. Zhao, W. Jiang and Q. Chen (2016). "Estimating net primary production of natural grassland and its spatio-temporal distribution in China." Science of the Total Environment **553**: 184-195.
- Zhang, M., R. Lal, Y. Zhao, W. Jiang and Q. Chen (2016). "Estimating net primary production of natural grassland and its spatio-temporal distribution in China." Sci Total Environ **553**: 184-195.
- Zhang, T., J. Su, C. Liu, W.-H. Chen, H. Liu and G. Liu (2017). Band selection in Sentinel-2 satellite for agriculture applications. 2017 23rd international conference on automation and computing (ICAC), IEEE.
- Zhang, X., Y. Bao, D. Wang, X. Xin, L. Ding, D. Xu, L. Hou and J. Shen (2021). "Using UAV LiDAR to Extract Vegetation Parameters of Inner Mongolian Grassland." Remote Sensing **13**(4): 656.
- Zhang, X., X. Chen, M. Tian, Y. Fan, J. Ma and D. Xing (2020). "An evaluation model for aboveground biomass based on hyperspectral data from field and TM8 in Khorchin grassland, China." PLoS One **15**(2): e0223934.

Zhang, Y., F. Chiew, L. Zhang, R. Leuning and H. Cleugh (2008). "Estimating catchment evaporation and runoff using MODIS leaf area index and the Penman-Monteith equation." Water Resources Research **44**(10).

Zhang, Y., S. Yang, W. Ouyang, H. Zeng and M. Cai (2010). "Applying multi-source remote sensing data on estimating ecological water requirement of grassland in ungauged region." Procedia Environmental Sciences **2**: 953-963.

Zhao, D., L. Huang, J. Li, J. J. I. J. o. P. Qi and R. Sensing (2007). "A comparative analysis of broadband and narrowband derived vegetation indices in predicting LAI and CCD of a cotton canopy." **62**(1): 25-33.

Zhao, Y., Z. Liu and J. Wu (2020). "Grassland ecosystem services: a systematic review of research advances and future directions." Landscape Ecology: 1-22.

Zhao, Y., Z. Liu and J. Wu (2020). "Grassland ecosystem services: a systematic review of research advances and future directions." Landscape Ecology **35**: 793-814.

Zhao, Y., W. Zhu, P. Wei, P. Fang, X. Zhang, N. Yan, W. Liu, H. Zhao and Q. Wu (2022). "Classification of Zambian grasslands using random forest feature importance selection during the optimal phenological period." Ecological Indicators **135**: 108529.

Zheng, G. and L. M. Moskal (2009). "Retrieving leaf area index (LAI) using remote sensing: Theories, methods and sensors." Sensors **9**(4): 2719-2745.

Zhengxing, W., L. Chuang and H. Alfredo (2003). "From AVHRR-NDVI to MODIS-EVI: Advances in vegetation index research." Acta ecologica sinica **23**(5): 979-987.

Zhou, H., G. Zhou, X. Song and Q. He (2022). "Dynamic characteristics of canopy and vegetation water content during an entire maize growing season in relation to spectral-based indices." Remote Sensing **14**(3): 584.

Zhou, S., R. A. Duursma, B. E. Medlyn, J. W. Kelly and I. C. Prentice (2013). "How should we model plant responses to drought? An analysis of stomatal and non-stomatal responses to water stress." Agricultural and Forest Meteorology **182**: 204-214.

Zhou, W., H. Li, L. Xie, X. Nie, Z. Wang, Z. Du and T. Yue (2021). "Remote sensing inversion of grassland aboveground biomass based on high accuracy surface modeling." Ecological Indicators **121**: 107215.

Zhou, W., H. Li, L. Xie, X. Nie, Z. Wang, Z. Du and T. Yue (2021). "Remote sensing inversion of grassland aboveground biomass based on high accuracy surface modeling." Ecological Indicators **121**.

Zhou, Y., L. Zhang, J. Xiao, S. Chen, T. Kato and G. Zhou (2014). "A Comparison of Satellite-Derived Vegetation Indices for Approximating Gross Primary Productivity of Grasslands." Rangeland Ecology & Management **67**(1): 9-18.

Zhu, G., Y. Su, X. Li, K. Zhang and C. Li (2013). "Estimating actual evapotranspiration from an alpine grassland on Qinghai-Tibetan plateau using a two-source model and parameter uncertainty analysis by Bayesian approach." Journal of Hydrology **476**: 42-51.

Zhu, L., G. I. Webb, M. Yebra, G. Scortechini, L. Miller and F. Petitjean (2021). "Live fuel moisture content estimation from MODIS: A deep learning approach." ISPRS Journal of Photogrammetry and Remote Sensing **179**: 81-91.

Zhu, X. X., D. Tuia, L. Mou, G.-S. Xia, L. Zhang, F. Xu and F. Fraundorfer (2017). "Deep learning in remote sensing: A comprehensive review and list of resources." IEEE Geoscience and Remote Sensing Magazine **5**(4): 8-36.

Zhu, Z. and C. E. Woodcock (2014). "Continuous change detection and classification of land cover using all available Landsat data." Remote sensing of Environment **144**: 152-171.

Zou, C. B., G. L. Caterina, R. E. Will, E. Stebler and D. Turton (2015). "Canopy interception for a tallgrass prairie under juniper encroachment." PLoS One **10**(11): e0141422.

Zumo, I. M., M. Hashim and N. Hassan (2021). "Mapping grass above-ground biomass of grazing-lands using satellite remote sensing." Geocarto International: 1-14.

APPENDICES

Appendix A: List of Publications

1. Masenyama, A., Mutanga, O., Dube, T., Bangira, T., Sibanda, M. and Mabhaudhi, T., 2022. A systematic review on the use of remote sensing technologies in quantifying grasslands ecosystem services. *GIScience & Remote Sensing*, 59(1), pp.1000-1025.
2. Masenyama, A., Mutanga, O., Dube, T., Sibanda, M., Odebiri, O. and Mabhaudhi, T., 2023. Inter-Seasonal Estimation of Grass Water Content Indicators Using Multisource Remotely Sensed Data Metrics and the Cloud-Computing Google Earth Engine Platform. *Applied Sciences*, 13(5), p.3117.
3. Bangira, T., Mutanga, O., Sibanda, M., Dube, T. and Mabhaudhi, T., 2023. Remote Sensing Grassland Productivity Attributes: A Systematic Review. *Remote Sensing*, 15(8), p.2043.
4. Vawda, M.I., Lottering, R., Mutanga, O., Peerbhay, K. and Sibanda, M., 2024. Comparing the Utility of Artificial Neural Networks (ANN) and Convolutional Neural Networks (CNN) on Sentinel-2 MSI to Estimate Dry Season Aboveground Grass Biomass. *Sustainability*, 16(3), p.1051.

Appendix B: List of Conferences Presentations

1. Masenyama, A et al. 2023, Inter-Seasonal Estimation of Grass Water Content Indicators Using Multisource Remotely Sensed Data Metrics and the Cloud-Computing Google Earth Engine Platform, International Association for Landscape Ecology (IALE) World Congress under Symposium/Paper session 'GeoAI, Machine Learning, and Big Data Analyses of Earth Observation Data for Climate Change and Ecosystem Resilience'. Nairobi, Kenya, from 10-15 July 2023.

Appendix C: Keynote Addresses

1. O. Mutanga. Multispectral Imaging and monitoring of Vegetation Ecosystem services in the face of Climate Change, Optica Sensing Congress, Munich, Germany 30 July-04 August 2023

Appendix D: Policy Briefs & Reports

1. Co-management of Communal rangelands in South Africa: Optimizing Communal rangeland management in South Africa through participatory approaches
2. Rangeland Management Plan as part of UMngeni Resilience Project
3. Rangeland management Plan Brochure & Poster

Appendix E: Policy Briefs & Reports

1. Co-management of Communal rangelands in South Africa: Optimizing Communal rangeland management in South Africa through participatory approaches
2. Rangeland Management Plan as part of UMngeni Resilience Project
3. Rangeland management Plan Brochure & Poster

Appendix F: Workshops

1. The stakeholders' workshop, 2022 (Two Days) – Purpose to analyse the problems affecting the rangeland for better understanding and in guiding the decision making on possible solutions to address the identified problems. Through stakeholders' discussions and agreement, a rangeland management goal was set, and management actions were also decided.
2. Vulindlela workshop, 15 February 2023, A focus Group discussion held with communities on explaining seasonal and long-term variability in grass productivity.

Appendix G: List of Post Doctoral Fellows and Graduated Students

Name	Degree Programme	University	Year
Xolile Zuma	MSc Environmental Science	University of KwaZulu-Natal	2021
Mohamed I Vawda	MSc Environmental Science	University of KwaZulu-Natal	2022
Anita Masenyama	MSc Environmental Science	University of KwaZulu-Natal	2022
Dr T Bangira	Geography & CTAFS	University of KwaZulu-Natal	2020